Improving the Convergence Rate of Seismic History Matching with a Proxy Derived Method to Aid Stochastic Sampling

Saleh Arwini

Submitted for the Degree of Doctor of Philosophy

Institute of Petroleum Engineering,

Heriot-Watt University

Edinburgh

Scotland

February 2013

Abstract

History matching is a very important activity during the continued development and management of petroleum reservoirs. Time-lapse (4D) seismic data provide information on the dynamics of fluids in reservoirs, relating variations of seismic signal to saturation and pressure changes. This information can be integrated with history matching to improve convergence towards a simulation model that predicts available data. The main aim of this thesis is to develop a method to speed up the convergence rate of assisted seismic history matching using proxy derived gradient method.

Stochastic inversion algorithms often rely on simple assumptions for selecting new models by random processes. In this work, we improve the way that such approaches learn about the system they are searching and thus operate more efficiently. To this end, a new method has been developed called NA with Proxy derived Gradients (NAPG). To improve convergence, we use a proxy model to understand how parameters control the misfit and then use a global stochastic method with these sensitivities to optimise the search of the parameter space. This leads to an improved set of final reservoir models. These in turn can be used more effectively in reservoir management decisions.

To validate the proposed approach, we applied the new approach on a number of analytical functions and synthetic cases. In addition, we demonstrate the proposed method by applying it to the UKCS Schiehallion field. The results show that the new method speeds up the rate of convergence by a factor of two to three generally. The performance of NAPG is much improved by updating the regression equation coefficients instead of keeping it fixed. In addition, we found that the initial number of models to start NAPG or NA could be reduced by using Experimental Design instead of using random initialization. Ultimately, with all of these approaches combined, the number of models required to find a good match reduced by an order of magnitude.

We have investigated the criteria for stopping the SHM loop, particularly the use of a proxy model to help. More research is needed to complete this work but the approach is promising. Quantifying parameter uncertainty using NA and NAPG was studied using the NA-Bayes approach (NAB). We found that NAB is very sensitive to misfit magnitude but otherwise NA and NAPG produce similar uncertainty measures.

This thesis is dedicated to my parents, my wife and my lovely sons

Mohamed and

Abd Alhai

Acknowledgements

In The Name of Allah, The Most Gracious, The Most Merciful

First and foremost, I would like to express my deepest gratitude and respect to my supervisor, Dr Karl D. Stephen. He has been supportive and very helpful since the days that I began working on the project. Karl has supported me academically through the rough road to finish this thesis. I thank him for his flexibility and supporting me with their never ending enthusiasm. His expertise in history matching and optimization provided numerous fruitful advices and has a valuable impact on the success of this research.

Furthermore, I would like to acknowledge my examining committee, Dr Remus Hanea from Delft University of Technology, The Netherlands and Dr Gillian Pickup from the Institute of Petroleum Engineering of Heriot Watt University for their time spending in the reading and evaluation of this thesis.

I would also like to thank my colleagues in SHM project and my office mates for their support. I also want to express my sincere thanks to all friends who made my stay at Heriot Watt University and Edinburgh an enjoyable and memorable.

I also want to thank the Schiehallion field partners: BP, Shell, Amerada Hess, Statoilhydro, Murphy Oil and OMV, for providing the data and permission to publish the results of this work. BP, ConocoPhilips, Shell and StatoilHydro are also thanked for funding of this research. Schlumberger Geoquest is thanked for use of the software. Malcolm Sambridge is thanked for use of the Neighbourhood Algorithm.

I would like to thank the institute of petroleum engineering at Heriot Watt University for providing the required facilities and for creating a unique work environment allowing students to work in friendly atmosphere.

Last but not least, I wish to thank my family, where the most basic source of my life energy resides. Special thanks to my wife who is always patient for the long time spending in the office. Also, the smiling faces of my sons Mohamed and Abd Alhai give me a lot of support and happiness during the hard times.

Publications

1. Arwini, S. and Stephen, K. D.: "Improve Convergence Rate of Seismic History Matching using NAPG," Extended Abstract, EAGE, the Integrated Reservoir Modelling Conference, Dubai UAE, 25 - 28 November 2012.
2. Arwini, S. and Stephen, K. D.: "Combining experimental design with proxy derived sensitivities to improve convergence rates in Seismic History Matching," paper SPE 143528, presented at the SPE EUROPEC/EAGE Annual Conference and Exhibition held in Vienna, Austria, 23–26 May 2011.
3. Stephen, K.D. and Arwini, S.: "Improving Stochastic Inversion Methods in History Matching using Proxy Models," ECMOR XII, 12th European Conference on the Mathematics of Oil Recovery, 6-9 September 2010, Oxford, UK.
4. Arwini, S. and Stephen, K. D.: "A New Method to Improve Convergence Rates with Seismic History Matching," paper SPE 131545, presented at the SPE EUROPEC/EAGE Annual Conference and Exhibition held in Barcelona, Spain, 14–17 June 2010.
5. Stephen, K. D., Kazemi, A., Sedighi, F., Arwini, S., Shams, A., MacBeth, C., Sagitov, I. & Said, A. "Improved reservoir description using seismic history matching" Production and Development Conference and Exhibition, DEVEX, Aberdeen Exhibition and Conference Centre, 12-13 May 2010.

ACADEMIC REGISTRY

Research Thesis Submission

Name*:*	**Saleh G. Arwini**		
School/PGI:	Institute of Petroleum Engineering		
Version: *(i.e. First, Resubmission, Final)*	First	Degree Sought (Award **and** Subject area)	Doctor of Philosophy (PhD) in Petroleum Engineering

Declaration

In accordance with the appropriate regulations I hereby submit my thesis and I declare that:

1) the thesis embodies the results of my own work and has been composed by myself
2) where appropriate, I have made acknowledgement of the work of others and have made reference to work carried out in collaboration with other persons
3) the thesis is the correct version of the thesis for submission and is the same version as any electronic versions submitted*.
4) my thesis for the award referred to, deposited in the Heriot-Watt University Library, should be made available for loan or photocopying and be available via the Institutional Repository, subject to such conditions as the Librarian may require
5) I understand that as a student of the University I am required to abide by the Regulations of the University and to conform to its discipline.

* *Please note that it is the responsibility of the candidate to ensure that the correct version of the thesis is submitted.*

Signature of Candidate*:*		Date:	

Submission

Submitted By *(name in capitals):*	**SALEH ARWINI**
Signature of Individual Submitting:	
Date Submitted:	

For Completion in the Student Service Centre (SSC)

Received in the SSC by *(name in capitals):*			
Method of Submission *(Handed in to SSC; posted through internal/external mail):*			
E-thesis Submitted (mandatory for final theses)			
Signature:		Date:	

Table of Content

List of Figures

Nomenclature

C_0	Constant coefficient
CCF	Central Composite Faced Designs
C_M	Covariance matrix
C_i	Linear coefficients
C_{i+nd}	Quadratic coefficients
C_{ij}	Cross term coefficients (interacting terms)
I	Impedance, m/L^2t, kg $m^{-2}s^{-1}$
I^{ij}	Impedance on the seismic grid, m/L^2t, Kg $m^{-2}s^{-1}$
I_{IJ}	Impedance on the simulation grid, m/L^2t, kg $m^{-2}s^{-1}$
I_{ij}^{interp}	Interpreted value of p impedance for the location of bins and between the simulation cells
I_p	Compressional acoustic impedance, Kg $m^{-2}s^{-1}$
it	Number of iterations
J	Total misfit function
J_j	Misfit for the j^{th} variable (j)
J_i	Misfit for the i^{th} variable Total misfit
J_{noise}	Misfit of the noise
κ	Bulk modulus, m/Lt^2, Pa
κ_f	Fluid bulk modulus, m/Lt2, Pa
κ_g	Gas bulk modulus, m/Lt2, Pa
κ_{gr}	Grain bulk modulus, , m/Lt2, Pa
κ_{inf}^r	Bulk modulus at STP, m/Lt2, Pa
κ_o	Oil bulk modulus, m/Lt2, Pa
κ_{dry}^r	Dry bulk modulus, m/Lt2, Pa
κ_{sat}^r	Saturated bulk modulus, m/Lt2, Pa
κ_w	Water bulk modulus, m/Lt2, Pa
K	Permeability, L^2, mD
K_h	Horizontal permeability, L^2 ,mD
K_Z	Vertical permeability, L^2 ,mD
n_d	Number of parameters
n_i	Initial sample size

M	p-wave moduli for sand-shale mixture, Pa
M^{sand}	p-wave moduli for sand, Pa
M^{shale}	p-wave moduli for and shale, Pa
Q^{obs}	Observed production data, m^3/t, bbl/day
Q^{cal}	Calculated production data, m^3/t, bbl/day
P	Pressure, m/Lt^2, Pa
P_{eff}	Effective (overburden – pore) pressure, m/Lt2, Pa
P_k^r	Stress sensitivity of the bulk modulus (r = sand or shale), m/Lt2, Pa
$p(m)$	Prior probability of the model
$p(m\|O)$	probability of each model m, given observations O
$p(O\|m)$	Likelihoods of the observed data O, given the model m
$P(d\|\theta)$	Probability for selecting one new parameter value given data, d
R^2	Correlation coefficient
S_g	Gas saturation
S_o	Oil saturation
S_w	Water saturation
V_p	P-wave velocity, m/t, Km/s
V_s	Velocity of shear wave, m/t, Km/s
w_{ijIJ}	Interpolated factor
φ	Porosity
ε_m	Model error
ε_d	Data error
σ_d	Standard deviation of the observed data error
θ_i	i^{th} element of the parameter vector, $\underline{\theta}$
$\underline{\theta}$	Parameter vector
ρ	Bulk density,kg/m^3
ρ_{solid}	Dry sand density, Kg/m^3
μ^r	Shear modulus (r = sand or shale), m/Lt^2, Pa

Subscripts and superscripts

d	Data
m	Model
mod	Modelled (predicted)
obs	Observed

prior	Prior information
i	Index
j	Index
I,J,K	x,y and z indices on the simulator grid
t	Time
x	x direction
y	y direction
z	z direction

Abbreviations

AHM	Assisted History Matching
API	American Petroleum Institute
cdf	Cumulative distribution function
ED	Experimental Design
gr	*Grain*
WOR	Water/oil ratio
GOR	Gas/oil ratios
WGR	Water/gas ratios
BHFP	Bottom hole flowing pressure
NA	Neighbourhood Algorithm
NAB	NA-Bayes
NAPG	NA with Proxy derived Gradients
NTG	Net-to-Gross Ratio
OF	Objective Function
pdf	Probability distribution function
PEM	Petro- Elastic Model
PPD	Posterior Probability Distribution
RMS	Root Mean Square
SCAL	Special core analysis
SEG	Society of Exploration Geophysicists
SHM	Seismic History Matching
TVD	True vertical depth, L
TVDSS	True Vertical Depth Subsea, L

CHAPTER 1

Introduction

Overview:

This chapter defines the problem statement of this research and also gives a brief introduction to History Matching and development optimization. The main objectives and contribution of this thesis have been listed. Finally, we end with a review of the following chapters showing the content of the thesis.

1.1 Statement of the Problem

Assisted history matching remains a challenging research topic. Effective updating of reservoir models and prediction of future performance with uncertainty continues to be a major challenge for the industry. One of the main problems of seismic history matching (SHM) problems is the speed of convergence of the misfit between observed and predicted data. It is important to optimise the number of models created during history matching so that the misfit is minimised while sufficiently sampling parameters. Therefore, the fundamental problem in the automated history matching process is the development of optimization algorithms to find optimal solutions in multidimensional search spaces.

In general, global methods (e.g. Genetic Algorithm, Neighbourhood Algorithm, etc) have slower convergence rates, compared to local methods based on gradient techniques (e.g. Adjoint method, Gauss-Newton method, etc). Local methods provide a single solution, which is the nearest local optimum to the initial guess. On the other hand, global optimization seeks to find the best possible solutions for given problems but the main disadvantage is the computational time to reach the global minimum. For this reason, improving the convergence rate of stochastic methods is an important issue that requires further research.

1.2 History Matching and Development Optimization

One of the major goals of any oil company is to optimise production and maximise profit. To achieve this, it is required to obtain the most accurate reservoir model. This plays a major role in field management and development. In many oil and gas assets, model based predictions are used to help with field management and can provide a large number of feasible production profiles. Thus, the field development decisions can be made based on the reliable reservoir-simulation models.

Reservoir simulation is an efficient method for helping engineers estimate the oil and gas reserves; practically all-major reservoir development disciplines somewhat utilize simulation results. In fact, reservoir development is comprised of geological and reservoir model building, history matching in case of mature fields, and forecasting. Data assimilation stems from the requirement to improve the output of the model. In particular, there is a need to reduce the parameter uncertainty, and increase prediction accuracy by incorporating production and (4D) seismic data. The available data for constructing a reliable and useful reservoir model are of different natures and can be classified as static or dynamic. Data that have originated from geology, electrical logs, core analysis, fluid properties and pre-production seismic surveys can be generally classified as static, whereas the information originating from well testing, repeat formation tests, production logs, production history, bottomhole pressure from permanent gauges, water cut, and gas-oil ratio can be classified as dynamic (Landa and Horne, 1997).

The data assimilation process of tuning unknown parameters in a reservoir simulation is known as history matching and has been studied extensively over the last four decades. History matching is exploited to improve reservoir characterization and to provide a better understanding of general flow mechanisms. However, this is not only mathematically and computationally challenging, but also non-unique in nature. This means that multiple models can generate the same response as the real data where none of them could be perfectly reliable. Generally HM is divided into manual, automatic and assisted history matching (Rwechungura *et al.*, 2011).

Manual history matching has been performed by trial and error, which largely depends on the engineer's experience and the resources available. Even for experienced

reservoir engineers, the process is very time consuming and, in general, a single adjusted scenario can be geologically inconsistent. Because reservoirs are usually very heterogeneous, grid cells should capture the interpreted heterogeneity in the reservoir by being populated with reservoir rock petro-physical properties such as porosity, permeability etc. The main drawback of the manual history matching workflow is that it is not easy to adjust a large number of parameters simultaneously since the behaviour of the reservoir models and the interdependencies among parameters is tremendously complex. For this reason, manual history matching is always associated with lots of uncertainties and is not reliable for long periods of forecasting.

Automatic history matching is the process of implementing changes to a model not by manual history matching, but rather, through algorithmic techniques that maintain adherence to certain restrictions of the input geological model. Automated history matching, usually based on gradient minimization, has been described in the literature. Automated history matching has seen good success in single-phase problems and in matching pressure. However, because of the large number of equations involved in a field-scale problem, the non-linear properties of flow parameters, and the subjective nature of 'matching,' automatic history matching has not had widespread practical use to date (Landa *et al.*, 1996; Kitandis, 1997; Alan *et al.*, 1998).

Assisted History Matching (AHM) is different from automated history matching and from traditional history matching techniques as well. AHM is the use of algorithmic techniques to *assist* the process of traditional history matching. Assisted history matching is proposed with the intention of alleviating manual work while honouring the data and allow engineers to better quantify the quality of the history match and develop a higher confidence level in parameter estimation and forecasts. The key motivation for AHM is that many geological realizations can be simply screened and history matched to observe if the geological realization fits. The advantages of using AHM with regard to manual history matching are obvious when the number of parameters to be calibrated is large. This is not straightforward in practice, as the choice of the parameters to be adjustd can be very difficult and not unique (Baker, 2001; Cancelliere *et al.*, 2011; Rwechungura *et al.*, 2011).

At Heriot-Watt University, an assisted history matching method has been developed where simulations are quantitatively compared to observed seismic and production data

and then updated in an objective manner as seen in Figure 1.1. We start with models generated in conventional form, conditioned to well and 3D seismic using a suitable geostatistical routine. A set of models are created using a suitable optimization method (e.g GA, NA. etc) and then forward reservoir simulation and Petrol-Elastic Modelling (PEM) are run to calculate the production and seismic responses of the reservoir model. Predicted versus observed data are compared using an appropriate misfit function to measure discrepancies between observed and predicted data. Once we have a misfit, a stochastic algorithm is used to choose new parameter values. The loop is run once per model but many hundred models may be run with 10's of models being run simultaneously on a Linux cluster. Finally, the uncertainty of the parameters and predicted behaviour may be analysed.

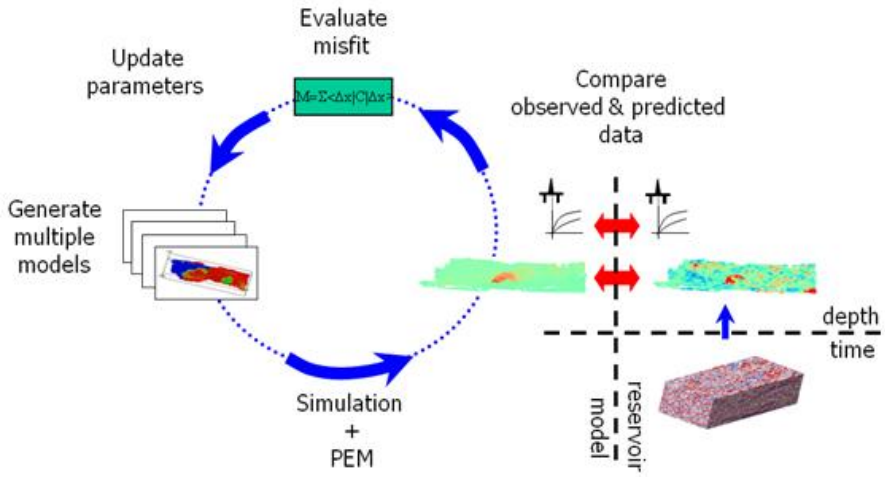

Figure 1.1: Automated seismic history matching workflow (Stephen *et al*., 2006).

A great effort has been made to automate the history matching process. However, limited success was achieved due to the complexity of the problem and also because of the high computational cost required by the practical applications. On the other hand, recent advances in employing permanent sensors for monitoring pressure, temperature, and flow rate has dramatically increased the amount of available conditioning data. This has added an extra level of complexity to the continuous model updating practices.

One of the main concerns for an integrated reservoir simulation study is the computational efficiency (CPU time) in which a large number of modelling scenarios are required to be evaluated. For this reason, clusters of PCs have become standard

tools for applying the parallel platforms for many optimization applications. Those clusters enable one to carry out a large number of simulation runs that before would have been impractical to perform because of excessively long run times. Furthermore, parallel processing using clusters has made it possible to parallelize the flow simulations so as to take the benefit of the possibly huge amount of distributed memory available in such cluster systems and also to decrease the clock time required for such simulations.

1.3 Literature Review

A brief literature review will be given here in this chapter. First, history matching both manual and assisted are reviewed and then a review about seismic history matching is summarized.

1.3.1 History Matching Review

Kruger carried out one of the first studies on history matching in 1961. He computed the areal permeability distribution of a reservoir (Kruger, 1961). Jacquard (1965) was the first to implement a perturbation technique to the problem of history matching. He used a steepest descent based method to calculate permeabilities in a one-dimensional model. Jacquard and Jain (1965) later extended the method to a two dimensional case. They also introduced the idea of zonation (subdividing the reservoir model into a limited number of constant parameter zones) to reduce the number of unknowns. Jahns (1966) used the Gauss-Newton method to solve for the updated parameters at each iteration. Coats (1970) used least squares and linear programming to solve for reservoir parameters using zonation. Wasserman *et al*. (1974) were among the first to use optimal control theory as a mathematical optimization method in history matching multiphase simulator models. An optimal control is a set of differential equations describing the paths of the control variables that minimize the objective functional (Chen *et al.*, 1974). However, instead of using a multi-phase optimal control theory, they used an adjoint equation only for the pressure equation. Chavent *et al*. (1975) studied history matching in single-phase oil reservoirs. They found that the implementation of automatic adjustment for single-phase reservoir models used in common practice was technically feasible for application of at that time. Hirasaki (1975) used sensitivity analysis to graphically display the effects that variations in

certain parameters had on recovery efficiency and cumulative oil production. Dougherty and Khairkhah (1975) used optimal control theory for history matching of a gas reservoir. Gavalas *et al.* (1976) used nonlinear regression and Bayesian estimation theory as a substitute for zonation in calculating porosity and permeability. The technique is only viable when sufficient statistics are available concerning the parameter to be calculated. Watson *et al*. (1979) studied history matching in two-phase petroleum reservoirs. Fasanino *et al.* (1986) investigated single-phase history matching of 2D gas reservoirs by means of the adjoint method in combination with geostatistical information and the pilot point method. Anterion *et al.* (1989) computed the gradients analytically using a commercial simulator and demonstrated how they could be used to aid in history matching. Significant work has been done using nonlinear programming to automate the process of history matching simulators to field data by varying formation properties such as porosity, permeability and relative permeability. Bi *et al*. (2000) studied the conditioning of three-dimensional stochastic channels to pressure data in single-phase reservoirs. Zhang and Reynolds (2002) concluded that the LBFGS method (The Limited-memory Broyden-Fletcher-Goldfarb-Shanno method) is the most efficient minimization method for typical history matching problems. Li *et al*. (2003) studied a three-dimensional history matching case using three-phase flow production data. The aim was to minimize the misfit in flowing wellbore pressure, water oil ratio (WOR) and producing gas oil ratio (GOR).

Nowadays, a number of pioneering global optimisation methods have gained popularity in research amongst oil and gas companies for tackling history-matching problems such as ensemble kalman filter, evolutionary algorithms, neighbourhood algorithm, swarm intelligence techniques and others. Stochastic techniques have been used in the petroleum engineering including Genetic algorithms (Goldberg, 1995; Romero *et al.*, 2000; Carter and Ballester, 2004; Erbas and Christie, 2007; Stephen and Arwini, 2010), Ant Colony Optimisation (Razavi and Jalali–Farahani, 2008a, 2008b; Hajizadeh *et al.*,2009; Hajizadeh, 2010), Particle Swarm Optimization (Kennedy and Eberhart 1995; Eberhart and Shi 2001; Mohamed *et al.* 2010; Rwechungura *et al.* 2011), Ensemble Kalman Filter Methods (EnKF) (Leeuwen, 1999; Corser *et al.*, 2000; Evensen, 2003; Haugen *et al.*, 2006; Aanonsen *et al.*, 2009; Hanea *et al.*, 2010; Szklarz *et al*.,2011) and the Neighbourhood Algorithm (Christie *et al.*, 2002; Subbey *et al.*, 2004; Stephen *et al.*, 2006; Rotondi *et al.*, 2006).

1.3.2 Seismic History Matching (SHM) Review

Seismic history matching (SHM) is an automatic procedure for matching both production and time-lapse (4D) seismic data. By combining the excellent areal resolution of the seismic data with the sparser data from wells, which include production rates and pressure measurements, it is anticipated that the parameters of the reservoir model can be more accurately estimated. In many fields, time-lapse seismic is collected routinely to capture the effect of changes in pressures and saturations spatially (Stephen and MacBeth, 2006b). The main value of time lapse (4D) seismic is the additional information to constrain or update a model of the reservoir. It also reduces the extent of non-uniqueness of traditional history matching. The possibility of incorporating 4D seismic information into history matching as additional dynamic data is an attractive proposal as it provides images of fluid movements between wells (Doyen, 2007). On the other hand, the use of 4D seismic data quantitatively in an assisted history matching procedure is not easy task.

In the literature, a number of publications have discussed the problem of using real time-lapse seismic data in history matching of reservoir simulation models to improve the characterization of permeability and porosity heterogeneity. Landa and Horne (1997) estimated reservoir parameters assuming that water saturation changes could be derived from the time lapse seismic. They included dynamic data observed from wells. Huang *et al.* (1997) utilized 4D seismic amplitude data and finite perturbation method to compute the required derivatives. Gosselin *et al.* (2001) suggested a gradient based optimization method to minimize the mismatch of all types of measured data simultaneously, including 4D seismic data. Waggoner *et al.* (2002) used acoustic impedance differences derived from time-lapse seismic data. Mezghani *et al*. (2004) used time-lapse acoustic impedance derived from pre-stack data to predict petrophysical properties using non-linear optimization based on derivatives with respect to the parameterization. Dong and Oliver (2005) matched both seismic impedance change data and production data in a medium scale problem. Stephen *et al.* (2006) applied a multiple-model history matching workflow based on simultaneous comparison of spatial data offered by seismic and production data for the UKCS Schiehallion reservoir and they used the Neighbourhood Algorithm in the context of 4D seismic history matching. Dong *et al*. (2006) used the ensemble Kalman filter (EnKF) to match production and time-lapse seismic impedance data and to improve estimation of the

porosity field. Andersen *et al.* (2006) have used 4D inverted elastic data to condition geological models in order to reduce the uncertainty in the facies distribution for the fluvial Ness formation in the Oseberg field. Roggero *et al.* (2007) studied the advanced parameterization methods to constrain fine scale geo-statistical models using gradual deformation method in the framework of time lapse seismic history matching of the Girassol field. Dong and Oliver (2008) applied an adjoint method to calculate the gradient of the data mismatch and a quasi-Newton method to estimate the search direction in the context of automatic history with the aim of incorporating 4D seismic data to a reservoir in the Gulf of Mexico. Dadashpour *et al*. (2008) calibrated porosity and permeability properties to estimate pressure and saturation changes from time-lapse seismic data by formulation of a nonlinear Gauss–Newton inversion scheme. Leeuwenburgh *et al*. (2010) showed the distribution of reservoir fluids and rock properties (porosity and permeability) can be better extracted from seismic amplitude data by combination of two inversion steps of both 3D and 4D data using two ensemble-based methods of the Kalman Filter and the randomized maximum. Trani *et al*. (2011) found the importance of the porosity in inversion of the changes in saturation and pressure from 4D seismic AVO (Amplitude Versus Offset) and time-shift of compressional and shear waves. There is a growing interest and necessity to incorporate 4D seismic data quantitatively in the workflow for reservoir management.

1.4 Improving the Convergence Rate of SHM

Alvarenga and Mateus define the optimization convergence as: "*An optimization algorithm has converged if it cannot reach new solution candidates anymore or if it keeps on producing solution candidates from a "small" subset of the problem space*" (Alvarenga and Mateus, 2004). In numerical analysis, the rate of convergence can be defined as the speed at which a convergent sequence approaches its limit. All local and global optimization methods have different rates of convergence. Figure 1.2 shows a characteristic curve for optimization showing a rapid progress at the beginning and flattening out at the end. Unluckily, global convergence usually requires a large number of iterations to approximate the solution. In fact, this cost is often too high for the reservoir history-matching problem, where the computation of the misfit is usually expensive. In seismic history matching, the convergence rate of SHM depends on the following factors:

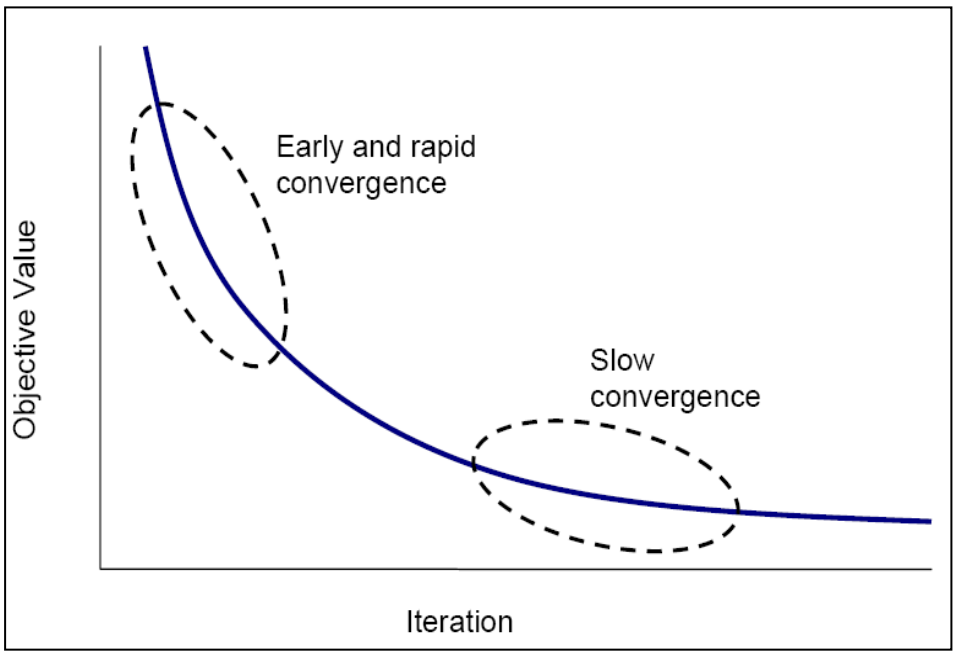

Figure 1.2: Typical convergence behaviour of optimization algorithms.

1. Exploitation: operations that generate new solutions from existing ones have a very big impact on the speed of convergence and populations diversity. This means that the information about the misfit surface may be used to improve parameter choices. The inversion method (e.g. NA) is used to generate an ensemble of reservoir models for which the forward problem is solved by means of a reservoir simulator. As a result, the information about the misfit surface may be exploited to get better parameter choices. Exploitative methods require more elaborate estimates of sensitivities but are susceptible to being trapped in local minima.

2. Exploration: in the context of optimization, exploration means finding new points in regions of the search space that have not been explored before. In other words, it refers to the width of a search of a parameter space. Exploration is a search the parameter space without considering what it has 'learned' from previous sampling. Figure 1.3 shows the balance between exploration (how wide we explore in the parameter space) and exploitation (how much we use the information from previous models) strength of various optimization algorithms (Sambridge and Mosegaard, 2002). Local methods are very strong in exploitation and they try to converge to the minimum of the misfit very fast. On the other hand, Global methods are less exploitative but they are stronger at

exploring the parameter space. Exploration is usually a very important issue for history matching of the reservoir because multiple various models get similar results, which ultimately defines various production scenarios in the reservoir. There should be a broad search over a reasonable range of various parameters in order to choose the most optimum combination of parameters that gives us a reliable reservoir model. In global optimization algorithms, preserving a set of diverse solution candidates is very significant as well. Losing diversity means approaching a situation where all the solution candidates under investigation are similar. Therefore, preserving diversity is directly related with maintaining a good balance between exploitation and exploration (Burke *et al.*, 2004).

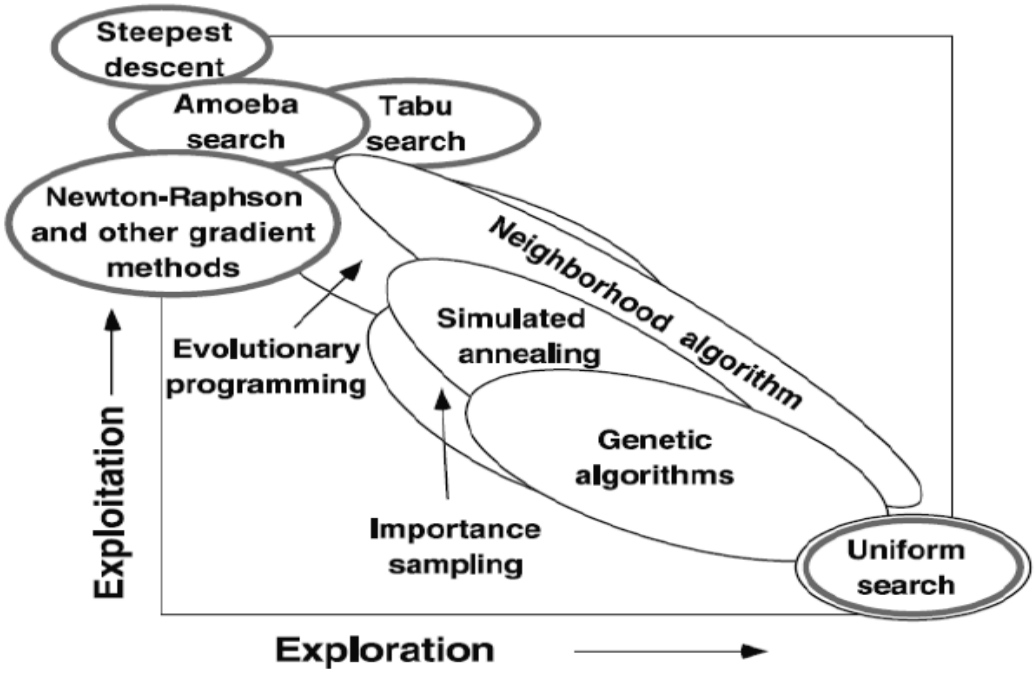

Figure 1.3: Exploration versus exploitation strength of optimization algorithms (Sambridge and Mosegaard, 2002).

3. Stopping criteria: a suitable stopping point is required in the iterative process during history matching. The stopping criteria could be, for example, a maximum number of simulations, a value of the objective-function below an estimated tolerance. We ask this question "*when is it possible to stop the assisted history matching process*?" The definition of an appropriate stopping criterion is complex and problem specific. The objective of stopping criteria is to ensure that the proper model(s) is (are) found given the data available. Therefore, the parameter space has to be sampled sufficiently to ensure the proper model is found. In addition, the definition of the stopping criteria is

related to the amount, quality, and type of constraining data available, and type of optimiser used. Especially for global optimisers it is important that the parameter space is properly sampled and the number of iterations is not too limited.

1.5 Research Objectives

The main objective of this research is to improve the convergence rate of SHM to create a user-friendly SHM framework. This research aims at the following objectives:

1. To develop a new approach named NAPG (NA with Proxy Derived Gradient) to improve the convergence rate with NA that directs the search in forwards greater probability of solution and then to steer the search towards better models.

2. To carry out a validation test to NAPG. Therefore, it is applied to analytical tests using a quadratic function with two minima and synthetic cases where we know the solution. In addition to assess the method by applying it to the Schiehallion field.

3. To develop approaches to update the regression equation sensitivities that are required for NAPG while we are progressing towards the minima. This will lead to improved accuracy of the regression equation sensitivities and to find models that are more accurate.

4. To combine experimental designs with the NAPG to explore the parameter space in an efficient way. This issue becomes critical when we have a high dimensional problem because of the requirement to use a large number of initial models to start NA or NAPG, which is extremely costly.

5. To investigate different approaches to define a criterion as a suitable point to stop the iterative loop of SHM.

6. To analyse the effect of using NA and NAPG on uncertainty and to use NA-Bayes approach to approximate the posterior probability and use it to estimate parameter uncertainty. This leads to finding more models that are reliable for prediction stage.

In conclusion, it can be said that the main theme of this research is to investigate different ways to improve the convergence rate of the SHM, which is needed in order to save CPU time where the computational cost is often too high for the reservoir history-matching problem.

1.6 Review of Chapters

A comprehensive reference list is attached at the end of the thesis. Most of the work has been published at conferences listed at the beginning of the thesis and later will be submitted to scientific journals. This thesis is divided into nine chapters.

Chapter 2 provides the basic building blocks of an inverse theory, optimization algorithms, 4D seismic and other relevant material to reservoir modelling such Petro-Elastic Model, pilot points and Kriging and barrier multipliers. The definitions of the systemic and random errors including data and model errors are discussed.

Chapter 3 explains the workflow that we used in this study in order to automatically update reservoir parameters during history matching. In addition, we present the neighbourhood algorithm (NA) as a stochastic optimization method that is used in this work to choose new parameter values. In this chapter, a new approach named NA with Proxy derived Gradients NAPG is presented and aims to speed up the convergence rate with original NA.

Chapter 4 describes the Schiehallion field, which is used for applications of the SHM approach, including geological settings, reservoir and management characterisation, time-lapse seismic data acquisition and model construction. It provides an overview of the selected area from the Schiehallion field (Segment 4) for seismic history matching applications.

Chapter 5 presents the verification tests that we carried out on the new approach (NAPG) to demonstrate that it is speeding the convergence rate of SHM. A number of synthetic cases where we know the true answer were applied to NA and NAPG such as analytical functions, synthetic models from Schiehallion field. In this chapter, different approaches to update sensitivities of regression equation were developed to improve performance of NAPG near minima.

Chapter 6 aims to combine the experimental designs with NAPG to reduce the number of initial models that we need to start NA and NAPG. In this work, Experimental Design (ED) is used to train the proxy model instead of the random selection used originally for the NA and NAPG. In this study, Central Composite Design (CCD) is used to sample the response surface because it is very useful for building a second order

(quadratic) model of the response variable. This approach is applied to a 10D real case from the Schiehallion field.

Chapter 7 investigates stopping criteria as it is one important factor that affects the convergence rate of the Seismic history matching. It presents different approaches to define the suitable point to stop the iterative loop of SHM or when we should search elsewhere to ensure that the proper parameter combination(s) is (are) found given the data available. In addition, the use of proxy models to calculate the misfit instead of the full misfit calculation is studied and is discussed the possibility of using proxy coefficients converge as stopping criterion.

Chapter 8 presents the uncertainty analysis of using NA and NAPG methods. NA-Bayes (NAB) which uses Markov chain Monte Carlo (MCMC) method is applied to approximate the posterior probability and is used to estimate parameter uncertainty. NAB uses the spatial properties of Voronoi cells to directly guide the sampling of parameter space.

Chapter 9 provides a summary, conclusion and recommendations for further work for the thesis.

CHAPTER 2

Inverse theory: Basic Concepts

Overview:

In this chapter, we will provide the basic building blocks of inverse theory, optimization and other relevant material to reservoir modelling. Most petroleum engineering applications deal with a subsurface that is not easily accessible and the properties controlling theses physical behaviours are numerous. For instance, some properties such as permeability and porosity require fine resolution in space, and others such as fluid saturation and pressure change in time. In such conditions, inversion is the only practical approach to integrate all available information.

2.1 Inverse theory

Inverse theory was introduced by Laplace and popularized for the first time by Gauss (1809). Inverse theory is the science of estimating model parameters from data. In other words, an inverse problem could be described as a problem in which the answer is known but the question is not. The problem of generating theoretical data for a given model is termed a forward problem since we choose a set of model parameter and calculate the predicted value and compares observations, while an inverse problem relates the data to the assumed model and uses mathematical "mapping" to estimate the model parameters. Figure 2.1 illustrates in a simple diagram the forward and inverse problem. Although the main purpose of inverse problem is to construct the model from a set of measurements, the theory has a considerably larger scope.

Applications of inverse theory in the petroleum industry are in two major areas. In geophysics, 'inversion of seismic data in oil and gas fields' is carried out, while in reservoir engineering 'inversion of reservoir history data' is performed. The purpose of inversion of seismic data is to recover the subsurface elastic properties (e.g. velocity and acoustic impedance). Many algorithms for this purpose have been developed (Tarantola 1984, Russell 1988). For example, Oldenburg *et al*. (1983) discussed the deterministic inversion for impedance, while Cao *et al*. (1989) illustrated an inversion method to

estimate velocity and impedance simultaneously. Landrø (2001) proposed a method to express the changes in amplitude as a function of variation of reservoir pressure and saturation. Ouair and Strønen (2006) proposed a global inversion method where all 4D vintages are inverted simultaneously.

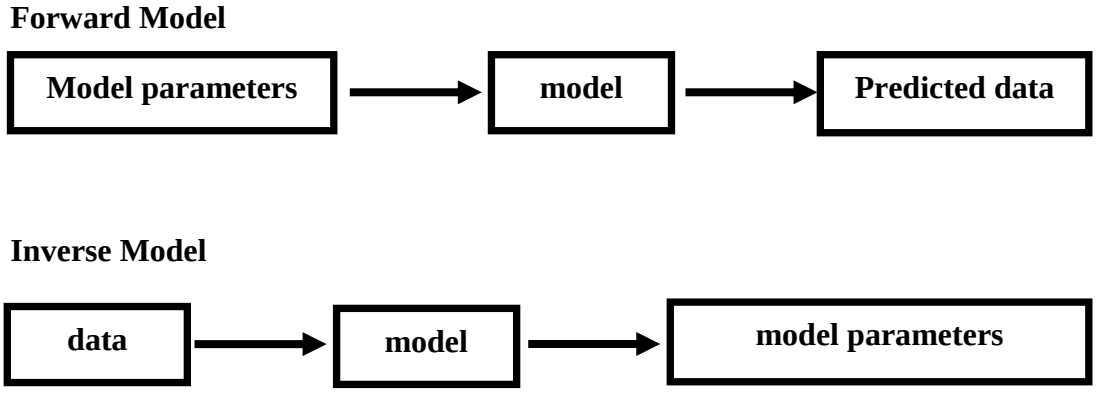

Figure 2.1: A simple diagram of Forward and Inverse problem.

2.1.1 Optimisation Algorithms

Optimization is one of the main approaches that every one in every area can encounter (Gill *et al.*, 1981), such as mathematics, applied science, engineering, economics, medicine and statistics. In the automated history matching procedure, an optimisation algorithm is employed to find the optimal solution by minimizing the objective function. The optimal solution is a combination of parameters that provides the best fit of the observed dynamic data, i.e. exhibits the smallest misfit. The type of optimiser to be chosen is problem-specific where type of objective function, amount of parameters and runtime of the simulation model affect the choice. From the reservoir engineering point of view any optimisation method must be simple, transparent, robust and results must directly relate to verifiable workflows, in order to establish trust and confidence. Assisted history matching has been investigated for at least a few decades, and there are abundant methods published in the petroleum literature (Schulze-Riegert, 2007). Generally, they can be classified into local and global algorithms based on the type of minima captured.

Local Algorithms

Gradient-based algorithms or deterministic algorithms are other synonyms of Local algorithms. The main advantage that they converge faster to a minimum than global algorithms but they provide only a single solution that is the nearest local optimum to the initial guess (Landa, 2005). Most local methods require the computation of sensitivity coefficients. Sensitivity coefficients are defined as the partial derivatives of the simulator output with respect to the parameters being adjusted. In implementation, the gradient of the objective function is calculated and the direction of the optimization search is then determined. Several algorithms have been discussed widely and even commercialized and they have been successfully applied to history matching problems such as Steepest Descent method, Gauss-Newton method, Levenberg-Marquardt method, Conjugate Gradient method and others.

Global Algorithms

Global optimization is about finding the best possible solutions for given problems. One of the most fundamental principles in our world is the search for an optimal state. The advantages of global algorithms can be summarized in the following:

1. They may generate a number of reservoir models and are more suitable to non-unique history matching problems, therefore.
2. They can be used to quantify the uncertainty of performance forecasting by using these models. Uncertainty quantification through stochastic history matching has become a hot topic.

On the other hand, the main disadvantage of applying global algorithms is the computational time to reach the global minimum. Because of the rapid development of computer memory and computing speed, global algorithms are receiving more and more attention. Several algorithms have been discussed widely and even commercialized such as Evolutionary Algorithm like Genetic Algorithms and Evolution Strategy, Simulated Annealing, Particle Swarm Optimization, Ensemble Kalman filter and Neighbourhood Algorithm. In this research, Neighbourhood Algorithm (NA) will be used as an optimization method to carry out Seismic History Matching.

Neighbourhood Algorithm (NA)

The Neighbourhood Algorithm (NA) was developed originally by Malcolm Sambridge to solve a seismic waveform inversion problem (Sambridge, 1999a). NA is categorized as a stochastic method searching for models with good match to the data. The neighbourhood algorithm uses simple geometrical constructs known as Voronoi cells (Voronoi, 1908) which are used to decompose the search space into *n* cells around *n* points by centring around the generated points. Each of these cells is the nearest neighbourhood region of the points, usually calculated by *Euclidean norm*. The neighbourhood algorithm begins the optimization with an initial random generation and after estimating the fitness of those models by using the objective function, NA finds out the nearest neighbour region of each model in the parameters space by constructing the Voronoi diagram. Then it chooses n_r best models according to their objective function value and creates n_s new models by a uniform random walk in the Voronoi cells of the models. The main advantages of the Neighbourhood Algorithm are:

1. the simplicity of its two-parameter tuning scheme in contrast to the more complicated tuning mechanisms of other methods, such as Simulated Annealing and Genetic Algorithms
2. similar to evolutionary algorithms, the selective sampling of good data-fit regions is achieved by exploiting information about all previously generated models thus enabling convergence to solution (Sambridge, 1999a)

NA has been applied to different ranges of problems, particularly to the problems in the field of seismology. A number of researchers have employed NA for different inversion problems in seismic (Sambridge and Kennet, 2001; Jansky *et al.*, 2006 and Yao *et al.*, 2008). In the oil industry, the neighbourhood algorithm is now applied for history matching problems. As a pioneering work, Christe *et al.* (2002) used NA to obtain multiple history matched models in the Teal South reservoir. In addition, history matching for both real reservoirs cases (Nicotra *et al.*, 2005; Valjak, 2008) and synthetic reservoir cases (Subbey *et al.*, 2003) has been performed using the neighbourhood algorithm. Stephen and MacBeth (2006a) and Stephen *et al.*, (2006) have applied NA for simultaneous history matching of production and 4D seismic data. Arnold (2009) has used the NA as the choice of sampling algorithm in a geologically parameterised

history matching framework, where the fault parameters or channel parameters are history matched. The Neighbourhood algorithm (NA) will be used in this work. It makes judicious use of all information obtained in every iterative stage, in sampling the parameter space and it will be discussed in details in Chapter 3.

2.1.2 Objective function

The misfit or objective function allows the ranking of different model realizations. It can give us the accuracy of each model by comparing the predicted data with the observed data. During reservoir history matching the reservoir model is conditioned to the observed history data such as seismic surveys, production data, field pressure etc. With the aim of measuring the extent of the conditioning, a mismatch between the simulation model output and the observed data is quantified. The mismatch quantification is referred to as the objective function. Moreover, in automated history matching the misfit function is used by the optimisation algorithm to determine how to perturb the inversion parameters. During subsequent iterations, the objective is to minimise the misfit function. The objective function can also be used in stopping criterion. When its value becomes less than a predefined (small) number, the reservoir model is considered to be history matched.

In the literature, there are several types of objective functions exist such as sum-of-squares, least-square and weighted least-square. However, the typical measure of the objective function is the square of the difference between simulated and observed historical data as defined in Equation 2.1. The general form of L2 norm or covariance-related norm of the objective function (Tarantola, 1987) may be expressed as:

$$J(\underline{\theta}) = \left[\underline{d}^{sim}(\underline{\theta}) - \underline{d}^{obs}\right]^T \underline{C}^{-1}\left[\underline{d}^{sim}(\underline{\theta}) - \underline{d}^{obs}\right] + \left[(\underline{\theta} - \underline{\theta}^p)\underline{C}_{prior}^{-1}(\underline{\theta} - \underline{\theta}^p)\right] \quad (2.1)$$

where: $\boldsymbol{d}^{obs}$ is the observed data of 4D seismic and production/injection (i.e. oil and water rate, and pressure), $\boldsymbol{d}^{sim}$ is their corresponding simulated response, and $\boldsymbol{\theta}$ is the vector of uncertain model parameters to be updated. $\underline{\boldsymbol{C}}$ is the covariance matrix and contains the correlated random error, which is calculated for the model and observed data. The prior term includes additional information on the expected average value $\underline{\theta}^p$ and the correlation matrix $\underline{C}_{prior}$. Both types of information are derived from geostatistics. This data can be added to the objective function, which is independent of the observed and simulated data. It is highly recommended to add prior information

term in the objective function to preserve features incorporated into a prior geological model. However, sometimes it cannot be determined and is left out as is the case in this work.

The objective function also provides weighting factors to scale the data of different type, magnitude and accuracy. In the case of integrating both production and seismic data in the objective function, there is another term for seismic. A weighting factor is considered as indicated in Equation 2.2 to bias towards data with higher accuracy.

$$J(\underline{\theta}) = \beta * M_p(\underline{\theta}) + (1-\beta) * M_s(\underline{\theta}) \tag{2.2}$$

M_p and M_s are production and seismic objective function respectively, β is the weighting factor between production and seismic objective functions. Choosing the appropriate value for the weighting factor could be a challenging decision in any history matching study. This factor should be a function of accuracy for production and seismic data. In this research, we use a sum of squares misfit and Stephen *et al*. 2006 found that errors are Gaussian and uncorrelated.

$$J(\underline{\theta}) = \sum_{all\ data} \frac{(d_i^{obs} - d_i^{sim})^2}{\sigma_{d_i}^2} \tag{2.3}$$

Where: d_i^{obs} is the observed data and d_i^{sim} is the simulated one and σ_d is the standard deviation of the errors in the observed data (normalization factor).

2.1.3 Parameterization

Parameterization is a critical step in the history matching procedure. The number of parameters that can be estimated or inverted using history matching is limited. The success in history matching depends on suitable choice of parameterization and the range of parameter values. An inadequate set of parameters would result in inaccurate uncertainty estimations, and introduce bias errors. A large number of parameters with a wide range requires a large computational time, increases the variance errors and decrease the stability of the solution. The type, number, and range of parameters are determined based on petro-physics, well test, and seismic and geological interpretations and experiences. Therefore, parameter selection must be done in close co-operation between geologists and reservoir engineers with the objective to provide reliable production forecasts.

Parameters that are optimised in most history matching techniques are primarily reservoir properties such as permeability, porosity, barrier/fault transmissibility, aquifer strength, and other flow-related properties. These properties do not directly represent the geometry of the reservoir. The geological structure of the reservoir model is determined early in the life of an oil field and sometimes it is adjusted, but more often kept fixed. However, in structurally complex fields, the reservoir geometry is one of the largest uncertainties and incorrectly identifying structural features like fault planes, badly placed wells, poor estimates of oil-in-place, by-passed hydrocarbon, and failure to find hydrocarbons trapped in compartments surrounded by no-flow boundaries or with anomalous flow paths because of the presence of faults. Geological parameterisation allows perturbation of these geological characteristics and objects as more relevant information becomes available during the life of a field. Common parameterization approaches are demonstrated in the following paragraphs (van Ditzhuijzen *et al.*, 2001; Oldenziel, 2002).

1. Grid Blocks

Grid blocks are the building units of a reservoir model. They can be in radial, rectangular, and unstructured shapes in one, two and three dimensions. In this method, all grid block values have been considered as independent parameters. Also, no preconceived idea about the geology of the reservoir is considered during history matching. Usually, porosity and directional permeability, NTG, relative permeabilities etc are assigned to each active grid block of a reservoir model. Since these parameters are estimated for single grid cells in the reservoir model, the number of model parameters is high, and therefore the problem will be undetermined. Thus, this method is not suitable for real reservoir cases (Smith *et al.*, 1992; Floris *et al.*., 2001; Dadashpour *et al*., 2007).

2. Zonation or Regions

Zonation is a method for reducing the number of parameters is by using homogeneous regions (Reynolds *et al.*, 1996). The goal of the zonation technique is to subdivide a formation unit into several different zones with different flow properties. Therefore, zoning assumes that a given zone of the reservoir has uniform parameter that is different to the other zone (Chung and Costas, 1990). The primary benefit of the regions approach is the use of less parameters to model the reservoir. On the other hand, the

drawback of the method is that it may not be sufficient for describing the actual heterogeneities of the reservoir properties, and may generate abrupt changes at the borders of regions, also some preconceived idea about the regions are not exact.

3. Pilot Points with Kriging

De Marsily *et al.* (1984) introduced one of the first geostatistical parameterisation techniques as a parameterization tool. The Pilot Point method with kriging involves the use of prefixed points to construct smooth variations in unknown reservoir parameters such as porosity and permeability fields throughout the reservoir. The method consists of three stages. First, the initial value for the property at pilot points is obtained by prior geo-statistical realizations conditioned to a variogram and the observed fix point values. Then, the property at pilot points is perturbed by the inversion routine. The third stage is to propagate the perturbation induced by pilot points to the nearby grid cells in the reservoir model using a spatial interpolation scheme such as Kriging. The Kriging–based techniques are well known for interpolating reservoir properties within the reservoir and were first developed by Matheron in 1971. There are different kinds of Kriging such as simple, universal, co-Kriging and factorial Kriging. In this work, we use the simple Kriging for interpolating property multipliers between the pilot points.

A particular benefit of the pilot point method is that we can change the reservoir smoothly while honouring the geostatistical prior information. On the other hand, a few weaknesses have been reported for the original pilot point method: the pilot points can be attributed unreasonable values and it disregards the possible correlations among the pilot point values. RamaRao *et al*. (1995) noticed that pilot points may be attributed unreasonably extreme values to force the fluid flow simulation to reproduce the measured dynamic data. In general, this method solves most of the troubles encountered by the zonation approach and provides a practical tool to be incorporated in history matching (Bissell *et al.* 1996; Gómez-Hernánez *et al.*,1997; Arenas *et al.* 2001; Backer *et al.*,2001; Floris *et al.*,2001; Stephen *et al.*, 2004; Le Ravalec-Dupin and Hu, 2007).

In this research, the pilot point method and Kriging are used for updating the reservoir parameters. Pilot points are used to directly control where changes are made to properties such as permeability and net:gross ratio (NTG). The change at the pilot point becomes the parameter of the inversion scheme where a multiplier vector is used for

each variable with specific limits and one specific value is chosen in this range. In order to further reduce the number of unknowns and to spread changes more smoothly, a set of pilot points may be grouped so that changes are applied all in the same way (Roggero, 1997). Figure 2.2 shows the location of pilot points (in a simple synthetic model) where the parameters will be changed (pink dots) compared to the rest of the reservoir where the reservoir kept unchanged as the base model that we start with (black dots). The decision about the location of pink or black dotes is a challenge because practically the whole reservoir is uncertain.

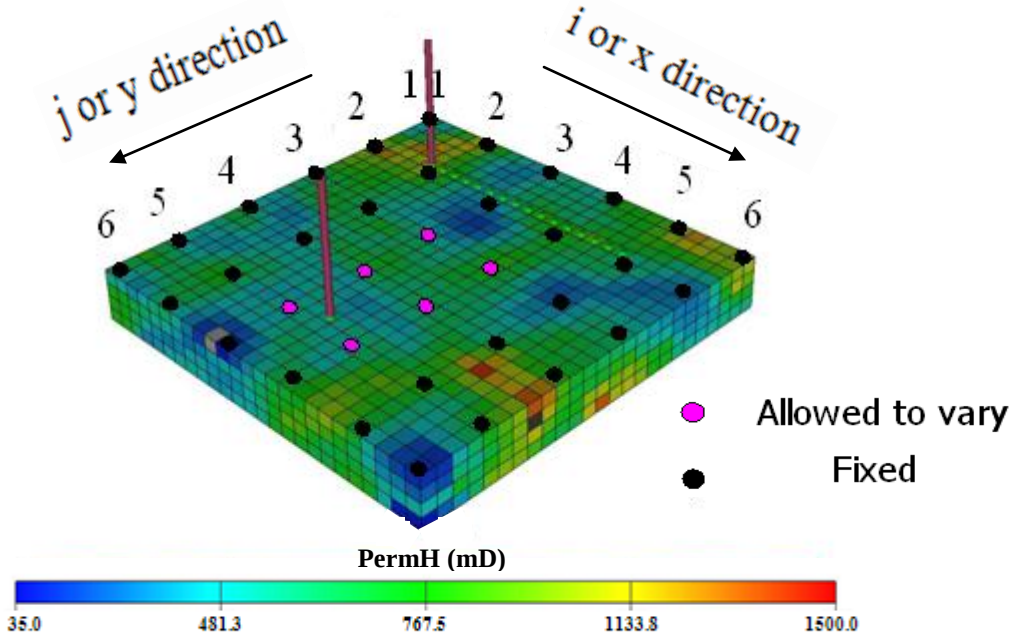

Figure 2.2: A synthetic models as an example of the location of pilot points where we make change (pink dots) versus black dots where no change is enforced (Stephen, 2007).

4. Gradual Deformation Method (GDM)

Hu *et al.* 2000 introduced Gradual Deformation Method (GDM) that is a geostatistical based inverse method, which reduces the unknown parameter space of the reservoir model to a few combination coefficients. Calibrating the reservoir model by fitting these combination coefficients preserves reservoir model structure. This method can be applied to modify the whole reservoir model or only certain sub-domains. The basic procedure starts with generation and combination of two geostatistical realizations in Gaussian space. The combined realization is then transformed into real space for

reservoir model input. The essential operation in gradual deformation is to form a new realization (Z_{new}) from a set of old ones as a simple linear combination:

$$Z_{new} = \sum_{i=1}^{n} \alpha_i Z_i \tag{2.4}$$

α_i is the weighting factor of i^{th} realization in gradual deformation. The coefficients α_i are required to satisfy

$$\sum_{i=i}^{n} \alpha_i^2 = 1 \tag{2.5}$$

The algorithm searches the optimum combination of different realizations to generate the reservoir model parameters in Gaussian space. There are many different variations of gradual deformation algorithm. The most basic form uses two realizations Z_1 and Z_2 with mean z_o and identical covariance: to form a new realization $Z(t)$:

$$[Z(t) - z_0] = [Z_1 - z_0]\cos(t) + [Z_2 - z_0]\sin(t) \tag{2.6}$$

where $\boldsymbol{t}$ is a deformation parameter between $[0,\pi/2]$, $\cos(t)$ and $\sin(t)$ are the combination coefficients making the method depend on only one parameter, $\boldsymbol{t}$. In this method, it is possible combining several independent realizations, which provides more flexibility for deforming realizations in history matching (Roggero and Hu, 1998). Then the number of deformation parameters equals the number of complementary realizations added to the starting one.

The advantage of this algorithm is the transformation of the history-matching problem into a one-dimensional optimization problem. On the other hand, the limitation of the gradual deformation method is that each new model is controlled by a set of deterministic parameters such as oil-water contact, fault transmissibilities, and bubble point pressure etc, which limits the accuracy of the gradual deformation technique. Also, Ravalec, Hu, and Noetinger (2000) revealed that the distribution of samples from the Gradual Deformation Method do not reflect the correct conditional distribution even for linear problems.

5. Faults and Barrier Transmissibility

The reservoir model can be parameterised by controlling fault transmissibility (Stephen *et al.*, 2006). The barriers significantly influence the depletion performance of reservoirs by inducing flow and pressure discontinuities, particularly in compartmentalized and channelized reservoirs (Yielding *et al*. 1999a). The flow barriers can be horizontal, such as shales, impermeable streaks, and vertical, such as faults or sub-vertical such as shale drapes. The barrier's distribution, location, thickness and transmissibility are hard to identify correctly from well test and log data. Although, barriers represent the borders of channels or faults may be identified in 3D/4D seismic maps. Properties of barriers are a source of uncertainty for reserve estimation (Lia *et al*., 1997) and are often picked as the parameters for calibrating reservoir models in history matching (Kruijsdijk, 2001, Stephen, 2006, and Edris, 2009).

During history matching, the structural and geological input to the reservoir model remains fixed. Given time-lapse seismic data, however, this procedure may differ. The dynamic content of time-lapse seismic data provides additional information on structural, geological and sedimentological characteristics. Barriers vary the efficiency of fluid communication from one part of the reservoir to the next (e.g. Yielding *et al.*, 1999a). In reservoir simulations, the effect of barriers on fluid flow is modelled using quantity called a 'transmissibility multiplier' (see Knai and Knipe 1998; Manzocchi *et al.*, 1999; Yielding *et al.*, 1999b). The properties needed to determine transmissibility multipliers, especially barrier zone thickness and barrier zone permeability, are usually not well understood or defined. Therefore, barrier transmissibility multipliers are usually considered a large source of uncertainty for reserve estimation (Lia *et al.*, 1997) and for reservoir management. Most flow barriers compare quite well with the borders of channels or faults observed in 3D seismic analysis. However, there seem to be some additional barriers, probably related to local channel boundaries, that are not identifiable using only 3D seismic data (Kruijsdijk, 2001; Stephen, 2006; Edris, 2009).

2.1.4 Response Surface Modelling (RSM)

The term of Response Surface Modelling is also referred to as approximation, surrogate, proxy, and metamodel. The basic reason for applying response surface modelling is to construct a simplified approximation of the complex and computationally expensive simulation to facilitate design optimization, design space exploration and reliability analysis (Sacks *et al*., 1989, Kleijnen *et al*., 1995, Anderson and Whitcomb, 2005). Response surface modelling has been used in history matching studies in the past to simplify a problem, mainly: i) through identifying parameters which are not significant and reduce the dimension of problem, ii) by finding interaction between parameters, and ultimately, and iii) when it is used to optimize production and investigation of the p10–p50–p90 uncertainty envelopes in the reservoir performance forecasts.

In the literature various response surface models have been used (e.g. polynomials, kriging, radial basis functions and neural networks). They should be used for different optimization roles. Therefore, criteria must be established for distinguishing goodness or weakness of each according to their applications (Barton and Meckesheimer, 2006). More important criteria to identify performance of response surface models in optimization are: i) approximation fidelity, ii) computational cost, and iii) global applicability. Fundamentally, in order to increase the fidelity of the proxy model, more complicated templates of models must be used. This in turn requires that the number of experimental simulation runs, and therefore computation cost be increased. Global applicability means that there is a wider variable design space with guaranteed fidelity of the proxy model. In order to increase the globality, computational cost increases. When approximation fidelity is taken as a constraint, there is a trade-off relationship between globality and computational cost as shown in Figure 2.3.

In history matching studies, several types of response surface models have been used, for instance Cullick *et al*. (2006) utilized an Artificial Neural Network (ANN) as a proxy. They found the results of history matching with proxy model are acceptable if an initial dataset of sufficient size can be used. Osterloh (2008) used a kriging model. Peng and Gupta (2004) compared kriging and polynomial for predicting uncertainty in Hydrocarbons Initially in Place (HCIP) and found no significant difference between results in each case. Li and Friedmann. (2005) proposed thin plate splines as proxy.

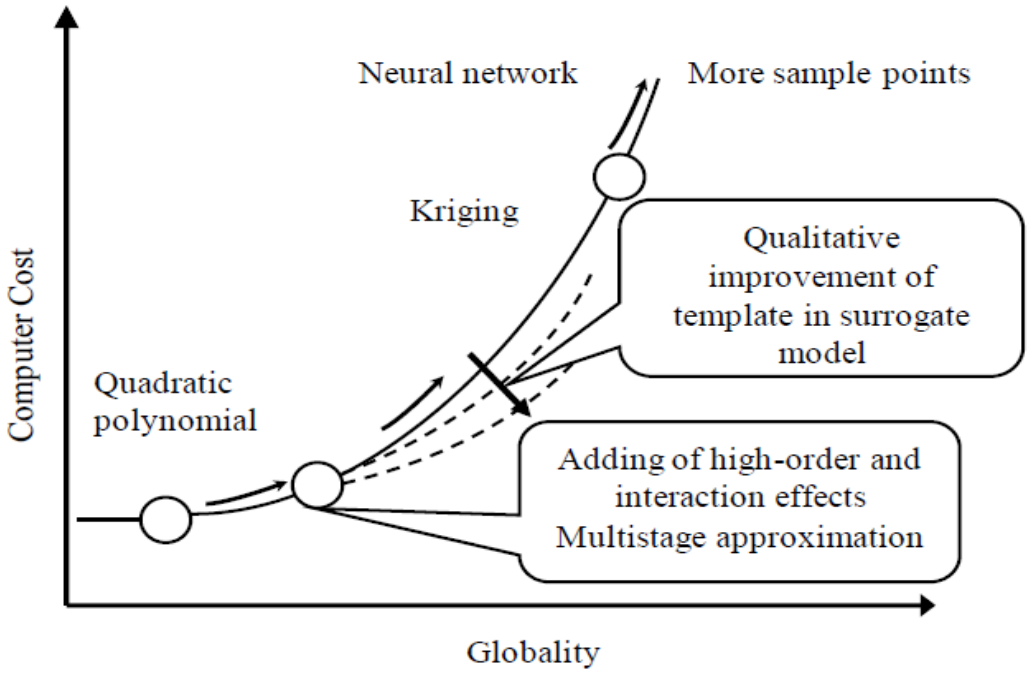

Figure 2.3: Computational cost versus globality in response surface modelling (after Fujita and Kounoe, 2005).

The Polynomial Response Surface is one of the proxy model that is widely used in petroleum science. In this research, we use this type as proxy model of the misfit (objective function). Albeit this kind of model does not precisely approximate the experimental data, polynomial regression models have been broadly adopted in the petroleum industry because of their ease of understanding, flexibility, and computational efficiency. The universal form of 2nd order quadratic polynomial regression model can be written as

$$J(\underline{\theta}) = C_0 + \sum_{i=1}^{nd} C_i\theta_i + \sum_{i=1}^{nd} C_{i+nd}\theta_i^2 + \sum_{i=1}^{nd-1}\sum_{j=i+1}^{nd} C_{ij}\theta_i\theta_j \qquad (2.7)$$

where $\underline{\theta}$ is a vector of input variables of length n_d, θ_i is a linear term, θ_i^2 is a quadratic term, $\theta_i\theta_j$ is a cross term and C_o,C_i ,C_{ii} ,C_{ij} represent unknown regression coefficients for constant, linear, quadratic and cross terms respectively. "*C*" terms may be estimated with a least squares approach or Singular Value Decomposition (SVD). A proxy model becomes very useful especially when the direct evaluation of the system is either impossible or too expensive and time consuming (Zubarev, 2009).

2.2 Observation Data

The type of observation data is usually split into two categories – production data and seismic data. Production data, such as gas-oil ratio, water cut, and bottom hole pressures, are extracted from well measurements. They provide valuable information, but have spatially sparse limitations. Seismic data, on the other hand, are spatially dense. Seismic data can either be 3D or 4D. 4D seismic data, or time lapsed seismic data, is the most used seismic data form used in history matching. The process of reservoir characterization for estimating reservoir properties usually involves the measurements, which are taken from boreholes, e.g. rock cores, rock cuttings, geophysical well logs, and pressure tests. These data are valuable because they represent in situ and direct measurements, but unfortunately, they only sample a very small fraction of the total reservoir volume. Seismic data, on the other hand, give a broader evaluation of the reservoir properties away from the wells, even though the overall resolution of the seismic data is only approximately 25 × 25 × 25 m. Repeatedly acquired seismic data is referred to as time-lapse seismic. It is a relatively new technology, which is believed to allow dynamic characterisation of a reservoir in a volumetric sense. The state of reservoir is characterised by pore (fluid) pressure, temperature, and saturation. Now, the major driver for time-lapse 3D seismic is its potential to indirectly measure the saturation and pressure changes. Knowing the reservoir's saturation distribution and its fluid flow behaviour, adds significant information and decreases risk in reservoir management.

The basic idea is that production and injection induced changes in the reservoir cause some changes in the recorded seismic signal over time due to changes in oil saturation and reservoir pressure. The essence of time-lapse is looking at differences in order to capture the variation of a system over time. The first seismic survey in a time-lapsed seismic project is referred to as a *baseline survey*. Surveys shot after the baseline survey is referred to as *monitor surveys*. By subtracting the base survey from the monitor survey static parameters and noise are cancelled out and dynamic parameters are emphasized. An example of 4D from the North Sea Gullfaks field and differences seen between the surveys results are shown in Figure 2.4. Therefore, time lapse seismic technology can be used to observe variations caused by production and/or the injection of fluids and gas to improve reservoir recovery.

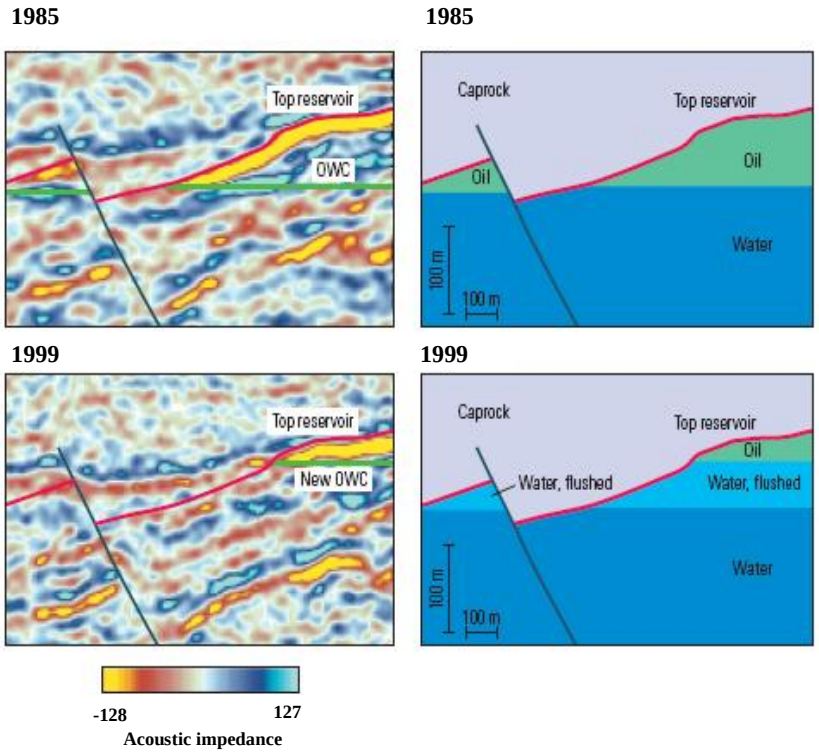

Figure 2.4: The changes in seismic reflection amplitude between the two surveys in 1985 and 1999 due to production. The difference in the signal strength of the top of the reservoir is related to decrease in oil saturation and original oil-column height. Red and yellow represent a reduction in acoustic impedance, while blue colours correspond to an increase (Traine, 2002).

The importance of time-lapse seismic has to be seen in the context of a better understanding of the reservoir properties. It offers the ability to detect the distribution of the inter-well bypassed and untapped oil; to monitor the effect of heterogeneity and to spot the non-uniform pressure variation away from wells. These can help increase the ultimate recovery, reduce production costs, and avoid the unexpected early breakthrough (Waggoner, 2000). Time-lapse (4D) seismic assists also in EOR processes, as it can provide information for creating more accurate reservoir models to support in better performance prediction and ultimate recovery. Time lapse seismic is not just utilized as a tool for understanding regions of bypassed oil that have been left in the reservoir, but also for monitoring the pressure depletion, which reveals vital information about reservoir connectivity and fault transmissibility (Koster *et al.*, 2000). Time-lapse seismic monitoring is a proven technology which has been successfully been applied in a variety of cases by the industry for more than a decade.

2.3 Challenges of 4D Seismic Data Integration

In a broad sense, the main challenge is to link the time-lapse seismic measurements and dynamic reservoir changes, which can alternatively be expressed as "*How can we benefit the most from time-lapse (4D) seismic?*" The answer to this question may result in broadening the adaptation of time-lapse seismic as a standard technique in reservoir engineering practice. However, the challenges on the road to attaining this optimal integration can be classified as follows (Harris and Henry, 1998; Vauthrin *et al.,* 1999; Marsh, 2004):

Acquisition - Processing of 4D seismic data remains a challenge. Even when one utilizes the same techniques for seismic acquisition of the base and the monitor surveys, one needs to decide whether to work with the surveys separately or use the differences. The latter may needed anyway special reprocessing to ensure the surveys can be compared to each other.

Visualisation - To date, much of the interpretation and integration is based on a mere visual comparison of data. Within the 4D data, recognition of patterns which are explainable in the context of expected reservoir changes gives an accessible method which needs limited specialist knowledge to apply, and can gain direct results.

Discipline Integration - Use of multi-source data requires teamwork and mutual technical understanding. The preferred scheme for work would be to have a development team with proper communication skills. Another problem is that the technical languages also differ. Geophysicists, Geologists, Petrophysicist and Reservoir Engineers have their own terminologies and share different views on the static and dynamic reservoir behaviour. Even within these main subject areas there are specialisms. This denotes that successful projects require team members to be able to understand and express the value and uncertainty of their own and others data.

Discrimination and Quantification of Pressure and Fluid Saturation - Changes in both pressure and fluid saturation are expected during the field life. The fluid substitution that occurs during the production of hydrocarbon reservoirs changes the compressibility of the pore fluids and rocks, thus changing the bulk velocity. However, the magnitude of the changes depends on the petrophysical properties of the dry rock frame and the filling pore fluids. These changes could have the opposite effects on the

seismic velocities. Figure 2.5 illustrates the effect of these changes on acoustic impedance (*I*) which has a combined response to pressure and saturation change. The time-lapse seismic response in general is a combination of these two effects (e.g. pressure and fluid saturation changes). Therefore, the polarity of the response depends on the increasing-decreasing trends of pressure change and the difference between the fluid properties at the beginning and the end of the survey.

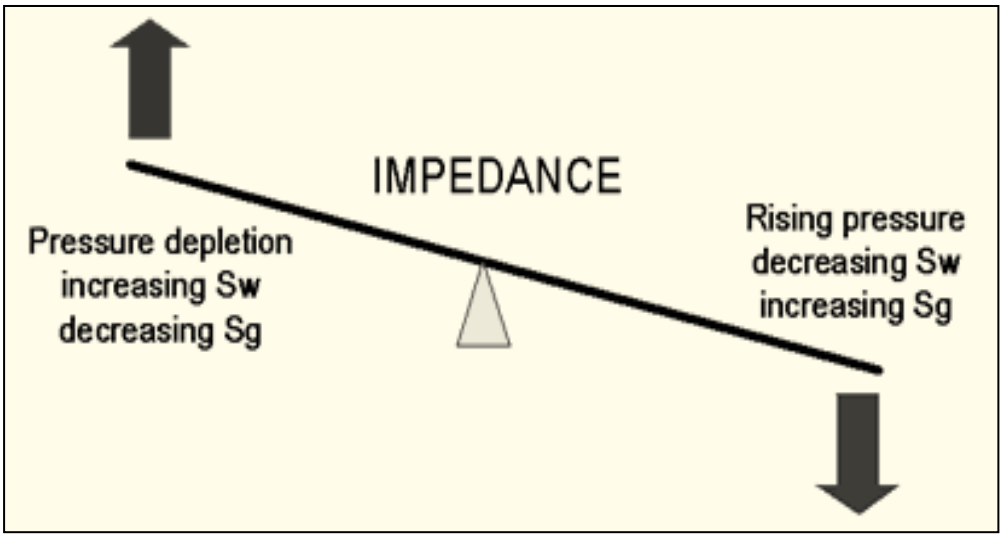

Figure 2.5: Change in acoustic impedance in response to production and injection (after Marsh, 2004).

Which Domain? - In addition to the above challenges, the choice of domain that we can compare real and predicted seismic data is another crucial issue in SHM. The model-based prediction of seismic may be compared to observations by using changes in amplitude, impedance/attribute or pressure and saturation as shown in Figure 2.6. Studies by others have already shown that the shape of the misfit surface, with respect to the model parameters, is different in each domain with unique minima that lead to alternative 'best' models. To date, the cause of the differences is unknown. Geophysicists often have a preference to use amplitude data to integrate the time-lapse seismic data for history matching purposes. This is mainly because it is the amplitude, which is recorded during any seismic survey, and this can be directly used to interpret the reservoir structures. Amplitude, however, depends both on the reflectivity between layers and on the properties of the source signature (i.e. the wavelet type). In SHM, there is no agreement on which domain (reflectivity impedance or saturations/pressures)

is best for seismic comparison (predicted versus observed). Perhaps the best 4D attribute to use is in the impedance domain since the petro elastic modelling (PEM) provides such a property and seismic inversion is a well-developed technique. The PEM will be explained in details later in Section 2.5.

There are various uncertainties and difficulties in each domain. If we start from the simulation model and generate synthetic seismic traces, the main sources of uncertainties come from the petro-elastic model and seismic modelling. The latter is moderately CPU intensive for convolution methods but too time consuming using full wave simulation. On the other hand, starting from measured seismic data to invert for pressure and saturation, the main important uncertainties come from the seismic inversion process used to calculate attributes and either from the petro-elastic model again or else from calibration issues via empirical inversion (Floricich *et al*., 2004; Stephen *et al.*, 2006; MacBeth, 2007). The optimum domain for the seismic comparison is still a topic of research.

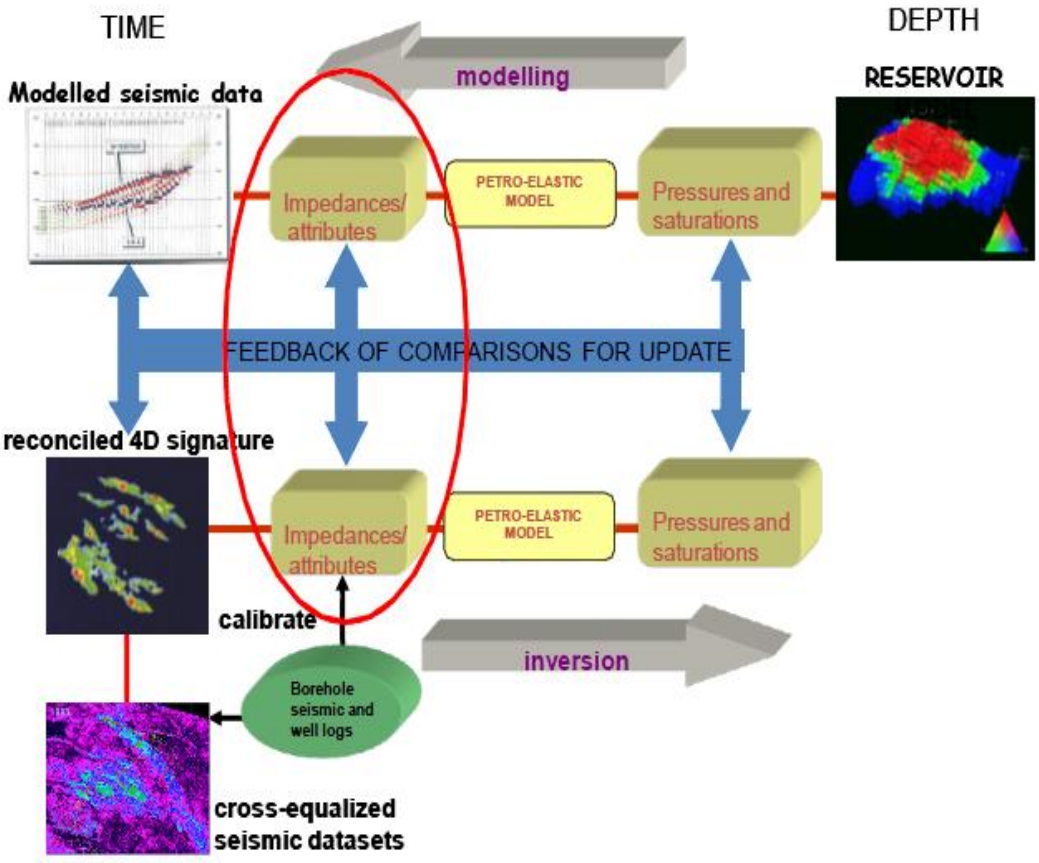

Figure 2.6: The various domains for comparison of measured and predicted seismic data (The red circle identifies the domain that we use in this work) (MacBeth, 2007).

2.4 Time-Lapse Data Normalization

In this study, we consider the impedance domain as the best place for comparing real and synthetic data to reach a balance between time and accuracy (Stephen *et al.*, 2006). In an automated seismic history-matching loop, the mismatch is evaluated between two attributes that are in a different seismic domain: predicted attributes are in the impedance domain while observed attributes are in the reflectivity domain as shown in Figure 2.7. For the observed data we do not actually know the units of real seismic data due to the relative nature of the processing and inversion methods that have been used. The range of values is totally different and therefore, normalization is needed and implemented prior comparison to bring the observed and synthetic data into the same units.

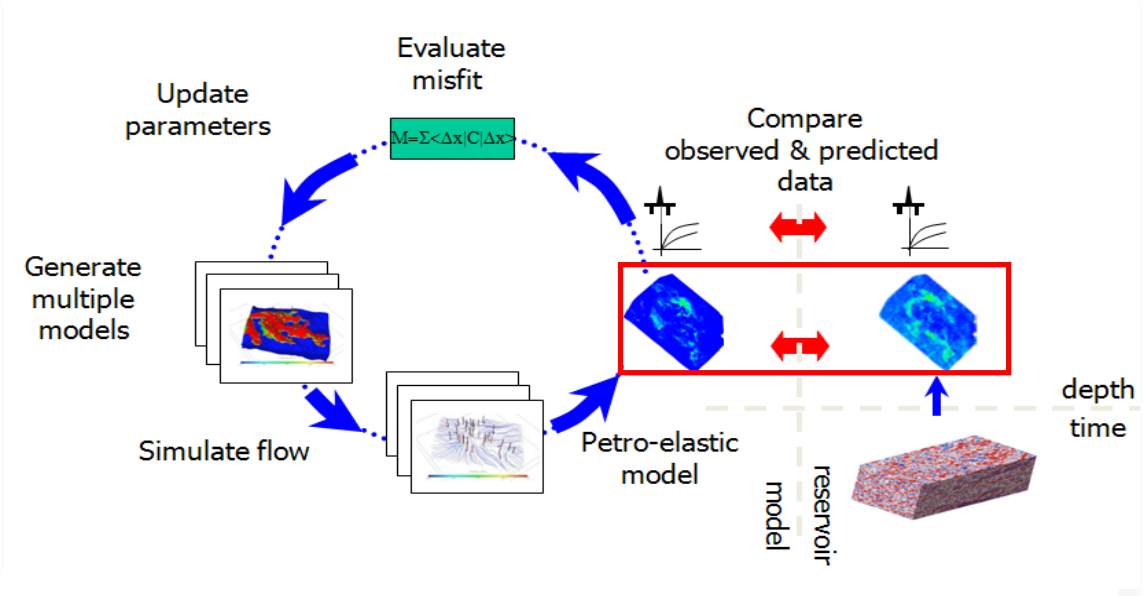

Figure 2.7: Seismic history matching workflow. The red box indicates normalization of time-lapse data as impedance maps takes place (Kazemi *et al.*, 2011).

This normalization step is based on the assumption that the effect of changing pressure and saturation induces an equivalent relative change in the reflectivities and impedance throughout the reservoir. For each domain, the surveys are normalised by subtracting the mean γ_A^0 of the baseline survey and dividing by its standard deviation σ_A^0. 4D attributes are calculated from the observed data by integrating over the reservoir time interval. Observations consist of relative impedance, so both observed and predicted attributes are normalised, scaling by the spread for each to obtain:

$$a(t,x,y,z) = \frac{A(t,x,y,z) - \gamma_A^0}{\sigma_A^0} \tag{2.8}$$

Where ***A*** and ***a*** are the raw and normalized attributes at monitor time ***t***, , γ_A^0 is the areal mean of seismic attribute *A* calculated for the pre-production survey, and σ_A^0 is the areal standard deviation of the attribute *A* calculated for the pre-production survey assuming equivalent pressure and saturation induced changes in both the observed and predicted data. Predicted impedances can now be compared quantitatively against the observed equivalent seismic attribute without the need for a full inversion.

2.5 Petro-Elastic Model (PEM)

A PEM is the abbreviation of Petro Elastic Model and is sometimes called it the rock physics model. The petro-elastic model is often composed of empirical laws calibrated to laboratory measurements and analytical formulas. PEM is used to convert changes in fluid saturations and pressures from the simulation into predicted impedance or other elastic properties for each simulation cell. A PEM is derived based on some laboratory work on core data, and ultimately it may be tested and calibrated by using petrophysical data from the logs. The output of the petro-elastic model will be elastic properties of the reservoir which will be used to generate the seismic data in the impedance domain or in the amplitude domain. For a PEM to be reliable within a 4D workflow it must be able to respond to changes due to the combined effect of pressure and saturation changes in the reservoir. Figure 2.8 shows the Petro-elastic modelling scheme for seismic comparison.

In this research, acoustic impedance is regarded as the preferred seismic inversion parameter for history matching purposes because it directly related to the values of the reservoir elastic parameters that are directly affected by the changes within the reservoir. Usually the PEM represents a combination of equations and different parameters consisting of two parts: one representing the shaly part of the reservoir and the other one representing the sandy part. The P-Impedance (I_p) is defined as follows

$$I_p = \rho V_p, \tag{2.9}$$

where ρ is bulk density, V_p is P-wave velocity. The P- and S-wave velocities (V_P and V_S) for a saturated porous medium are functions of saturated bulk modulus (K_{sat}) and shear modulus (μ_{sat}) and saturated bulk density (ρ_{sat}):

$$V_p = \sqrt{\frac{1}{\rho_{sat}}\left(K_{sat} + \frac{4}{3}\mu_{sat}\right)} \tag{2.10}$$

The velocity of shear wave is

$$V_s = \sqrt{\frac{\mu_{sat}}{\rho_{sat}}} \tag{2.11}$$

Consequently, the saturated moduli and bulk density need to be calculated. It is assumed that fluids do not affect the estimated shear modulus; thus, the shear modulus remains the same regardless of the fluid filling the rock pores:

$\mu_{sat} = \mu_{dry}$

Also, the density of saturated rock ρ_{sat} is given by:

$$\rho_{sat} = \rho_f \emptyset + (1 - \emptyset)\rho_m \tag{2.12}$$

Where $\emptyset$ is the effective porosity of the medium, and ρ_m is the matrix density, and ρ_f is the fluid density, which is a volume average of the individual fluids:

$$\rho_f = \rho_w S_w + \rho_o S_o + \rho_g S_g \tag{2.13}$$

where S_w, S_o and S_g are the water, oil and gas saturations respectively, and ρ_w, ρ_o and ρ_g are the densities of the water, oil- and gas-phases respectively. Gas, oil and water density are estimated using the Batzle and Wang empirical correlations expressed in **Appendix A**. Gassmann (1951) derived an equation to compute bulk modulus of a fluid-saturated porous medium. The Gassmann equations divide the bulk modulus of a fluid saturated rock into three elements:

- bulk modulus of the porous rock frame
- bulk modulus of the pore-filling fluids, and
- bulk modulus of the mineral matrix

The Gassmann formulation is based on several assumptions: i) rocks properties are homogeneous and isotropic, ii) pores in rocks are well connected, iii) wave frequency is low enough to achieve equilibrium, iv) viscosities of the fluids are negligible, and v) no

chemical effects occur between fluids and rock (Smith *et al.*, 2003, Wang, 2001). Gassmann equations can be written as the following formula:

$$k_{sat}^{r} = k_{dry}^{r} + \frac{(1-\propto)^2}{\frac{\emptyset}{k_f} + \frac{\propto - \emptyset}{k_{gr}}} \tag{2.14}$$

Where the superscript *r* indicates rock type (sand/shale), and ∅ is the porosity, k_{gr} is the bulk modulus of the mineral,$\alpha = (1 - \frac{K_{dry}^{r}}{K_{gr}})$. And k_f is the fluid modulus is given by the saturation weighted harmonic average of the individual phase bulk moduli:

$$\frac{1}{k_f} = \frac{S_w}{k_w} + \frac{S_o}{k_o} + \frac{S_g}{k_g} \tag{2.15}$$

where K_w, K_o and K_g are the water, oil and gas moduli respectively and obtained using Batzle and Wang (1992) and lab data for the field (see appendix A). MacBeth and Stephen (2008) investigate the scale dependence of this equation assuming an improved representation in cases where statistics of the fine scale properties of the reservoir are known. However, we assume in this study that Equation 2.15 may be used and inaccuracies may be captured by model error analysis following Stephen (2007). Table 2.1 shows the values of moduli that we used in the study.

Table 2.1: Typical petro-elastic transform parameters for Gassman's Equation, 2.14 and the saturation Equation 2.15 (Stephen et *al.*, 2006).

k_{gr} in GPa	k_w in GPa	k_o in GPa	k_g in GPa
37	2.58	1.18	0.035

Stress-dependency of k_{dry}

Gassmann's formulation requires knowledge of the dry bulk. Typically, dry rock properties are measured in the laboratory from core samples as a function of porosity, pressure and temperature. In this study, the stress dependency of the rock is captured in an empirical relationship (MacBeth, 2004):

$$k_{dry}^{r} = \frac{k_{inf}^{r}}{1 + E_{k}^{r} \exp\left(-\frac{P_{eff}}{P_{k}^{r}}\right)} \tag{2.16}$$

where the superscript *r* identifies rock type (sand or shale), and the parameters K_{inf}, represent the dry bulk modulus at Standard Temperature and Pressure, and E_{κ} is the excess compliance present in the rock as a result of geological or mechanical processes, and P_{κ} is the stress sensitivity respectively. They are determined from lab measurements or by history matching (Stephen *et al.*, 2006) as shown in Table 2.1. P_{eff} *is* the effective pressure, which is the difference between the overburden pressure and the pore pressure. The overburden pressure is calculated at the centre of each grid cell using an average overburden pressure gradient of 1 psi/ft.

Table 2.1: Default stress-sensitivity parameters for the dry bulk modulus in Equation 2.16. Sand and shale have the same parameter values unless otherwise stated (Stephen *et al.*, 2006).

k_{inf} in GPa	P_k in MPa	E_k	μ_{inf} in GPa	P_μ in MPa	E_μ
9.78	6.71	1.00	6.28	6.84	1.00

Effective p-Impedance for the interval

The P-wave modulus for sand and shale are calculated from $M^r = k_{sat}^r + 4\mu^r/3$ (shale is assumed to consist of dry frame only) and the shear modulus is unaffected by saturation) and the value for each cell, M_{cell} , is obtained from the harmonic mean of the sand and shale values, weighted by the respective fractional volumes using net: gross (NTG). This is a valid practice for vertical wave propagation in a layered model (Backus, 1962). Using this, the acoustic impedance, ***I***, for a column of cells in the simulation model is calculated as below:

$$I = \sqrt{\langle \rho \rangle \langle \frac{1}{M} \rangle^{-1}} \tag{2.17}$$

Where:

$$\frac{1}{M} = \frac{(1 - V_{shale})}{M^{sand}} + \frac{V_{shale}}{M^{shale}}$$

And ρ is the bulk density of the cell obtained by averaging the densities of the rock frame and the fluid densities. The brackets, "< >", indicate a vertical volume weighted average over the reservoir interval. M, M^{sand} and M^{shale} are p-wave moduli for sand-shale mixture, sand, and shale, respectively (Stephen, 2007). This approach is suitable for reservoir beds that are less than one tenth of the seismic wavelength thick, and to reservoir units of around one quarter wavelength thick. A typical wavelength is 50 to 100 m (MacBeth, 1995). For the Schiehallion field, the reservoir units are around 25 m thick, equivalent to one quarter of a wavelength in many places, and the predicted impedance typically represents a cell of approximately 100 m × 100 m × 6 m.

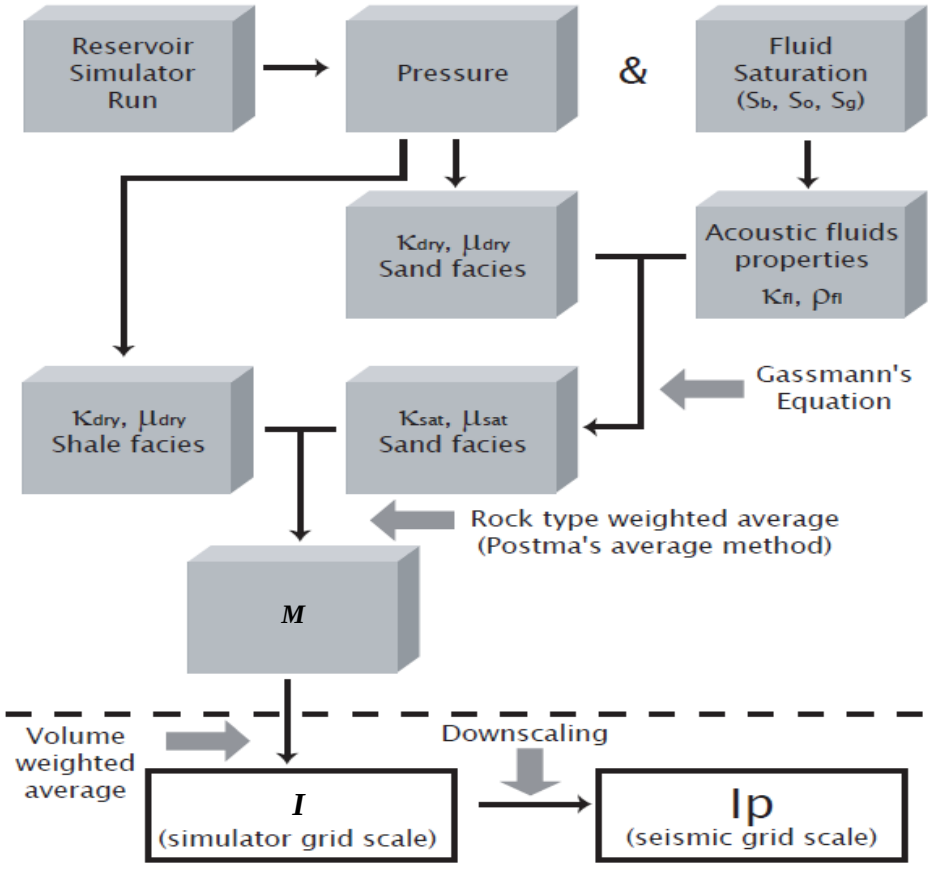

Figure 2.8: Petro-elastic modelling scheme for seismic comparison (Soldo, 2004).

2.6 Data Error

In SHM applications, errors in observed data can occur both in time-lapsed seismic and well measurements. Time lapse (4D) seismic data are often contaminated by several sources of non-repeatable noise, those errors need to be suppressed before any time-lapse anomalies linked to production can be included in the objective function. Observed production data also have an error component due to the constraints of instrumental measuring of pressures and rates and allotting accurate well completion intervals. For instance, wellhead-sampling can introduce big uncertainty in water-cut data and the method fails when excessive GOR (gas-oil ratio) production is encountered, for example after gas breakthrough and during gas lift operations (Kabir and Young, 2004). If the error in observed data is large, the estimated parameter vector may be a biased relative to the true parameter value, and the model prediction will not closely reproduce the true behaviour (Stephen, 2007).

During the inversion, and assuming a Gaussian distribution of the observed data errors, the covariance matrix can be used in order to represent the degree of uncertainty in the estimations (Tarantola and Valette, 1982). Generally, the observed data errors are related to the noise contained in the high frequency of the data (e.g. Robinson and Treitel, 1980; Yilmaz, 1987; Sheriff and Geldart, 1995). They are obtained by applying low frequency filter to the data, the noise structure in space (for the case of the errors related to the seismic data) and time (for the case of production data errors). Many algorithms can be found in literature for data analysis and filtering (e.g. Davis, 1986; Hohn, 1999).

2.7 Model Error

There are various model errors that may affect the solution of the history matching such as: reservoir simulation errors, rock physics modelling errors and upscaling and downscaling simulated seismic properties. In fact, induced errors in the modelling can affect the reliability of the predictions in history matching. When the errors in the simulation are considered during history matching, the updated parameters of flow simulation models would be more accurate. The mean model error significantly reduces the bias effects while the covariance gives a realistic spread from the mean prediction (O'Sullivan and Christie, 2006; Stephen, 2007; Sedighi**,** 2011).

In the reservoir simulation errors, there are three errors, which are results of Partial Differential Equation (PDE) discretization. These errors are truncation, round-off, and stability errors. The truncation error consequences from the substitution of the partial derivatives in the differential equation with approximate finite differences. Round-off error is the discrepancy between the calculated approximation of a number and its exact mathematical value. In reality, every computer carries a finite number of digits; round-off errors do occur, resulting in non-exact solutions. As the number of operations increases, so does the cumulative round-off error. For very large systems of equations, it is possible for the round-off errors to grow uncontrollably to the point of generating unrealistic results and even instability. Stability errors arise from the approximation method used in transforming the Partial Differential Equation into a numerical model and the PDE itself. Instability in numerical solution can be described as a feedback process whereby one error leads to one more error (truncation or round-off errors, respectively). As the error increases, the rate of error growth increases which causes the true solution to be lost (Peaceman, 1977; Brand *et al*., 1991; Eriksson *et al.*, 1996; Peaceman, 1979).

In the rock physics modelling errors, the seismic attribute simulation can be affected by this source of model error. Petro-Elastic Modelling (PEM) is another name of rock physics modelling. Rock physics transforms are based on data generated in the laboratory at the scale of centimetres or in the well at the scale of metres. However, they are used at the seismic scale in tens of metres. The substantial discrepancy between these scales may lead to error. Stephen (2007) calibrated the scale dependence of the model errors to reduce this effect. They showed that the error due to scale dependent simulation and subsequent petro-elastic transformation are of equal size and produce a non-zero minimum misfit, which affects the ability to history match to a degree that is equivalent to errors in the observed seismic data.

In upscaling and downscaling simulated seismic properties, the amount of well log and seismic data, available computer memory, and processing power often constrain the cell size and scale of gridded reservoir models. Upscaling can be described as the averaging of data from a finer to a coarser sample interval. Downscaling is the opposite technique. Upscaling can often cause the loss of information that makes downscaling non-unique. Therefore, the downscaling process must be consistent with the upscaling method in terms of conservation of volumes (Roggero *et al.*, 2007). Generally, finer

grids are necessary in any area in which you expect large changes in terms of fluid saturation and pressure. For example, you may prefer a finer grid in high permeability zones, and in a low permeability region, a coarse grid may be sufficient. The key idea behind any upscaling process should keep the saturation and pressure differences (flow responses) equivalent in both resolutions. For example, the areal interpolation of predicted impedances at the simulation scale (~ 100 m × 100 m) down to the seismic scale bins (25 m × 25 m) adds to the model error. Sharp transitions of the fine grid impedances, which may be due to saturation changes at the waterfront or at geological variation such as at faults, cannot be captured accurately (Stephen, 2007).

2.8 Scale dependence in SHM

Simulation and seismic data is not straightforward to integrate because these are two different domains, each with its own geometry and resolution. The seismic bins are typically spaced by 10's of m (12.5 m in our field study) while the wavelet may sample 25 m vertically, the same as our predicted data. The predicted seismic property grids are typically coarser horizontally but they are finer vertically. The predicted seismic impedance is calculated on a grid that is typically of the size 100 m × 100 m × 25 m that is the scale of reservoir simulation model (for our case study) as illustrated in Figure.2.9.

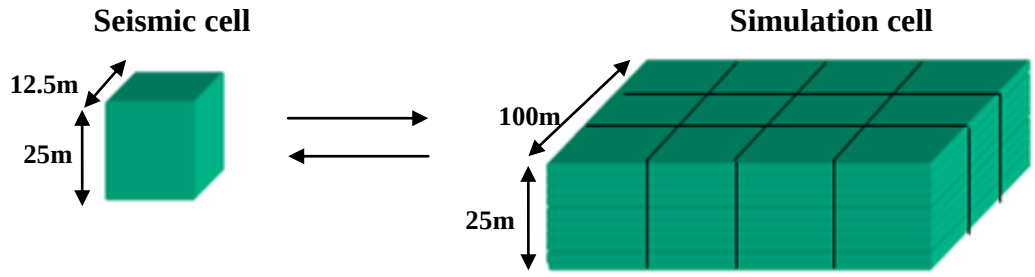

Figure 2.9: Scales of seismic and reservoir simulation cells.

For the calculation of the misfit we require that the observed and predicted seismic data represent the same volume. Upscaling and possibly downscaling is therefore required to bridge the gap between these two scales. Once the flow simulation model results are obtained, the elastic parameters of the reservoir are calculated for each cell through petro-elastic modelling to convert the simulation output into seismic attributes. Vertical

upscaling is used (Backus, 1962) then downscaled into the seismic grid with an inverse exponential distance weighting in order to compute the predicted impedances and compare them with the time-lapse seismic observations as depicted in Figure 2.10.

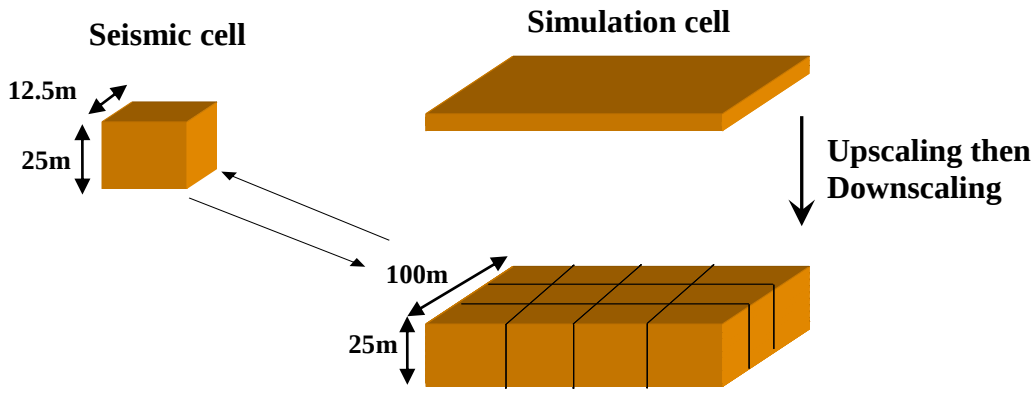

Figure 2.10: Schematic of upscaling and downscaling process in SHM. It starts by upscaling the simulated seismic properties vertically during the PEM calculation, and then downscaling the predicted seismic to the observed seismic bin horizontally.

The observed seismic data are obtained as a set of points on a grid defined by the acquisition inline and crossline co-ordinates but also by the bin centre in UTM (Universal Transverse Mercator) co-ordinates (e.g. Figure 2.11). In the field studied here, the Schiehallion field, the seismic and model grids are independent although the latter is aligned at approximately 45 degrees to the former (Stephen *et al.*, 2006). Due to scale differences between seismic and simulation, some conversion is therefore needed so that predicted and synthetic data can be compared: so far the areas are different but thickness is equivalent. The observed data could be upscaled areally, but it is preferable to interpolate the predicted data using an inverse exponential distance weighting. The interpolated impedance is obtained from:

$$I_{ij}^{fine} = \frac{\sum_{IJ} W_{ijIJ} I_{IJ}^{coarse}}{\sum_{IJ} W_{ijIJ}} \qquad (2.18)$$

where:

$$W_{ijIJ} = \exp\left(-\beta(|\underline{r}_{IJ} - \underline{r}_{ij}|\right)$$

Where indices *I* and *J* are the x and y indices on the simulation grid and *i* and *j* indicate seismic bins where I_{IJ} is obtained from Equation 2.17. $\underline{r}$ is the position of a simulation cell centre. It was found previously that $\beta = 0.05$ m^{-1} gave the best results, minimising the representivity error (Stephen *et al.*, 2006).

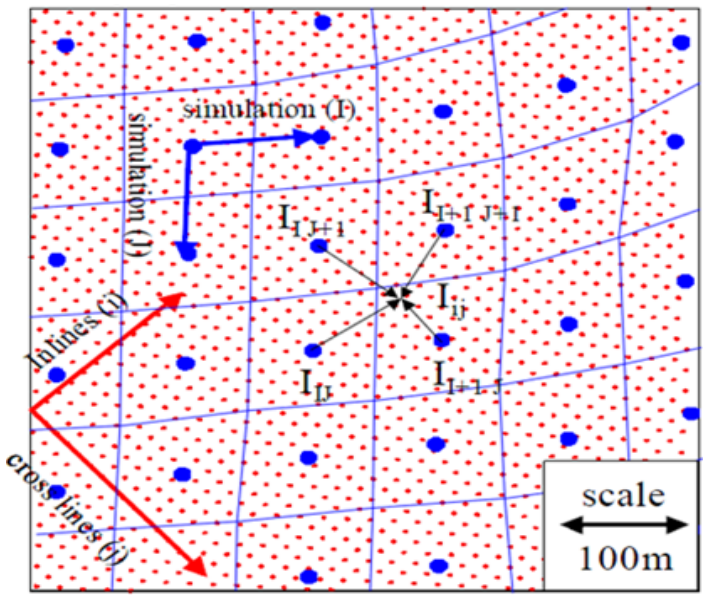

Figure 2.11: Comparison of the seismic and simulation grids in the present study. Blue lines indicate the simulation cells and large blue symbols the location at which the impedances are predicted. Equation 2.18 is used to interpolate the impedances to obtain values at the small red symbols, i.e. where the observed seismic data is measured. Solid blue and red arrows indicate the principal directions of the simulation axes and seismic grids respectively (Stephen *et al.*, 2006).

2.9 Summary

Inverse theory is commonly formulated to find a model for a physical system that agrees most with a given observation dataset. Reservoir history matching is a non-linear optimization problem, which involves the minimization of an objective function that measures misfit between observed and simulated data. The use of all gradient-based algorithms (local algorithms) is most efficient if the objective function exhibits the following characteristics: nearly quadratic response surface, symmetric and convex, one global minimum, and continuous. Nevertheless, in the most real cases of reservoir modelling the shape of the objective function strongly differs from the above given simplified assumptions. The main causes for these are: the non-linearity, complicated topology, many local minima, and discontinuity of the objective function. For this reason, the non-convex nature of the history-matching problem is conceptually better tackled using global (stochastic) methods, where the parameter space is explored by randomly generated trajectories, until a satisfactory minimum is reached. The main advantages result in the following: (i) we do not make any assumption about topology of the objective function and (ii) we can obtain a complete picture of parameter sensitivity and well- or ill-posedness of the inverse problem. In particular, direct search optimization techniques seem to be very promising. Unluckily, however, global convergence even to an approximation of the solution usually needs a large number of iterations. In fact, this cost is often too high for the reservoir history-matching problem, where the calculation of the objective function is mostly expensive. In general, the type of optimiser to be used is problem specific which may affected by different issues such as type of objective function, amount of parameters and runtime of the simulation model.

Production data used in the process of history matching measures pressure and saturations at discrete well locations, and it is necessary to constrain dynamic reservoir parameters such as permeability and the effect of faults. Time-lapse seismic analysis has the potential to provide the missing information, but it lacks precise details of the pressure and saturation states. The process of seismic history matching is an effort to merging the benefits of both types of information to improve estimates of the reservoir model parameters. Because of the huge amount of data (including the time-lapse seismic data and the model parameters) involved in a history matching problems, it is

customary and necessary to reduce the number of model parameters by using a suitable parameterization method.

Incorporating the 4D seismic in the reservoir history matching procedure is relies on the integration of a reliable petro-elastic model (PEM) with a dynamic flow simulation model together with a suitable optimisation method to tune the reservoir parameters. A PEM is a set of equations that relates reservoir properties (such as pore volume, pore fluid, fluid saturation, reservoir pressures, and rock composition) to seismic elastic parameters (such as P-wave and S-wave velocities, V_p and V_s, respectively and density). Gassmann's equation is usually takes account of fluid substitution in pore rocks. Bulk of dry rock moduli may vary significantly with stress.

Finally, parameter estimation by inverse modelling is based on a comparison between measured values and the corresponding model output. Measured and calculated variables must be consistent. There are several sources of errors in a 4D workflow comprising simulation errors, errors due to insufficient model characterization, and measurement errors. The numerical model errors are a result of model approximation or due to upscaling or downscaling. In addition, there are errors due to the different scales at which petro-elastic modelling is applied compared to observations. The parameter deficiency errors are the result of not capturing the reservoir heterogeneity or due to incomplete and incorrect choice of geological features description. The aim is to reduce the effect of such errors by finding the best solution of history matching.

CHAPTER 3
A New Method to Improve Convergence Rates with SHM

Overview

In this chapter, we develop a new method to speed up the convergence rate of Seismic History Matching (SHM). The new method is a modification of the original Neighbourhood Algorithms (NA) and we call this approach the ***NA with Proxy derived Gradients*** (NAPG). In addition, a detailed workflow approach adopted for the implementation of seismic history matching will be presented, where simulations are quantitatively compared to observe seismic and production data and then updated in an objective manner.

3.1 Seismic History Matching Workflow

It is becoming more and more common to use Assisted History Matching methods to find various combinations of reservoir simulation models that agree with available production and time-lapse seismic data. At Heriot-Watt University, an assisted history matching method has been developed to include as much reservoir data as is necessary and sufficient, including core and well logs, seismic, production data, SCAL etc (Stephen *et al.*, 2006). In this workflow, simulations are quantitatively compared to observed seismic and production data and then updated in an objective manner as shown in Figure 3.1. The observed seismic attributes are generated from 3D cubes as maps of surveys or differences. Multiple flow simulations are generated simultaneously using a suitable parameterization of the reservoir description. These models are converted to forward simulations of the production process and compared to the observed data using a misfit. The Neighbourhood Algorithm is then used to choose new parameter values. The Neighbourhood Algorithm is a stochastic optimization algorithm initially aimed at seismic inversion problems. Similar to simulated annealing and genetic algorithms, it tries to find models of acceptable data in a multidimensional parameter space. The SHM loop is run once per model but many hundred models may be run with 10's of models being run simultaneously on a Linux cluster. The process is

repeated a number of times until the misfit is reduced. Finally, the uncertainty of the parameters and predicted behaviour is analysed. Prior to history-matching time-to-depth conversion is used to create maps of observed seismic which can then be compared to predict seismic along with production data.

The basic aims of seismic history matching are:

- To improve the reservoir characterisation by adding additional constraints given by the 4D data.
- To quantify the model predictions and uncertainties via statistical parameters obtained after inversion (i.e. standard deviation, mean, etc).
- To understand the fluid-flow directional patterns throughout the life of the reservoir.

This history matching loop consists of several components with the application of the stochastic Neighbourhood Algorithm (NA) (Sambridge, 1999a).

Generation of Multiple Models: A set of models are created and converted into forward simulations of the production process. Forward modelling is performed in order to obtain changes in dynamic properties of the reservoir (such as pressure and fluid saturations) using a commercial finite difference simulator (Eclipse 100). Conventionally, geological models are constructed at a fine scale and upscaled (Christie, 1996) while in our approach the models are updated at a scale appropriate for simulation. This speeds up the generation process and reduces the potential for upscaling errors.

We use the Pilot Point Method with Kriging (e.g. de Marsily, 1984) to reduce the number of unknown permeability values in the model and to enable efficient updating. A number of cells are identified as pilot points and their properties modified independently, while neighbouring cells are updated using Kriging, effectively an interpolation. In this way, we can update net:gross, porosity, and permeability parameters. Fault properties and barriers may also require modification. Fault locations are very difficult to determine as part of an automated scheme (Staples, *et al.*, 2004) and perhaps should be defined during the model building process. Their flow properties, the transmissibility multipliers, can be included in the seismic history matching process.

Seismic to Reservoir Model Comparison: We predict impedances via a petro-elastic model (PEM). Once the predicted and observed seismic attribute maps are mapped in a common grid, they are normalised prior to comparison. This normalisation is done since the mismatch is evaluated between two attributes that are in different seismic domains (Stephen *et al.*, 2006).

Evaluation of the Misfit: The degree of discrepancy between prediction and observations are estimated by the misfit objective function. A single misfit objective function is obtained for each model incorporating a comparison between observed and predicted production and seismic data.

Sample from the parameter distribution: The multiple model approach relies on sampling the parameter space a number of times and simultaneously running forward simulations to obtain a misfit. Currently we use the Neighbourhood Algorithm as an optimization method to sample the parameter space. Resampling takes place by dividing the parameter space into Voronoi cells. The best n_r models are selected and n_s/n_r (typically 2 in this work) new models are randomly located in each Voronoi cell in this sub-sample (Sambridge, 1999a). The process is repeated to build an approximate Posterior Probability Distribution (PPD), which may be resampled later as part of the uncertainty analysis. Large values of n_s and n_r improve the chances of avoiding local minima and should be increased with the dimension of the parameter space (Sambridge, 2001). The neighbourhood algorithm will be explained in detail later in this chapter.

Uncertainty Analysis: Using Bayes theory, the misfits provide the conditional likelihood of each model for the given data and these are used to update prior model probabilities. The updated probabilities is similar to Markov Chain Monte Carlo methods (MCMC) as part of the uncertainty analysis of the unknown parameters giving a set of probability distributions. These probabilities can also be used as weights to determine the ensemble average and the spread of variables such as saturation or pressure in each cell when predicting long-term reservoir behaviour. Since we refine the parameter space near most likely models.

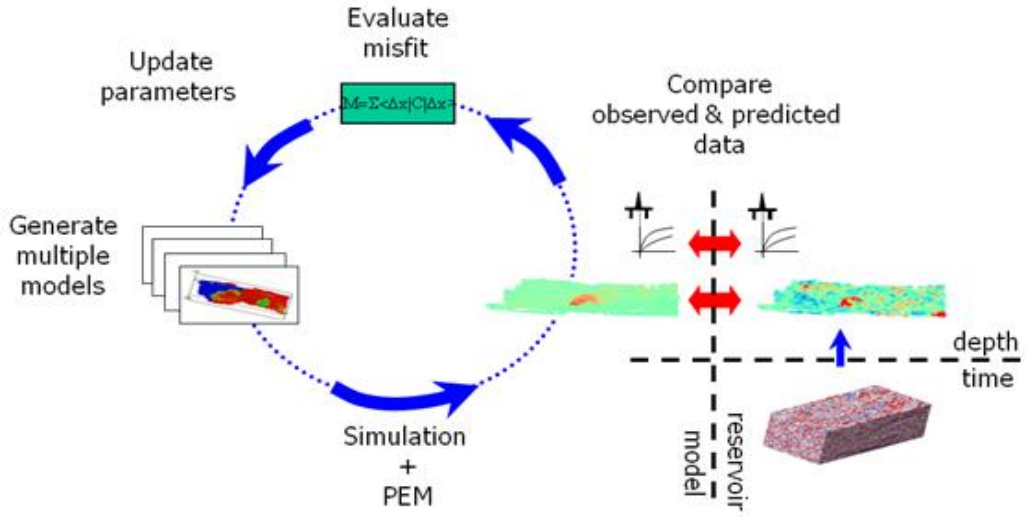

Figure 3.1: Seismic and production history matching workflow (Stephen *et al.*, 2006)

3.2 Likelihood and least-square misfit Function

In order to make quantitative comparisons of new reservoir models to the observed data, we need to define a misfit function. This misfit function can give us the accuracy of each model by comparing the measured data with the observed data. In this work, the objective function was based on the L2 norm formula (Tarantola, 1987) which is already defined in Chapter 2 (Section 2.1.2, Equation 2.1). In Equation 3.1, we assumed that there is a Gaussian distribution of the errors in the observed data and this error is additive to each datum. E.g. for seismic data:

$$d_s = d_s^{truth} + \varepsilon \tag{3.1}$$

where ε is data error in observed impedance data relative to the true value d_s^{truth}. Data errors in the production history are usually expressed statistically and are incorporated into the likelihood function. For example, Floris *et al*. (2001) assumed that time-series data errors would be distributed independently and follow a Gaussian distribution. These approximations resulted in a well-known form of logarithmic probability dependent on the sum of the squares of each discrepancy.

To demonstrate how we apply the likelihood function, we assume that the data measurement errors are normally distributed (Gaussian) around zero with a variance σ^2 at any given time and there is no simulation error. The probability that the true value of observed data is equal to simulated value is:

$$P(O|m)_t = \frac{1}{\sigma\sqrt{2\pi}} exp\left\{-\frac{1}{2}\frac{\left(d^{obs} - d^{sim}\right)_t^2}{\sigma^2}\right\} \tag{3.2}$$

where t is the time step, σ is the standard deviation of the error and d^{sim} is the model output. Assuming measurement errors are independent at each time step, the likelihood of the model is obtained from the product of the probabilities of individual measurements:

$$P(O|m) = (\frac{1}{\sigma\sqrt{2\pi}})^N \prod_{t=1}^{N} exp\left\{-\frac{1}{2}\frac{(d^{obs} - d^{sim})_t^2}{\sigma^2}\right\} \tag{3.3}$$

where N is the number of the data points. Since $(\frac{1}{\sigma\sqrt{2\pi}})^N$ is constant, Equation 3.3 can be written as

$$P(O|m) = \alpha\ exp\left\{-\sum_{t=1}^{N}\frac{(d^{obs} - d^{sim})_t^2}{2\sigma^2}\right\} \tag{3.4}$$

Thus, if we define the misfit M as

$$M = \sum_{t=1}^{N}\frac{(d^{obs} - d^{sim})_t^2}{\sigma^2}$$

Hence, the likelihood function is:

$$P(O|m) \propto\ e^{-M/2} \tag{3.5}$$

In this study, the production data that will be used in history matching; for example well oil and water flow rates are estimated for total monthly volume and for this case uncorrelated assumption for observe data is valid. For seismic data, we usually deal with a lot of data because the bin size is small and there are many bins. Therefore, it is very important to determine whether or not the data errors are correlated. If they are correlated, it is important to include the inverse of the covariance matrix. However, it is not easy to calculate that matrix and including that matrix in the objective function can make a big difference in terms of CPU time (Aanonsen *et al.*, 2003; Gosselin *et al.*, 2003; Soldo 2005). For the Schiehallion field, Stephen *et al*. (2006) found that the observed 4D signature is an uncorrelated Gaussian over the length of the simulation cells.

3.3 The Neighbourhood Algorithms

The Neighbourhood Algorithm (NA) is a recent stochastic optimization method that was proposed by Malcolm Sambridge (1999a). This method was not designed specifically to perform global optimisation, but has been used by other authors (Sambridge and Kennett, 2001; Sambridge, 2001) in that sense. The main objective of this algorithm is to sample the region of parameter space that contains models of acceptable data fit and to extract robust information from the resultant ensemble of models. The neighbourhood algorithm arose with the intention of responding to the next question:" *How can a search for new models be best guided by all previous models for which the forward problem has been solved?"* In this algorithm, the previous models are used to approximate the objective function everywhere in model space (Sambridge, 1999a; Subbey *et al.*, 2002). Sambridge and Mosegaard 2002 have classified optimization algorithms in terms of exploitation and exploration as shown in Figure 1.3 and they put NA in between exploration and exploitation axes when classifying several search and optimisation algorithms.

The motivation for using NA is that it makes use of all previously models at each iteration including all the models generated to guide the search (self-adaptive). In addition, NA is simple to use because the simplicity of its parameter-tuning scheme in contrast to the more complicated tuning mechanisms of other methods, such as Simulated Annealing and Genetic Algorithms. NA, similar to evolutionary algorithms, has the advantage of finding an ensemble of models by exploiting information about all previously generated models, which are good data fitting, rather than seeking a single optimal model. On the other hand, there are a few drawbacks to using the NA as optimization method. In high dimensional space, NA requires a large number of initial models both for the initial ensemble and in the search for minima of the misfit function. NA as other stochastic methods, the convergence rate is slow and requires a huge number of iterations to find the optimal solution. Therefore, the price is often too high for the reservoir history-matching problem, where the computation of the objective function is usually expensive.

3.3.1 NA parameters

There are four parameters that control the performance of the neighbourhood algorithm, which are:

n_i : initial number of models needs for NA initialisation (initial sample size)
n_r : number of best models resampled by the NA
n_s : number of models per iteration, and
it : number of iterations.

The convergence performance of the algorithm depends on n_s and the ratio of n_s/n_r as tuning parameters. They control the explorative and exploitative behaviours of the algorithm respectively. Setting NA parameters for greater exploration, i.e. small n_s to n_r ratio, increases the chance of finding the global minimum compared with less explorative NA runs. Setting NA parameters for greater exploitation, i.e. high n_s to n_r ratio could result in trapping in a local minimum although convergence is faster. At each stage of the exploitation and the sampling procedure, selective sampling of the good data-fit regions is achieved by exploiting information about all the previously generated models. Elabed (2003) investigated the efficiency of NA and assessed the robustness of the algorithm in searching the misfit surface of a history-matching problem. She states that for a fixed n_s by keeping n_s/n_r ratio high one can achieve good exploitation of the best fit regions and lower n_s/n_r ratios will result in good exploration of the parameter space. She reports that sampling is likely to get trapped in local minima if the first best models are all located in the same regions of the search space, forcing the algorithm to discard other regions for exploration.

In addition to the above, in many direct search problems, e.g. global optimization, an increase in the number of unknowns (n_d) makes the problem considerably harder to solve (Sen and Stoffa, 1995). This is the so-called '*curse of dimensionality*'. Sambridge (2001) recommends that the initial models n_i should be at least equal to 2^{nd} to saturate the parameter space and avoid undersampled and oversampled space, where n_d is the number of unknown parameters in the optimization problem. Also, Erbas and Christie (2007) found that the size of initial population (n_i) affects the quality of results especially in high-dimensional search spaces, as higher n_i provides more information from explored search space and leads the algorithm towards more diverse solutions throughout the search space. On the other hand, it has been claimed that in cases where

multiple minima exist, each initial random population may lead to convergence to distinct solutions (Erbas, 2007) if the ensemble is too small. This effect is more severe in high dimensional problems (e.g. updated grid cells properties) and also in a wide range of model parameters.

3.3.2 Voronoi Diagram

The NA uses a direct search method by using the spatial properties of Voronoi cells to find optimal minima. In mathematics, a Voronoi diagram (named after Georgy Voronoi 1868-1908) is a special kind of decomposition of a given space. The NA algorithm makes use of the simple geometrical concept of Voronoi cells to guide the search in the model space. The Voronoi cell is a unique way of dividing the n_d dimensional model space into regions. That is, the Voronoi cell of the generator point $m^{(i)}$ is the polygon containing all the points in the space that are closer to $m^{(i)}$ than to any other point $m^{(j)} \in P, j \neq i$. Constructing these nearest neighbour polygons for all points in P results in the *Voronoi diagram* of P. Each point in the search space that has one unique nearest neighbour $m^{(i)} \in P$ is located in the inside of the Voronoi cell generated around $m^{(i)}$, while points that are equidistant from exactly two elements of P are lying on the edge between the two corresponding Voronoi polygons. Finally, points having the same distance from at least three elements of P form the vertices of the diagram. In this way, the set of points P defines a unique partition of the entire space into N Voronoi cells.

For any distribution and density of samples, the structure of Voronoi cells would be unique and the space filling and size of the cells are inversely proportional to the sampling density (Sambridge, 1999a).

3.3.3 NA Sampling Algorithm

The main principle which the NA algorithm is based on is that at every stage of the search process the model space is represented by the Voronoi diagram of all previously sampled models and that this representation helps the algorithm to concentrate sampling on the most promising regions.

In the very first step, an initial set of uniformly distributed points in the model space is generated and their Voronoi cells are constructed. After computing the misfit values for all initial samples, the n_r models with the lowest misfit are chosen, where n_r is a control parameter specified by the user. Since models with low misfit values give reason to

believe that there could be more good points or even better points located within their close neighbourhood, the Voronoi cells belonging to the chosen n_r best samples are considered to be the currently most promising areas. Consequently, the n_s new models generated in the second iteration are sampled in these cells, where n_s/n_r models are uniformly randomly generated in each cell. The misfit values of these samples that have been added to our ensemble are then calculated and the Voronoi diagram is updated to include all points collected so far. Again, of all these models, the n_r points with the lowest misfit values are selected and the search goes on.

The working mechanism of the neighbourhood algorithm (NA) is illustrated in Figure 3.2. The NA algorithm can be summarized in the following steps:

1. Generate an initial set of n_i models uniformly in the model space
2. Calculate the misfit function for the most recently generated set of n_i models and determine the n_r models with the lowest misfit of all models generated so far;
3. Generate n_s new models by performing a uniform random walk in the Voronoi cell of each of the n_r chosen models (i.e., n_s/n_r samples in each cell);
4. Go to step 2.

This procedure is repeated until a predetermined stopping criterion is met (see Chapter 7 for full stopping criteria diagram). A question that crucially affects the algorithm's computational efficiency is how the new samples can be chosen in the n_r chosen cells. Constructing the complete Voronoi diagram would be prohibitively expensive, even for low-dimensional problems. However, Sambridge suggested an efficient approach where new models are collected by performing a uniform random walk within each relevant cell. This is done using a Gibbs sampler illustrated in Figure 3.3 using a two-dimensional example (with parameters x and y) where three points are generated within the centre cell. Starting from a point (x_0,y_0), a new value x_1 for the first parameter is randomly chosen from the interval $[a, b]$ between the intersection points of the cell boundaries with an axis drawn through (x_0,y_0) in the direction of the current parameter. That is, the conditional probabilities required for the Gibbs sampler to simulate a random walk within one cell are simply defined to be uniform for the models within the Voronoi cell and set to 0 outside the cell. Then, the value of the second parameter is manipulated analogously resulting in the new model (x_1,y_1). This procedure can be transferred to higher-dimensional spaces, and all the information that is needed are the

aforementioned intersection points with the cell boundaries, which can be calculated using an efficient formula given in Sambridge 1999a. From the assumption that the misfit value is uniformly constant in each Voronoi cell at each iteration new samples are concentrated in the cells with better data-fitting models.

To sum up, the main idea behind the algorithm is that the misfit of each of the previous models is representative of the region of space in its neighbourhood defined by the Voronoi cells. Consequently, at each iteration new samples are concentrated at the neighbourhoods surrounding the better fitting models. In this way, the algorithm exploits the information contained in the previous models to adapt the sampling. The size and shape of the neighbourhoods are not imposed by any external information but more exactly determined automatically and uniquely by the previous samples and is geometrically determined by the Voronoi partitions, which will be analysed in each iteration. On the other hand, the algorithm only requires models to be considered for their relative fit to the data, because it uses the misfits as a rank (i.e. by difference) or to calculate the ratio of likelihoods. This is very useful because of the fact that sometimes it is a lot easier to answer the question *'is model X a better fit to the data than model Y?'* instead of estimating the difference in a precise way. Lastly, an absolute measure of the data fit is needed to estimate if any models satisfy the data.

In addition to the above, sampling makes use of multidimensional geometrical structures of ordinary the Voronoi diagram together with a decision criterion to guide the search process towards the best regions of the misfit surface. Figure 3.4 shows a set of Voronoi cells which was calculated by NA for 10, 100 and 1000 irregularly distributed points in a 2D example.

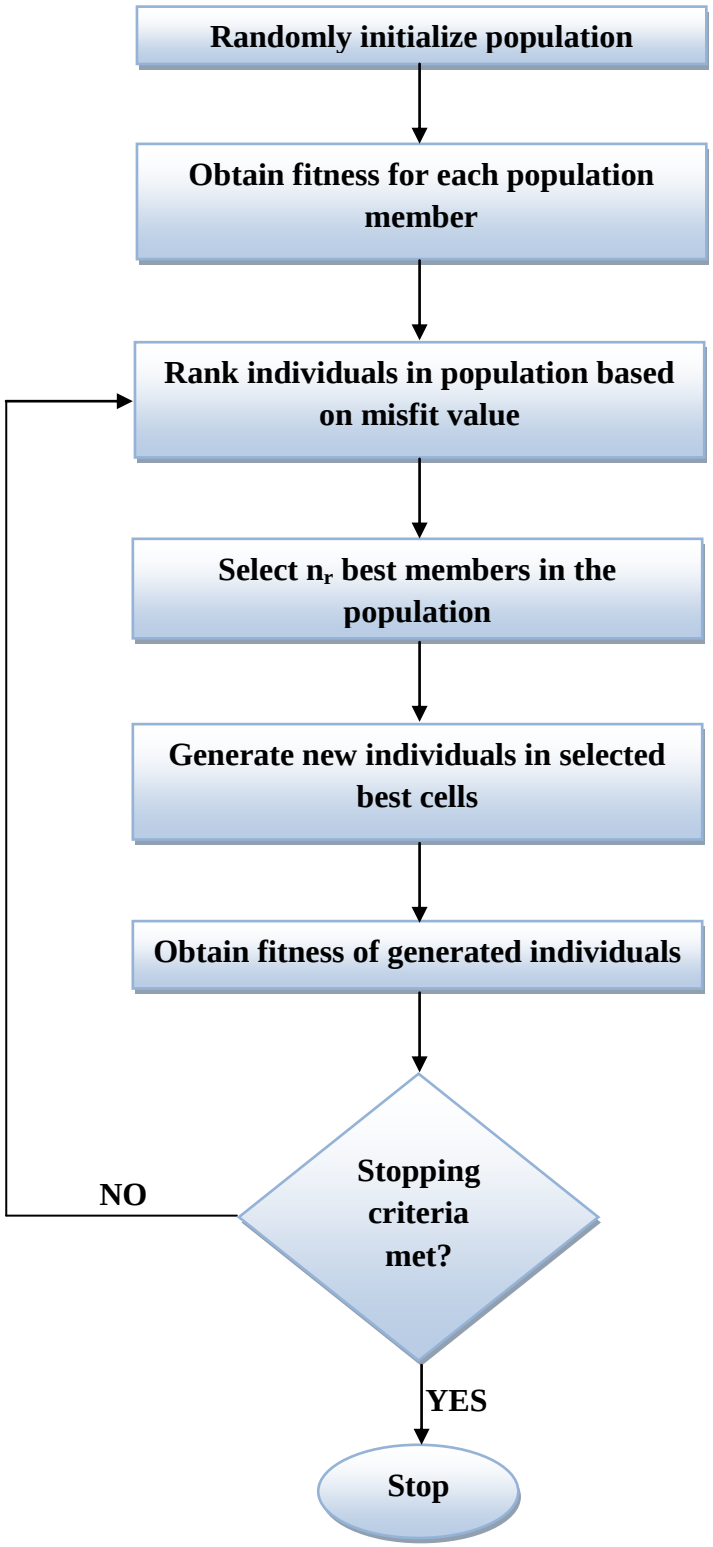

Figure 3.2: Flow chart of the NA Sampling Algorithm (Hajizadeh, 2011).

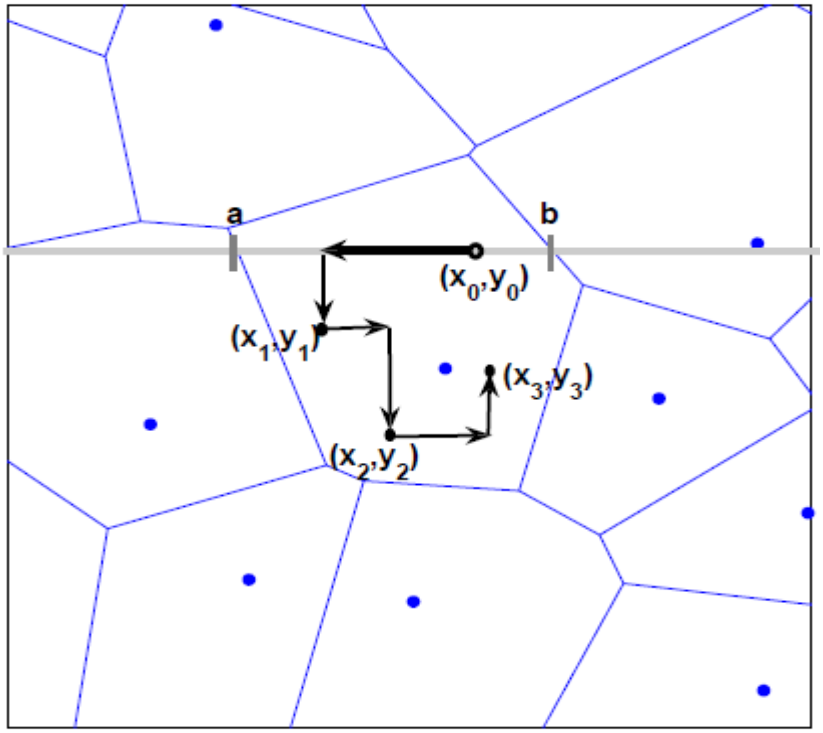

Figure 3.3: Schematic diagram of NA– Gibbs Sampler. Uniform walk within one cell generating three new points (x_1, y_1),(x_2, y_2) and (x_3, y_3) (Subbey *et al.*, 2003).

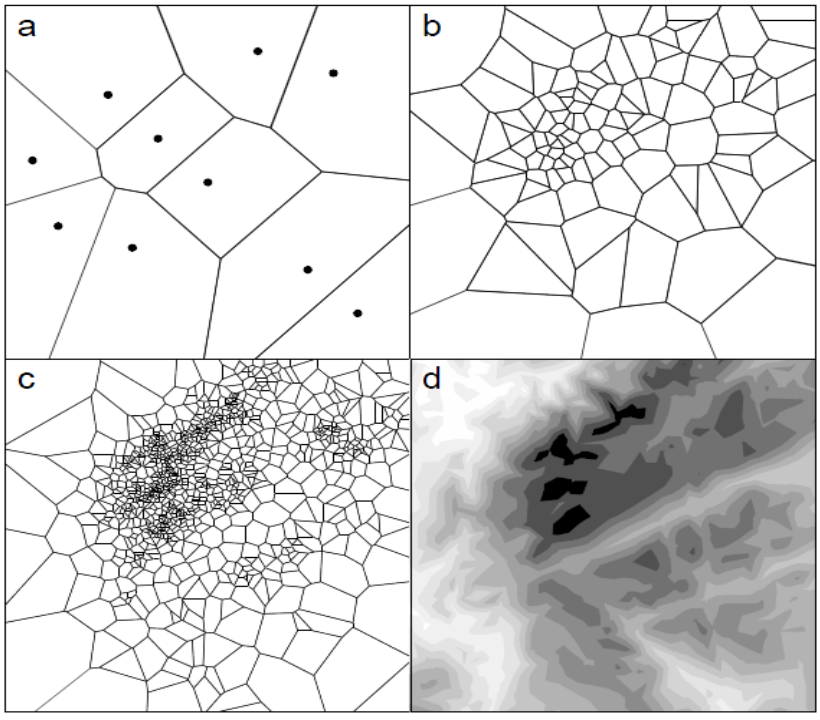

Figure 3.4: Quasi-uniform random points and Voronoi cells for a) 10 points, b) the Voronoi cells of 100 points generated by the neighbourhood approximation, c) as b but for 1000 points and d) contours of the test objective function. The black dots in Figure belong to the misfit value of different models (Sambridge, 1999a).

3.4 A New Method to Improve Convergence Rates with SHM

Stochastic inversion algorithms often rely on simple assumptions for selecting new models by random processes. In this work, we improve the way that such approaches learn about the system they are searching and thus operate more efficiently. To improve the efficiency of sampling, we seek to replace the uniform distribution that we sample from with one that reflects the information learned about the misfits as we proceed through the iterative process of HM. We can improve this approach by approximating the probability of the models within the Voronoi cell as being a linear function of the parameter values instead of using sampling from a uniform distribution. We derive a proxy model of the misfit response surface and use that to derive sensitivities of the misfit with respect to the parameters that we modify to steer the search towards better models. We combine a global method with a gradient-like one to speed up the convergence and take advantages of exploitation of the global method, which will lead to further interpret the misfit of surface to guide the stochastic parameter search.

To explain the improvements that we make to the NA approach, we use the 2D synthetic misfit surface (Figure 3.5a) which contains many minima. The NA begins with a purely random sample of the parameter space such that ten new models are chosen (Figure 3.5b). The best five models are identified and new models are located in their neighbourhood (obtained by generating Voronoi cells) by further random sampling with a uniform distribution across each cell. This last step can be inefficient in large dimensional problems. Further exploitation is possible if information about the relationship between the misfit and the parameters can be obtained. Such sensitivities can be used to direct the search towards regions expected to have higher probability (Figure 3.5c). In this new approach, we use a proxy model to represent the surface, which can then be differentiated to get first order derivatives of the misfit with respect to each parameter. These can then be used to transform a uniform probability into a linear probability. The new approached is named the NA with Proxy derived Gradients (NAPG).

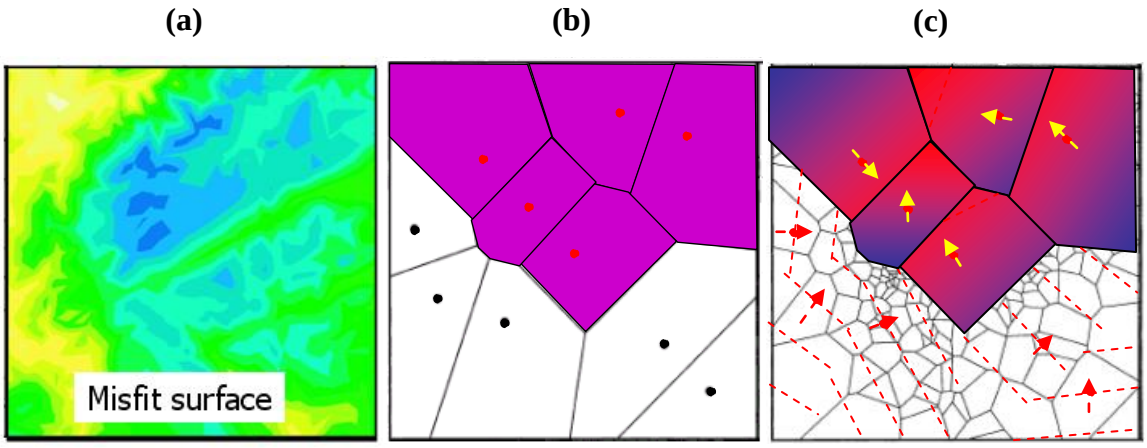

Figure 3.5: Schematic of the Neighbourhood Algorithm and how we improve it: (a) synthetic 2D misfit surface, blue indicates lower values (b) Voronoi cells used to identify neighbourhoods around models, the best 5 models are identified and randomly sampled with a uniform distribution in each cell (c) probability contour plots estimated from the misfit showing the areas identified as having a better chance of finding an improved match with red indicating highest probability; arrows indicate preferred direction of search. Discontinuities of probability at the Voronoi cell boundaries indicate the nature of the approximation.

3.4.1 Mathematical Derivation of NAPG

The aim in this work is to find an appropriate sampling strategy that improves the efficiency, as high dimensional problems require a search of a very large hyper-volume. Selection of new parameter values within a Voronoi cell makes use of an approximated probability based on the misfit.

We begin with the likelihood of the data, d, given the model, θ, from the misfit, J, via:

$$P(d|\theta) \propto \exp\left(-\frac{J(\underline{\theta})}{2}\right) \tag{3.6}$$

where $\underline{\theta}$ is the parameter vector. We calculate $J(\underline{\theta})$ for each model in an ensemble from Equation 2.3. We can therefore see that if the misfit increases with the parameter, the likelihood decreases. For any one of these models, we can apply 1st order Taylor expansion:

$$P(d|\theta) \propto \exp\left(-\frac{J(\underline{\theta}^*)}{2}\right)\left(1 - \frac{1}{2}\sum \frac{\partial J}{\partial \theta_i}(\theta_i - \theta_i^*) + \cdots\right) \tag{3.7}$$

where θ_i^* is the current variable.

The probability of θ_i is approximated by:

$$P(d|\theta_i) = P^*[1 + k(\theta_i - \theta_i^*)] \tag{3.8}$$

Where $k = -\frac{1}{2}\frac{\partial J}{\partial \theta_i}$ and p^* is the current model probability.

We can then use Equation 3.8 to obtain the cumulative distribution function, *cdf*, for a given parameter, θ_i, by integrating over the range of the parameter from θ_1 to θ_2 obtained from the boundaries of the Voronoi cell. We normalise this integral so that it is unity over the whole range:

$$cdf = \frac{\int_{\theta_1}^{\theta} P d\theta}{\int_{\theta_1}^{\theta_2} P d\theta} = \frac{k\theta^2 + 2(1 - k\theta^*)\theta - k\theta_1^2 - 2(1 - k\theta^*)\theta_1}{k\theta_2^2 + 2(1 - k\theta^*)\theta_2 - k\theta_1^2 - 2(1 - k\theta^*)\theta_1} \tag{3.9}$$

If we randomly generate the *cdf* value between 0 and 1, then we can solve this equation to get θ (see Figure 3.6). Hence, if we define

$$\tau_j = k\,\theta_j^2 + 2(1 - k\,\theta^*)\,\theta_j \qquad \text{where j} = 1,2 \tag{3.10}$$

Then we can re-write Equation 3.9 as

$$0 = \tau_\theta - \tau_1 - cdf(\tau_2 - \tau_1) \tag{3.11}$$

By substituting Equation 3.10 into Equation 3.11, we obtain

$$0 = k\theta^2 + 2(1 - k\theta^*)\theta - \tau_1 - cdf(\tau_2 - \tau_1) \tag{3.12}$$

The solution for θ is:

$$\theta = \frac{-(1 - k\theta^*) \mp \sqrt{(1 - k\theta^*)^2 + k(\tau_1 + cdf(\tau_2 - \tau_1))}}{k} \tag{3.13}$$

We assume that the probability $P(d|\theta_i)$ has to be greater than or equal to zero ($P(d|\theta_i)$>=0). This means that we have to place limits on the value of *k* to prevent $P(d|\theta_i)$<0. In practice if k has such a large magnitude that if the linear expansion leads to a negative value then it means the Taylor expansion has failed. However, we can still make use of the approximation as a guide. To solve this, we define four limits:

1. If k is negative, $k \geq k_{min}$ and $k_{min} = -1/(\theta_2 - \theta^*)$. If $k=k_{min}$ then $P=0$ at $\theta=\theta_2$.

2. If k is positive then $k < k_{max}$ and $k_{max}= 1/(\theta^* - \theta_1)$. If $k=k_{max}$, then $P=0$ at $\theta = \theta_1$.

3. If $k>k_{max}$, we can say then that $P/P^*= (\theta-\theta_2)k_{max}$ and k is set to k_{max}. Then our solution for θ is:

$$\theta = \theta_1 + (\theta_2 - \theta_1)\sqrt{cdf} \tag{3.14}$$

4. If $k<k_{min}$, we can say then say that $P/P^*=(\theta-\theta_2)k_{min}$ and k is set to k_{min}

$$\theta = \theta_1 - (\theta_2 - \theta_1)\sqrt{1 - cdf} \tag{3.15}$$

As a result, instead of randomly sampling between θ_1 and θ_2, with a linear cumulative distribution around θ^*, we use a square root function to approximate the linear probability distribution to distribute the new models inside the voronoi cells. To estimate the likelihoods we therefore need the gradient of the misfit with respect to each of the parameters as illustrated in the next section, Section 3.4.2. Analysis of the proxy derived gradients method illustrated that in one dimension as shown in Figure 3.6, we assume extreme probability gradients to speed up the search. The blue dots represent some models for which we have calculated the misfit. We then fit a quadratic equation through these points. A random number from 0 to 1 is used to give the *cdf* and then that function is inverted to give the new value of the parameter. The search space is then identified for one or more of the best models where it runs from the midpoints between models. Of course, at the minimum the gradient changes and the solution to the cdf flips over. If we are not careful, and we do not take this into account we may see inefficient sampling resulting from new values being picked from the other side of the minimum.

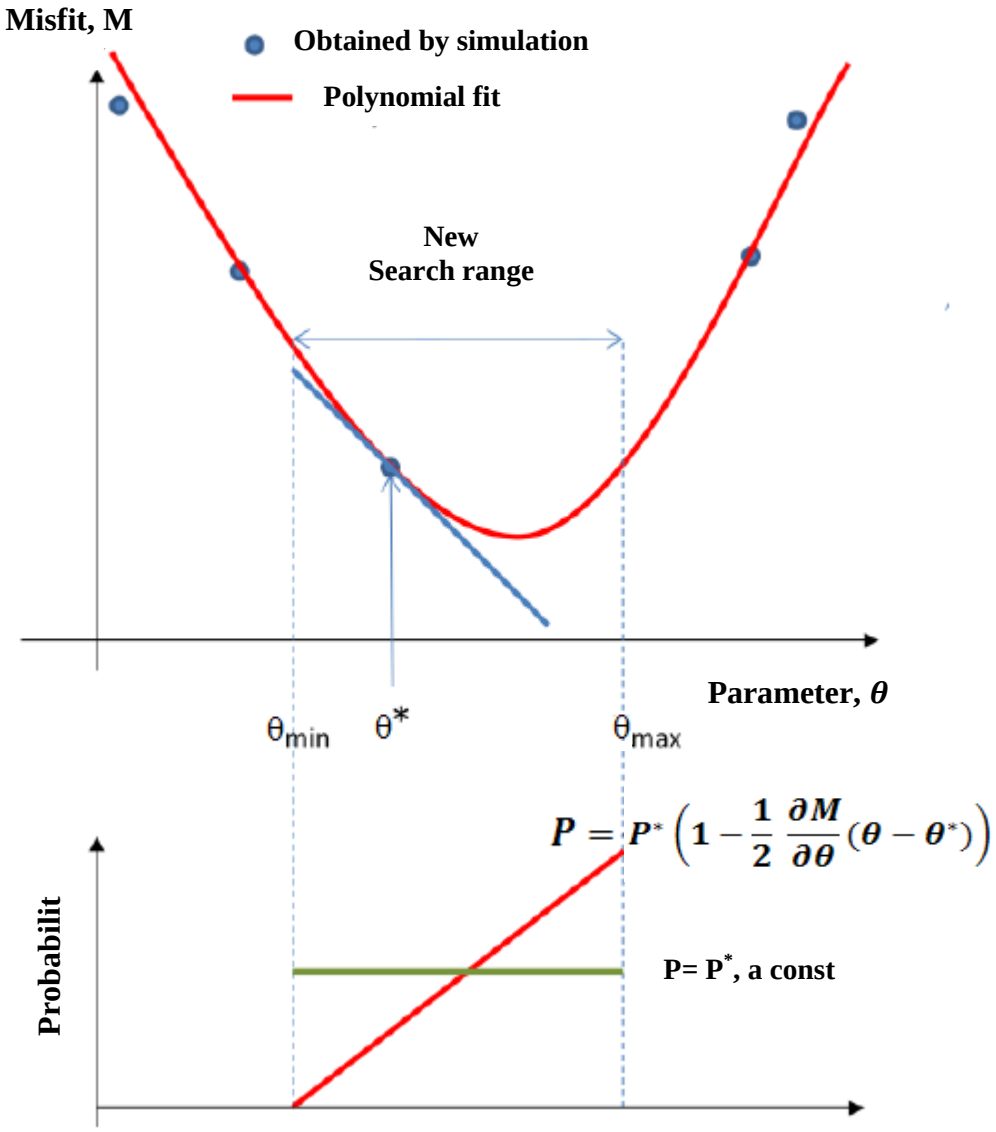

Figure 3.6: Schematic of using gradient to pick a new value of parameter, θ and derive a linear probability.

3.4.2 Proxy Response Surface

To complete the process above, we need to obtain *k* for which we use a proxy response surface as a representation of the real misfit. Response surfaces are often constructed with polynomial regression techniques. In this study, the Singular Value Decomposition technique with least square regression (Montgomery *et al.*, 2000; Press *et al.*, 2007; Sedighi and Stephen, 2010, Stephen and Arwini, 2010; Arwini and Stephen, 2010) is used to fit the data and the coefficients and to construct 2nd order polynomial misfit function.

The proxy model of the misfit is then:

$$J(\underline{\theta}) = C_0 + \sum_{i=1}^{nd} \mathrm{C_i}\theta_\mathrm{i} + \sum_{\mathrm{i=1}}^{\mathrm{nd}} \mathrm{C_{i+nd}}\theta_\mathrm{i}^2 + \sum_{\mathrm{i=1}}^{\mathrm{nd-1}} \sum_{\mathrm{j=i+1}}^{\mathrm{nd}} \mathrm{C_{ij}}\theta_\mathrm{i}\theta_\mathrm{j} \tag{3.16}$$

where $\boldsymbol{C_0}$, $\boldsymbol{C_i}$, $\boldsymbol{C_{i+nd}}$, and $\boldsymbol{C_{ij}}$ are the coefficients of the polynomial equation and represent the constant, linear, second order, and parameter interaction terms. Indices $\boldsymbol{i}$ and $\boldsymbol{j}$ are parameter counters, and $\boldsymbol{n_d}$ is the number of parameters. In practice the above equation utilizes the normalized sampled parameters to avoid distortion effects. In the SHM workflow, we also tend to sample the parameters on a $\log_{10}$ scale and hence the parameters are represented in this form. Therefore, a linear scaling transformation is applied on parameter values to map them onto the domain of [-1,1], on a $\log_{10}$.scale. This linear transform is then:

$$\theta_i' = \frac{\theta_i - \theta_i^{mid}}{\theta_i^{max} - \theta_i^{min}} \tag{3.17}$$

$$\theta_i^{mid} = \frac{\theta_i^{min} + \theta_i^{max}}{2} \qquad where\ i = 1,2,\ldots\ldots,nd \tag{3.18}$$

Where θ_i' is the normalized parameter, and θ_i^{min}, θ_i^{mid}, and θ_i^{max} are the minimum, middle and maximum of the range of the $\boldsymbol{i^{th}}$ element of parameter vector $\boldsymbol{\theta}$, respectively.

The derivative of this polynomial is then:

$$\frac{\partial M(\underline{\theta})}{\partial \theta_i} = C_i + 2C_{i+nd}\theta_\mathrm{i} + \sum_{\substack{j=1 \\ j\neq i}}^{nd} C_{ij}\theta_\mathrm{j} \tag{3.19}$$

where the cross term sum does not apply when $\boldsymbol{i}$ is equal to $\boldsymbol{j}$. Thus for a given model we can calculate an updated parameter value using Equation 3.13

3.5 Summary

We perform seismic history matching starting with a reservoir simulation model created by conventional methods where 3D seismic, well logs and cores, well test data and other pre-production data are used to condition a geological model. This has been upscaled for flow simulation and then used as a base case. A multi-model approach to history matching including seismic data has been explained in this chapter, and this will be applied to obtain a good match to production and 4D seismic data. A full description for each individual part of a loop was discussed. The neighbourhood approximation (NA) algorithm and its use as a sampling algorithm was presented, along with details about the objective function, voronoi cell properties and NA parameters.

In this chapter, we presented a method where the NA approach can be improved by using sensitivities derived from a proxy model. The proxy model itself points to a simple structure to the misfit response and we will use the NA and NAPG approaches to find the minima on that surface. In history matching, high dimensional problems are still a real challenge especially in respect of CPU time cost. In other words, the real problem of seismic history matching is the dimensionality of the problem. In many direct search problems, e.g. global optimisation, an increase in the number of unknowns makes the problem considerably harder to solve. This is so-called the '*curse of dimensionality'*. With the NA, the main affect of increasing dimension is on the topology of the Voronoi cells. The new approach is designed to improve exploitation and exploration with the NA especially in high dimensional problems.

Chapter 4

Schiehallion Field

Overview:

A description of the Schiehallion field is provided in this chapter. This includes geological settings, reservoir development, management, and static modelling. Regular acquisition of 3D and 4D seismic data over field life has been the key to advancing the understanding and resolution of fluid and pressure changes in the reservoir over more than 10 years of field development. Such information is very useful in order develop understanding of the reservoir and to make reasonable decisions for reservoir updating through history matching. A brief summary including some statistics from the Schiehallion field can be found at the end of this chapter.

4.1 Schiehallion Field overview

The Schiehallion Field is located 175 kilometres (110 miles) to the West of Shetland; 10 km from the Foinaven Field (see Figure 4.1). The Schiehallion and adjacent Loyal field were jointly developed by BP on behalf of the Schiehallion field partners; BP, Shell, Amerada Hess, Murphy Oil, Statoil and OMV, and the Loyal field partners; BP and Shell. The Schiehallion field together with Foinaven and Clair fields, form the frontier area generally termed as the West of Shetland. The Schiehallion field was discovered in 1993 by the semi-submersible drilling vessel Ocean Alliance drilling the third exploration well in block 204 (well 204-3). The field is located in blocks 204/20 and 204/25 of the United Kingdom Continental Shelf in a water depth of 350 to 450 metres (1,150 to 1,480 ft). The Schiehallion Paleocene turbidite reservoir sands lie at a depth of 1800–2064 m. Horizontal wells were steered through the four 10–50 m thick sand bodies to ensure that 300–1000 m of net rock is contacted to produce at a sufficiently high rates (Walder *et al.*, 1999; Dobbyn and Marcus, 2001; Govan *et al.*, 2006; Gainski *et al.*, 2010).

The oil is close to bubble point, and to prevent significant gas breakout and deliver sweep, sub-vertical water injectors are employed. However, the effective use of the water flood demands a high level of connectivity between injectors and producers. This is a significant issue in a turbidite system that is inherently heterogeneous. The field has been producing since 1998 through subsea horizontal wells, which are tied back to the Schiehallion FPSO (Floating Production Storage and Offloading vessel) (Parr and Marsh, 2000; Gainski *et al.*, 2010) .

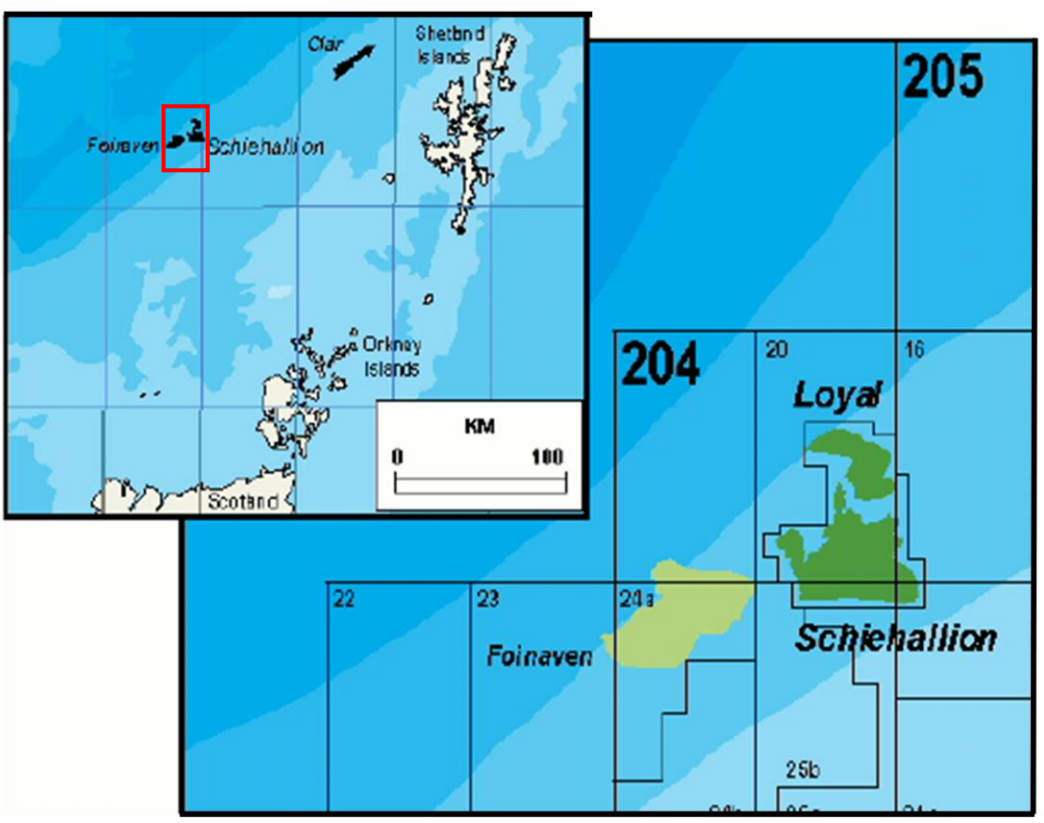

Figure 4.1: Location of the Schiehallion Field, to the West of Shetland (Parr and Marsh, 2000).

The multiple reservoir sands are siliciclastic turbidites, with seismic interpretation and attribute mapping revealing them to be highly channelised units. Reservoir quality varies in character from thinly interbedded sands to massive sands (Lancaster *et al.*, 2000), with the massive sands being of better quality. Classically, the sands are fine to medium grained, with 23–32% porosity and 250–2000 mD permeability. The Schiehallion reservoir fluids are geochemically mixed source oils, with oil gravity in the range of 22–28° API. It has been estimated that high levels of gas have come out of

solution in some areas, particularly early on in field life. Several seismic surveys have been acquired in Schiehallion (preproduction in 1993 and 1996, as well as monitor surveys in 1999, 2000, 2002 and 2004). .

4.2 Field Geology and Reservoir Characterisations

The operator named the Paleocene–Early Eocene sequence in the West of Shetland as the 'T-sequence'. More comprehensive and detailed descriptions of the Paleocene deep-water sandstones can be found in Lamers and Carmichael (1999). In this thesis, we use this convention in order to refer to the reservoir. The description of the T-sequence has been developed over the last two decades by incorporating seismic and well log data constrained by biostratigraphical analysis as seen in Figure 4.2. The Schiehallion reservoir is encapsulated within the T30 Paleocene Sequences, which are equivalent to the Andrew Member according to the North Sea lithostratigraphy and are represented as siliciclastic turbidite sandstones that are the result of the erosion of the uplifted Scottish Massif to the southeast (Lamers and Carmichael, 1999).

The T30 interval is also subdivided into a number of sequences (e.g. T31, T32), based upon well log and seismic data interpretation. Within these sequences, three different sets of episodes of sandstones depositions are known in the Schiehallion field, namely T31, T34 and T35, and contain the main reservoir of the field. Reservoir sand quality increases from thin interbedded sands to massive sands. The sandstone packages are fine to medium grained, and porosity ranges from 23% to 32%, with structure dip of 2–3° to the northwest, crossed by a series of east–west faults dividing the field into four structural segments as shown in Figure 4.3. In April of 1995, an Extended Well Test (EWT) was carried out in a high-angle well drilled in main channel sand in the T31 sequence to identify possible flow barriers at the edge of the identified channels (Richardson *et al.*, 1997). From the interpretation of the EWT, it was concluded that the reservoir is quite well connected throughout the main channel sands, with good communication of fluids within each segment defined by the structural interpretation. There also appeared to be some degree of decrease in the transmissibility in the areas around channel edges (Lamers and Carmichael, 1999).

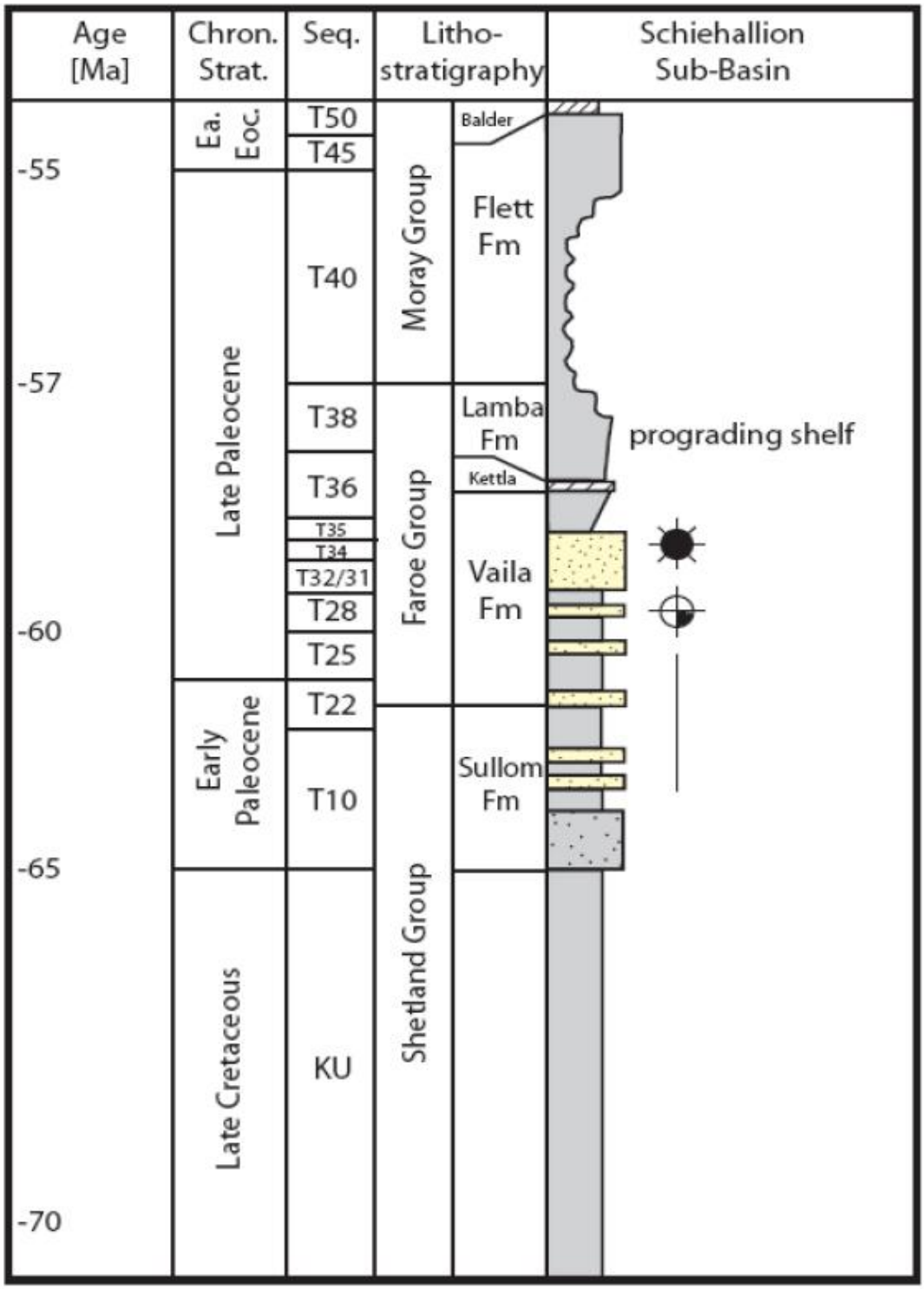

Figure 4.2: Paleocene stratigraphy template for the Schiehallion field and its relationship with the operator's regional stratigraphic sequence. (After Lamers and Carmichael, 1999).

Most of the oil in place in the reservoir that was mapped by the operator is located within the two southernmost blocks of the field (i.e. Segments 1 and Segment 4) as shown in the below figure. The density of faults in these two segments increases towards the west providing a possible flow barrier while in the east the throw of the faults is less than the thickness of the T30 sandstones reservoir. Over geological time scale, the main fault system that separates Segment 1 from Segment 4 does not represent a flow barrier. This was confirmed by geochemical analysis of the oil in the reservoir and flow gradient measurement in wells. Nevertheless, these faults could represent a flow barrier in terms of the life of the reservoir production time scale.

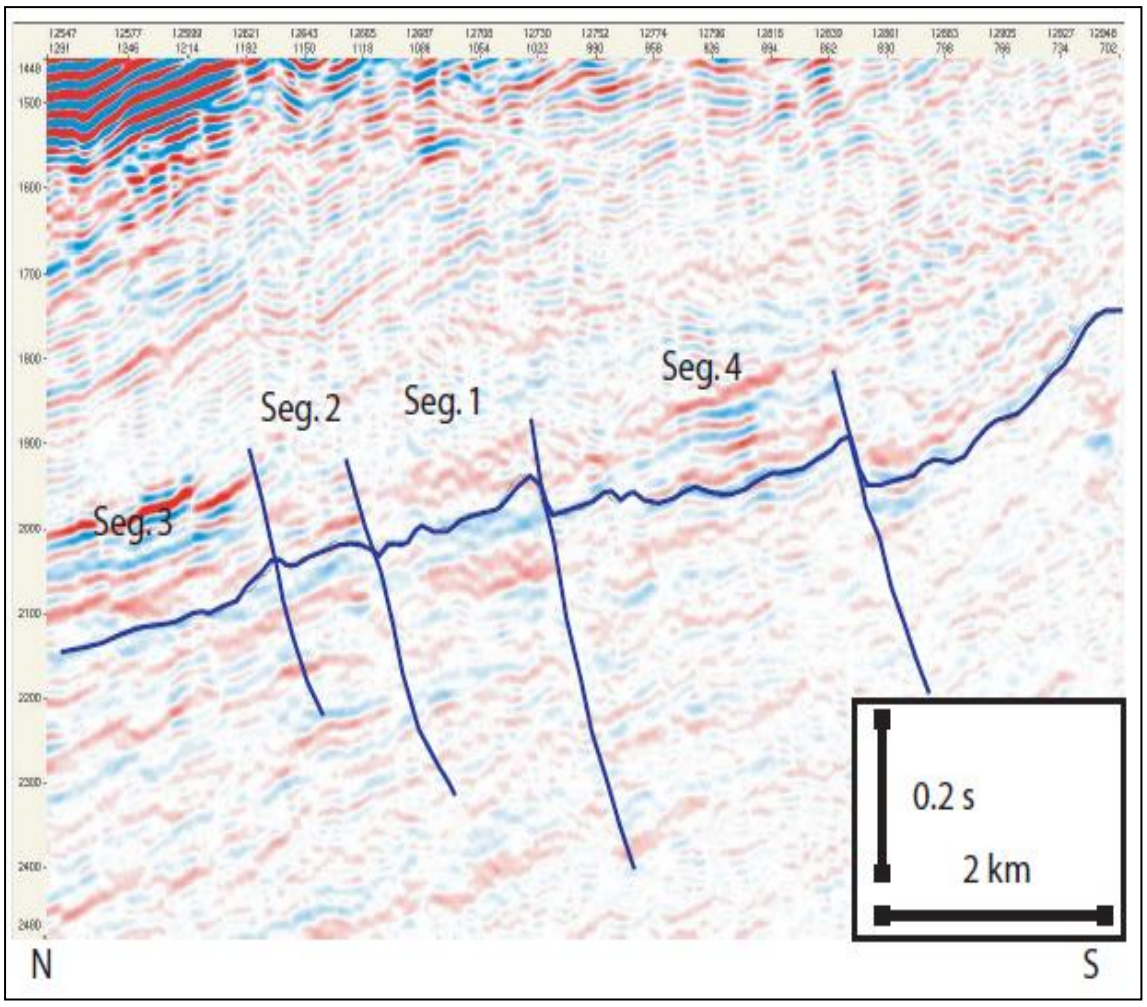

Figure 4.3: North-south cross section of the Schiehallion field, showing the reservoir segmentation through a normal fault system (Leach *et al.*, 1999).

4.3 Seismic Data - Acquisition and Interpretation

Several seismic surveys have been acquired in Schiehallion (pre-production in 1993 and 1996 as well as monitor surveys in 1999, 2000, 2002 and 2004). A 3D seismic survey was acquired over the West of Shetland covering 2000 km^2. Acquisition and interpretation of this data was used to determine the extension of the fields within this sub-basin and to plan the well location and appraisal approach for a later field development. An ongoing programme of seismic data acquisition is expected, whilst active infill drilling continues, with the next planned survey in 2012 and every two years thereafter. A 4D seismic survey involves a vessel towing a number of cables carrying hydrophones and air gun sources through the water column. The hydrophones record pressure waves generated by the air gun sources. No cables or equipment are placed on the seabed for the survey. The array's position within the water column is controlled by a series of flotation devices, which are remotely controlled by the survey vessel to ensure that the array remains at a constant depth below the sea surface. The survey vessel towing the air gun array will in general sail along around 100 or so prime sail lines, each of which will be on average 20 km in length and nominally 400 m apart. In order to prevent the array cables becoming entangled, the vessel will have to make a wide turn before commencing the next survey line. Each line turn is expected to take up to three hours to complete (Parr *et al.*, 1999; PBQuad204Project, 2010; Govan *et al.*, 2006).

The seismic signature of the reservoir for Schiehallion can be explained by the classical bright spot technology. When favourable physical circumstances are presented within the reservoir, seismic reflection can create effects that can be detected. For instance, local decreases in amplitude creates what are called dim spots while a local waveshape change can be identified as a polarity reversal or local phasing (Sheriff, 1992; Brown, 1999). This type of physical phenomenon depends on the impedance contrast being present in the surroundings of the reservoir. For a water-saturated reservoir rock with a lower acoustic impedance than the surrounding rock, the presence of hydrocarbons usually increases the contrast and a high-amplitude bright spot results, this is a very common situation for Tertiary clastics, (see, Benabentos *et al.*, 1975; Huston and Backus, 1998; Benabentos *et al.*, 2002) and has been applied also in 4D interpretation (Watts *et al.*, 1996; Parr and Marsh, 2000). As a result of this seismic characteristic, a

window based attribute extraction technique was used for interpretation of the spatial distribution of reservoir properties in the reservoir.

The map on Figure 4.4 shows the RMS (Root Mean Square) amplitude taken from the 1993 seismic survey in an asymmetric time window (-5/+25 ms) around the T31 picked horizon. The estimation of this time window was based upon the seismic calibration. It shows the main channel features with external meander geometries, spatial distribution and complexity of the reservoir for the T31 sequence. The T31 sequence shows by a decrease in acoustic impedance (or a high-to-low impedance contrast). As a consequence of this, the wavelet that represents the top of the reservoir can be identified in a trough-over-peak assuming zero phase and normal SEG polarity. In general, the impedance contrast is weak in the non oil-bearing regions of the reservoir but as we enter the mineralised zone this contrast is stronger as seen in Figure 4.5. Since the quality of the seismic data is very good, the distribution and complexity of the channels and facies can be obtained through seismic attribute interpretation. The central portion of the field has a low sinuosity channel system, perhaps showing a greater lateral stacking/amalgamation (Chapin *et al.*, 2000; Brook *et al.*, 1993).

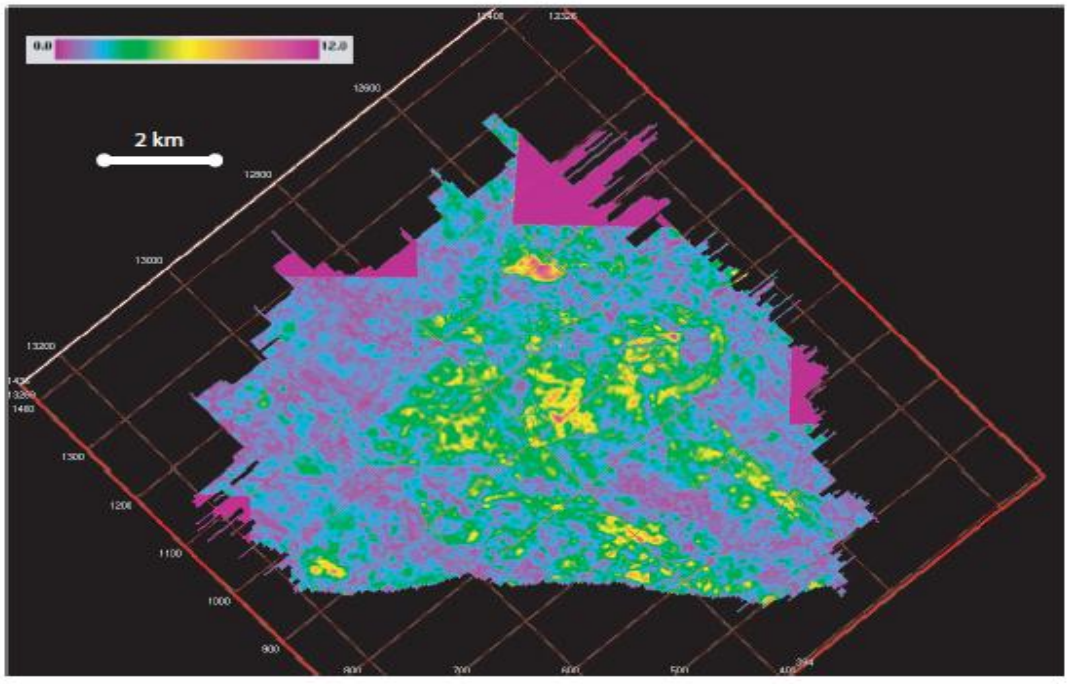

Figure 4.4: Map showing the RMS amplitude based on an asymmetric window taken from the 1993 seismic dataset. Note the channel complexity determined by the interpretation of the seismic data. The main channel features appear in the North-East and South-East of the T31a mapped reservoir (Chapin *et al.*, 2000).

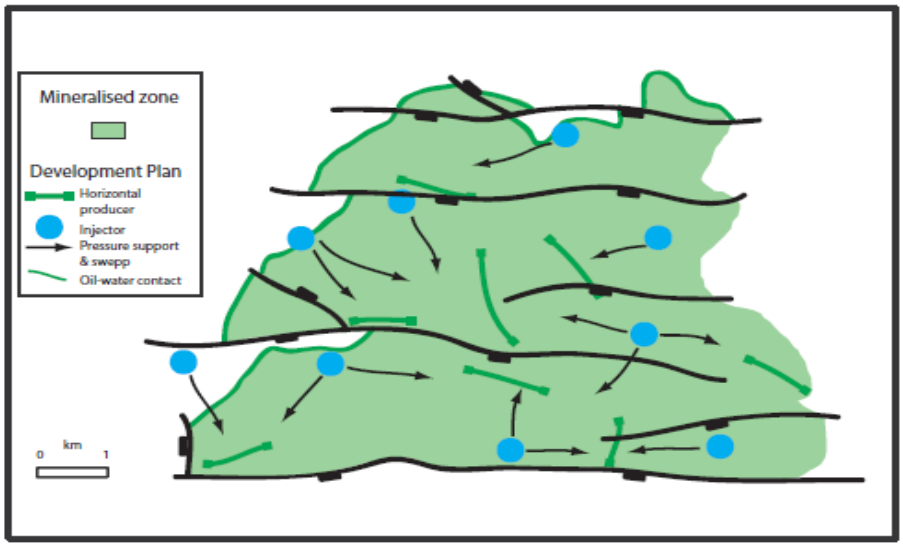

Figure 4.5: Mineralised zone, Schiehallion Field (Leach *et al.*, 1999). The impedance contrast is weak in the non oil-bearing regions of the reservoir, but as we enter the mineralised zone, this contrast is stronger.

The data set used in this thesis consisted of two P-wave seismic volumes: migrated stack and coloured inversion stack (A superior fast track method for the inversion of seismic data). The operators performed the process of cross-equalization, calibration, transformation of migrated stack and it was transformed by combination of phase rotation and filtering to derive coloured inversion stack (e.g. Figure 4.6). The main advantages of coloured inversion are ease of interpretation and quick inversion. The inverted data is used as a layer-based superior fast track attribute to evaluate the reservoir response. (Lancaster and Whitcombe, 2000). In addition, coloured inverted seismic data is being used to drive 4D attributes over the top and base T31a sand (e.g. Figure 4.7). By time-to-depth conversion, the location of the reservoir horizons were provided by the operator also and used to generate maps of Root Mean Square (RMS) attributes from the migrated stack by integrating the signal over a suitable time window. Then, the pre-production RMS attributes were mapped to Net:Gross (NTG), given the almost uniform porosity of the sand (Stephen *et al.*, 2006). Time lapse seismic data were obtained using differences of the RMS attributes of the migrated stack. These attributes were used as a pseudo-impedance to detect pressure and saturation effects via the time-lapse seismic map of differences between the surveys (Lancaster and Whitcombe, 2000). The attribute maps were normalised to the baseline by subtracting the mean and dividing by its standard deviation to get a comparable change in magnitude and signs between surveys.

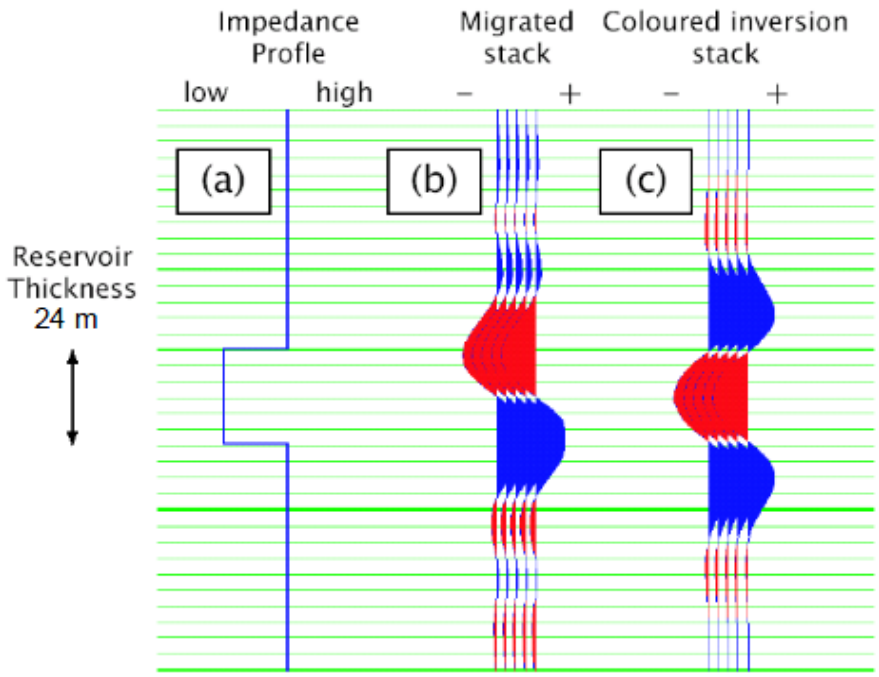

Figure 4.6: Coloured inversion schematic showing (a) a P-wave impedance profile with a thickness of 24 m (approximate thickness for our reservoir); (b) the zero angle seismic stack and (c) the coloured inversion stack. The reservoir is located between the two zero crossings for the case of the Coloured Inversion Stack and the shape of the wavelet is similar to that of the impedance profile (Stephen *et al.*, 2006).

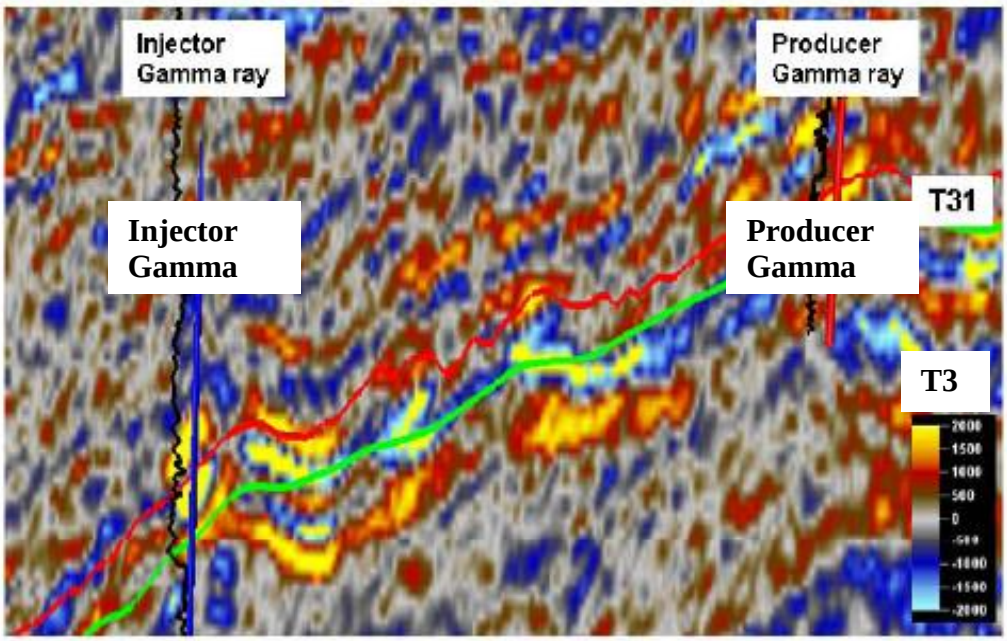

Figure 4.7: Coloured inversion product for the full offset migrated stack vintage 1996. The green and red lines indicate top and bottom of the T31a sand (Lancaster and Whitcombe 2000).

In the early years, the 4D response was dominated by gas breakout in many parts of the field, which is relatively easy to interpret. However, by 2004 the emphasis had shifted to imaging water movement. Therefore, a new seismic survey was planned for 2004 in order to help identify zones swept by water. However, feasibility studies have shown the 4D signal expected for water flood is smaller than the 4D signal for gas breakout. To optimise the potential for the detection of weak 4D signals over Schiehallion, the 1996 dataset was used as the baseline, thereby taking advantage of the acquisition improvements between the 1993 and 1996 datasets. Changes in water saturation give a more subtle 4D response and, in order to image it accurately, the 2004 survey was shot with a high specification and with great care to repeat the streamer locations corresponding to the 1996 preproduction survey. Figure 4.8 shows the Segment 4 where the resulting 4D difference maps clearly show the water movement in several areas of the field, notably from injectors CW15 and CW19 towards producer CP01 and from injectors CW13 and CW17 towards producer CP06 (Govan *et al.*, 2005).

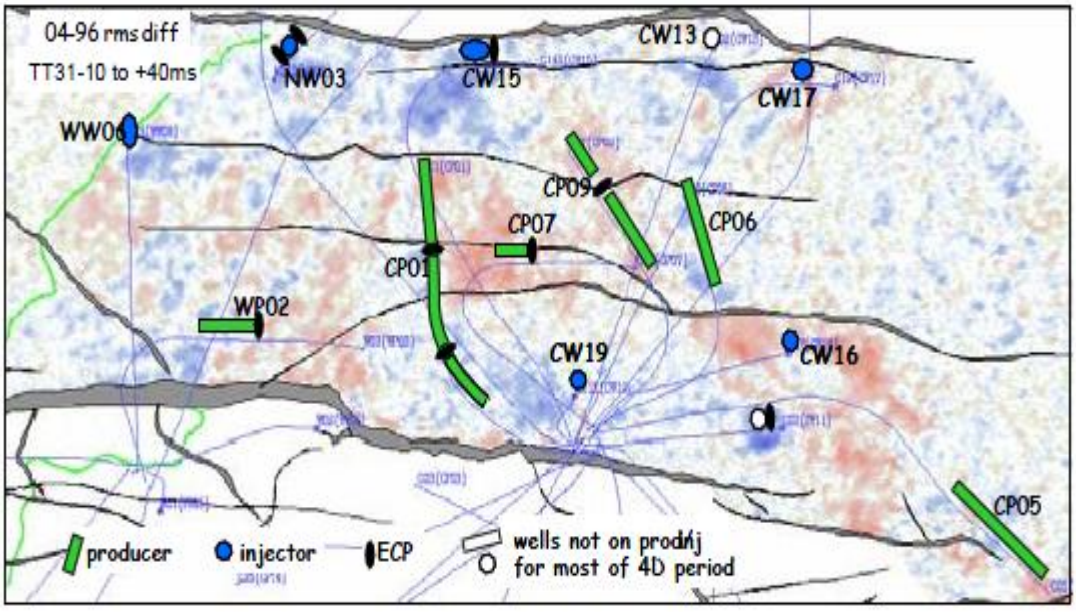

Figure 4.8: 4D difference map of Segment 4 (2004-1996) (blue = increased S_w, red = increased S_g or increased pressure) (after Govan *et al.*, 2005). ECP refers to Eastern Counties Pumps type.

4.3.1 Time-lapse Seismic Response

3D time-lapse seismic was successfully applied to the Schiehallion field in order to monitor changes in the dynamic properties of the reservoir. Following the successful results obtained from the Foinaven project (Cooper *et al.*, 1999a, b, c), in 1999 - and after one year of production - a third full 4D acquisition survey was acquired. Time-lapse signals were detected from pressure and saturation variations. Floricich (2006) introduced a full feasibility study to estimate the possible 4D signal expected between the 2004 and 1996 seismic surveys. A stochastic fluid replacement procedure was used to examine the impedance changes due to fluid saturation changes in the reservoir. The mean and standard deviation for the fluid properties were taken from the published literature for the Schiehallion area. Floricich (2006) concluded that the variations in acoustic impedance are due to the combined effect of changes in water saturation and reservoir pressure for the Schiehallion area in a rock of 27% porosity. An increase in reservoir pressure has an opposite effect to an increase in water saturation on the acoustic impedance change (Figure 4.9). In addition, the exsolution of gas within the reservoir, since pressure reached bubble point, has stronger effect on the impedances changes and thus the resulting effect is a decrease in the amplitude.

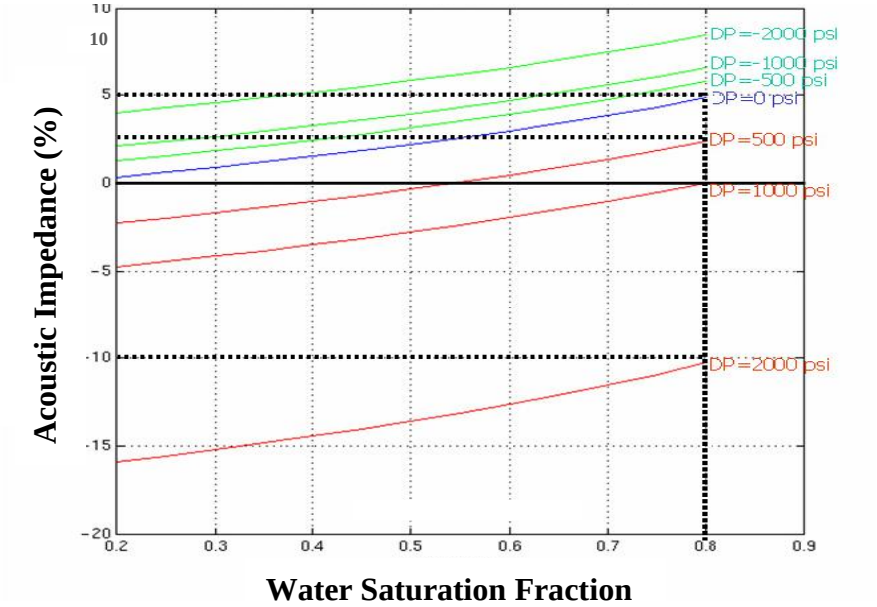

Figure 4.9: Estimated changes in acoustic impedance due to change in water saturation and reservoir pressure. (Floricich, 2006).

In the case of Schiehallion, an increase in pressure of 500 psi could reduce the acoustic impedance change due to water flood to half the value if no change in reservoir pressure is present. Most importantly, an increase in reservoir pressure of 1000 psi or more could mask the change in acoustic impedance due to water flood. The 4D signal is a combination of both effects, and separating and quantifying these production effects would provide additional value to the field reservoir management (Floricich, 2006).

4.3.2 Seismic coherency data derived barriers

Seismic coherency data were used to define possible barriers to flow in the T31 Upper reservoir (Macdonald *et al.*, 2004). Production data and 4D seismic surveys have shown that the Schiehallion field is compartmentalised: fluid is strongly impacted by non-fault related flow barriers. A total of 215 such barriers were mapped from the coherency data as shown in Figure 4.10. Initially they tried to discretise these barriers onto the faces of the simulation grid cells by treating them as surfaces in much the same way as the discretised shales. It is difficult to convert the seismic coherency picks into surfaces with a sufficient number of points on them to be able to definitely 'snap' the surfaces to the correct faces of the simulation grid cells: the coherency data picks tended to be inclined, and not vertical, making the surfaces true three-dimensional objects. To overcome this problem barriers have been represented vertically (in a simulation k-direction sense) and by approximately discretising them areally. Figure 4.11 shows a cartoon of the areal grid in (i,j) space, with the structural faults shown as the thick dark lines and all 215 seismic coherency data derived barriers shown as the thin dark lines (Leach *et al*., 1999; Macdonald *et al.*, 2004).

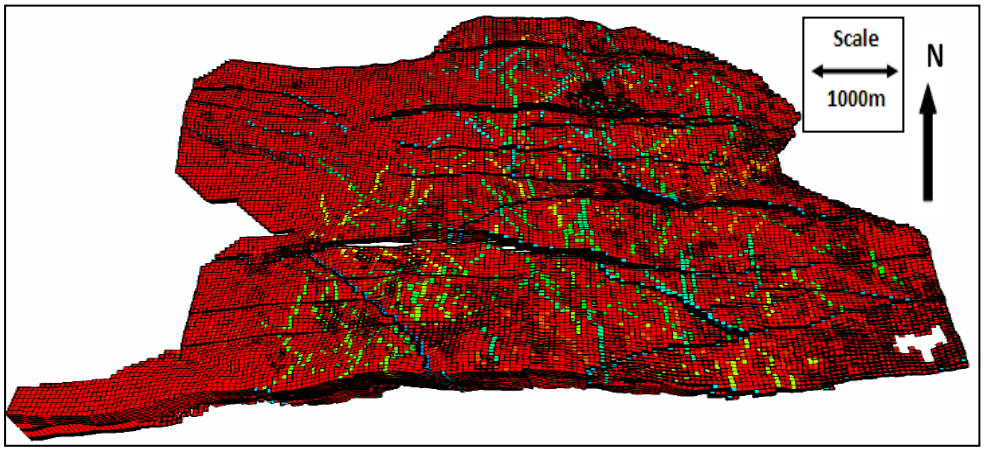

Figure 4.10: Top-view picture showing the x-direction barriers in the T31 reservoir (Macdonald *et al.*, 2004).

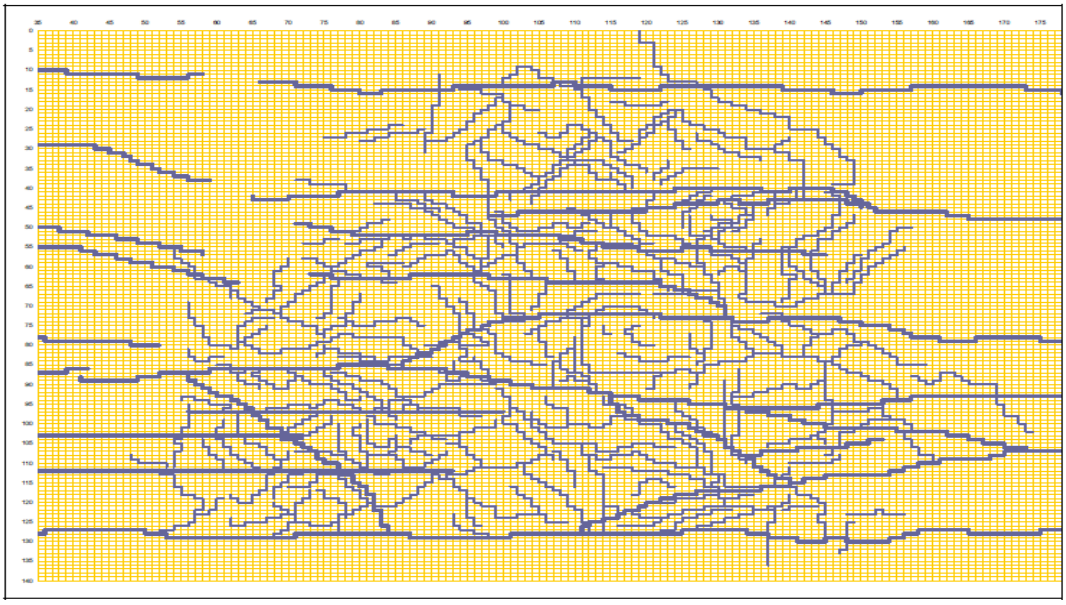

Figure 4.11: Schiehallion Field barrier network (Macdonald *et al.*, 2004).

4.4 Schiehallion Reservoir fluid properties

Fluids and conditions at the Schiehallion field are relatively favourable, i.e. the oils are not at a high temperature or pressure; they are classed as medium crudes and contain a relatively low proportion of volatile components. The Schiehallion reservoir hydrocarbon fluid has three phases (oil, gas and water) with gravity that varies between 22 to 28° API (Figure 4.12). The initial reservoir pressure is 2907 psia at a datum depth of 1940 m TVDss. Typical values for the gas–oil ratio (GOR) and bubble pressure are 342 scf/bbl and 2677 psia respectively. High wax content (9%) and asphaltenes (0.3%) results in high viscosities ranging from 1.5 to 4.5 cp (Figure 4.13). PVT properties have a high uncertainty, derived from the difficulty in obtaining single-phase samples, because the reservoir pressure is close to bubble point pressure (Leach *et al.*, 1999). There is a slow decreasing vertical variation on the gravity down to 1980 m TVDSS. Below this depth, this decreasing variation is more pronounced, probably due to the proximity of the hydrocarbon to the oil water contact at 2064 m TVDSS. A biodegradation induced trend also impacts on the fluid viscosity and gas-oil ratio observed on the wells. At the original reservoir pressure, and using the data available at start of production, the field appears to be close to the bubble point, and since there is no clear aquifer support, water injection must be provided to maintain reservoir pressure high.

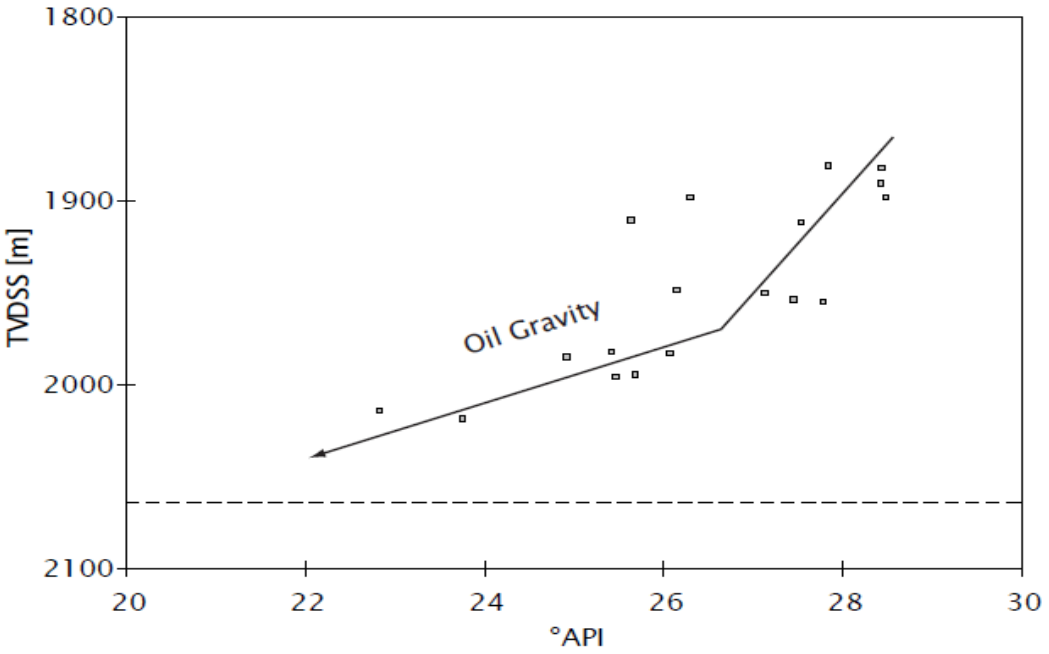

Figure 4.12: Operator's oil gravity trend as a function of depth. On dashed line, the OWC. After: Leach *et al.* (1999).

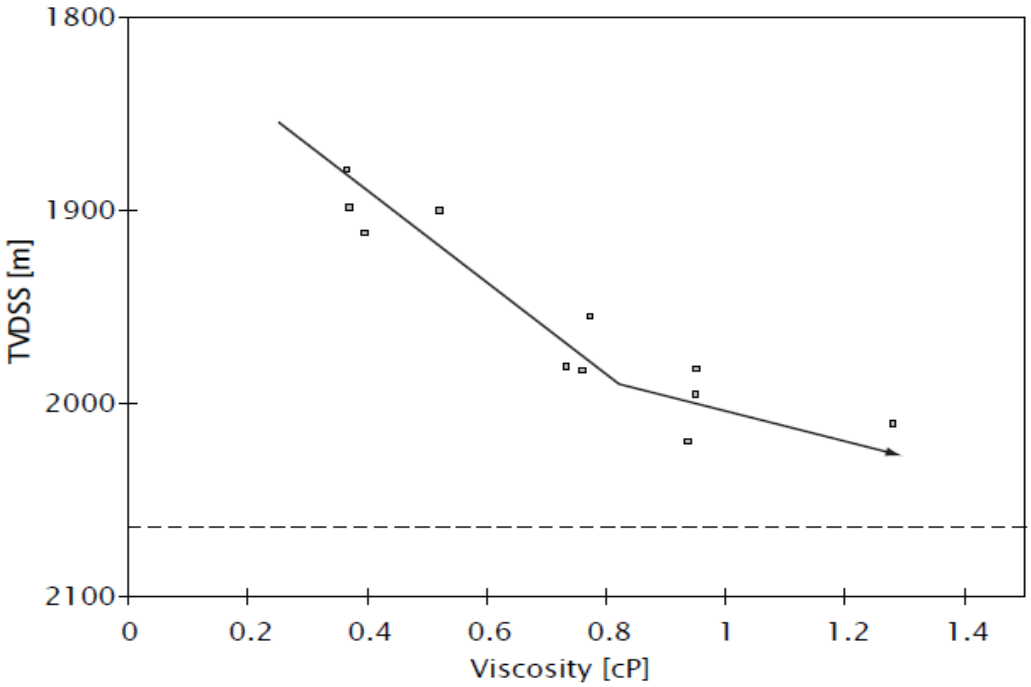

Figure 4.13: Operator's dynamic viscosity trend of stock tank oil as a function of depth. On dashed line, the OWC. After: Leach *et al*. (1999).

4.5 Field Development Strategy and Production History

The original development strategy aimed to avoid placing injectors and producers in the same channel, in order to avoid early water breakthrough and therefore to maximise sweep efficiency. However, owing to the poor connectivity, especially in the eastern part of the field, it quickly became clear that many of the producers did not achieve the pressure support from the injector wells. For the first 3-4 years, the reservoir management plan was largely about gas management, with a focus on the infill drilling of water injectors to recover reservoir pressure and reduce GOR production (Figure 4.14). The success of the infill drilling campaign has been driven strongly by effective use of 4D seismic and pressure data to understand connectivity. Based on seismic attribute analysis, the horizontal production wells are placed horizontally in the 10-50m thick sand bodies to ensure that 300-1000m of net rock is contacted so that the wells produce at sufficiently high rate. As the field has matured, water production has inevitably increased and the field water cut is now around 30%. Consequently, reservoir management focus has shifted to managing sweep and water cut (Fletcher *et al*., 2005). Water injection rates are constrained by plant capacity, and one of the levers for optimizing production is to optimize the water injection distribution among the available wells. Most of the injectors support more than one producer, and vice versa (see Figure 4.15), and the sweep pattern is further complicated by co-mingling of flow from two or three zones in some of the wells (Govan *et al.*, 2005).

The Schiehallion field and Loyal field produced over 2 billion barrels of oil in situ and have produced at rates of 140 Mstb/day of oil. The Schiehallion field alone had produced 212 MMstb by the end of 2004 (Fletcher *et al*., 2005). First oil was brought through flowlines from these drill centres into the purpose built Schiehallion F.P.S.O. (Floating Production Storage and Offloading) vessel in late July 1998. All producers have functioning bottom hole and wellhead pressure-temperature gauges. The injection wells all have functioning wellhead pressure-temperature gauges (Dobbyn and Marsh, 2001).

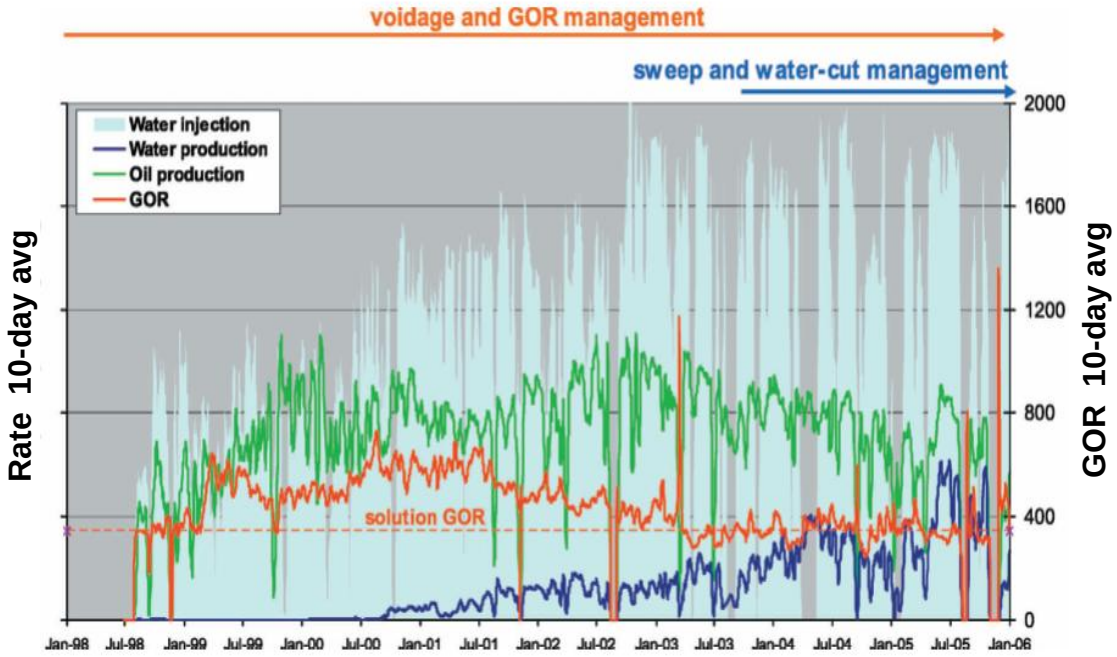

Figure 4.14: Production history of Schiehallion field including GOR, oil rate, water production rate and water injection rate (note: y-axis scale omitted for confidentiality) (after Govan *et al.*, 2006).

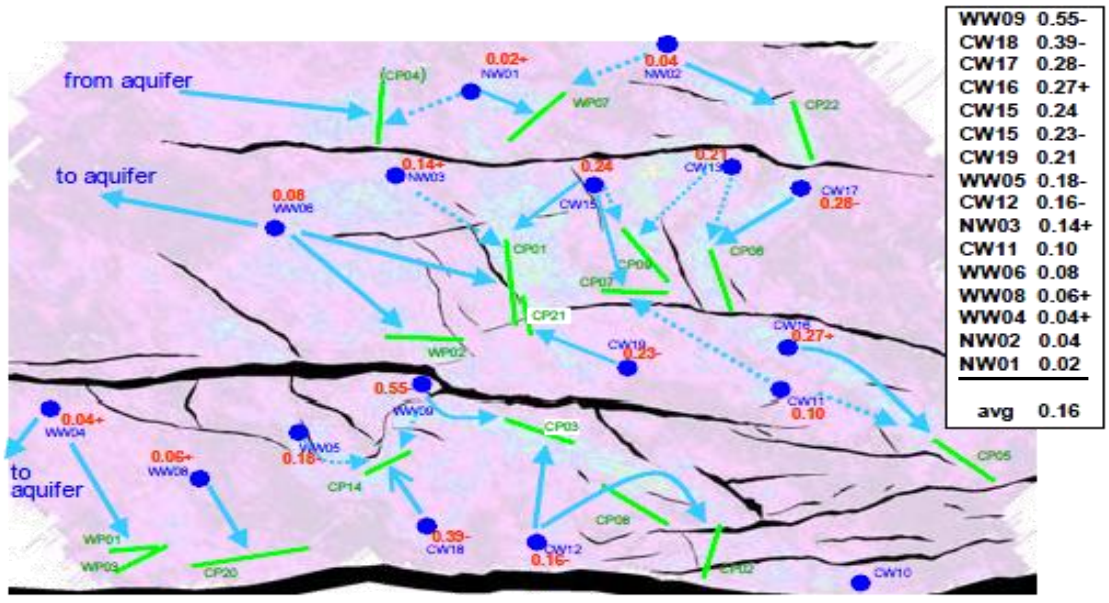

Figure 4.15: Map showing the development strategy for Schiehallion showing connectivity map with WI (Water Injection) value per well in bbls oil per bbl water injection (Govan *et al.*, 2004).

4.6 Aquifer representation

Initially, the operator applied an infinite radial analytical aquifer model to the western side of the model to provide aquifer support with 8 mD effective permeability as depicted in Figure 4.16. Subsequently, a numerical aquifer has been used on the western side of the model that has water-bearing cells with increased pore volumes, to provide aquifer support. These aquifer cells have an NTG ratio of 1, a permeability of 8 mD and a porosity of 20% (Macdonald *et al.*, 2004).

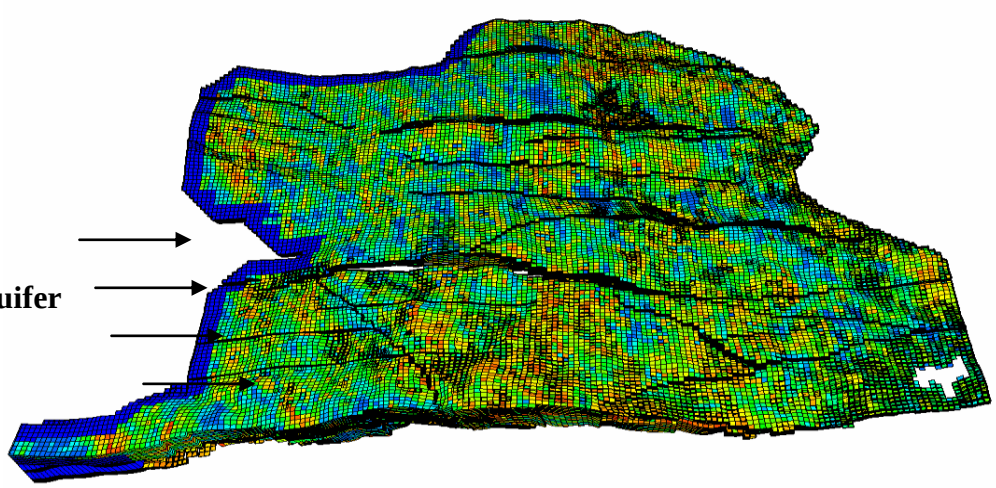

Figure 4.16: Location of aquifer cells (blue band on western side of model) (Macdonald et al., 2004).

4.7 Schiehallion reservoir model

FFM2000 static model was provided by the operator and it has been used by SHM project at Heriot Watt Institute. The operator provided another updated version of the static model called FFM2003 that we used in this work. The main differences are faults and barriers network in terms of the location and the density. The new model FFM2003 has more faults and barriers than the FFM2000 model and it has been updated as additional wells and reprocessed seismic data have been included. Therefore, the new model has been built with more data to improve planning of the field development. It is also needed for planning future seismic surveys. The final model was built in a fine grid scale vertically (typical cell size is 100 m × 100 m × 0.5 m) in order to obtain a detailed description. For the simulator to be used for field management, upscaling was applied to decrease computational run time.

In addition, incorporating new production and pressure data suggests a high degree of compartmentalisation. An object-based facies technique was used to construct the base-case geological model. It was constrained using depth converted seismic (Elastic Impedance) volumes (as in Leach *et al.*, 1999) and by the well data. The seismic data were used to identify large-scale channels and overbank regions as well as to guide stochastic facies modelling. Five genetic units in total were modelled, and geomodel cells were typically 100×100 by 0.5 m. The resulting facies distribution was found to compare well, qualitatively, relative to the Brushy Canyon outcrop, Western Texas, and also to maps of Net:Gross derived from seismic. Well logs and core plugs were used to derive porosity and permeability trends for each genetic unit, and these were then used to derive cellular porosity and permeability values.

4.7.1 Segment 4 - Simulation Model

The base-case simulation model for the field, supplied by the operator, took a day for full simulation using ECLIPSE 100, including 6 years of production, on a single 2.50GHz processor of our cluster with 3 GB of RAM. To reduce CPU time and the number of variables that should be varied for such a large model, we focused on a smaller independent sector of the reservoir as shown in Figure 4.17 (segment 4), which represents the T31 layer, which contains more oil compared to other segments. In this work, Segment 4 was extracted and then upscaled vertically to 8 layers by a factor of 4 using arithmetic averaging for NTG and porosity and geometric averaging for permeability to speed up simulation time. For history up to 2000, each Segment 4 simulation takes around 38 minutes while the upscaled simulation model takes around 9 minutes on 2.50 GHz processor. If we include six years of production up to 2004, then the simulation time will be about 150 minutes but only 22 minutes for the upscaled model. This sector contained 146 × 44 × 8 (26616 active cells typically measuring 100 × 100 × 6 m). Note that the segment was four cells thick vertically in many parts, but to the East side of the model, it extended to eight cells in the aquifer. The barriers and baffles have been represented vertically, in a simulation k-direction, and by discretising areally, so that they stair-step through the simulation grid at the top of the reservoir.

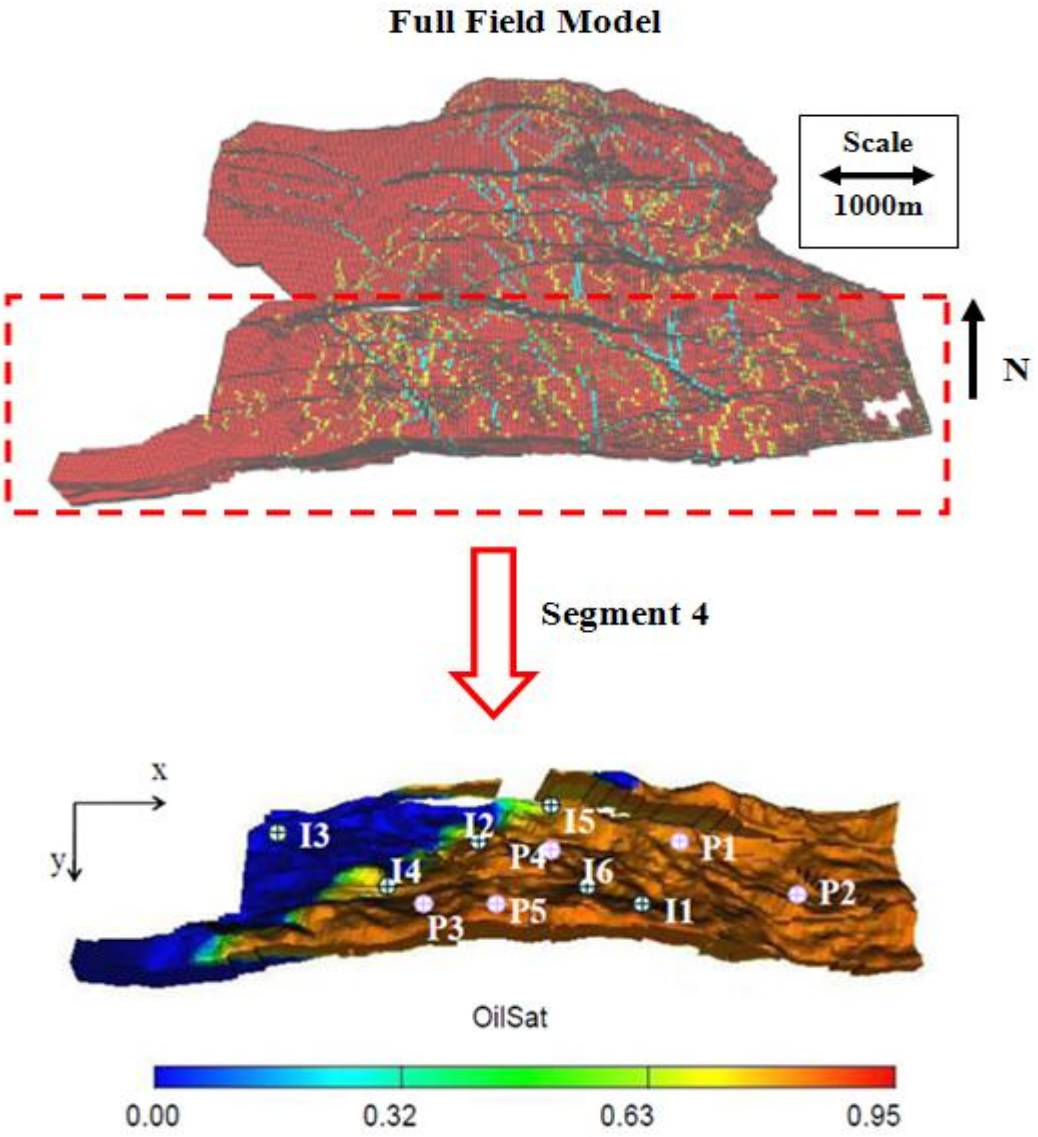

Figure 4.17: Location of the extracted Segment 4 in the Full Field Model (top figure) and the bottom figure is the reservoir simulation model of Segment 4. (Macdonald *et al.*, 2004).

The Segment 4 has been producing from August 1998 to now. However, in this thesis, we focus on the production history period up to 2004 and we have two pre-production surveys as baseline and four monitor surveys. There are eleven wells completed in the T31 sandstone sequence as shown in Table 4.1. In the model, the well controls were set to oil rate for producers and water rate for injectors. The observed seismic attribute maps for Segment 4 are depicted as differences in impedances for 6 time intervals in Figure 4.18. The difference between the baseline and the first-survey (1993-1999 map) shows a very strong effect around the injector I2, though not for I3, which was also

active in this period. The time-lapse effect around I2 appears to be pressure-dominated, with brightening of the RMS amplitudes of the migrated stack and dimming of the colored inversion occurring as a function of pressure buildup. Injector I2 was switched off just after the 1999 survey and the reservoir pressure relaxes back to equilibrium (Saxby 2001). In 2003, another newly drilled injector (I5) was switched on generating a pressure up signal. This has shown the effect of compartmentalization and poor well performance (Leach *et al*., 1999; Floricich *et al*., 2008). Additional time-lapse effects are largely caused by noise at the non-sealing faults. To sum up, there is clearly a high degree of compartmentalisation and heterogeneity, perhaps due to a combination of faulting and channelised structures in the reservoir, which is recognisable by 4D differencing (Stephen *et al.*, 2005).

Table 4.1: Well list for Segment 4 in the Schiehallion field for the history period starting from August 1998 up to August 2004.

Well Name	Type	Active Since
P1	Producer	July 1998
I6	Injector	July 1998
P4	Producer	July 1998
I3	Injector	September 1998
I2	Injector	November 1998*
I1	Injector	May 1999
P3	Producer	December 2001
P2	Producer	June 2002
I4	Injector	June 2002
I5	Injector	May 2003
* Switched off in September 1999		

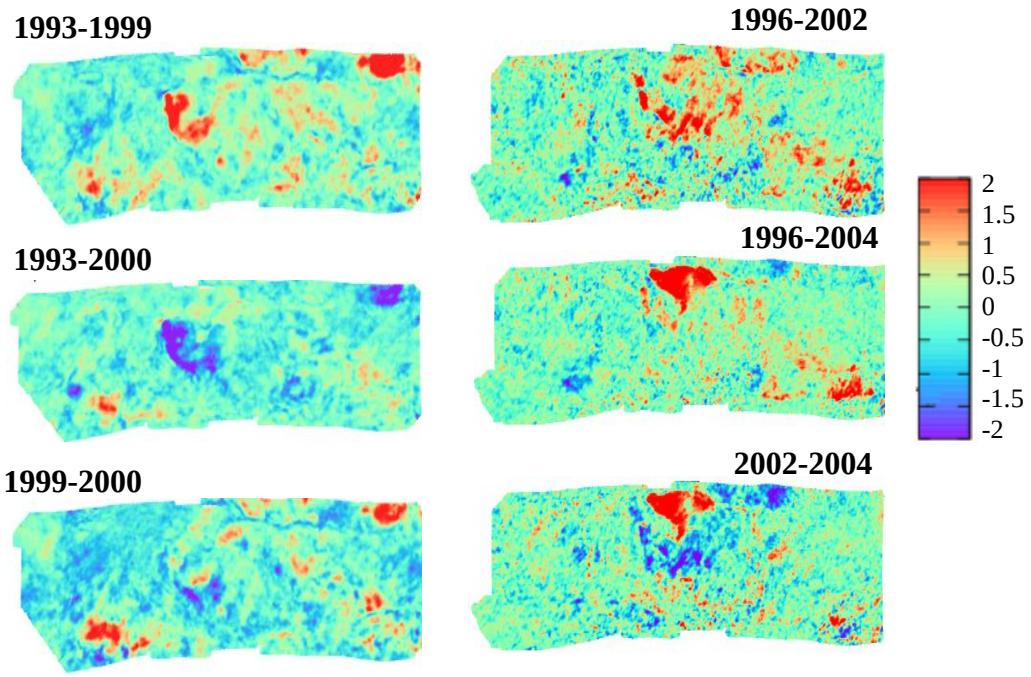

Figure 4.18: Maps of the observed seismic data as a difference in pseudo-impedance for 6 time steps. They show old minus new where, red indicates pressure up or gas displacing oil, blue indicates water displacing oil or drawdown. The 4D signatures are normalised by subtracting the mean (μ) of the pre-production maps in 1993 and 1996 and dividing by its standard deviation (σ), and differences are presented in this scale.

4.7.2 Identifying key reservoir uncertainties

The 2001 reservoir uncertainty study used a more sophisticated Monte Carlo approach than the 1999 study: it recognised that varying parameters independently could mask correlation effects and also that each sensitivity run would impact the quality of the history match. The following variables were investigated in the 2001 reservoir uncertainty study:

- off channel quality
- horizontal and vertical permeability
- NTG (net:gross ratio)
- gas mobility, oil viscosity and relative permeabilities
- connate water saturation
- maximum water cut
- voidage replacement ratio
- channel communication (barrier)

Experimental design techniques were used to reduce the full matrix of sensitivity cases and to look at the impact of varying more than one parameter at a time (Macdonald *et al*., 2004). In the Schiehallion field the physical barriers to flow are still a major uncertainty after 10 years of production. From the operators understanding and interpretation, they define some uncertain parameters. Updating of the fault transmissibility multiplier inversion was done by applying a single multiplier or scaling factor to a group of faults multipliers taken from the base case provided from the operator. A Single fault multiplier is difficult to use because of the high degree of uncertainty that the whole system has to changes of pressure and saturation. The first group of multipliers are taken from the neighbourhood of an active well, either injector or producer, in order to calibrate this first set of multipliers in the region where the largest change in impedance is expected (Soldo, 2004). Figure 4.19 illustrates the location of identified barriers (10 barriers labelled 'a' to 'j') around the injector I2 that we will update to improve the prediction of the seismic anomaly around that well in the seismic history matching in this study. In the base case, the transmissibility multipliers of 10 barriers were updated by setting to 0.001.

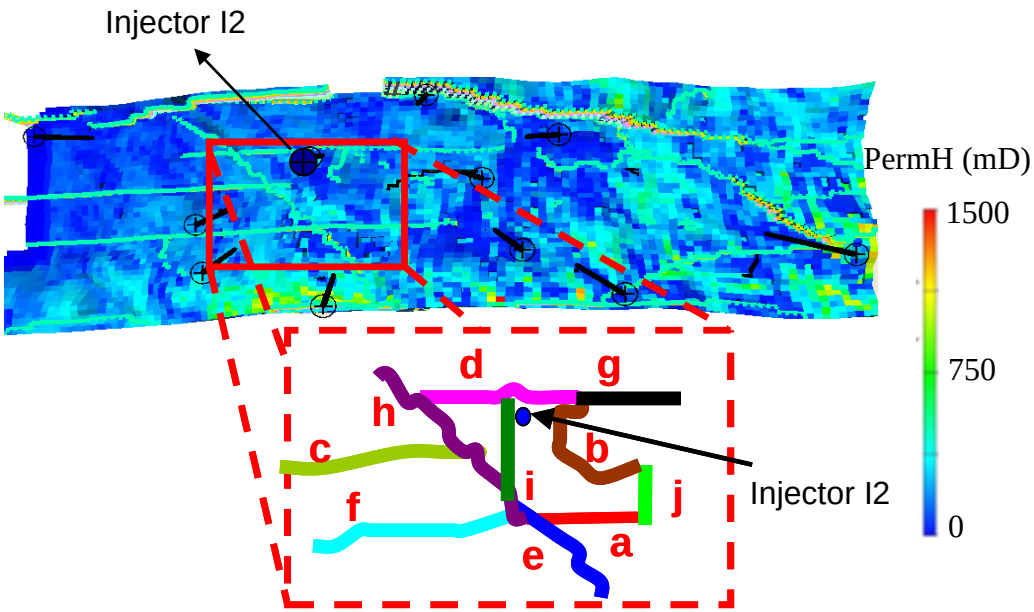

Figure 4.19: location of ten barriers around the injector I2 that can be updated to improve the prediction of the seismic anomaly around that well in the seismic history matching.

4.8 Summary

A brief description of the Schiehallion field was given in this chapter. This included geological settings, reservoir development & management and reservoir simulation model. Schiehallion field has four segments and we focus on Segment 4 to reduce simulation time. Geological barriers to flow are still a major uncertainty after 10 years of production in the Schiehallion Field. The Schiehallion Field development experience has clearly shown that compartmentalization can have a large impact on static and flow-connected volume estimates, and the associated development planning. A section on time-lapse seismic response and 4D signature analysis was also given, confirming that the seismic acquired in the field could provide qualitative data for interpretation and monitoring. In addition, the operator demonstrated that the Schiehallion field is a good candidate for seismic history matching as a static reservoir model.

CHAPTER 5

Verification of the Proposed Method

Overview

In this chapter, the new approach described in Chapter 3 will be verified using various synthetic test cases where we know the answer. Analytical functions along with a six dimensional problem will be applied to the original NA and NAPG to assess the behaviour of both algorithms in searching and sampling the parameter space. In addition, we will apply NA and NAPG on a higher (10D) dimensional case from the Schiehallion field. The results of the original NA and the new method NAPG will be compared based on the misfit evolution and parameters convergence. In this chapter, we will also develop different approaches to update the regression equation sensitivities to improve the performance of NAPG near the minimum.

5.1 Analytical Functions

There are many mathematical test functions in the literature to check the performances of optimization algorithms where the solution of these functions is known. The main aim of applying such analysis is to investigate the behaviour of the NA and NAPG in respect of finding the solution and the convergence rate. The following standard test functions will be used to investigate the performance of NA:

1. 6D-Fourth order polynomial function with two global minima
2. 6D-Branin Function

To carry out this test, the above two functions will be applied with three different scenarios; under sampled, well sampled and over sampled parameter space cases. In order to fill the space to the same degree, we should follow the rule of thumb for estimating n_i which is $n_i = 2^{nd}$ or $2^{(nd+1)}$ data points where n_d is the dimension of the problem. The NA parameters (described in Chapter 3, Section 3.3.1) for three cases are shown in Table 5.1. Generally, in low dimensions it will usually be possible to

oversample a parameter space and in higher-dimensional problems one will almost always undersample the space (Sambridge, 2001).

Table 5.1: Three different scenarios to assess both NA and NAPG.

Scenario	n_i	n_s	n_r
Under-Sampled	2	2	2
Well-Sampled	64	32	32
Over-Sampled	10000	128	128

5.1.1 Fourth Order Polynomial Function

A six dimensional fourth order polynomial is used to assess NA and NAPG algorithms. This function has two global minima in its usual two-dimensional form (n_d=2) as shown in Figure 5.1. The form of the 6D fourth order polynomial is:

$$y = (\theta_1 - 1)^2(\theta_1 + 1)^2 + \sum_{i=2}^{6} \theta_i^4 \qquad \underline{\theta} \in R; \tag{5.1}$$

$$\theta^{min} = \begin{Bmatrix} (+1 & 0 & 0 & 0 & 0 & 0) \\ (-1 & 0 & 0 & 0 & 0 & 0) \end{Bmatrix}$$

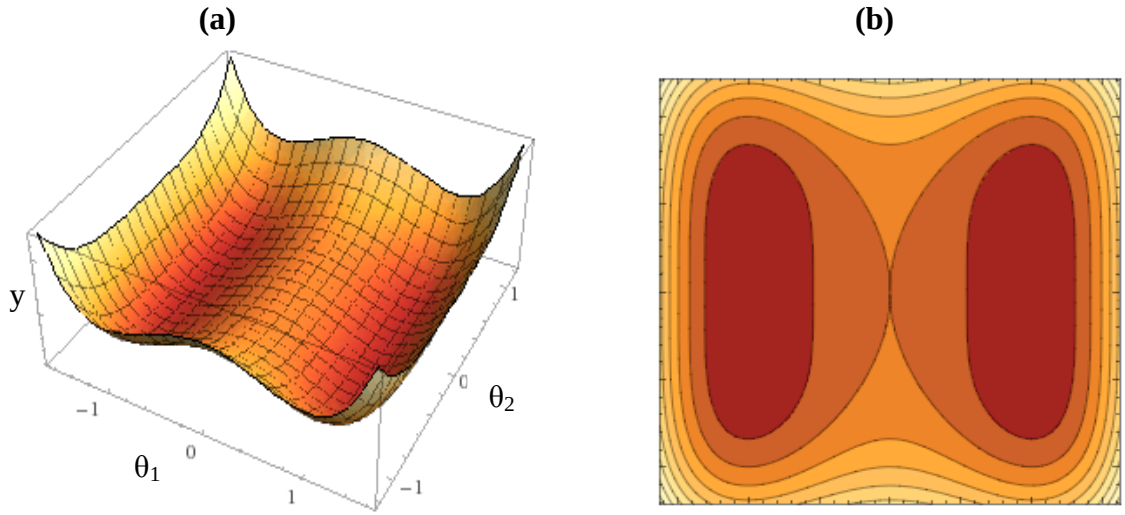

Figure 5.1: (a) fourth order polynomial plot **(b)** contour plot of the fourth order polynomial showing two global minima.

In this work, the NA and NAPG are applied to a 6D dimensional problem, which is a challenge, especially in respect of CPU time cost. The ratio n_s/n_r is kept to unity to achieve good exploration of the 6D parameter space. It can be seen from the misfit evolution of three scenarios that the convergence rate is considerably improved for the 6D fourth polynomial equation with NAPG comparing to original NA as shown in Figure 5.2.

For the under-sampled scenario, Figure 5.3 shows that NA and NAPG capture different solutions and they found only one minimum out of the two. This is because the number of best models resampled by the NA (n_r) is too low (under sampled), which causes the lack of concentration in the sampling. This scenario is the most likely in a high dimensional problem and should be avoided in real history matching applications. Therefore, it requires a larger number of initial models to saturate the parameter space and to capture both minima.

For the well-sampled scenario, the parameter convergence is better than the under-sampled case as both algorithms found the same solution as shown in Figure 5.4. This sampling strategy is the most preferable in real history matching applications.

For the over-sampled scenario, the NA and NAPG found the same solution but the rate of convergence is fast with the NAPG comparing to NA as seen in Figure 5.5. This sampling strategy should be also avoided as under-sampled case in real HM applications.

In Chapter 8, we confirm the above results of the three scenarios (under-sampled, well-sampled and over-sampled) using Neighbourhood Bayesian Inference algorithm (NAB) as the solution to the inverse problem from the Bayesian point of view is the posterior probability density function (PPD).

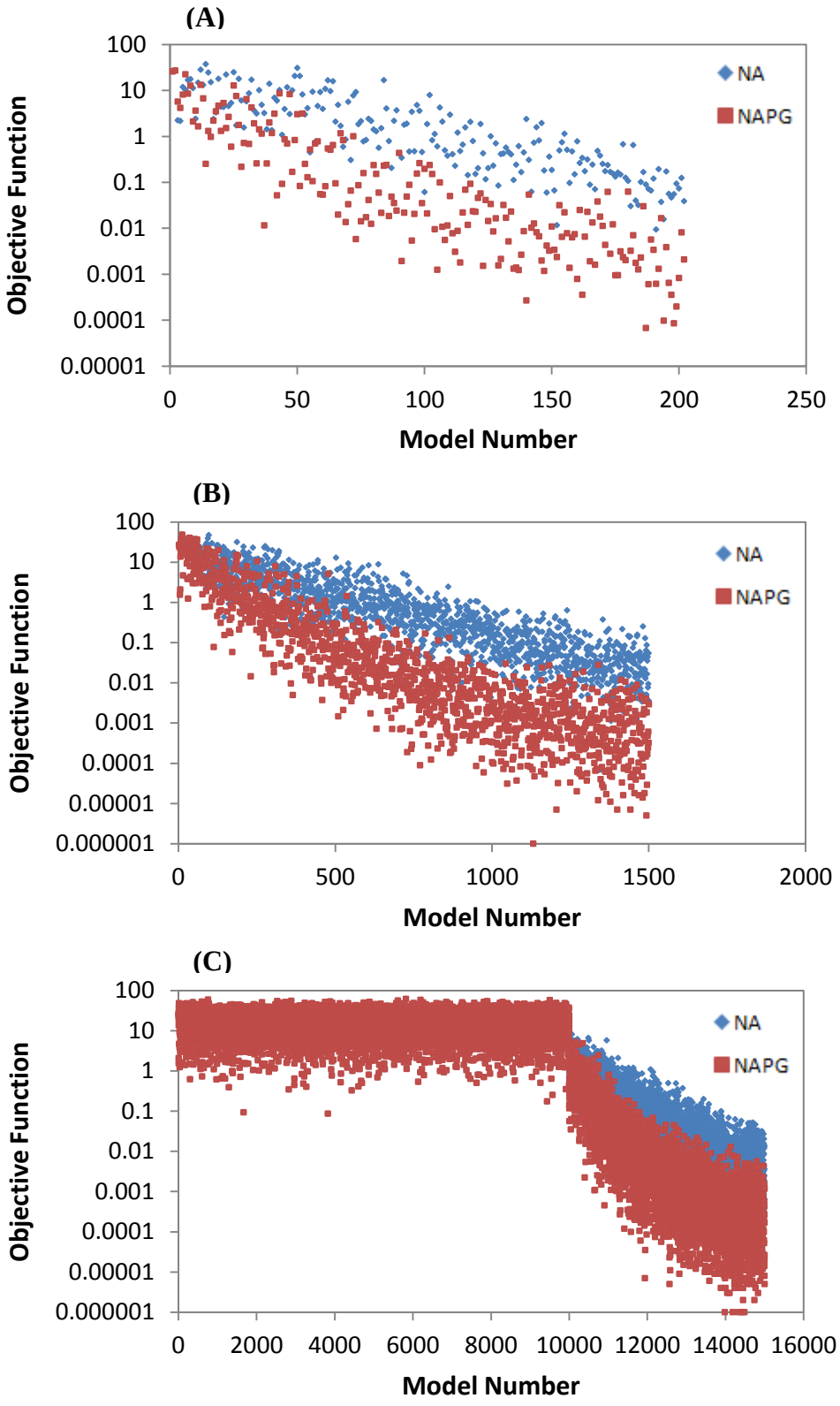

Figure 5.2: Misfit evolution when sampling using the 6D fourth order polynomial with two global minima as we have **(A)** under-sampled **(B)** well-sampled **(C)** over-sampled cases with NA and NAPG.

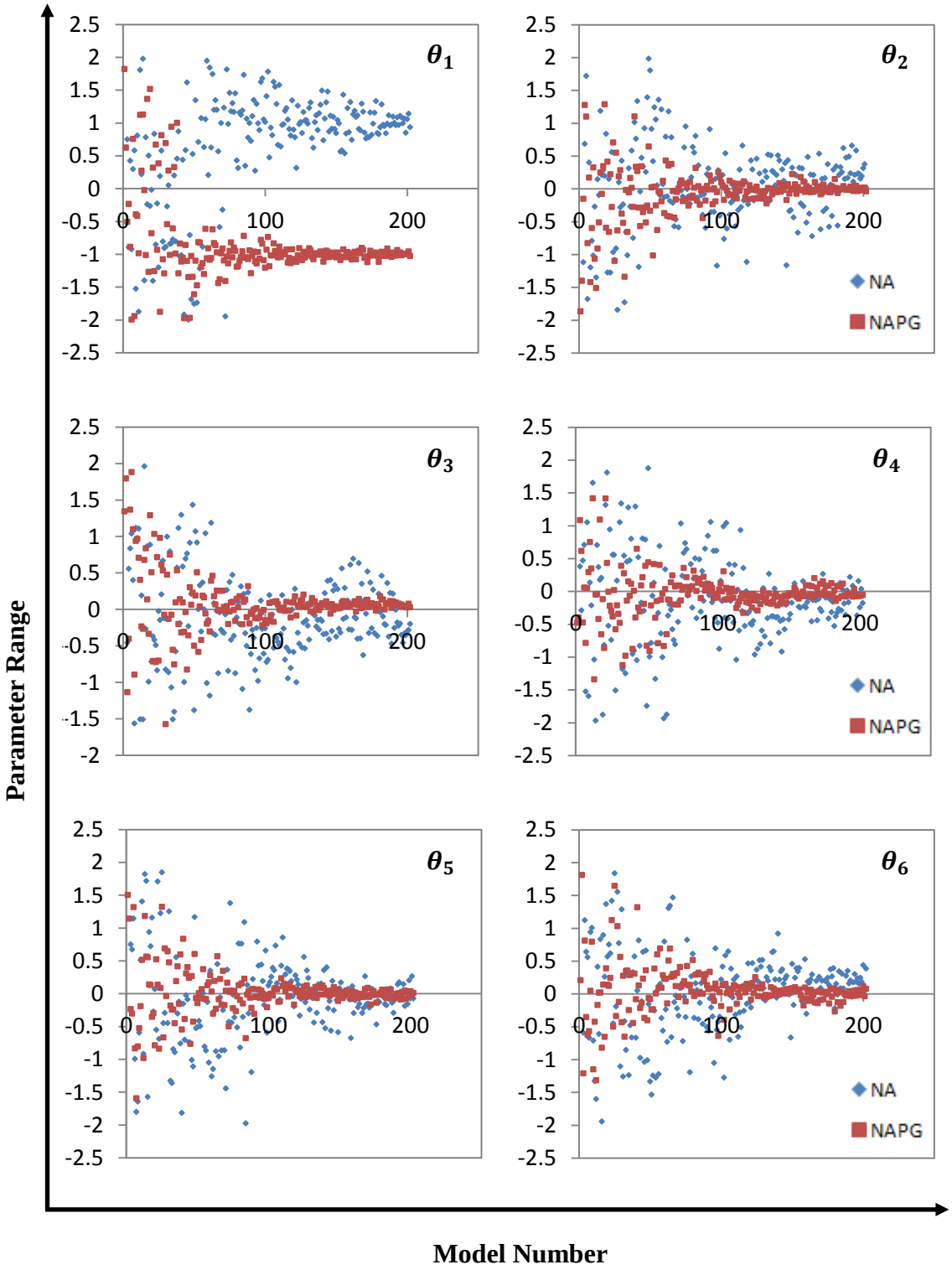

Figure 5.3: Under-Sampled case. Convergence of the 6-parameters for both NA and NAPG as we use the fourth-order polynomial function with two global minima.

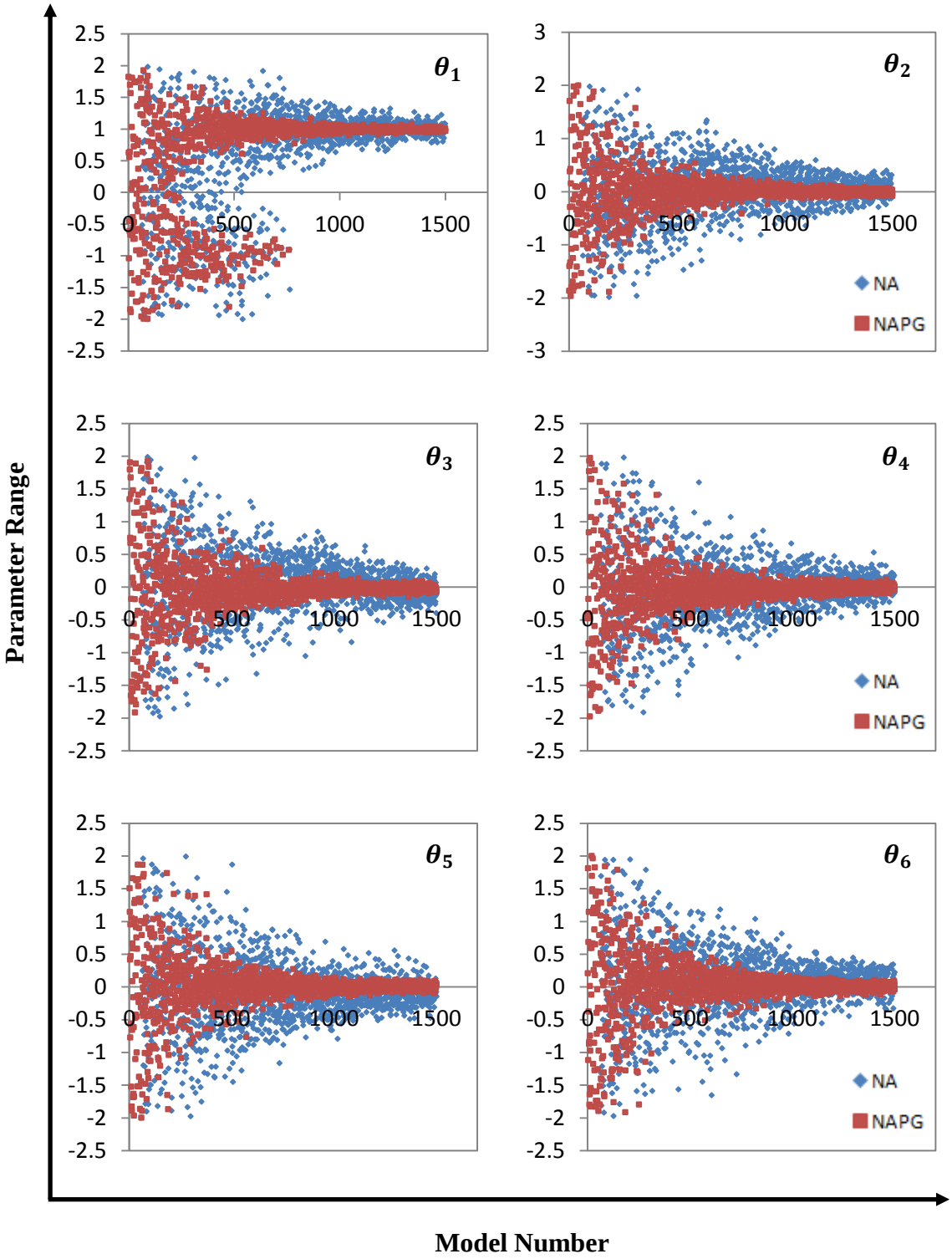

Figure 5.4: Well-Sampled case. The 6-parameters convergence for both NA and NAPG when we use the fourth-order polynomial function.

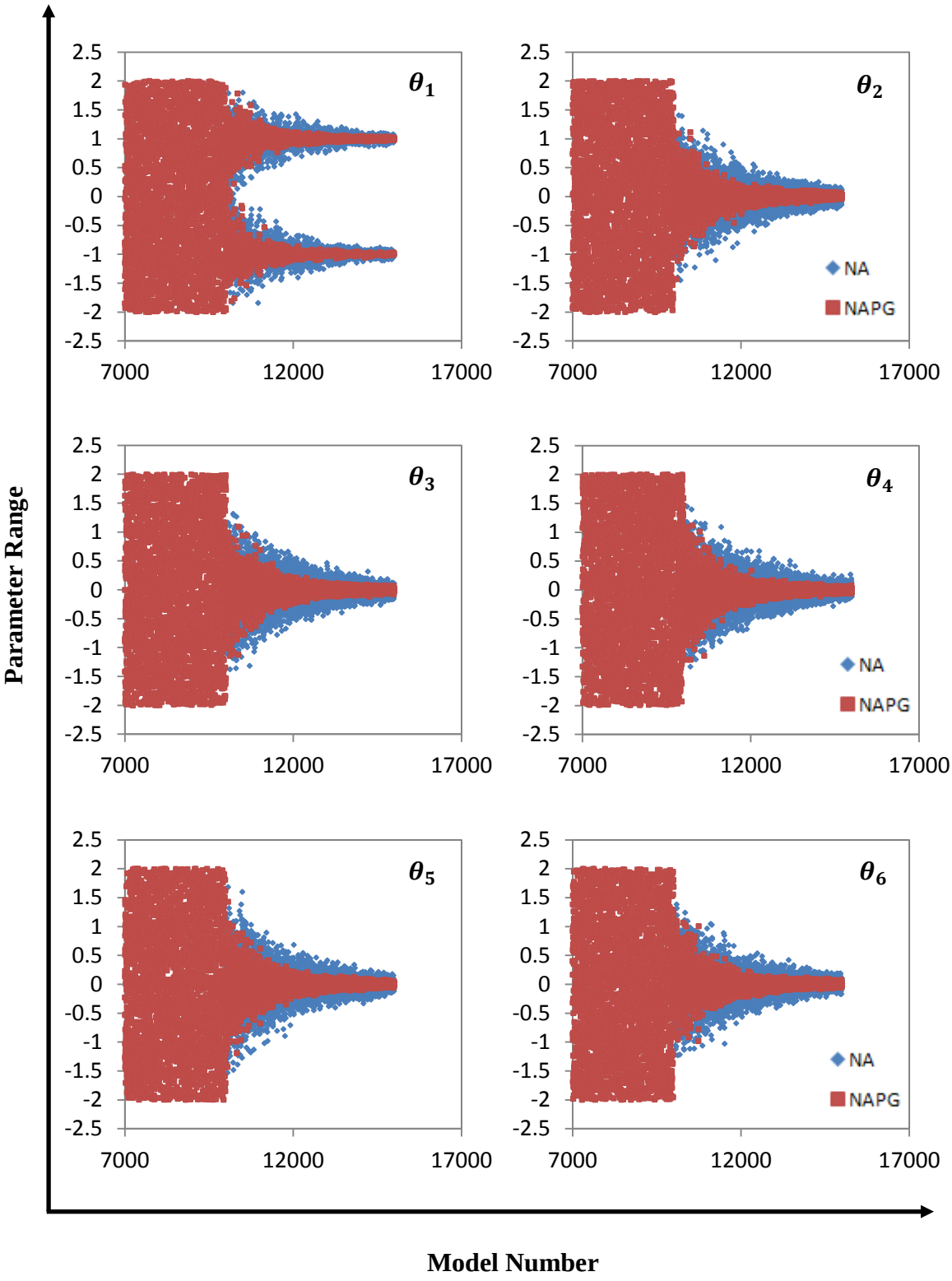

Figure 5.5: Over-Sampled case. The six parameters convergence for both NA and NAPG when sampling using the fourth-order polynomial function.

5.1.2 Branin Function

The Branin function is another mathematical function often used for testing optimization algorithms and has five global minima in its usual two-dimensional form (n_d=2). This function is more complicated than the previous 4th order polynomial function as shown in Figure 5.6 in 3D. We set up the equation as a six dimensional problem by summing it three times. We deliberately constructed this difficult problem as a test of the NA and NAPG methods. In 2D there are 5 global minima, in 6D there are 125 (Stephen and Arwini, 2010).

$$f(\theta) = \sum_{i=1}^{nd/2} (1 - 2\theta_{2i-1} + \frac{1}{20}\sin 4\pi\theta_{2i} - \theta_{2i-1})^2 + (\theta_{2i} - \frac{1}{2} sin2\pi\theta_{2i-1})^2 \qquad (5.3)$$

$$\theta^{min} = \begin{Bmatrix} (1.000000 & 0.000000), \\ (0.148696 & 0.402086), \\ (0.402537 & 0.287408), \\ (1.59746 & -0.287408), \\ (1.85130 & -0.402086) \end{Bmatrix} \quad \text{for each pair.}$$

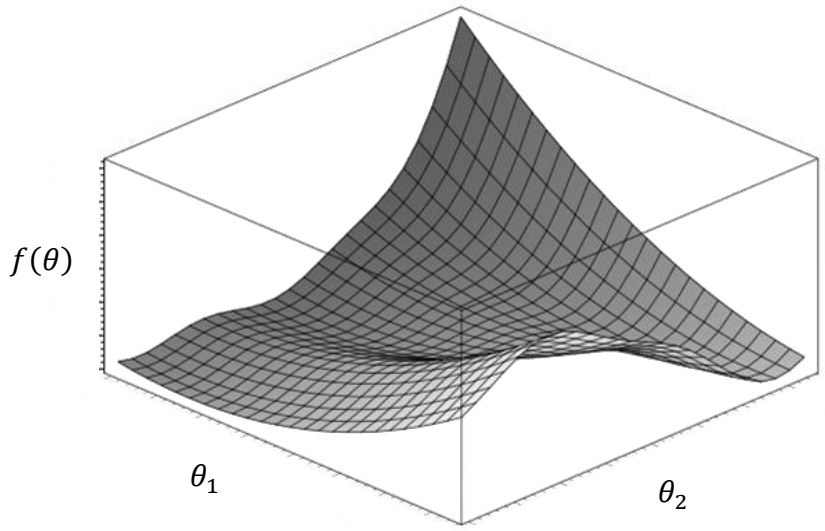

Figure 5.6: Branin function plot for n_d=2.

Although this function is more complicated than the previous polynomial function, our approach tended to speed things up somewhat compared to the original NA as showed in Figure 5.7. The parameter convergence of the under sampled, well sampled and oversampled cases is depicted in Figure 5.8, Figure 5.9 and Figure 5.10 respectively. We found that both NA and NAPG failed to capture all five minima and they required more tuning of the parameters (n_i, n_s and n_r) to explore the space sufficiently. Therefore, according to those sets of parameters in Table 5.1, both algorithms NA and NAPG found different solutions except for the oversampled case which captured most of the five minima.

Arwini and Stephen (2010) used a different choice of (n_i, n_r, n_s) for the 6D Branin function case with both NA and NAPG. They initialised the ensemble with 20000 models (n_i). Then they generated 256 new models (n_r) per iteration and. selected the best 128 models (n_s). Figures 5.11a showed that the misfit reduction is slow. In this figure, the first 20,000 models as these are identical in each case. The NAPG method has a tendency to speed up the convergence rate but the improvement for the NA was less apparent. Figure 5.11b shows that the multiple minima were sensed by the optimization routines and indeed, they have had to use quite large number of models to do this.

The study of the Branin equation is an example where NAPG offers some speed for more complicated response surfaces but still thousands of models can be saved with NAPG. For computationally expensive problems like history matching, it is desirable to reduce the number of models generated to minimise the objective function. This drawback will be solved by using experimental design to train a proxy model of the misfit so the proxy model can be obtained from experimental design approaches. The cost of the proxy model estimation is relatively cheap. Both NA and NAPG methods require a large initial sample of models anyway and so the estimation of the proxy model costs very little. In addition, the control parameters of the NA must be adjusted for each particular problem in hand where tuning requires trial and error, which is also costly.

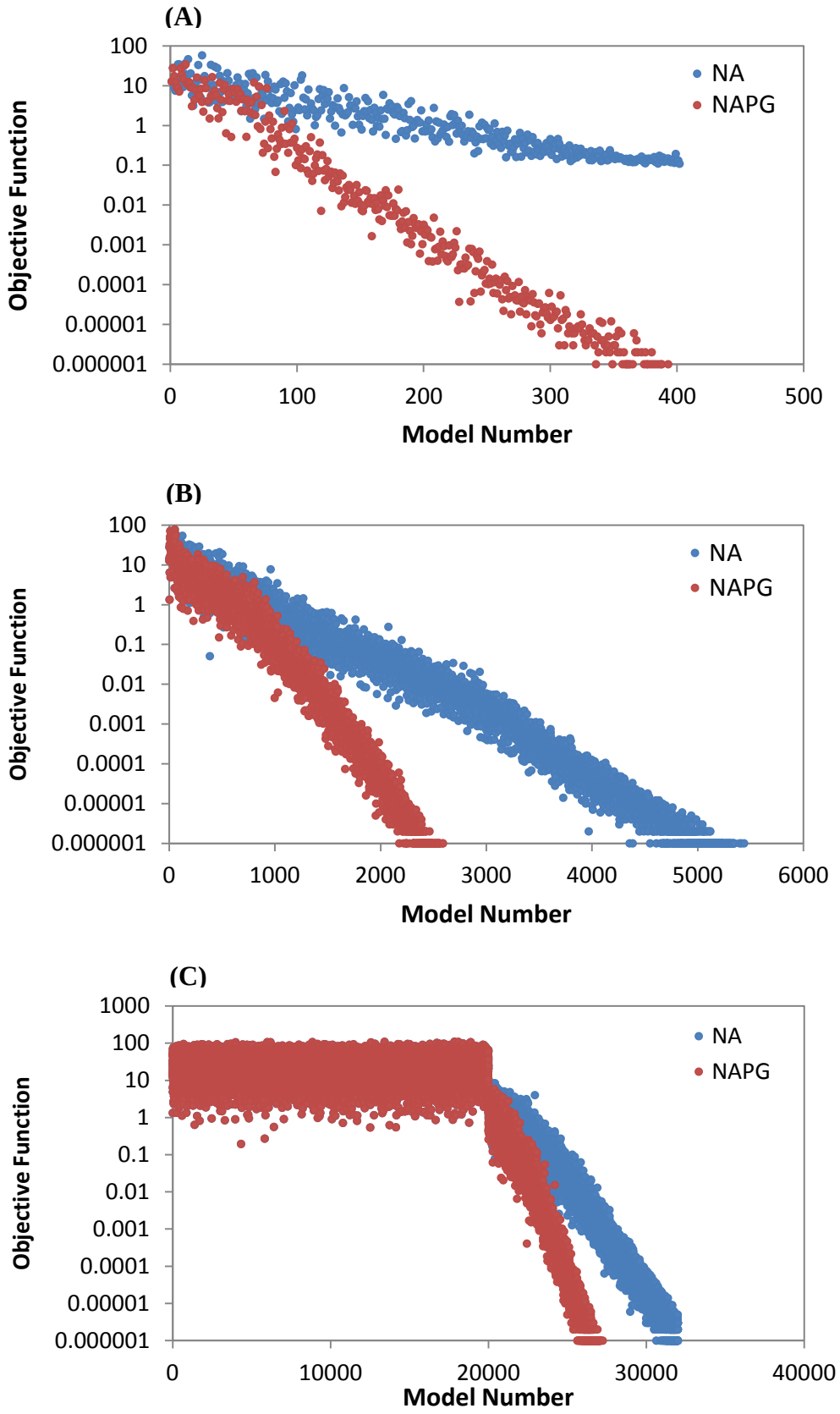

Figure 5.7: Branin function in 6D case. Misfit evolution for both NA and NAPG for **(a)** Under-sampled case **(b)** Well-sampled case and **(c)** Over- sampled case.

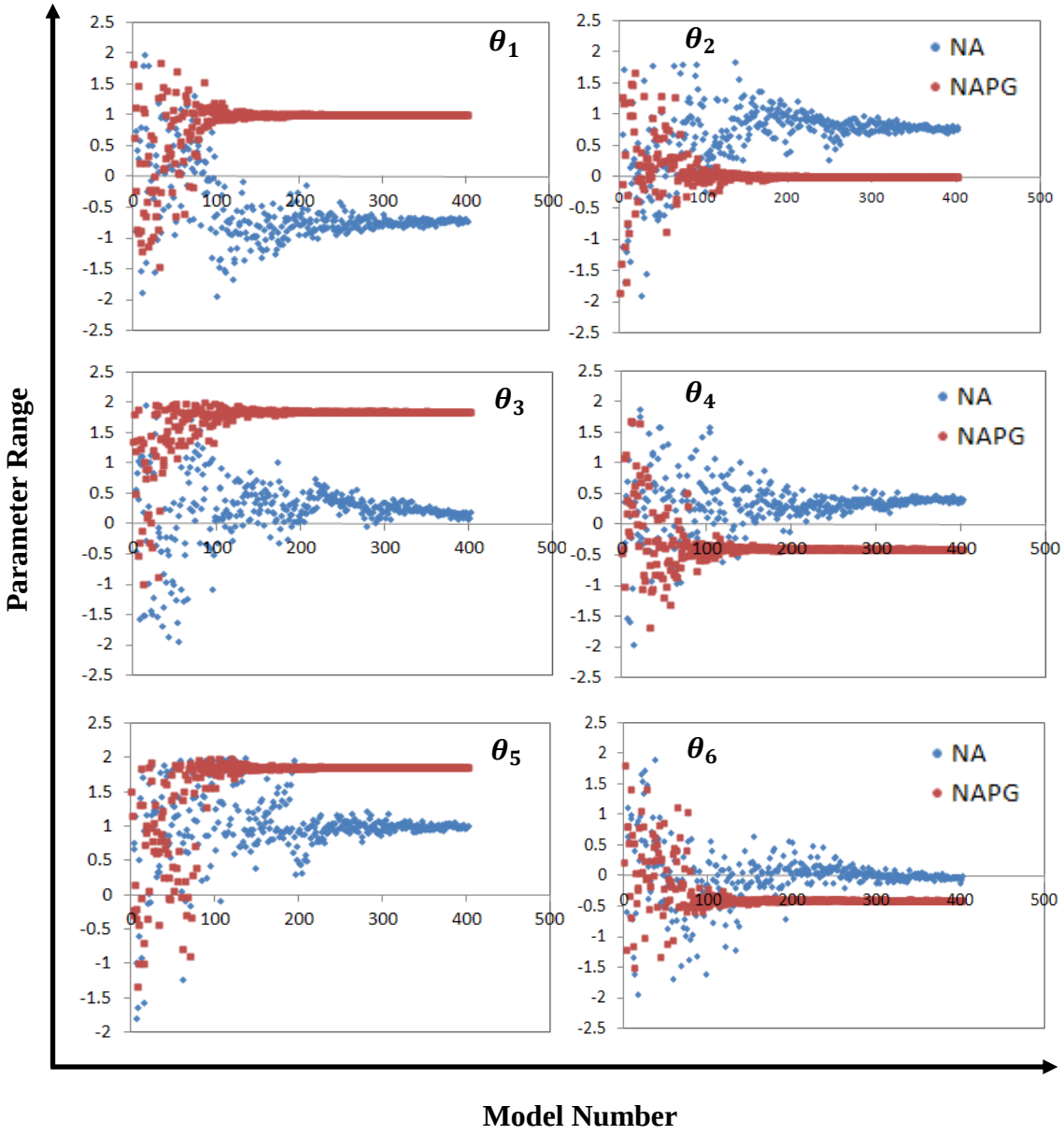

Figure 5.8: Branin function in 6D case - Under-Sampled case. Convergence of the six parameters ($\boldsymbol{\theta_1}$ to $\boldsymbol{\theta_6}$) for NA and NAPG. As the space is not sufficiently saturated, they found different solutions.

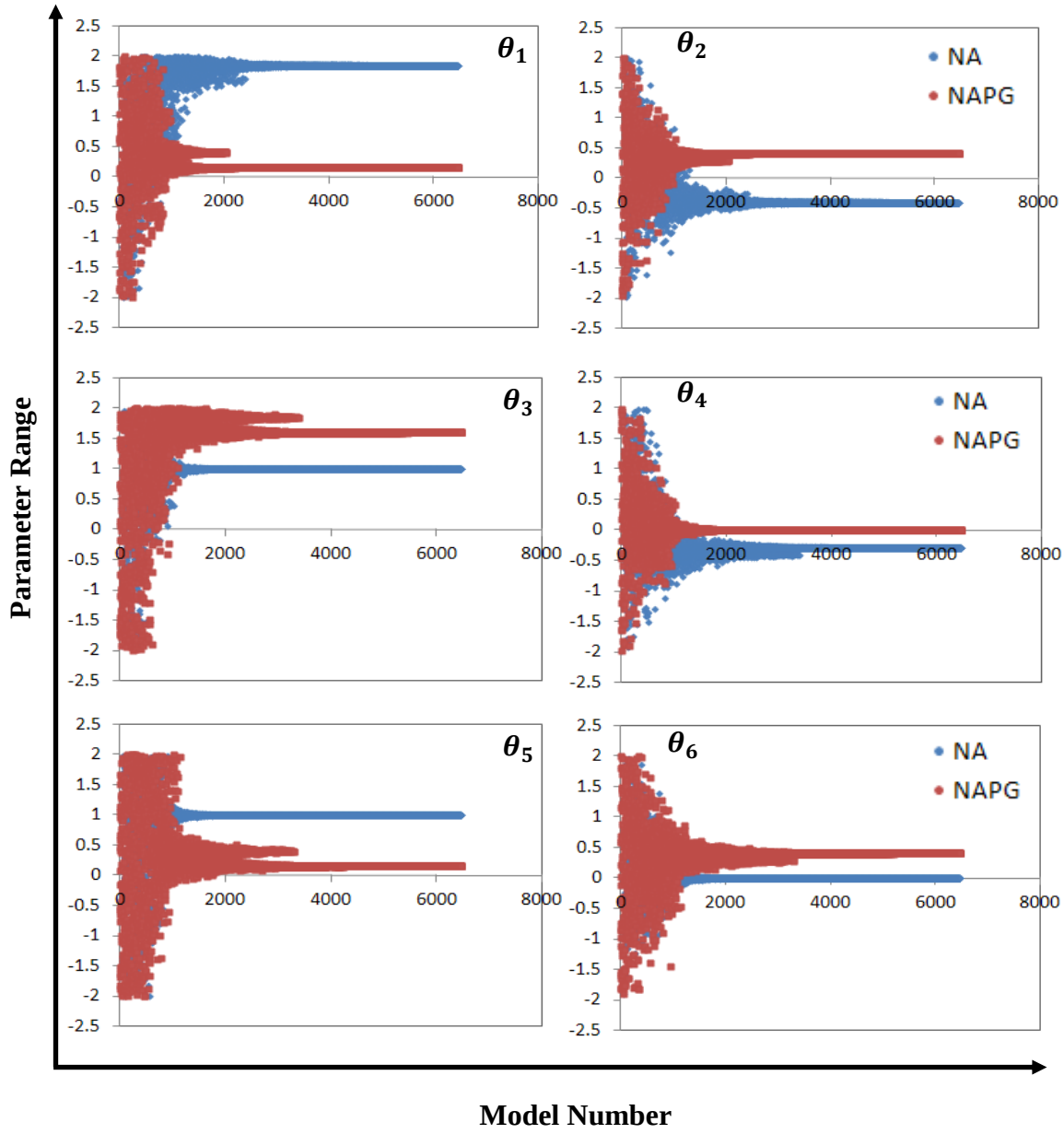

Figure 5.9: Branin function - Well-Sampled case. The six parameters ($\boldsymbol{\theta_1}$ to $\boldsymbol{\theta_6}$) converge for both NA and NAPG. Both algorithms also found different solutions when the space is not sufficiently saturated.

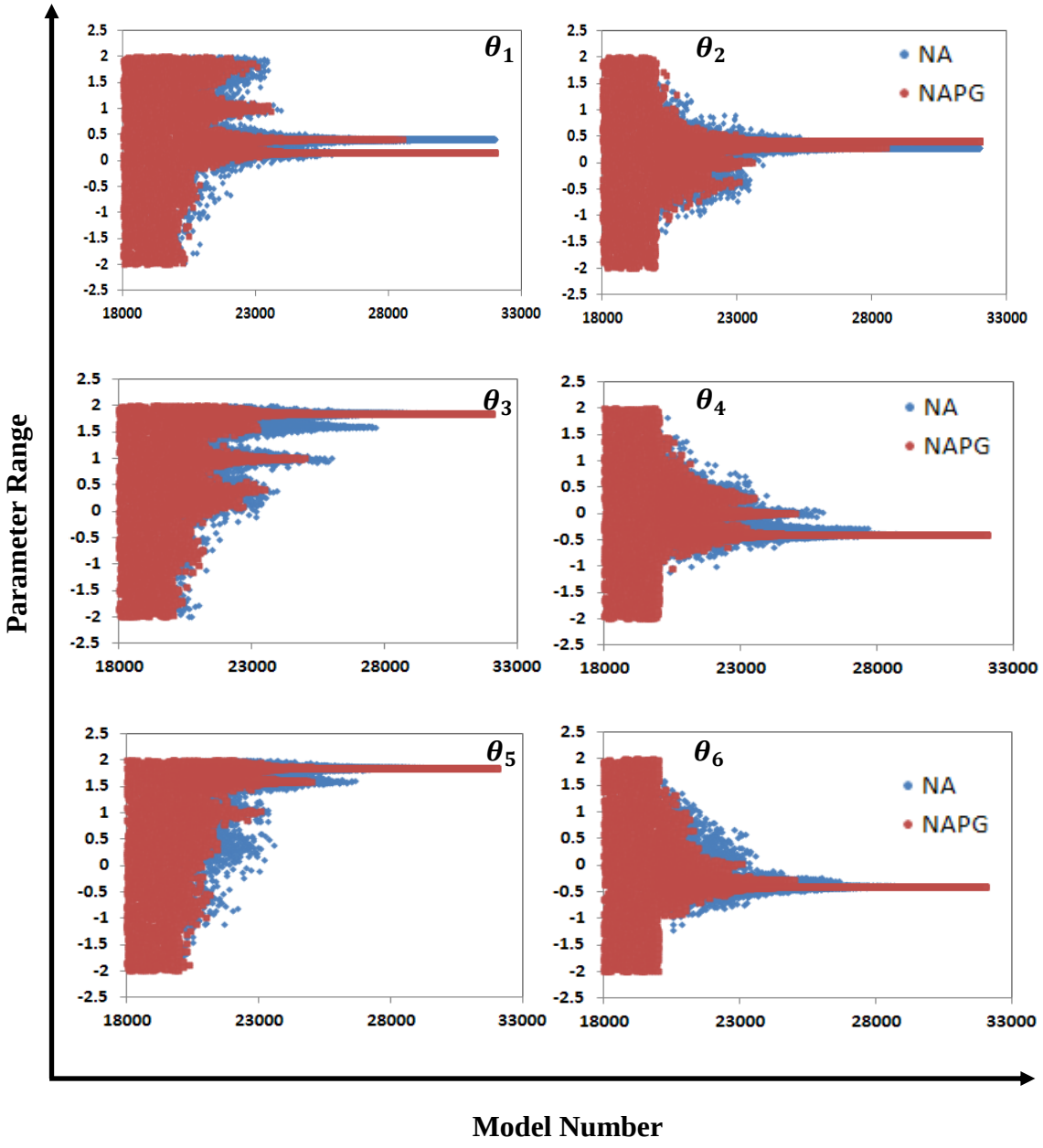

Figure 5.10: Branin function in 6D - Over-Sampled case. The six parameters ($\boldsymbol{\theta_1}$ to $\boldsymbol{\theta_6}$) convergence when sampling using NA and NAPG. When the space is over saturated, both NA and NAPG found the same minima.

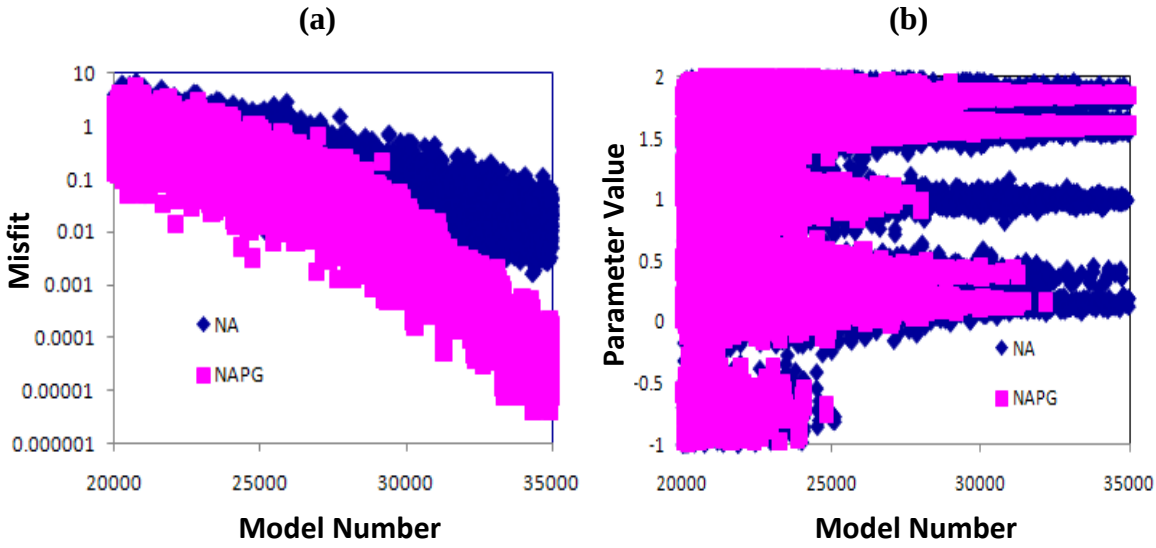

Figure 5.11: 6D Branin misfit function **(a)** Misfit convergence of NA and NAPG **(b)** Parameter evolution plots. The first n_i models are not shown and the number of models required reflects the complex multi-minimum problem (Arwini and Stephen, 2010).

5.2 Case Study I: 6D Simple Model

The first simulation case consists of synthetic case analogous to the Schiehallion field and the model is very fast to run. The simulation grid size is 25 x 25 x 4 and the simple grid allows for the cross-sectional modelling of a waterflood between vertical injector and a horizontal producer as shown in Figure 5.12. The reservoir has a uniform porosity of 20%. The reservoir pressure was maintained by water injection, and the producer well was controlled by liquid rate with production rate of 18000 STB/day. In this study, the horizontal permeability values for each of the four geological layers are the parameters that are being modified in history matching using pilot points (as described in Chapter 2). Therefore, horizontal permeabilities (K_h) will be modified using the pilot point method by selection of six permeability multipliers at various locations in the reservoir model as seen in Figure 5.13. A super-grid consisting of 5 x 5 x 1 cells is used to locate pilot points. Each super-grid cell consists of 5x5x4 fine grid cells. In the picture, K_h at the pink pilot points are varied by history matching and the rest are fixed with multipliers of 1. These parameters are labelled from 1 to 6 in this figure. In the truth case simulation model, the value of each multiplier was 1.0 (i.e. the parameters were 0.0 in the log10 scale).

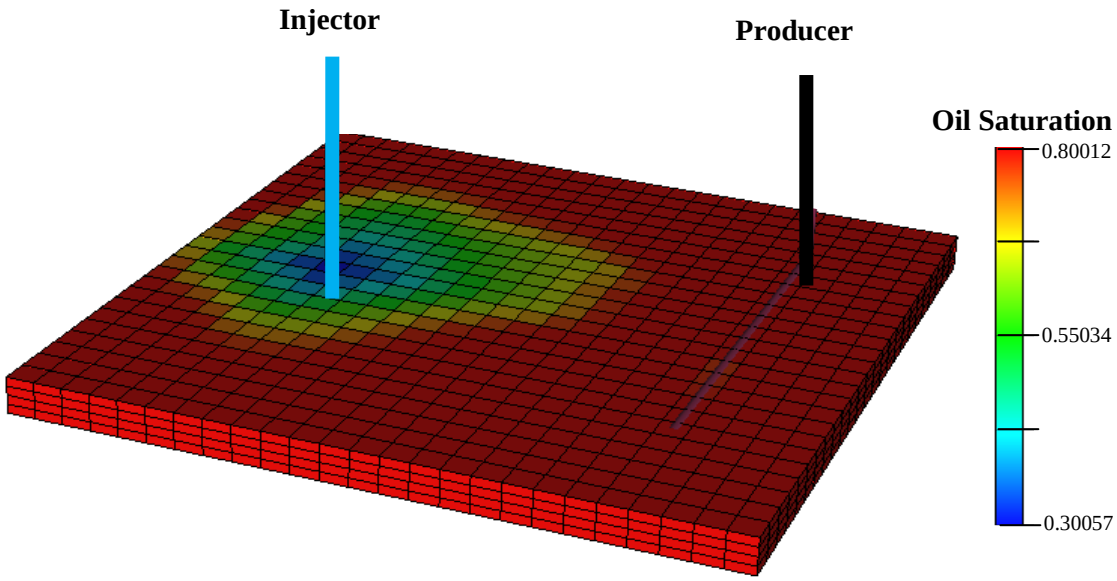

Figure 5.12: Simulation grid model (25 x 25 x 4 cell grid size) of synthetic case showing location of injector and horizontal producer.

Pressure trends and production history of both producer and injector are shown in Figure 5.14 and Figure 5.15 respectively. In this case, the steady state WBHP profiles are well established within thirty days of the start-up of production and injection and so by this time the two wells are in full communication with each other. The production data is measured/predicted at every month up to 30 months.

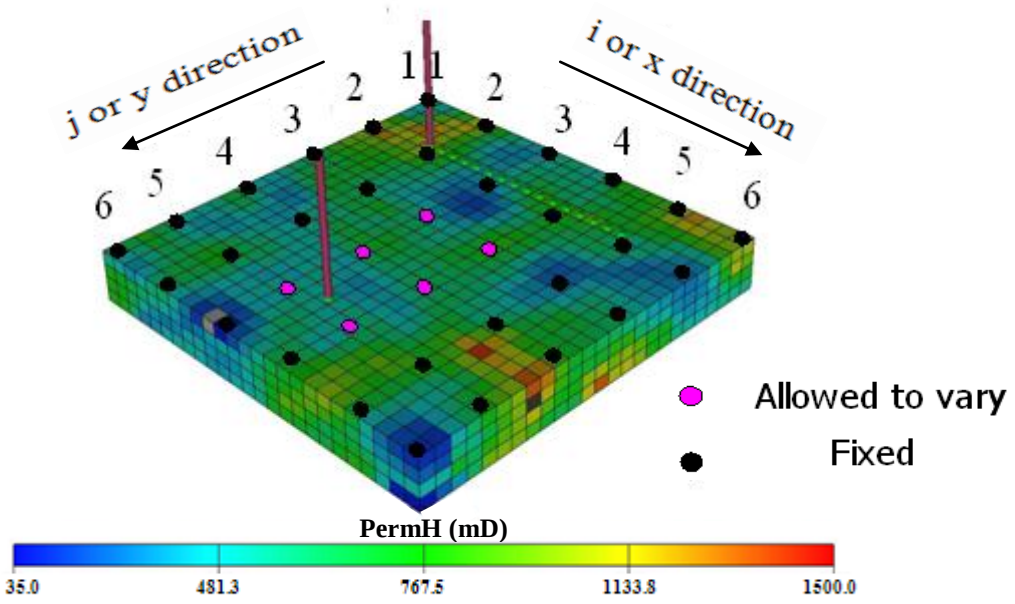

Figure 5.13: Pilot point locations. Six-dimensional parameter space has been defined to adjust horizontal permeability.

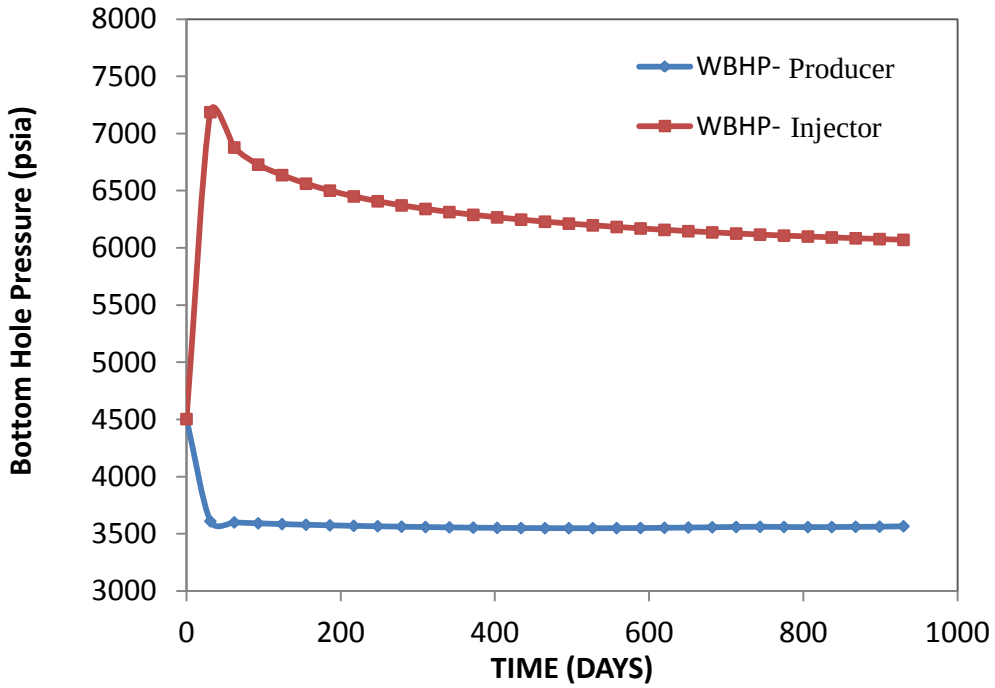

Figure 5.14: Bottom Hole Pressure trends over first 900 days for both the horizontal producer and the injector.

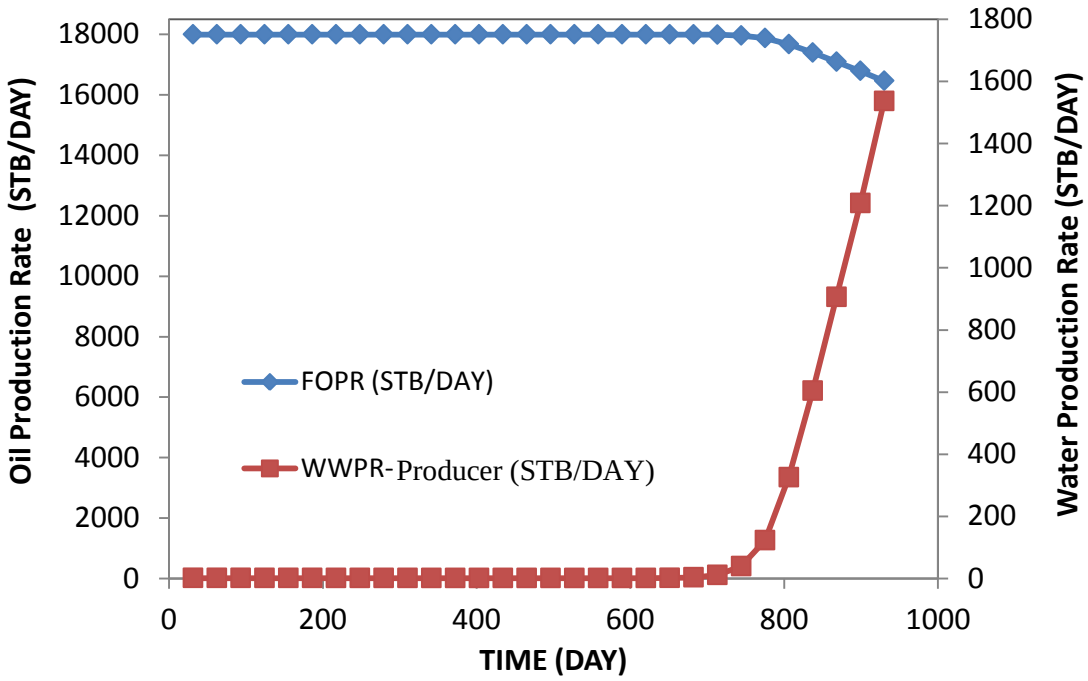

Figure 5.15: Oil and water production rates used as history data for the horizontal producer.

The seismic data is taken in three surveys: the first survey, shot prior to production (month zero), is the baseline survey, the second and third are shot after 12 months and 24 months respectively. Both the second and third surveys are compared to the baseline to visualize the changes in acoustic impedances due to changes in pressure and saturation. Synthetic seismic data as a difference in impedances are generated from the observed seismic data and they become the truth case. We applied seismic and production misfits to the SHM loop combined with NA and NAPG to see how much we could speed up the convergence rate. The NA parameters were n_i = 128, n_s = 64 and n_r = 32. In the history matching process, a number of simulations, n_i, are generated initially and their misfit calculated. The regression equation was obtained using Singular Value Decomposition techniques (see Chapter 3, Section 3.4.2). Figure 5.16 shows the cross plot of misfit from the regression equation against the actual value and we obtained a high correlation factor R^2 (0.94) for the training data. The sensitivity analysis of six uncertain parameters was carried out by changing one parameter at a time to assess how the shape of misfit surface as shown in Figure 5.17. It can be seen from Figure 5.18 and Figure 5.19 that the convergence rate is significantly improved with NAPG compared to NA and thousands of models can be saved with the new approach. Seismic maps as differences in impedances for the base case and best models for both NA and NAPG are shown in Figure 5.20. Both algorithms found identical 4D signature as the truth case but NAPG converged faster than NA.

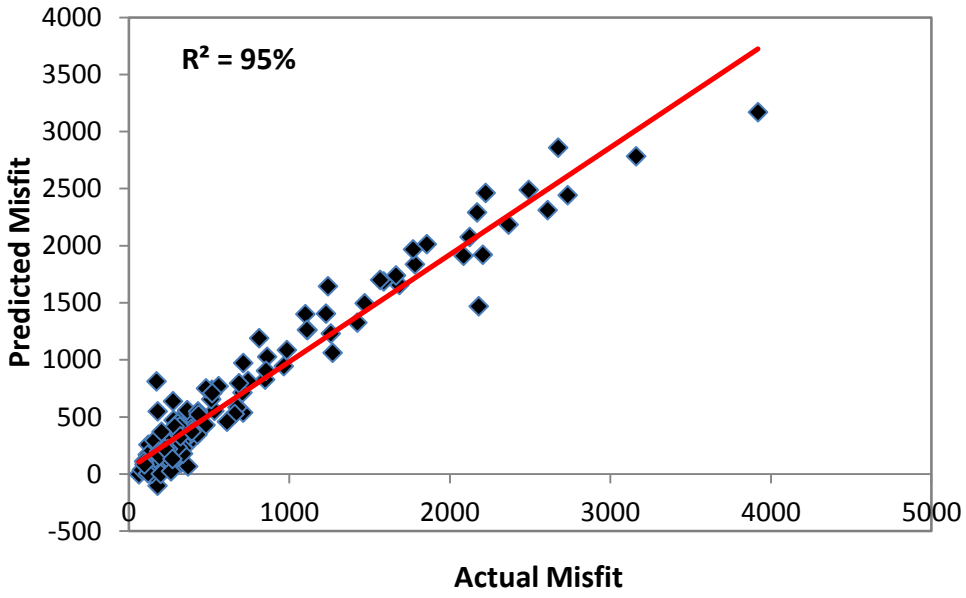

Figure 5.16: Cross plot of the misfit predicted by polynomial response surface against the actual misfits.

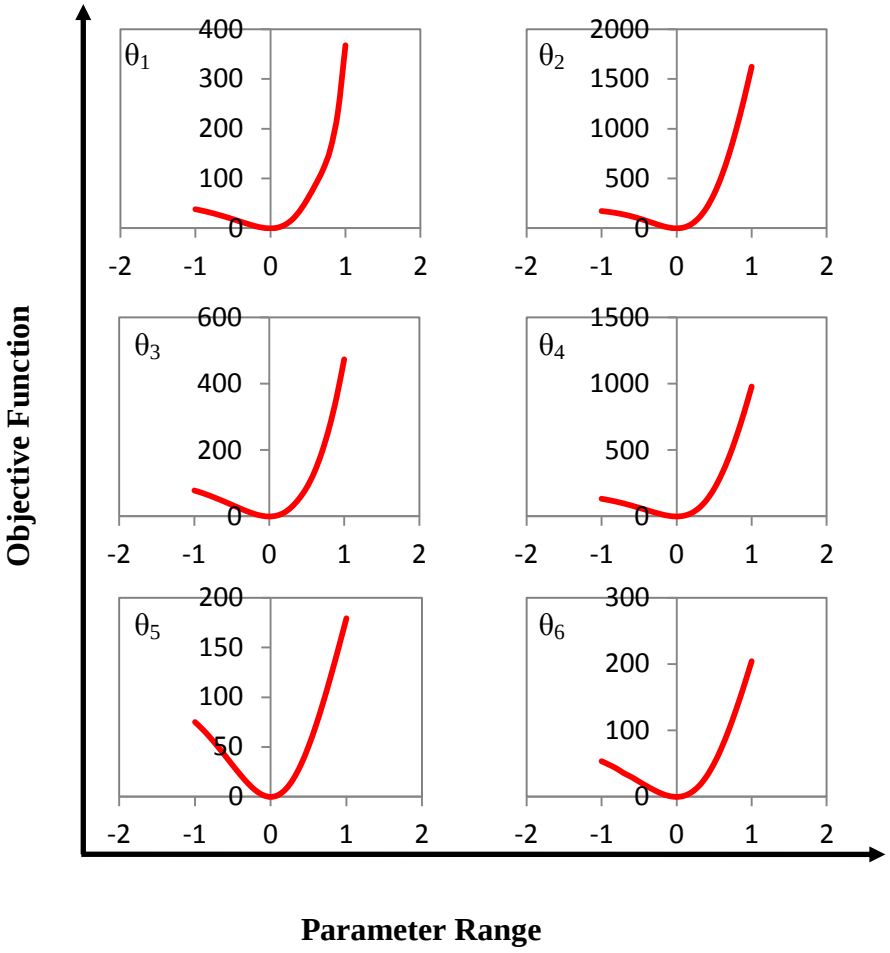

Figure 5.17: Sensitivity of misfit to parameters in the interval of [-1,1] in the log10 scale. The permeability multipliers of 6 pilot points were changed in the base case model in one parameter at a time.

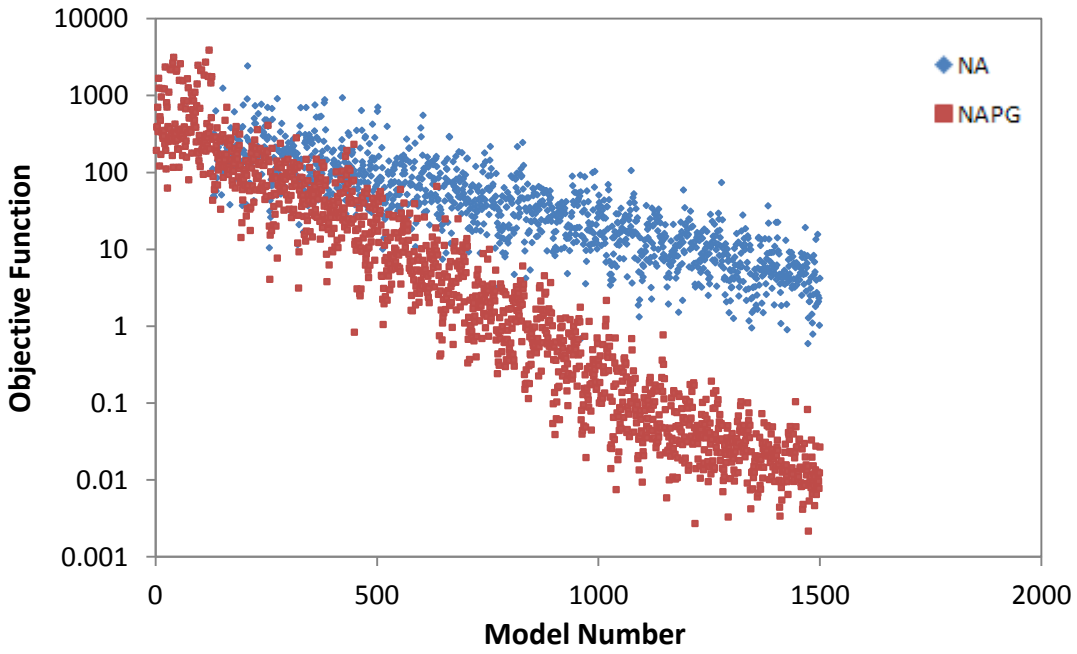

Figure 5.18: Misfit evolution for both approaches (NA vs. NAPG).

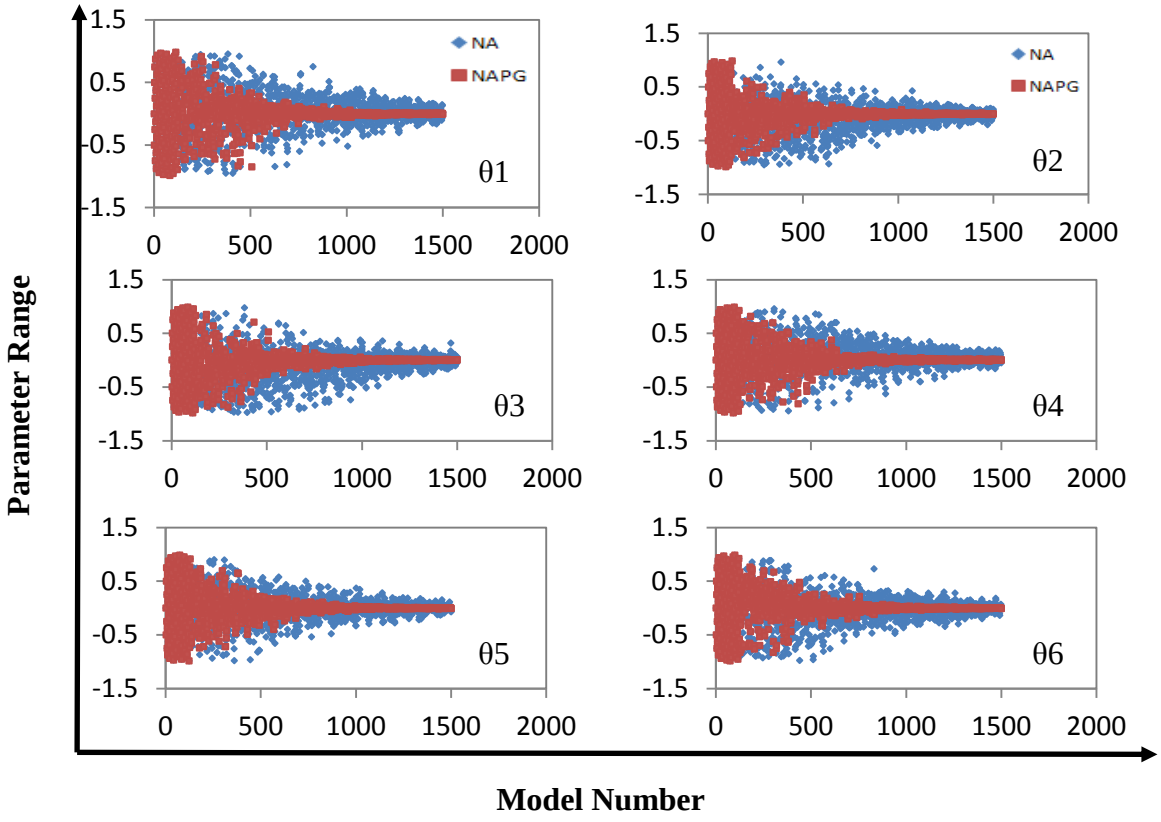

Figure 5.19: Six parameters (θ_1 to θ_6)convergence for both approaches (NA vs. NAPG).

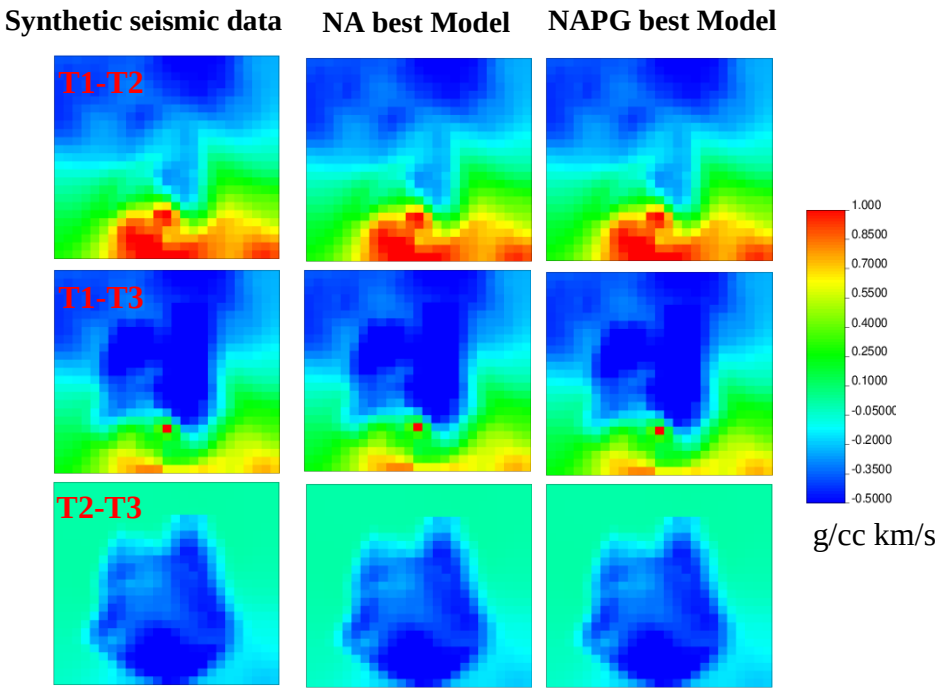

Figure 5.20: Truth and best model predicted maps as difference in impedance over two years of production for both NA and NAPG. (old - new) positive number (red) corresponds to a decrease in effective pressure, (due to an increase in the pore pressure) or increase in gas coming out of the solution. Negative impedance (blue) is either linked to a decrease in pore pressure or increase in water saturation.

5.3 Case Study II: 10D Synthetic SHM -Schiehallion Field Case

As mentioned in Chapter 4, the Schiehallion field is situated to the west of Shetland on the UK Continental Shelf (UKCS). The original model of this heavily faulted turbidite reservoir was constructed by the field operator using a conventional approaches to map reservoir properties to the simulation model. The model used for this study has already described in Chapter 4. The focus here is on better capturing the 4D signatures around a particular injector well, by updating the transmissibility of 10 barriers and faults nearby as shown in Table 5.2 as shown in Figure 4.19

Table 5.2: Barrier multiplier range on log scale.

Fault	Barrier Transmissibility multiplier of base case	Range of Parameter	
		Min	Max
a	0.001	-2.0	1.0
b	0.0009	-2.0	1.0
c	0.0009	-2.0	1.0
d	0.0009	-2.0	1.0
e	0.0009	-1.0	2.0
f	0.001	0.0	3.0
g	0.0009	-1.0	2.0
h	0.0009	0.0	3.0
i	0.0009	-2.0	1.0
j	0.0009	-1.0	2.0

In this study, we applied NAPG on the synthetic acoustic impedance prediction that is derived from the Schiehallion field model of Segment 4. To test the improvement to the NA via the NAPG, we consider a base case as the truth and use it to generate a 4D seismic signature as observed data. Therefore, the predicted 4D seismic signature from that model, in the form of acoustic impedance change, will be used as truth data along with the production data. From the output of the simulator, we calculate acoustic impedance maps using the approach in Stephen *et al.* (2006). This involves calculating the density, shear and bulk moduli for each cell in the model and then upscaling the p-wave modulus vertically using Backus formula (Equation 2.17).

In this section, we focus on the seismic misfit. In the Schiehallion field, the well causing the 4D signature of the field reached its pressure limit (Sedighi and Stephen, 2007) and this can affect in-fill wells (Edriz and Stephen, 2009) but in this part of the study, we ignore the well misfit.

5.3.1 Uncorrelated Gaussian Noise

In a purely synthetic case, there is no data error so the misfit reduces to a sum of squares. For increased realism, we add uncorrelated Gaussian noise to the predicted acoustic impedance for each survey. Stephen *et al.* (2006) found that the observed 4D signature was uncorrelated over the length of the simulation cells. We also show that we can remove the effect of this kind of noise from the misfit as in the following paragraph.

A sum of squares misfit (Equation 5.5) is used for each variable that we compare. We assume for this synthetic study that observed data contain uncorrelated Gaussian noise with zero mean and standard deviation σ_d^2, which is used in the misfit as a weighting term.

$$J(\underline{\theta}) = \sum_{\mathrm{i}=1}^{\mathrm{N}} \frac{\left(d_i^{obs} - d_i^{mod}\right)^2}{\sigma_{\mathrm{d_i}}^2} \tag{5.5}$$

Where ***N*** is number of data points. We then consider the observed and modelled data as perturbations on the truth:

$$d_i^{obs} = d_i^{truth} + \varepsilon_{di} \tag{5.6}$$

$$d_i^{mod} = d_i^{truth} + \varepsilon_{mi} \tag{5.7}$$

And for $\varepsilon_m = 0$

$$\therefore \sigma^2 = \frac{\sum \varepsilon_{d_i}^2}{N}$$

where truth refers to the true response without noise. When we set the model to be the same as the truth (i.e. $\boldsymbol{\varepsilon_m}$ = 0), we could substitute the above relations in the Equation 5.5. We would obtain $M_{noise}=N$, which represents the "data error" in the misfit, if we ignore the model error. This is also called "misfit of the noise".

For $\varepsilon_m \neq 0$, we can substitute Equations 5.6 and 5.7 into Equation 5.5 to get:

$$J = N - 2\frac{\sum \varepsilon_{di}\varepsilon_{mi}}{\sigma^2} + \frac{\sum \varepsilon_{mi}^2}{\sigma^2} \tag{5.8}$$

In most cases, the middle term on the right hand side can be neglected because data and model errors are unlikely to be correlated and in seismic data, N is large. The third term is the misfit we would get if the observed data contained no noise. So,

$$J \approx N + \frac{\sum \varepsilon_m^2}{\sigma^2} \tag{5.9}$$

The misfit of the noise is identified as the number of measurements (Equation 5.9) which can be subtracted from the total misfit to obtain a misfit as if there was no noise present.

5.3.2 Case Study II - Results

In this case, we add noise to the seismic survey such that the standard deviation of the noise on the difference of impedances, σ_d, is 20% of the truth 4D signal. Figure 5.21 shows the observed and synthetic seismic maps as impedance differences for three time steps. They show old minus new 4D maps where, red indicates pressure up or gas displacing oil, blue indicates water displacing oil or drawdown. The pressure build up seen in the (1993-1999) map disappears very quickly once the injector is switched off in the second year resulting in negligible signal over the two years of production.

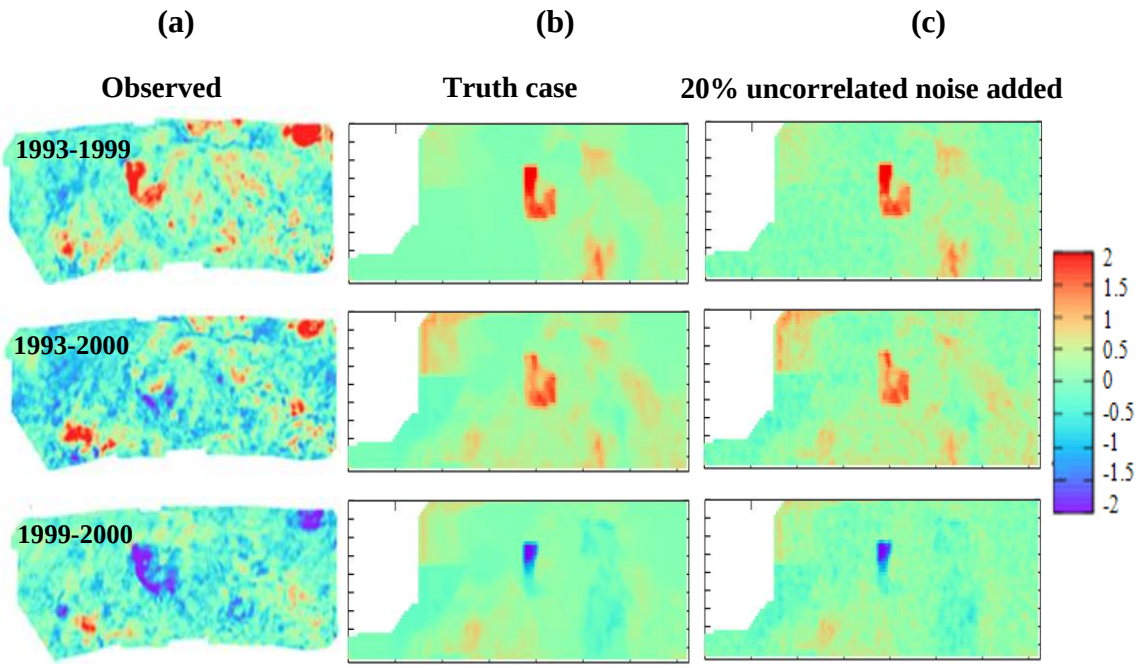

Figure 5.21: Synthetic 4D signature maps as acoustic impedances differences (normalized to the mean and standard deviation of the pre-production survey) **(a)** Observed seismic maps **(b)** truth case, **(c)** truth case with 20% uncorrelated noise added.

We use two truth cases in the study; the first one is noiseless and the second case is noisy with 20% uncorrelated noise added to the noiseless truth case. In the history matching process, a number of simulations, n_i, are generated initially and their misfit calculated. NAPG will use the same number of models that would be used by the NA method to initialize the ensemble of models. The regression equation (Equation 3.16) is then obtained and 66 coefficients were derived.

I. Noiseless case. The Pareto plot of the significant effects on the misfit polynomial is shown in Figure 5.22. In this figure, the most significant coefficients of the polynomial misfits are shown for those effects that capture 95% of the total true misfit behaviour. Figure 5.23a shows the cross plot of misfit from the regression equation against the actual misfit for the noise-less case. We obtained a high R^2 (97%) for the training data. We used the first n_i models in the conventional NA run and plot the misfit evolution in Figure 5.23b. We then plotted the regression versus actual misfits for the models obtained from the NA loop to test the regression equation. We found that the NA derived models no longer lie on the original regression equation line. In fact, the regression equation predicts negative misfits. The latter is not a problem in itself if we are only interested in relative misfits, as is the case with the NA. In general, however,

we cannot be sure *a priori* whether the minima of the real misfit surface are accurately represented in the proxy model. We will use the full misfit in the NAPG to begin with albeit with sensitivities from the regression equation. Later we will test the regression equation itself as a quick way to estimate the misfits.

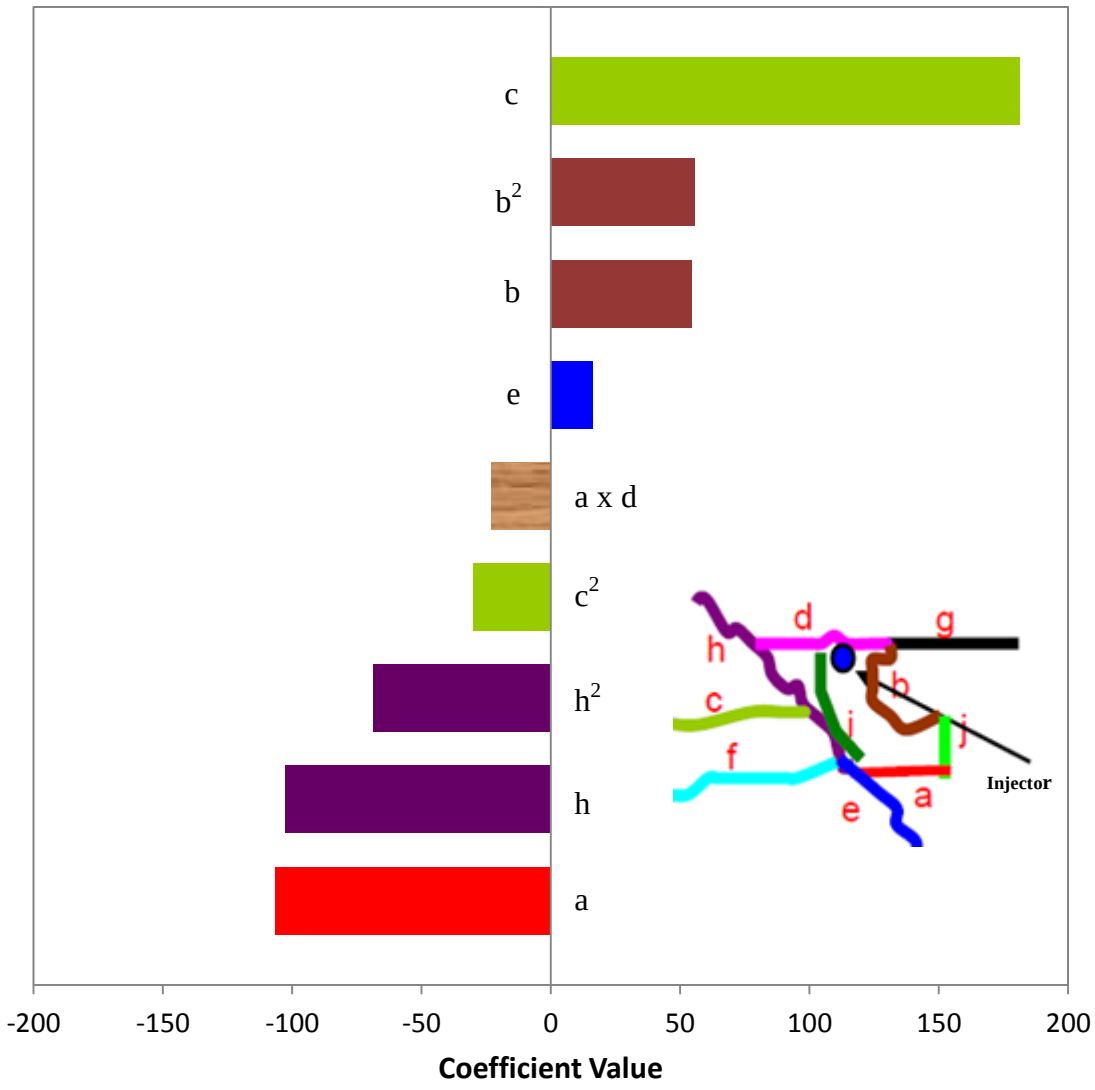

Figure 5.22: Pareto charts of significant effects from the regression polynomial of the total seismic misfits for noiseless case. The single character shows a linear effect, squared letter indicates quadratic effect, and cross product of two letters (e.g. a×d) and texture fill represent interaction effects.

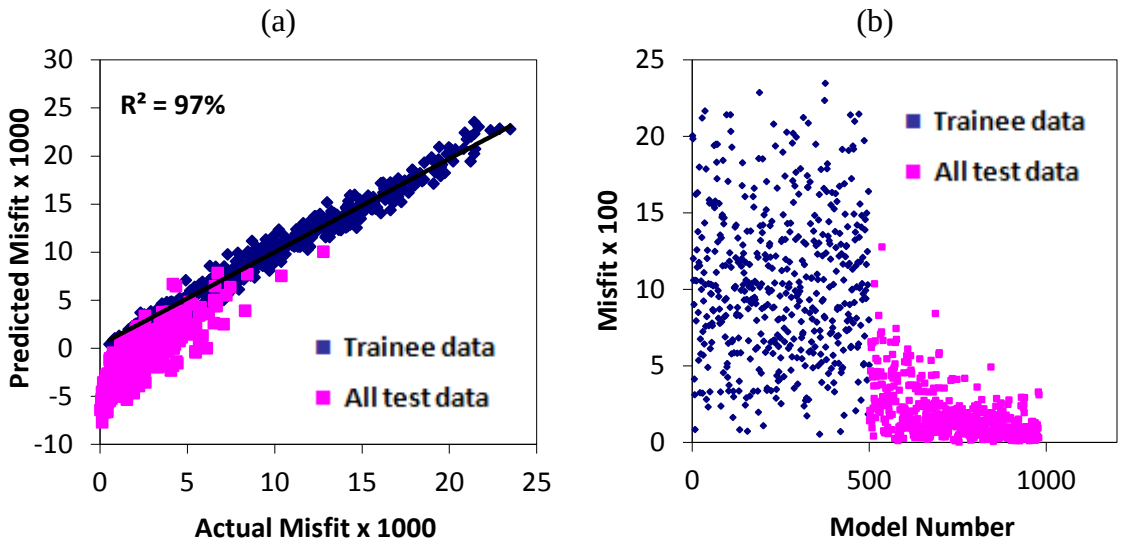

Figure 5.23: (a) Cross plot of the misfit predicted from the polynomial response surface against the actual misfits for the noiseless case and **(b)** Misfit evolution when the NA is run where the blue points are used to generate the regression equation and the pink points are used as test data.

The sensitivities of the parameters of the regression equation are then used in a history matching case with the NAPG. The NA parameters were n_i = 500, n_s = 64 and n_r = 32. Figure 5.24a shows the misfit evolution for the original NA method and the new NAPG method for the noiseless case. The convergence rate with the new method is much improved compared to the original approach with a factor 2 speed up. The histogram of the best ten models is shown in Figure 5.24b and it can be noticed that the misfit value is reduced more with the NAPG compared to the original NA.

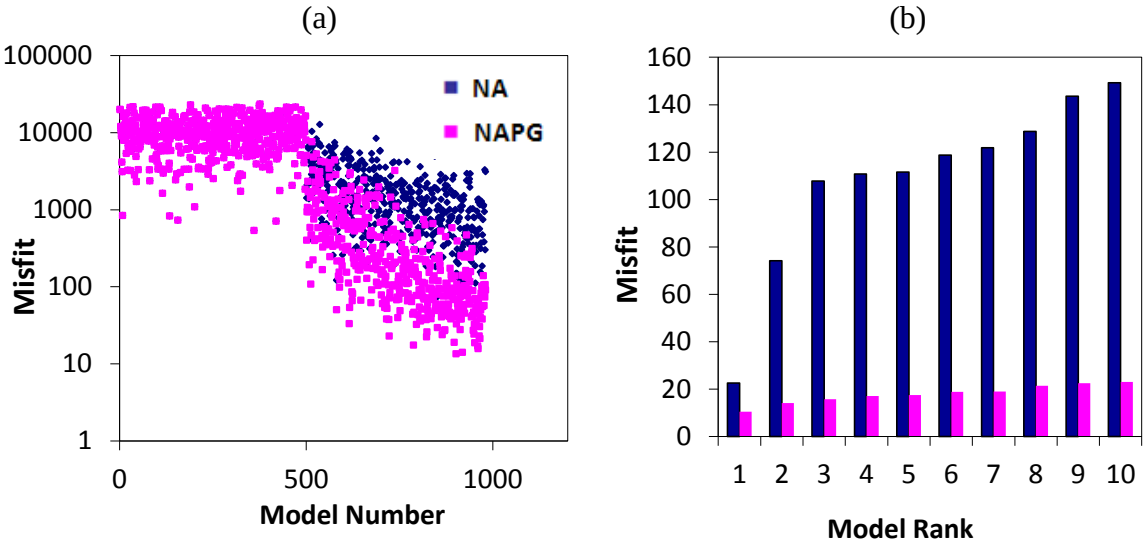

Figure 5.24: (a) Misfit evolution for both NA and NAPG for noiseless case on log plot and **(b)** NA vs. NAPG histogram chart of the best 10 models.

2. Noisy case. We carried out the same analysis on the noisy case. The equivalent plots for the case where noise is added to the truth case. The most significant coefficients on the proxy misfit are similar to the noiseless case as shown in Figure 5.25 and Figure 5.26. There are some difference in the proxy coefficients magnitude and order due to noise affect. In addition, the correlation factor R^2 is still high (94%) indicating a good correlation between actual and predicted misfit. We also apply the NAPG to the noisy case and the convergence rate is improved with the new method but we found that the misfit value cannot be reduced below the noise induced floor. If we remove the effect of the Gaussian noise from the misfit by subtracting *N* we retrieve the noiseless misfit, albeit with some variation in results due to changes to the choices made during parameter generation (Figure 5.27a). The histogram chart of the misfit of the best ten models (Figure 5.27b) shows that the misfit value is reduced further with the new method compared to the original NA method and seismic maps of impedance differences are shown in Figure 5.28. The final match is very good.

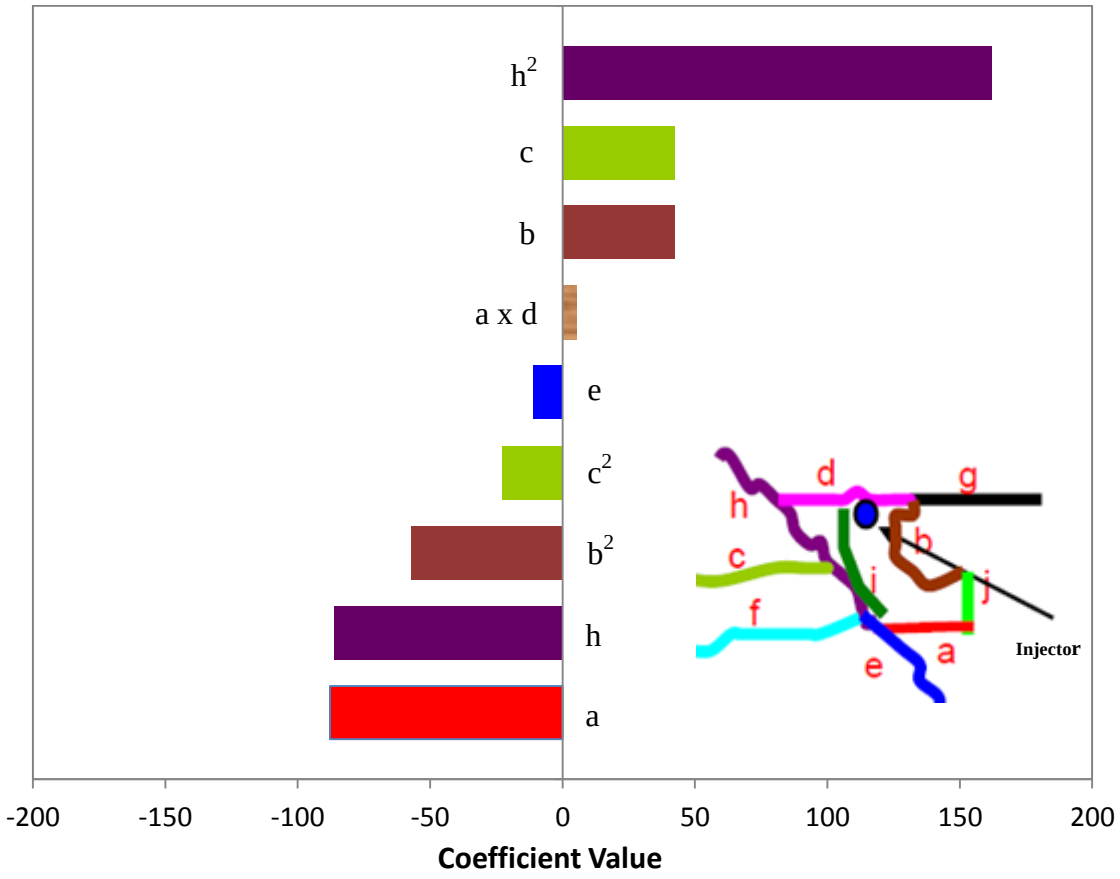

Figure 5.25: Pareto charts of significant effects from the regression polynomial of the total seismic misfits for noisy case. The single character and shows a linear effect, squared letter indicates quadratic effect, and cross product of two letters (e.g. a×d) and texture fill bars represent interaction effects.

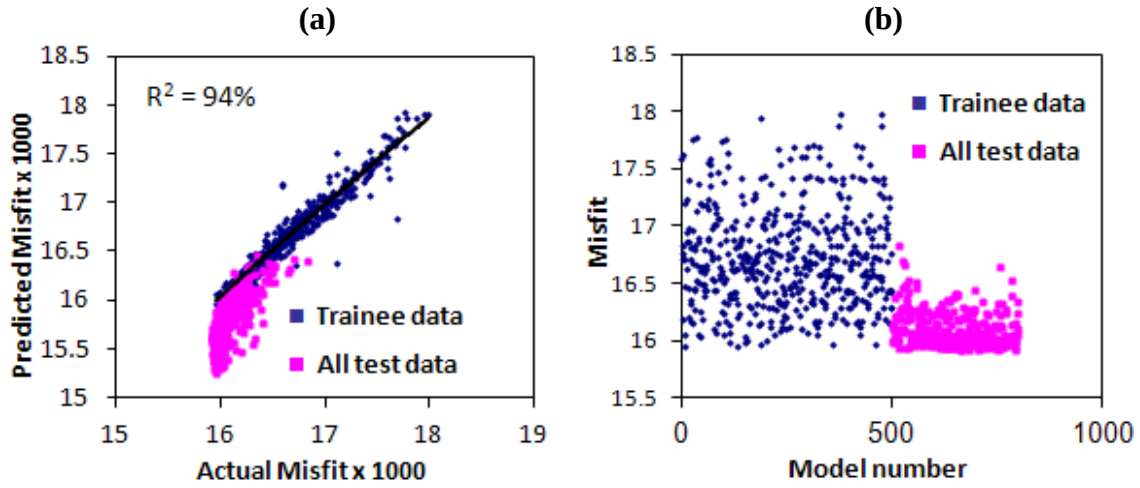

Figure 5.26: (a) Cross plot of the misfit predicted the polynomial response surface against the actual misfits for the case with 20% noise added and **(b)** Misfit evolution when the NA is run where the blue points are used to generate the regression equation and the pink points are used as test data.

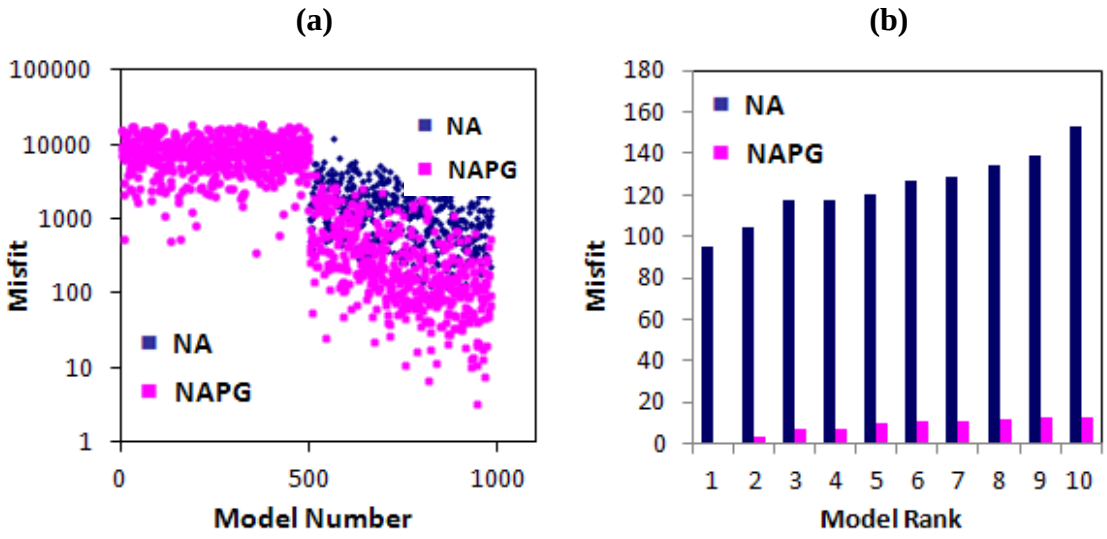

Figure 5.27: (a) Misfit evolution for both approaches (NA vs. NAPG) for noisy case on log plot after removing Gaussian noise according to Equation 5.9 and **(b)** Histogram chart of the best 10 models.

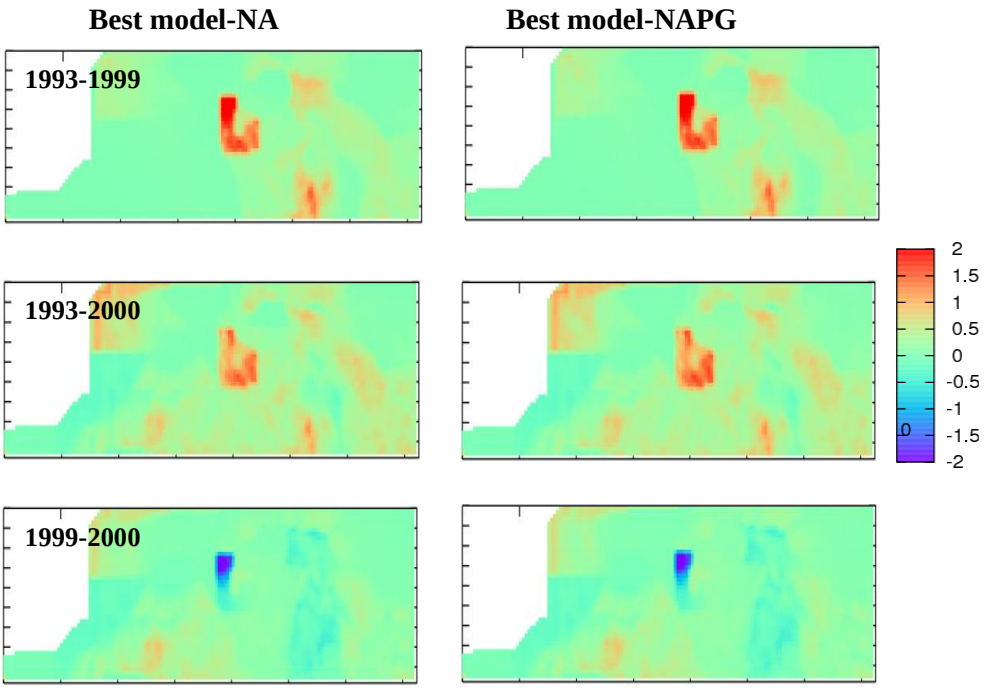

Figure 5.28: Seismic maps as impedance differences for the best model in both approaches (Noisy Case) normalized to the mean and standard deviation of the pre-production survey.

5.4 Usefulness Test of the Regression Equation Sensitivities

In the new method, the gradient of the misfit M($\underline{\theta}$) with respect to parameters $\underline{\theta}$ is calculated and is used to steer sampling in Voronoi cells. A fast option might be to use the regression equation directly instead of a full misfit calculation via simulation and petro-elastic transform calculation. The aim of this test is to investigate the results from such an approach and compare them to the use of the full misfit via simulation. We determine whether or not the regression equation can find the truth case set of parameters accurately.

There are two steps to perform the test:

1. Perform NA and NAPG on the regression equation misfit
2. Take the best 10 models from each case, calculate full misfit and compare that to the best 10 NA and NAPG using full misfit.

The regression equation predicts negative misfits in the no noise case but the NA and NAPG methods simply rank misfits so from an operational perspective this is not a problem. It can be seen from Figure 5.29a that the convergence rate is improved with the NAPG compared with original NA. The histogram chart of the misfit of the best 10 models is shown in Figure 5.29b. In the noisy case, the convergence rate is also improved with the new method in this case and as we have found before that the misfit cannot be reduced below noise misfit level (Figure 5.30a). The histogram chart of the best 10 models is shown in Figure 5.30b.

We take the parameters of 10 best models from the regression misfit case and we recalculate the misfit using the full misfit equation (Equation 2.3). We find that the regression misfit equation fails to predict at lower misfits and does not recover the original solution (see Figure 5.31). It can be concluded that using the proxy model of the misfit instead of full misfit calculation is a very attractive approach as it is very cheap but it still needs further investigations especially when we are approaching the minima.

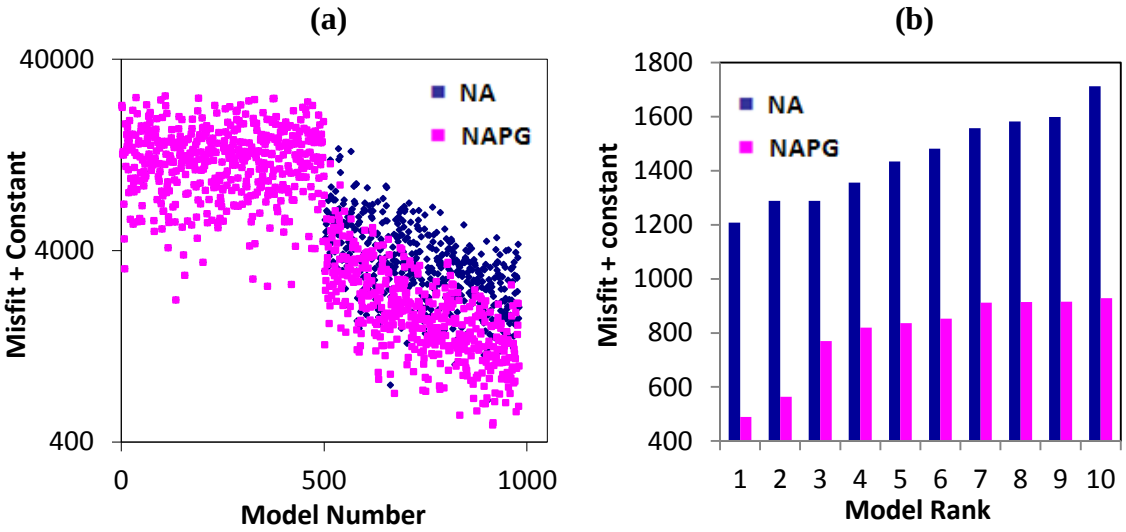

Figure 5.29: Regression misfit calculations for no-noise case showing **(a)** Misfit evolution for both NA and NAPG where we added a constant to total misfit to show negative misfits on log scale **(b)** NA vs. NAPG Histogram chart for 10 best models.

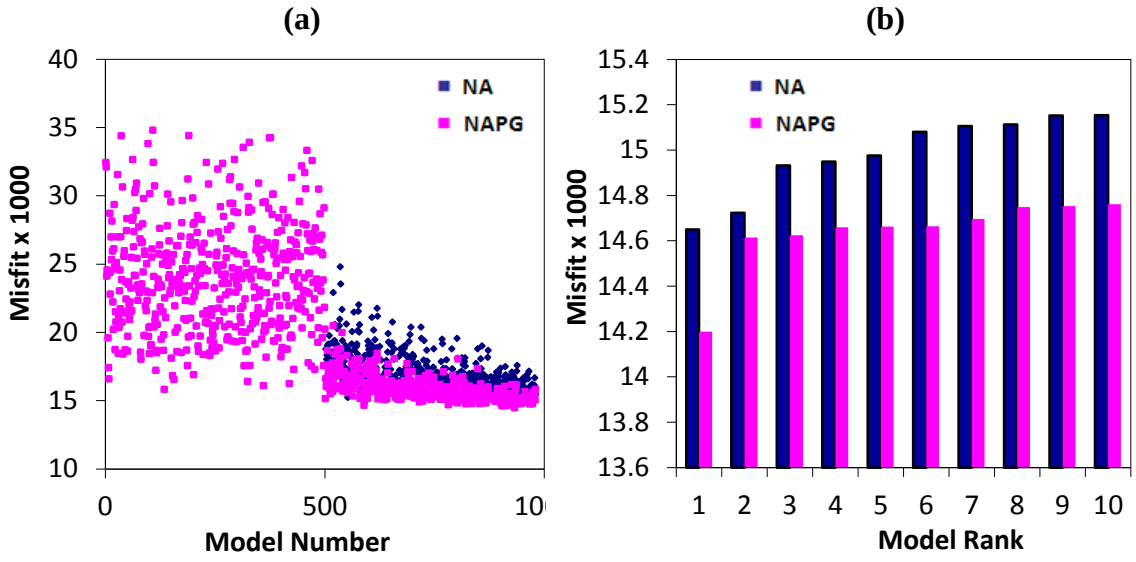

Figure 5.30: Regression misfit calculations for noisy case showing **(a)** Misfit evolution for both NA and NAPG **(b)** histogram chart of the best 10 models.

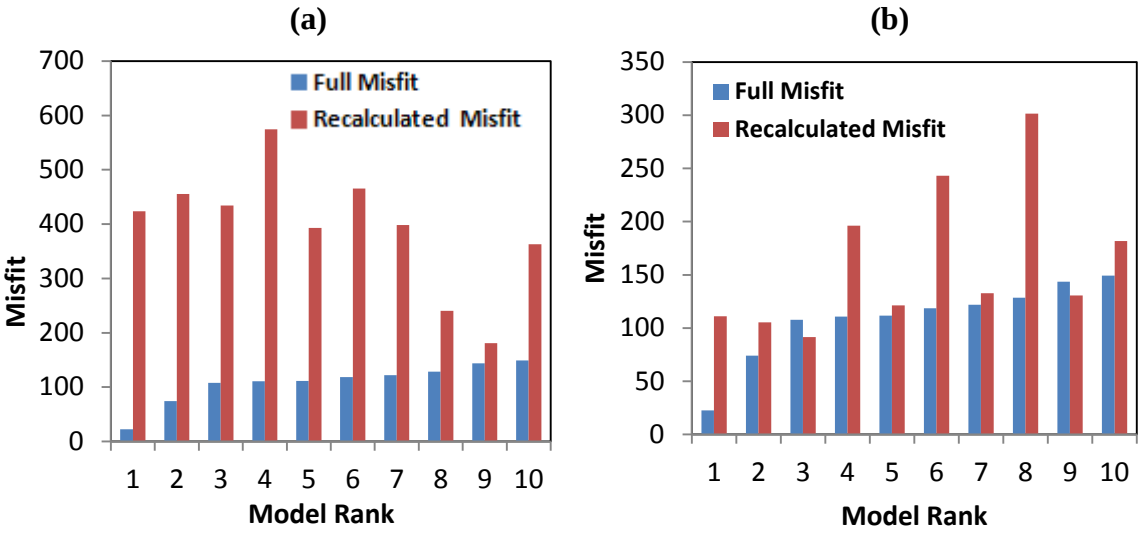

Figure 5.31: Histogram chart of no noise case for the 10 best models following application of **(a)** NA and **(b)** NAPG comparing the use of regression equation against full misfit. The misfits of the best 10 models from the regression misfit case are recalculated with the full version.

We perform another test of the parameter convergence using the full misfit and regression misfit in a very long run using different NA parameters (n_i=200, n_s=40, n_r=20 and n_s/n_r =2). The Pareto plot of the significant effects of the misfit polynomial is shown in Figure 5.32. In the full misfit case, the parameters converge to zero indicating

no change as shown in Figure 5.33a. When using the proxy model misfit, the convergence is good but the final answer does not match the truth case as depicted in Figure 5.33b. The regression equation fails to find the correct minimum. This means the truth case has not been recovered from the history-matching run. On the other hand, using the regression equation sensitivities with full misfit calculation gives better results as shown in Figure 5.34a and Figure 5.34b.

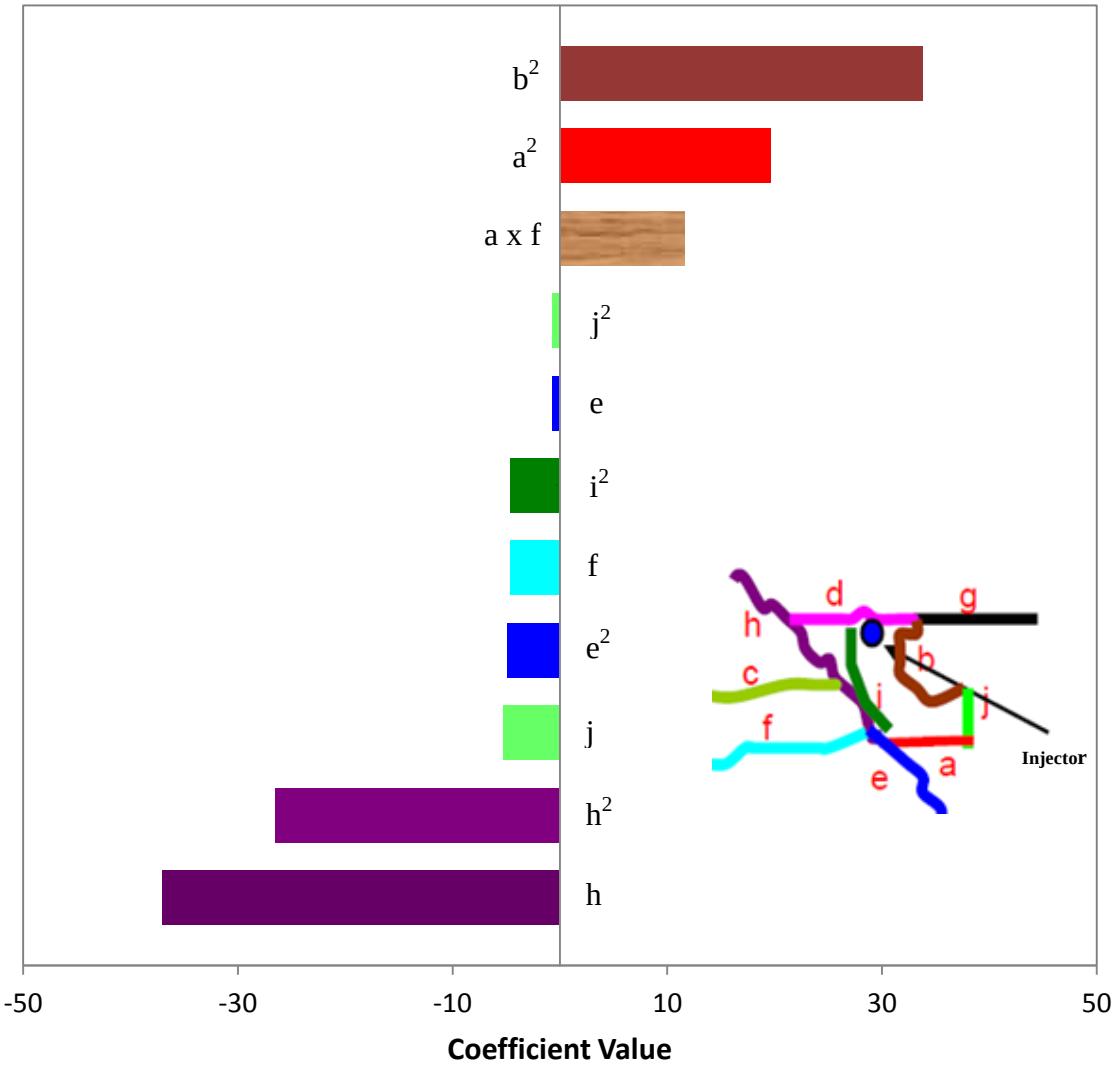

Figure 5.32: Pareto charts of significant effects from the regression polynomial of the total seismic misfits for noisy case. Single letters shows linear effects, letters to the power of two shows quadratic effects, and product of letters and texture fill bars are interacting effects.

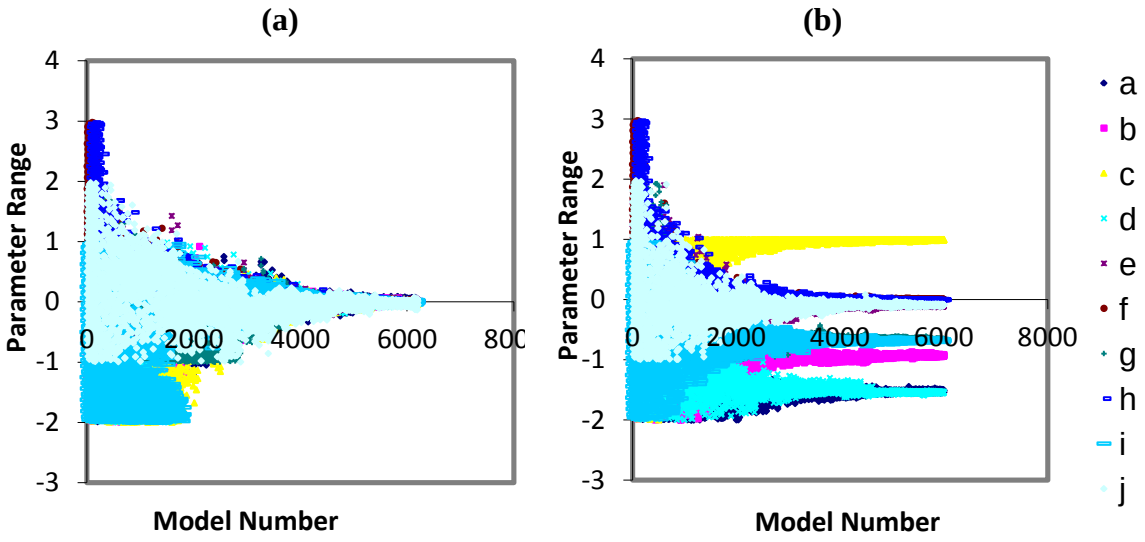

Figure 5.33: Convergence for no-noise case for long run using **(a)** Full misfit calculation and **(b)** Regression Misfit calculation.

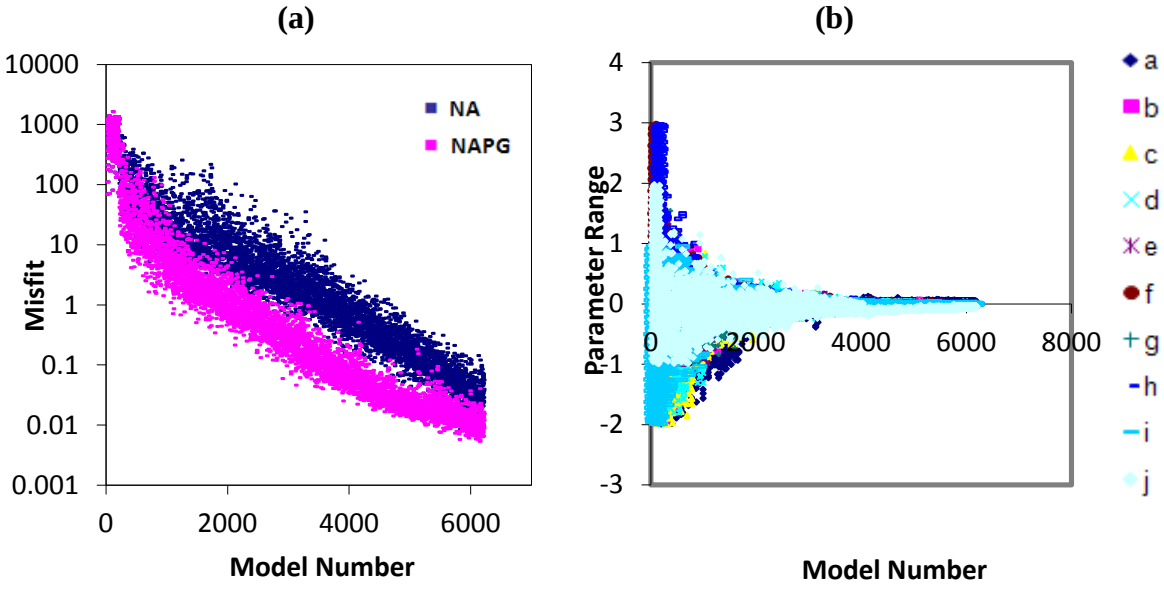

Figure 5.34: Long SHM run. **(a)** NA vs. NAPG misfit evolution with full misfit calculation and **(b)** Ten parameters convergence when using NAPG.

To sum up, in the Schiehallion synthetic field case, the locations of the minima are different in the regression equation from the true misfit. It is therefore possible that we lose the benefit of the proxy model sensitivities and they could even work against us by directing the search in the wrong direction. We could have opted for a direct solution to find the zero gradient locations on the surface. However, we found that the proxy

model could be concave with a maximum in some parameters. We also search on a limited range of parameters, which may not contain the zero gradient location. There may be multiple minima and they may lie at the extrema. This makes this approach somewhat more cumbersome and besides we wanted to test the NA and NAPG directly. To solve such a problem, we consider three approaches to update the regression equation coefficients while we are progressing. This will lead to improved accuracy of the regression equation at the extrema.

5.5 Updating Regression Equation Sensitivities

We found in the previous section that the regression equation fails somewhat as the proxy and its gradients are used close to minima. This suggested that we should update the regression equation as part of the iterative process. Figure 5.35 shows the revised workflow, which includes updating the coefficients of Equation 3.16 that are required for NAPG. The same synthetic case from the Schiehallion field was used to investigate the importance of updating the regression equation during history matching. We considered three ways of updating the regression equation coefficients. These reflect the accuracy that we are likely to obtain in representing the misfit surface close to the minimum. We consider using different sets of models are used as follows.

1. Full ensemble

All models generated so far are used in the updating. This is the most straightforward approach and the hope would be that simply adding information from the most recent models would update the regression sufficiently. Whilst it is the simplest, the regression equation would still be biased by the extreme misfit values, which could slow down convergence because the proxy model is still inaccurate.

2. Best so far

A number of the best models generated so far are used. This approach would ensure that we only use the models closest to the minimum as found so far and this is a definite attraction. On the other hand, the latest models may be selected from inaccuracies in the proxy and this could lead to noise. In this study, the best 200 models were used.

3. Latest models

Models from the latest iterations are used. This means that some of the more extreme models are used and this can improve the shape of the misfit surface. In this study, the latest 100 models were used consisting of all models used in the last five iterations of NAPG. The number of models in the proxy updating process is obviously tunable but we fix the numbers here.

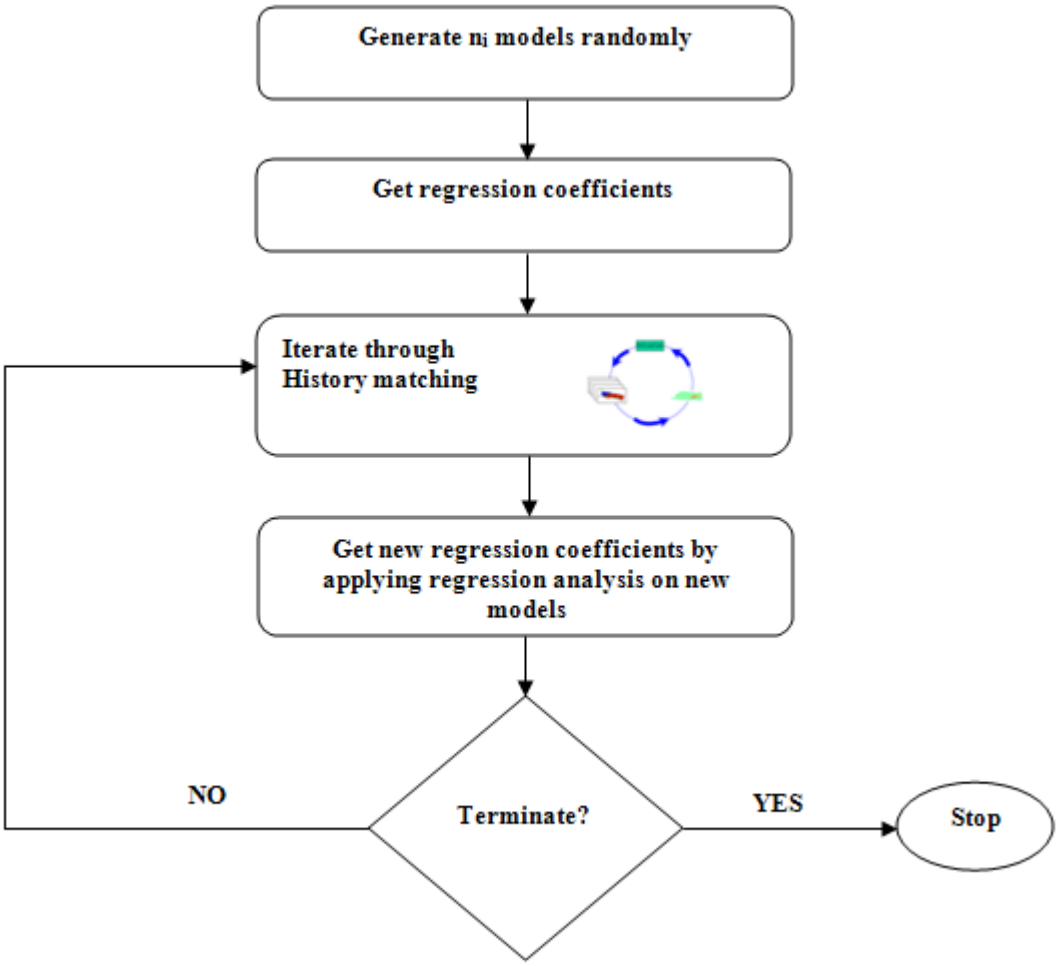

Figure 5.35: Workflow of NAPG as optimization method with updating regression equation sensitivities.

The misfits of the initial set of models of the NA approach were used to build the regression equation initially. History matching was carried out using the NA method but then we also used the NAPG method where the coefficients of this equation were used to calculate misfit gradients.

We used three difference sets of models to update the regression equation coefficients. It can be seen from the misfit evolution plots of the three scenarios as shown in Figure 5.36 that the Latest Models case, using the latest 100 models from the last five iterations, gave the best results. The misfit was reduced most quickly. The histogram (Figure 5.37a) shows the lowest 10 misfits of each approach after an equivalent number of simulations. Naturally, as a synthetic study, the truth case was recovered in all cases. Figure 5.37b shows the correlation coefficient between the data used in the calculation of the regression equation at each step plotted against the number of models generated. We see that for the full ensemble case, the correlation is very stable indicating that the poorly fitting models from initialization are significant. The Best So Far case has quite a low correlation indicating that the misfits of best models fail to match the proxy model. This means a poorer subsequent estimate of the proxy is obtained. The misfit evolution and ten-parameter convergence when updating with the Latest Models are shown in Figure 5.38 and Figure 5.39. The updated equation significantly collapses the parameter range and also improves the speed at which the misfit declines.

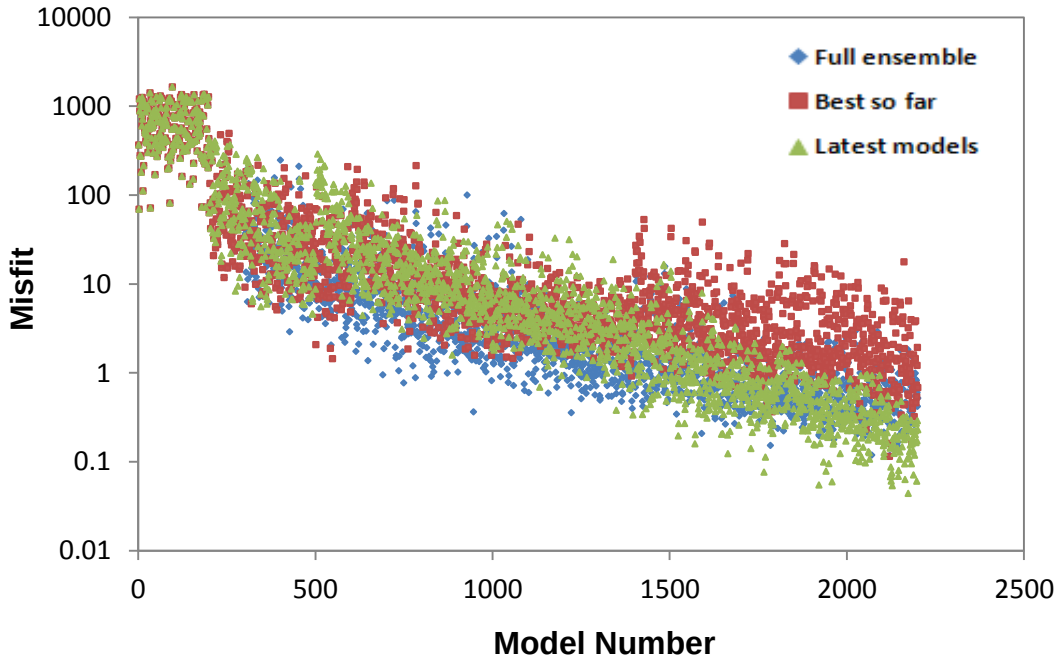

Figure 5.36: Misfit evolutions of three scenarios to update regression equation sensitivities.

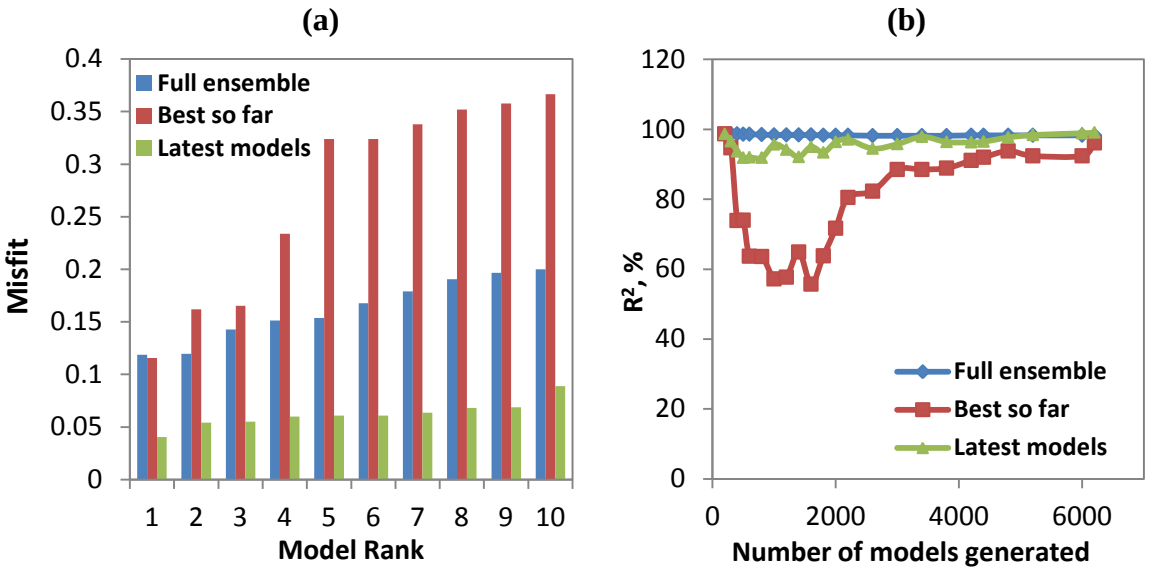

Figure 5.37: (a) Bar chart showing the lowest 10 misfits of each approach. **(b)** Correlation coefficient (R^2) plot for three approaches. Each symbol indicates a single iteration of NAPG.

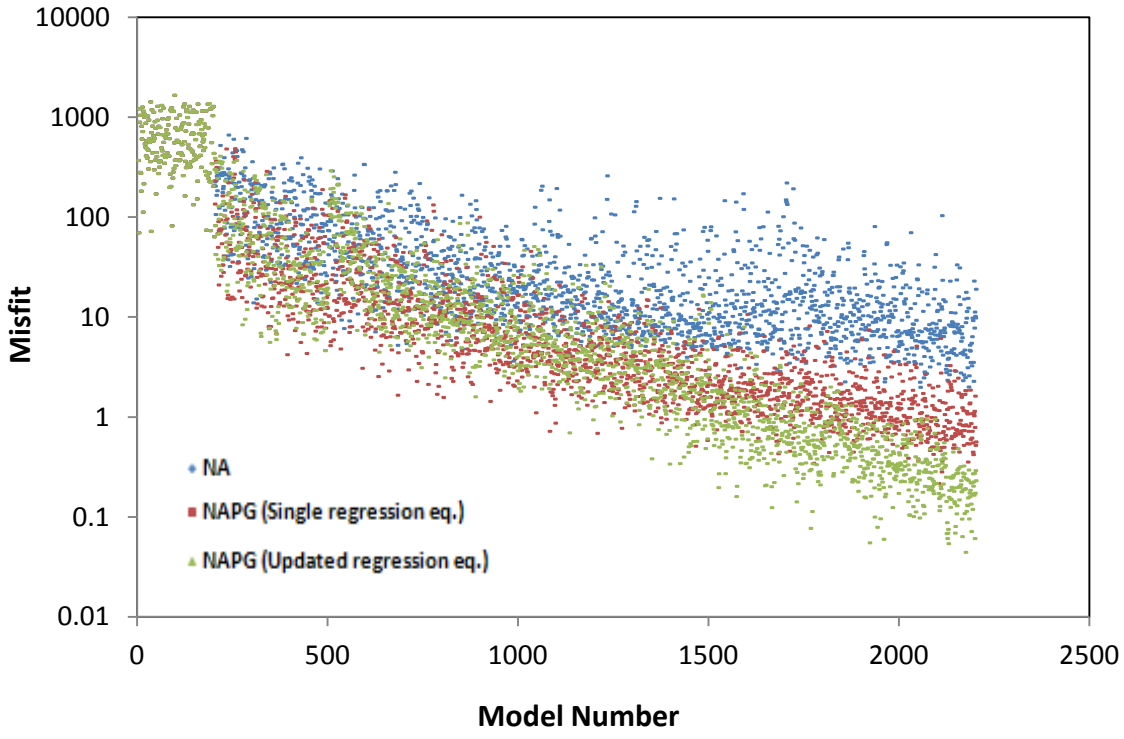

Figure 5.38: Misfit evolution plot of NA and NAPG with and without updated regression equation sensitivities using the Latest Models approach.

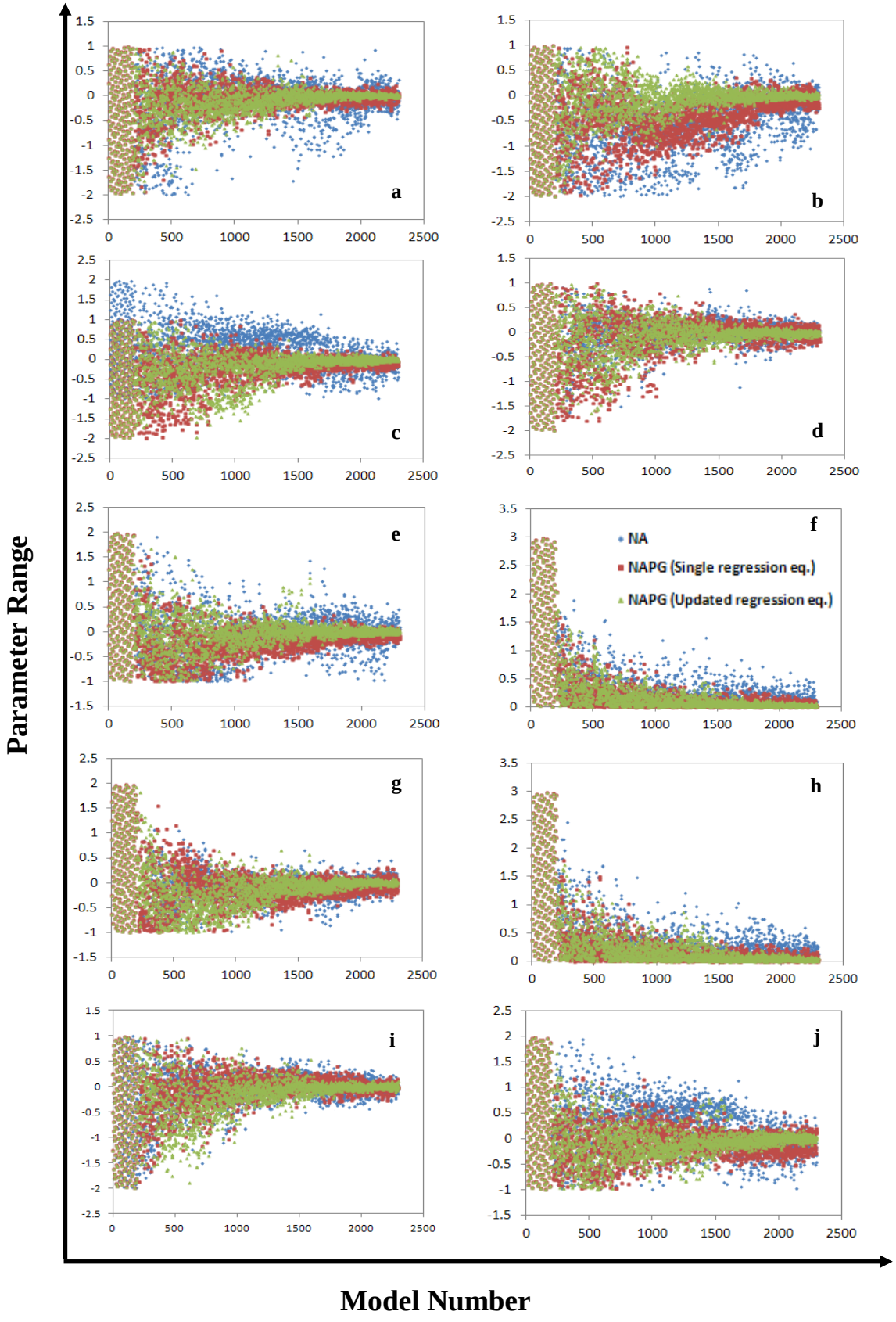

Figure 5.39: Ten-parameter convergence when updating with the Latest Models. Blue indicates NA, red indicates NAPG using single regression eq. and green indicates NAPG using updated regression equation sensitivities.

5.6 Summary

Sampling in high-dimensional spaces is still a difficult task and makes the SHM problem considerably harder to solve. The main affect of increasing dimension is on the topology of the Voronoi cells where sampling always has the potential to move into any region of parameter space. In the case of low-dimensional (oversampled) problems the potential exists to become trapped in local minima of the objective function (because the voronoi cells are isolated), and so the algorithm should be tuned more for exploration. In high-dimensional (undersampled) cases, the opposite problem is more likely to occur, i.e. a lack of concentration in the sampling (because the sampling always has the potential to move into any region of parameter space).

In this chapter, a set of verification tests were carried out on the proposed approach NAPG. Two analytical functions, 4^{th} order polynomial and Branin functions, 6D synthetic model and 10D synthetic case from Schiehallion field were used to examine the NA and NAPG behaviour. Comparisons of the evolution of the misfits for those different cases were carried out and we found that the convergence rate with NAPG is faster than NA in all cases.

In the Schiehallion field case, we added uncorrelated Gaussian noise (20%) to the predicted acoustic impedance for each survey added noise. We found that the sensitivities of the proxy model to the misfit for both noiseless and noisy case helped to explore the parameter space in efficient way and the convergence much improved with the proposed NAPG method. However, we found that the misfit value cannot be reduced below the noise induced floor for the noisy case and if we remove the effect of the uncorrelated Gaussian noise from the misfit by subtracting N we retrieved the noiseless misfit with some variation in results as a result of changing the choices made during parameter generation.

In addition, we concluded the proxy model of the misfit fails somewhat as the proxy and its gradients are used near minima. We suggested that we should update the regression equation as part of the iterative process. Therefore, we found those sensitivities can be improved by updating the regression equation while we approach the solution. We considered three approaches to update the regression equation coefficients while we are progressing and we found that the Latest Models case, using the latest 100 models from the last five iterations, gave the best results.

CHAPTER 6

Combining experimental design with proxy derived sensitivities to improve convergence rates in SHM

Overview

The aim of this chapter is to study the results of combining experimental design with proxy-derived sensitivities to improve convergence rates in SHM. It includes a literature review of Experimental Design (ED) methods and their advantages and disadvantages. In this work, ED is also used to train the proxy model instead of the random selection used originally for the NA. It potentially reduces the number of initial models that we need to start NA or NAPG and samples the parameter space in an optimally efficient way. This approach will be applied to the real data from Schiehallion field.

6.1 Response Surface Modelling (RSM)

Response Surface Modelling (RSM) is a set of mathematical and statistical techniques that are used for modelling, and analysis of problems in which a response of interest is influenced by a number of variables and the purpose is to optimize this response (Montgomery, 2005). In the history matching studies, RSM has been used widely simplify problem. In such approaches, first an initial of sample of reservoir models is obtained to determine the sensitivity of parameters to simulator outputs and to identify the significant parameters. Next, the proxy models of numerical simulator responses, e.g. initial oil in place and oil recovery, are constructed as a function of significant parameters. The proxies may then be used many times as an input in a Monte Carlo-Bayes practice for estimating the probability distribution of the responses and uncertainty analysis (Fishman, 1996, Guyaguler *et al*., 2000; White and Royer, 2003; Badru and Kabir, 2003; Peng and Gupta, 2004; Li and Friedmann, 2005, Yeten, 2007;

Yu *et al*., 2008; Scheidt and Caers, 2009). Due to the high computational efficiency of proxy-models, extensive sampling then can be achieved.

Generally, the response surface model is essentially an equation derived from the multiple regressions of all the main parameters that affect the reservoir response. It is an approximate model that links the parameters within a specified uncertainty domain to the measurable variables, referred to as the response, of the reservoir. At least, two values (low and high) are required to generate a linear response surface model and three values (low, middle and high) are required for a quadratic response surface model (Ghosh and Rao, 1996; White and Royer 2003).

6.2 Experimental Designs (ED)

Design of Experiments (DOE) is a method used to select simulations to maximize the information gained from each simulation and to evaluate statistically the significance of the different factors. In other words, ED is the use of statistical methods to determine the number and the location of the experiments in order to get the most information about a system (reservoir) at the lowest experimental cost (i.e. reservoir simulations). An experimental design study is used to generate response surfaces that identify the various factors that cause changes in the responses and also predicting these variations in a simple mathematical form. In ED each factor or input variable is set to two or more levels. Then the term design denotes a matrix with a column of samples of factors, usually in coded levels, and each row represents a particular combination of levels for all factors used in the experiment. Kleijnen (2005) concluded that there is no a unique plan for using the design of experiments in engineering problems because the same problem may be addressed through different designs.

Proxy models combined with design of experiment are widely used for sensitivity analysis in history matching. One-parameter-at-a-time scenarios are used for linear sensitivity analyses and quadratic experimental designs are used to determine correlation and higher order effects. Yeten *et al*. (2005) studied different experimental designs and found that polynomial, kriging and splines proxies along with space filling designs are proficient to predict uncertainties in the field performance.

In this research, we use ED to train the proxy model instead of the random selection used originally for the NA. Hence, ED is used to reduce initial models that we need to

start NA or NAPG by sampling the parameter space in a more efficient way, which leads to reduce CPU time. Experimental designs have been used in history matching by several studies (White *et al*., 2003; Castellini *et al*., 2004, Peake *et al*., 2005, Sedighi and Stephen, 2009; 2010, Arwini and Stephen, 2010; 2011; Wolff, 2010). A comprehensive survey can be found in the literature describing the design of experiments theory (e.g. Box and Draper, 1987; Myers and Montgomery, 1995; and Montgomery, 1997). In the next section, common different ED methodologies are given.

6.2.1 Full Factorial Designs

The full-factorial approach to experimentation covers all combinations of factors, providing valuable information on interactions. A *factorial* experiment is an experimental strategy where design variables are changed together, rather than one at a time. A common experimental design is one with all input factors set at two levels each. These levels are named 'high' and 'low' or '+1' and '-1', respectively. If there are **k** factors, each at 2 levels, a full factorial design has $\mathbf{2^k}$ runs,.i.e. examine each of **k** factors at two levels and simulated all combination effects, while three levels design (-1,0,+1) require $\mathbf{3^k}$ experiments. In general, **m** levels per factor results in $\mathbf{m^k}$ samples. Figure 6.1a shows the geometry of 2^3 factorial designs. Considering more complex metamodels of second-order, the experiments would be performed at three levels (-1,0,+1) per factor, resulting in 3^k experiments as shown in Figure 6.1b. In general, *m* levels per factor results in m^k samples. It may be possible to use mixed levels for factors, i.e. employing higher levels for more important factors to enable to examine degree of nonlinearities of the response surface in respect to them (Ghosh and Rao, 1996; Montgomery, 1997).

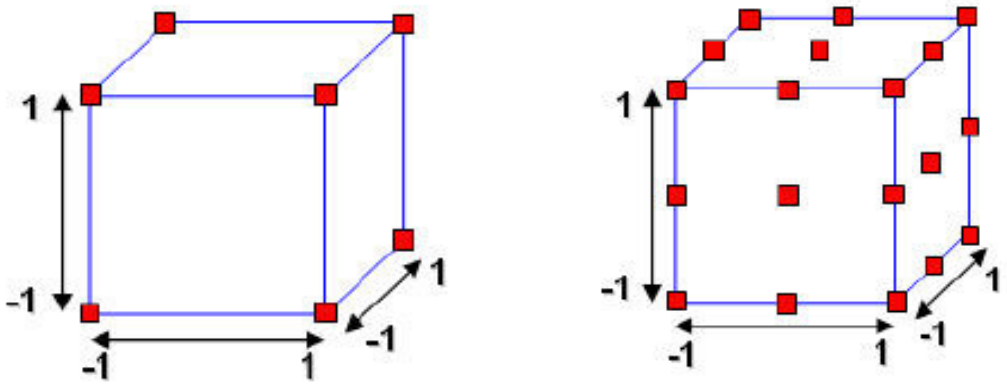

Figure 6.1: Full Factorial Designs. **(a)** 2^3 factorial Design **(b)** 3^3 factorial designs.

6.2.2 Fractional Factorial Designs

The full-factorial approach to experimentation includes all combinations of factors given that valuable information on interactions. However, the number of experimental runs increases rapidly. Fortunately, by resorting to a "fractional factorial", you can study many factors and still keep the experiment to a reasonable size. Fractional Factorial Designs consists of m^{k-p} runs to reduce the cost, where m is the number of levels of each factor investigated, k is the number of factors investigated, and p describes the size of the fraction of the full factorial used. For instance, a 2^{5-2} design is 1/4 of a two level, five factor factorial design. So instead of the 32 runs that would be required for the full 2^5 factorial experiment, only eight runs are required for this experiment. Generally, we choose a fraction such as ½, ¼, etc. of the runs called for by the full factorial (Montgomery, 1997; Myers and Montgomery, 2002; NIST/SEMATECH, 2012).

6.2.3 Quadratic Designs

This section discusses designs for adjusting quadratic models that are much more efficient, using three or five levels for each factor, but not using all combinations of levels. Central Composite Design (CCD) and Box-Behnken Design are the most common quadratic designs as explained below.

Central Composite Design (CCD)

CCD contains five levels of each factor: low axial, low factorial, center, high factorial, and high axial. With this many levels, it generates enough information to fit a second-order polynomial called a "quadratic" (Montgomery, 1997). This is a remedy for dealing with significant curvature in two-level factorial design to add more points. By locating the new points along the axes of the factor space, you can create a "central composite design" (CCD), which was introduced by Box and Wilson (1951). If constructed properly, the CCD provides a solid foundation for generating a response surface map. As the most common RSM design, CCD is divided into three parts as shown in Figure 6.2:

- Factorial points. Two-level full or fractional design (the core)
- Axial points (outside the core)
- Centre points

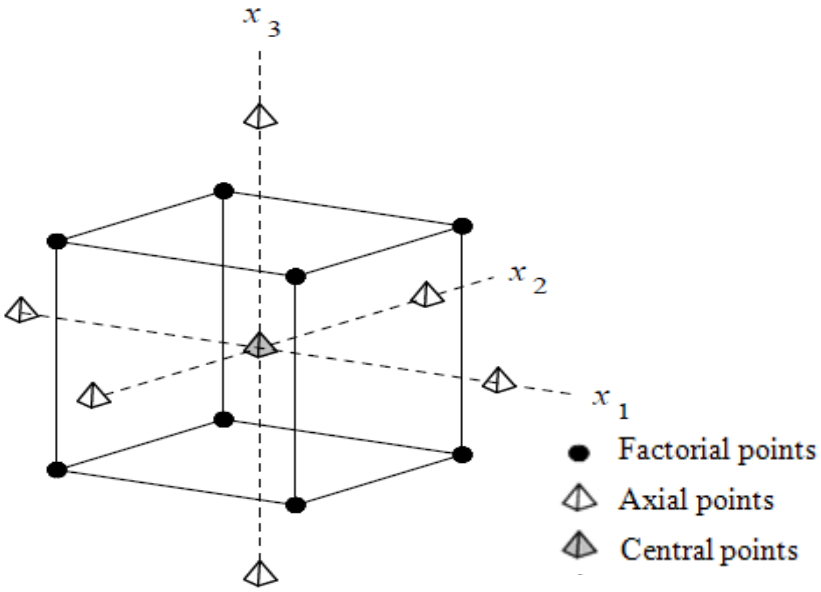

Figure 6.2: Central composite design for 3 design variables at 2 levels.

The two-level factorial design contains all possible combinations of the +1 or -1 levels of the factors. Axial points, often represented by stars, emanate from the centre point, with all but one of the factors set to zero. There are three kinds of CCDs - circumscribed, inscribed, and faced as depicted in Figure 6.3. Each design consists of a factorial design (the corners of a cube) along with *centre* and *star* points that allow for estimation of second-order effects. For a full quadratic model with k factors, CCDs have enough design points to estimate the $(k+2)(k+1)/2$ coefficients in a full quadratic model with k factors (Montgomery, 1997; Myers and Montgomery, 2002; NIST/SEMATECH, 2012).

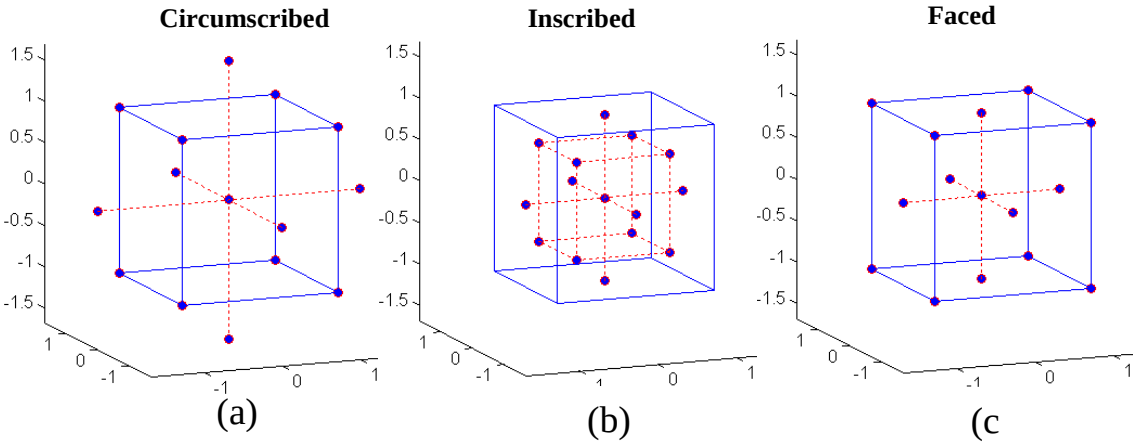

Figure 6.3: geometry of CCD for **(a)** circumscribed **(b)** inscribed, and **(c)** faced.

2. Box-Behnken Design

In the case of two-level factorial designs, Plackett and Burman (1946) developed highly fractionalized designs to screen the highest number of major effects in the least number of experimental runs. The equivalent in the case of three-level factorial designs are so-called Box-Behnken designs (Box and Behnken, 1960). Figure 6.4 shows the geometry of a Box-Behnken design. This design needs 15 experiments for three factors, including three at the factor centerpoint (all factors assigned to their centerpoint values). and this decrease becomes more vital as the number of factors increases. For five factors, a Box-Behnken design requires 41 experiments, compared to 243 experiments required for a full three-level factorial and 32 for a full two-level factorial. There is no straightforward formula relating the number of required experiments to the number of factors for Box-Behnken designs; however, the number of experiments required will always be between 2^k and 3^k. However, the designs are economical and therefore particularly useful when it is expensive to perform the necessary experimental runs (Montgomery, 1997; Myers and Montgomery, 2002; NIST/SEMATECH, 2012).

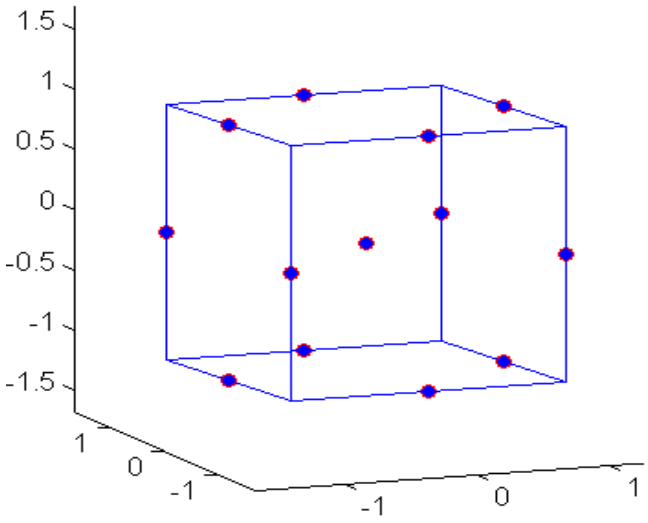

Figure 6.4: geometry of a Box-Behnken design.

6.2.4 D-Optimal Design

D-Optimal Designs are computer optimization routines that seek to minimize the covariance of the parameter estimates for a specified model. This is equivalent to maximizing the determinant $D = |X^TX|$, where X is the design matrix of model terms evaluated at specific treatments in the design space. The usual approach is to specify a model, determine the region of interest, select the number of runs to make, specify the optimality criterion, and then choose the design points from a set of candidate points that the experimenter would consider using. There are several popular design optimality criteria. They are characterized by letters of the alphabet and, as a result, are often called alphabetic optimality criteria. The best-known and often-used criterion is the D-optimal criterion. D-optimality is based on the concept that the experimental design should be chosen so as to achieve certain properties in the moment matrix (Montgomery, 1997; Myers and Montgomery, 2002; Box and *et al*. 2005; NIST/SEMATECH, 2012).

6.3 Case Study: Using ED in the Schiehallion Field

In this case, the history matching began in 1998 and continued up to the end of 2004. Six years of injection and production data and six seismic surveys data were used in this model. The baseline surveys were acquired in 1993 and 1996 while monitor surveys were acquired in 1999, 2000, 2002 and 2004 in the form of 3D migrated stack volumes of coloured inversion data. In this case, we include seismic data and eleven wells (including 6 producers and 5 injectors) data in the misfit calculations. The location of producers and injectors are shown in Figure 6.5. The observed seismic attribute maps for Segment 4 as differences in impedances for six time intervals are shown in Figure 4.18. Initial studies showed that we could not improve the injection match significantly by updating the faults and barrier transmissibilities alone. NTG as well as permeability (horizontal and vertical) were then considered to be appropriate parameters to vary as well. The history matching focussed on capturing the 4D signatures around the injectors 1 and 5 by updating the transmissibility of six barriers, NTG and permeabilities. Eighteen uncertain parameters have been considered in total. The case study included the previous 10 transmissibility multiplier of barriers ‘a’ to ‘j’ plus transmissibility multipliers of 2 new barriers (‘k’ and ‘l’) that have impact on the later history data (i.e. history added from 2000 up to 2004). In addition, 6 new parameters that

take account of two multipliers of net:gross (NTG), two multipliers of horizontal permeability (K_h) and two multipliers of vertical permeability (K_z) are included. The pilot point method with Kriging (de Marsily, 1984) is used to modify permeability and net:gross which we sample on a log scale (For more details see Section 2.1.3 of Chapter 2). In each group, several individual pilot points were changed to control the petro-physical properties locally in the area with high seismic mismatch particularly where there are strong seismic anomalies around the injectors I2 and I5. The pilot points as shown in Figure 6.5 were located to find a match to the 4D signal by following one of the identified channels in the field.

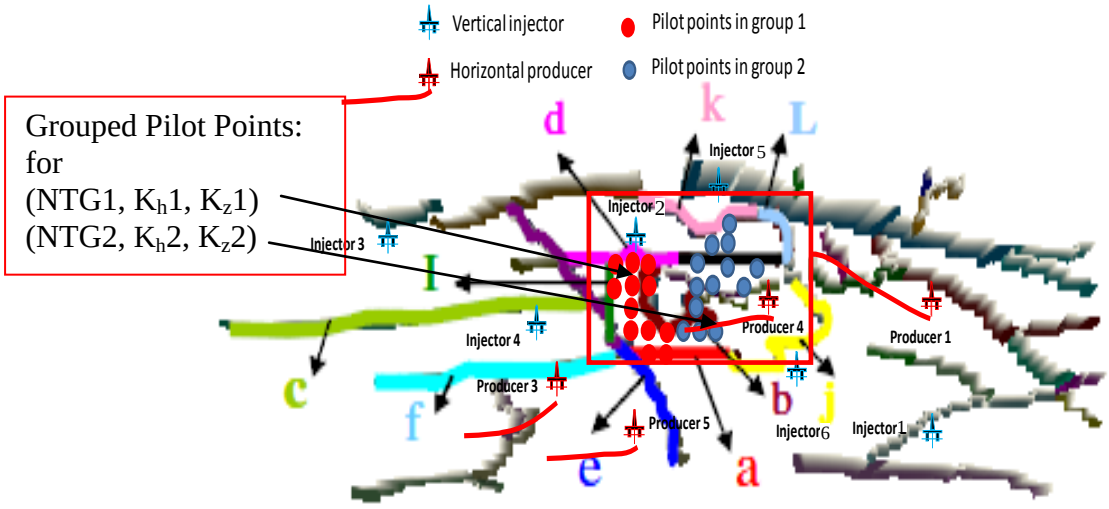

Figure 6.5: Faults and barriers in the simulation model of Segment 4. Barriers modified by history matching are colour coded and there are two groups of pilot points indicated by red and blue circles. Wells are also indicated.

In this study, we used a spider diagram to show the results of the sensitivity study on those 18 uncertain parameters to eliminate the variables that do not have sufficient impact on the reservoir simulation model results. Removing less important variables for the following steps will therefore decrease the dimension of the problem, which means fewer simulations to run and less time and effort to be spent in problem solving. The sensitivity analysis was conducted through one parameter change at a time fixing other parameters to the base case value. For some parameters, the change to the misfit was very small. We therefore reduced the dimensionality of the problem according to this sensitivity study by removing those that have little effect as shown in Figure 6.6. The results confirmed that some parameters have considerable influence and cause non-

linear effects in the parameter space. The problem was reduced to a 10D problem. We kept 6 barriers around injector 1 and 2 groups of NTG and 2 groups of K_h. We defined a set of ranges over which we allow the NA algorithm to search (Table 6.1). This range represents a constant prior uncertainty in a Bayesian sense. The limits of the parameter values were chosen according to anticipated extrema obtained by reservoir characterization. The maximum fault or barrier multiplier was set so that the transmissibility did not exceed that calculated in the absence of a fault. This 10 dimensional problem was then history matched.

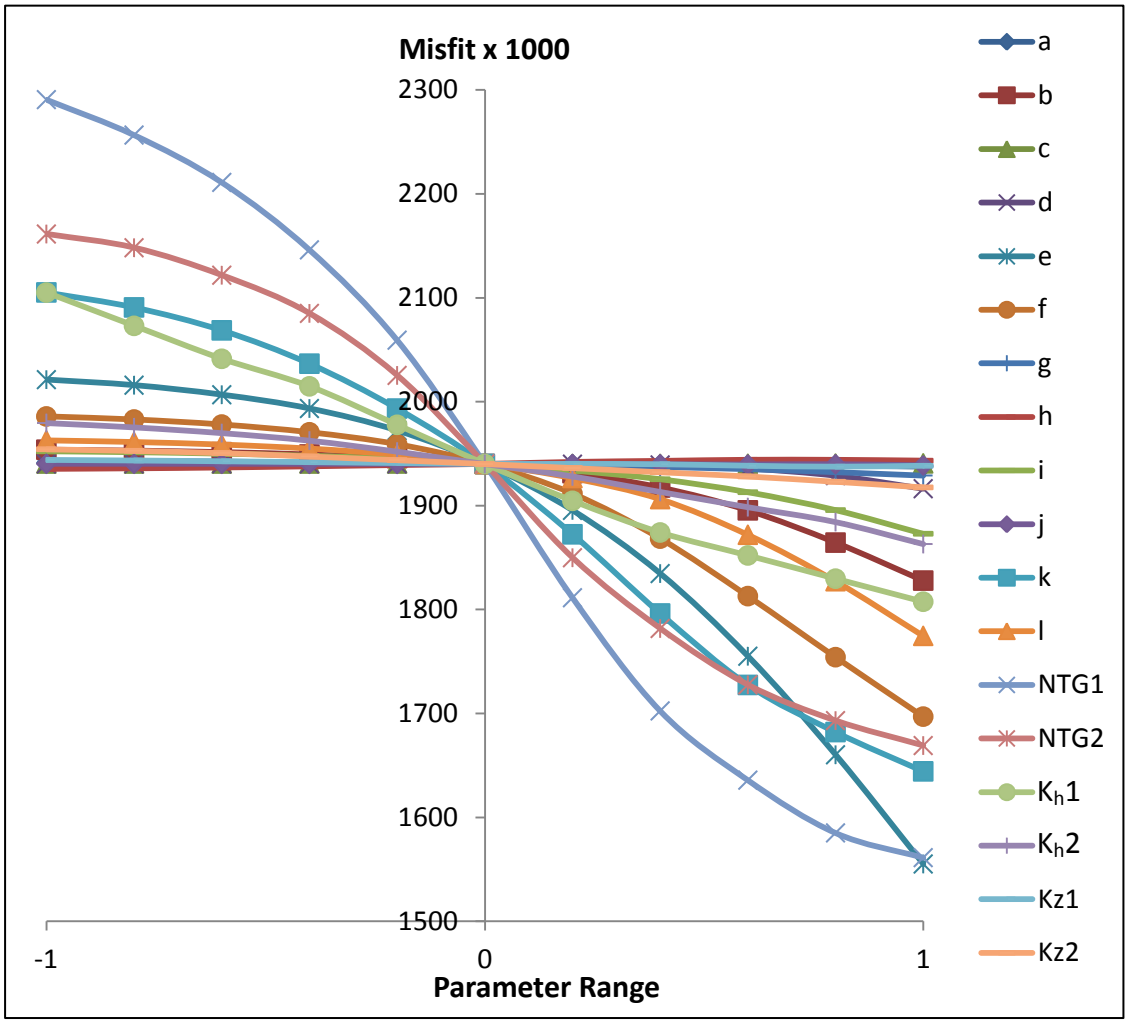

Figure 6.6: One parameter changed at a time plot for 18 updated parameters. They consist of 10 barriers, 2 groups of NTG, 2 groups of horizontal permeability and 2 groups of vertical permeability.

Table 6.1: Absolute base case multiplier for the barriers and ranges of the modifiers to transmissibility expressed on a log10 scale.

Parameter	Multiplier Base case	Range	
		MIN	MAX
Barrier a	0.001	-2	1
Barrier b	0.0009	-1	2
Barrier d	0.0009	0	3
Barrier e	0.0009	0	3
Barrier g	0.0009	-2	1
Barrier i	0.0009	-1	2
NTG1	1	-1	1
NTG2	1	-1	1
K_h1	1	-1	1
K_h2	1	-1	1

6.4 Combining ED with NAPG

Experimental designs and NAPG were combined in one approach and then applied to the 10D real case from the Schiehallion field. In this study, we used the Central Composite Face-centered (CCF) design as shown in Figure 6.3c to sample the response surface because it is very useful for building a second order (quadratic) model of the response variable without the need to use a complete three-level factorial experiment. The Matlab 7.0.1 statistical toolbox was used to generate these designs (for more details see Statistical Toolbox of Matlab software). In this research, ED is used to train the proxy model instead of the random selection used originally for the NA. This will lead to sample the parameter space in an optimally efficient way and potentially reduce the number of initial models that we need to start NA or NAPG.

As we have mentioned before, Sambridge (2001) suggests that theoretically, for NA, we need 2^{nd} models for initialization to fill the parameter space to get better misfit minimization. This saturates the parameter space and reduces inefficiencies in the search process when trying to locate the minimum. For this reason, we select an initial ensemble of 1024 models for 10D case to start NA and NAPG. This is a large number however and we used ED along with NAPG ("NAPG+ED") to initialize the proposed SHM workflow in Figure 3.1. By applying fractional ED, we need only 149 models instead to construct the proxy model. Then all three approaches are progressed generating n_s=20 models per iteration and n_r =10. Figure 6.7 and Figure 6.8 show the coefficients of the response function indicating the most important parameters. When we use ED to start NA or NAPG, we found that more coefficients play an important role to control the proxy model to misfit. Figure 6.9 shows the cross plot of misfit from the regression equation against the actual value for ED and ED+NAPG. As can be seen, we obtained a high correlation factor R^2 (0.98) for the training data.

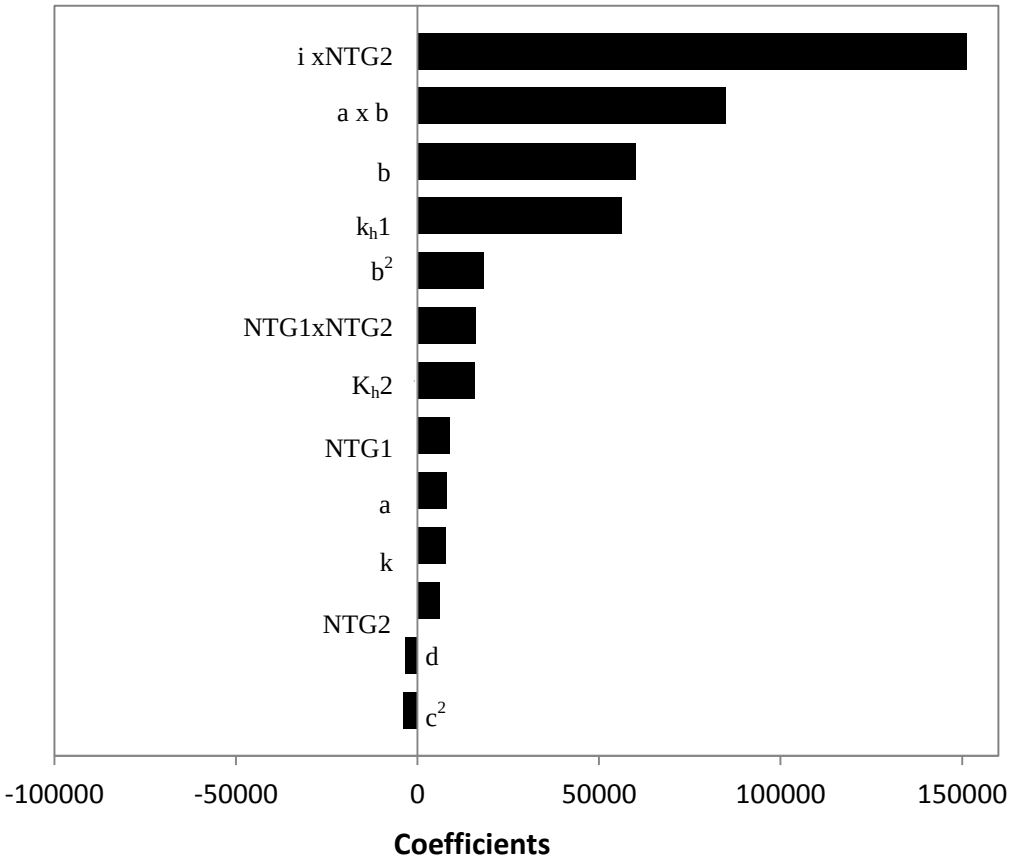

Figure 6.7: Pareto charts showing the major coefficients obtained for the polynomial proxy model for initial *ni* (1024 models). The single character shows a linear effect, squared letter indicates quadratic effect, and cross product of two letters (e.g. a×d) and orange represent interaction effects.

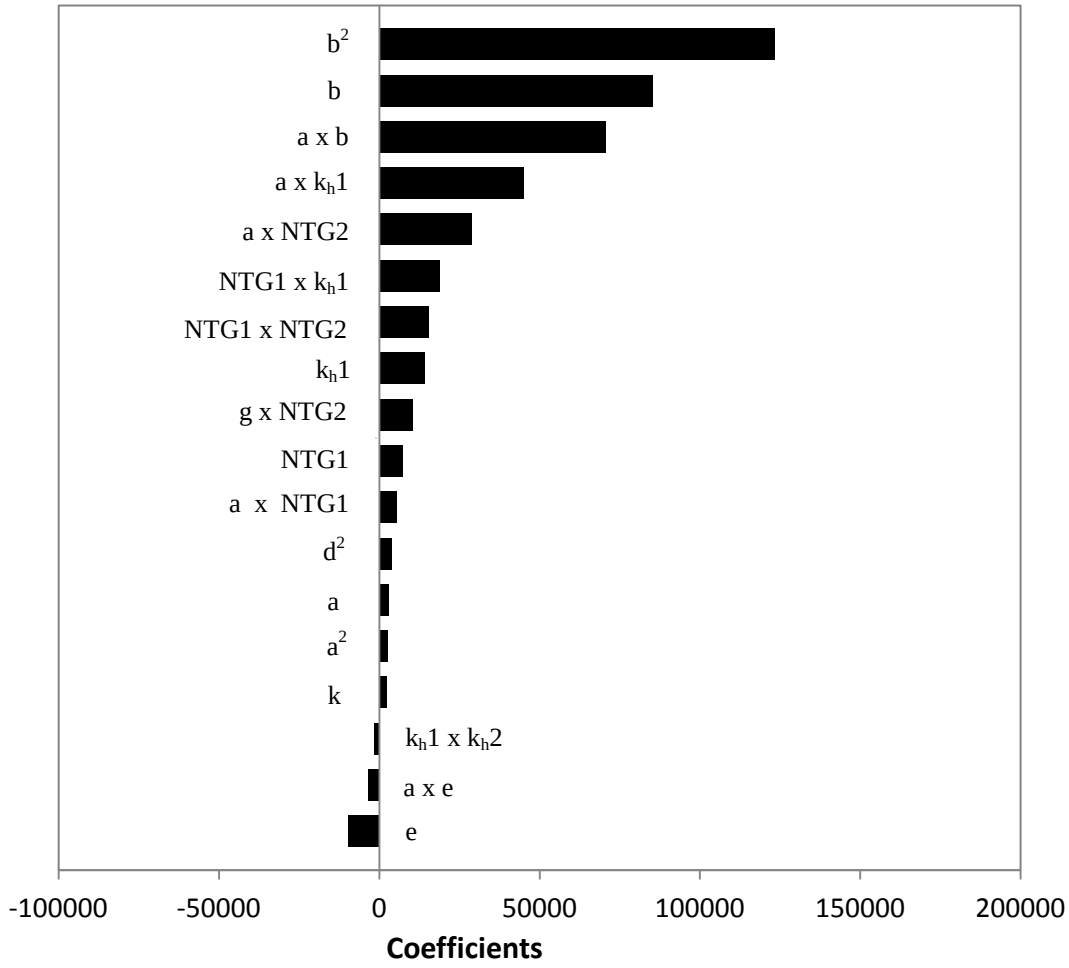

Figure 6.8: Pareto charts showing the major coefficients obtained for the polynomial proxy model for only 149 models for ED+NAPG method. The single character shows a linear effect, squared letter indicates quadratic effect, and cross product of two letters (e.g. a×d) and orange represent interaction effects.

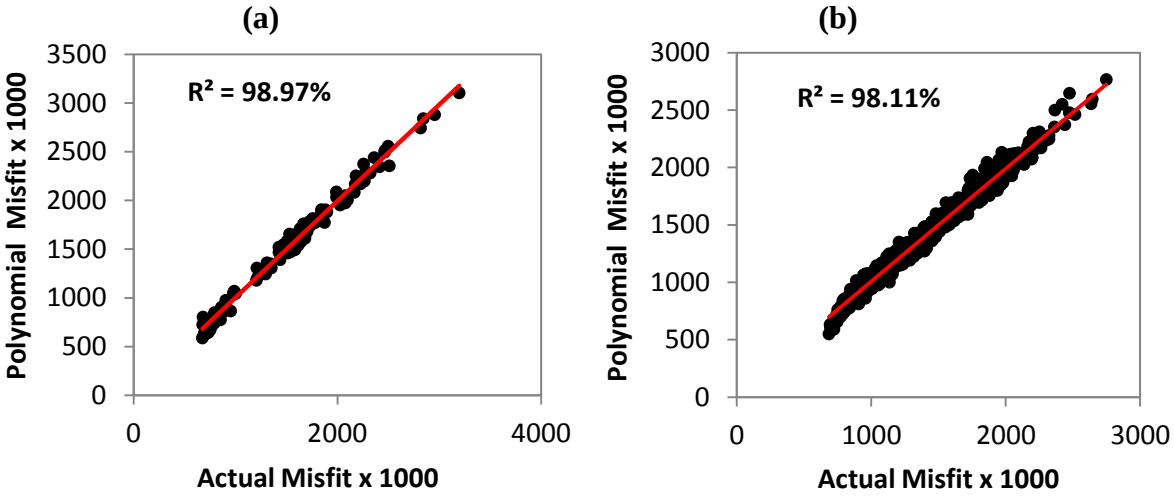

Figure 6.9: Misfits predicted by polynomial response surface against the true misfit for **(a)** ED case and **(B)** ED+NAPG case.

A comparison of parameters updated by the three different history-matching cases is shown in Figure 6.10. The random initialization is shown by a large cloud of data for NA and NAPG while NAPG+ED has a much smaller initialization. The three cases were run for the same number of iterations after initialization. It can be seen that the misfit declines in all three cases after initialization and NAPG and NAPG+ED converge better than the original NA. Although all three cases are converging to a minimum that is quite large, the total misfit is reduced by a factor of three almost. The minimum reached is a combination of noise in the seismic map as well as features that we do not try to alter the model to match. We also plot the misfits of the best 10 models in each case in Figure 6.11. The NAPG+ED case provides the best model overall. The experimental design models actually make a good starting point for NA thus saving the n_i models.

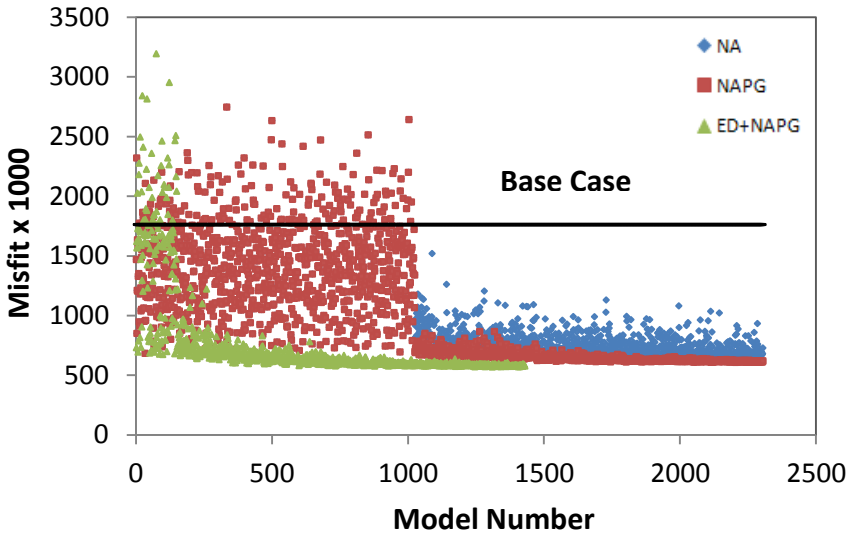

Figure 6.10: NA, NAPG and NAPG+ED methods showing the misfit evolution plot for the 10D problem (black line indicates base case model).

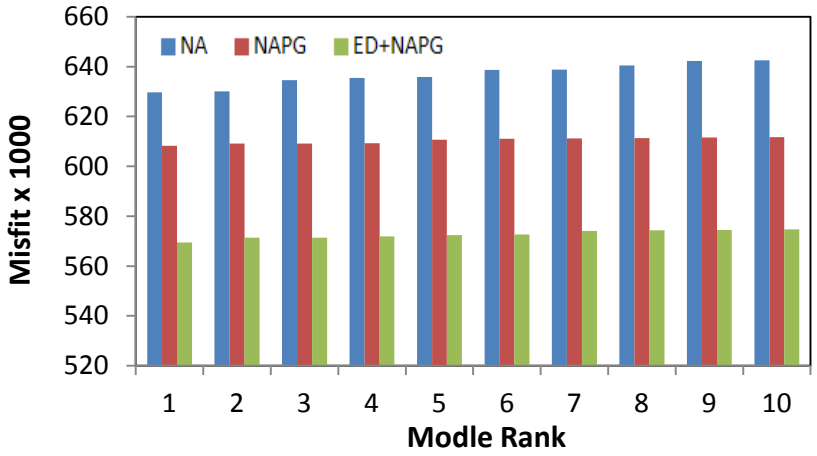

Figure 6.11: NA, NAPG and NAPG+ED methods showing the histogram for 10 misfits of the best models.

The convergence of the ten parameters for each approach is shown in Figure 6.12. The final solution for each is similar except for barrier g and K_{h1} but NAPG achieved better convergence rate. We examine the ultimate parameter values for the best model from each case in Figure 6.13. NAPG and NAPG+ED gave similar solutions generally although in some cases the error bars, indicating the degree of convergence, do not always overlap (e.g. parameter 'd'). In addition, for barriers 'g' and 'K_{h1}', there are a few discrepancies between the various methods. These results may signify the non-uniqueness of this history matching problem and the existence of the multiple solutions that have been obtained using different search methods.

The reduction of the production and seismic misfits as percentages relative to the base case in are shown Figure 6.14a and Figure 6.14b. In absolute terms, the reduction is approximately equivalent for both misfits. The data estimated errors have been used to weight the seismic and production in a natural manner towards fitting the most accurate data. Although the number of measurements is greater for the 4D seismic data, the production data is more accurate. We also observed that for 4D seismic, the reduction of the misfit is somewhat lower than for production data as shown. This is because the change in 4D signature is quite localized and much of the 4D misfit actually comes from noise in the non-reservoir region or from signal that we have not tried to better predict. The production misfit is actually very much localized and is going to be relatively more affected by changes during SHM. For the majority of producers (except producer 4 and Producer 5) and most the injectors (except Injector 2), their historical rates are predicted quite well by the reservoir base case model. The improvements to the predictions of injection and production data are shown in Figure 6.15, Figure 6.16 and Figure 6.17. The injector well was significantly under injecting in the base case and the NA method had not quite found the right properties to apply. The permeability near the injector was too low. This had little effect on the seismic behaviour near that well because the signal was pressure dominated and the well was reaching its pressure limit. Ultimately, the injector rate was matched. Producers 4 and 5 were also significantly improved in terms of the oil production rate. By speeding up convergence, the degree of improvement was greater for NAPG and NAPG+ED.

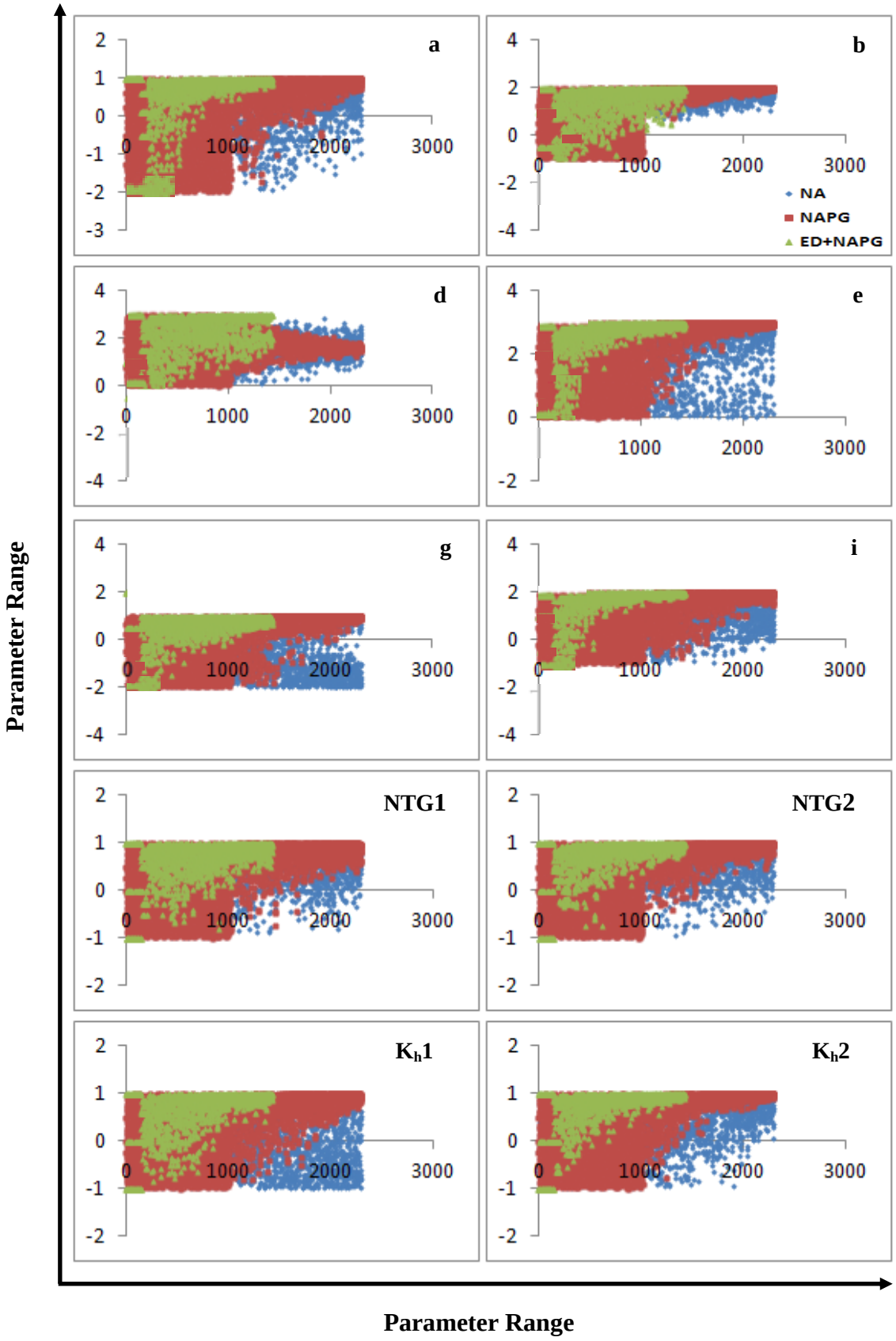

Figure 6.12: Convergence of ten parameters for the three approaches (NA, NAPG and ED+NAPG).

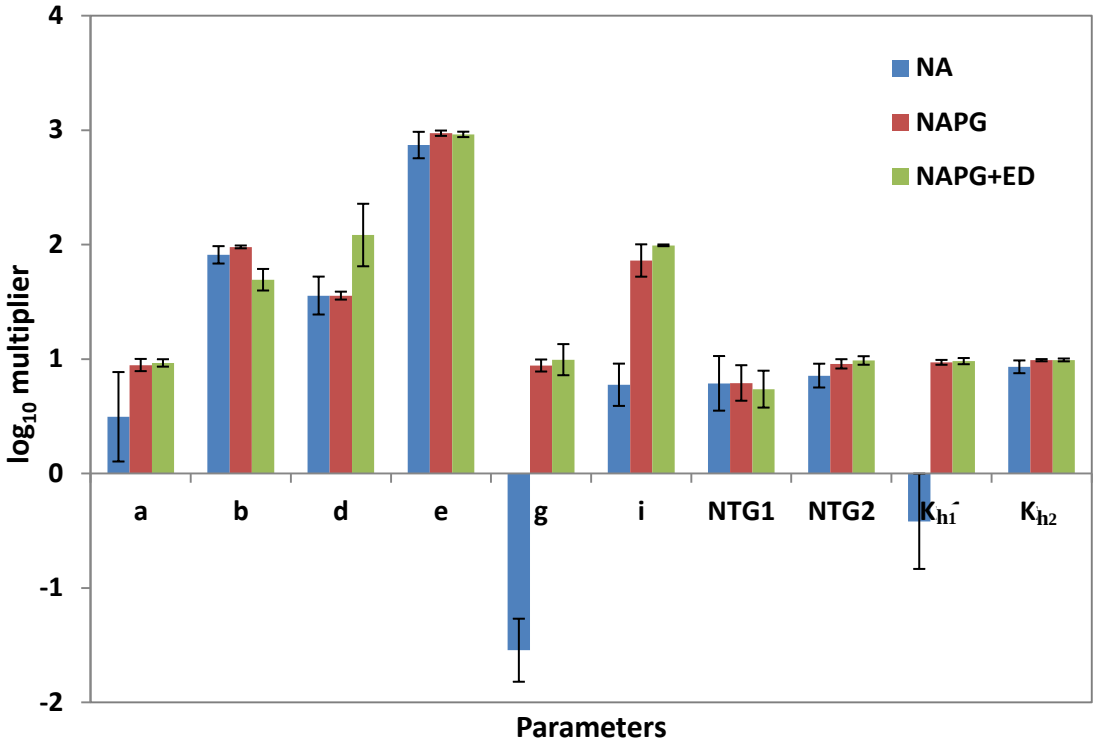

Figure 6.13: Parameters of the best model of each method. Error bars indicate the standard deviation in values over the best 10 models overall, assuming equal likelihood.

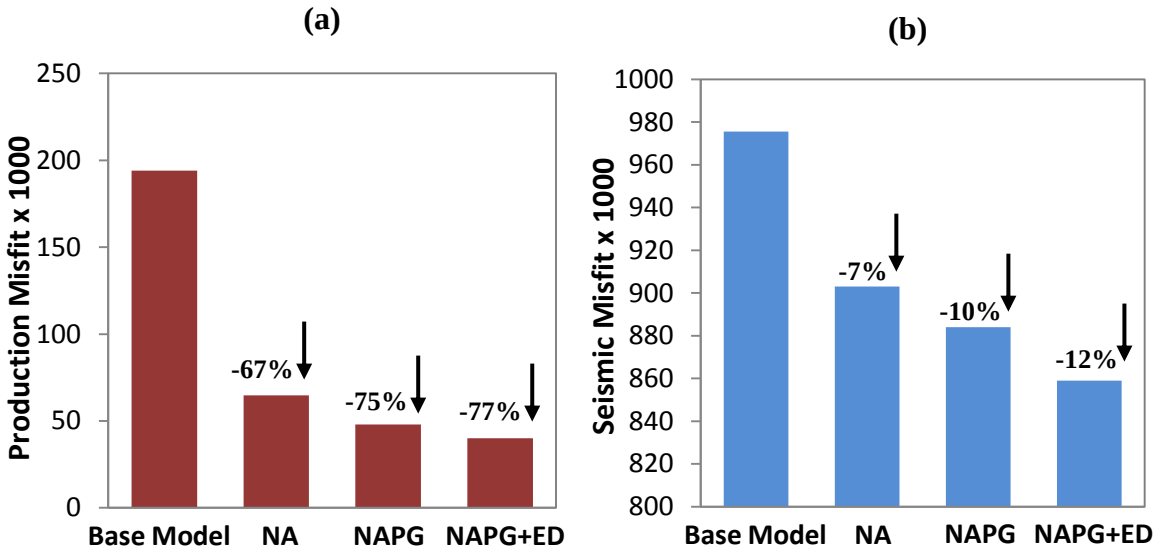

Figure 6.14: (a) Production misfit reduction by percentage for the best history matched model of each method and **(b)** Seismic misfit reduction by percentage for the best history matched model of each method.

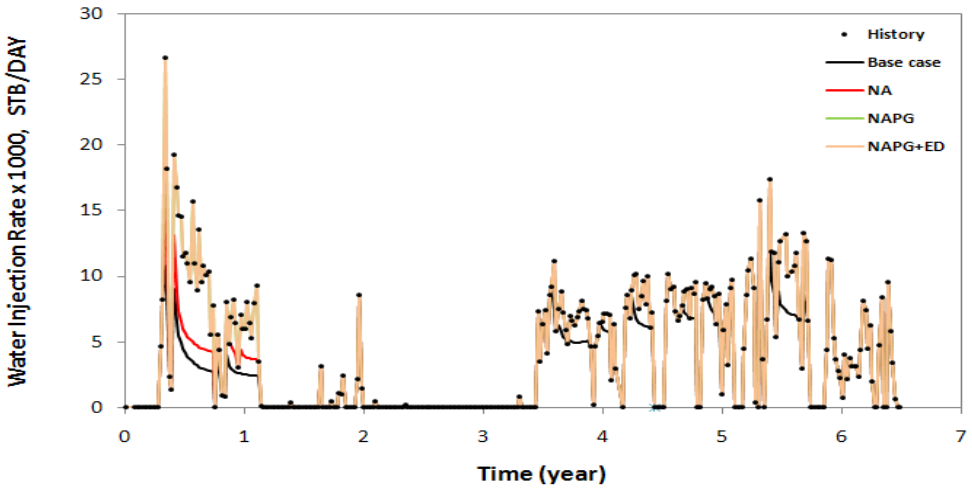

Figure 6.15: Predictions and history data for Injector 2 obtained from the three methods. Symbols indicate the observed data.

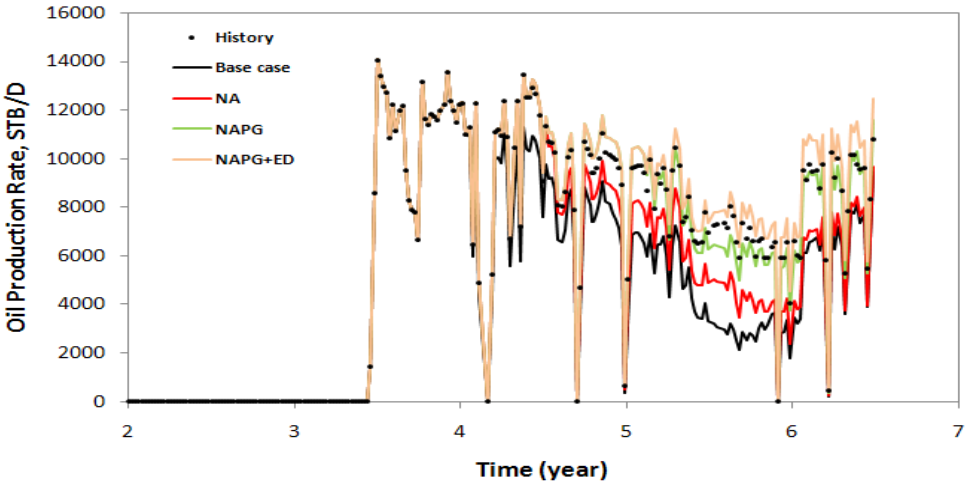

Figure 6.16: Predictions and history data for Producer 4 obtained from three methods. Symbols indicate the observed data.

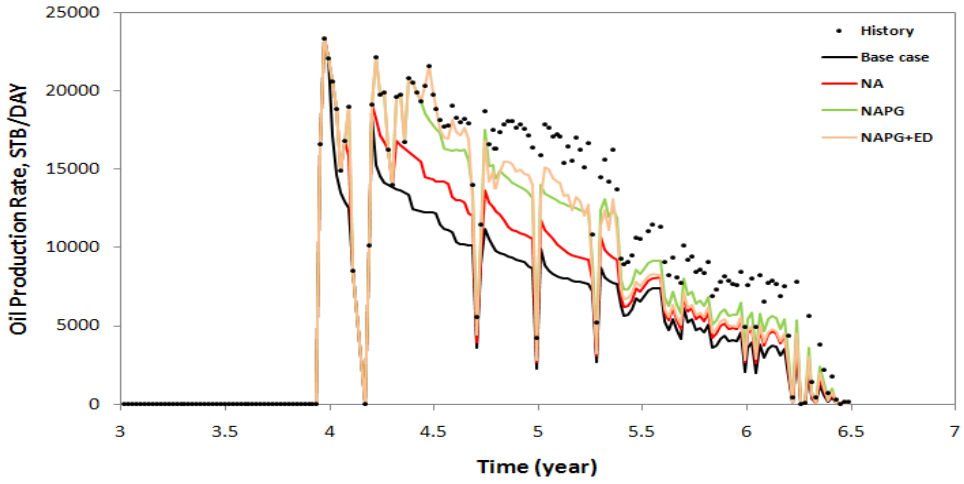

Figure 6.17: Predictions and history data for Producer 5 obtained from three methods. Symbols indicate the observed data.

Seismic maps as impedance differences for six time intervals are shown in Figure 6.18, calculated from the base case model as well as the best models from NA, NAPG and NAPG+ED cases. The base case model is actually quite similar to the best models from the NAPG and NAPG+ED cases. The NA seems to have pulled the search away from fitting the seismic maps. Later, in the process, as more models are generated, the maps are more like the NAPG cases.

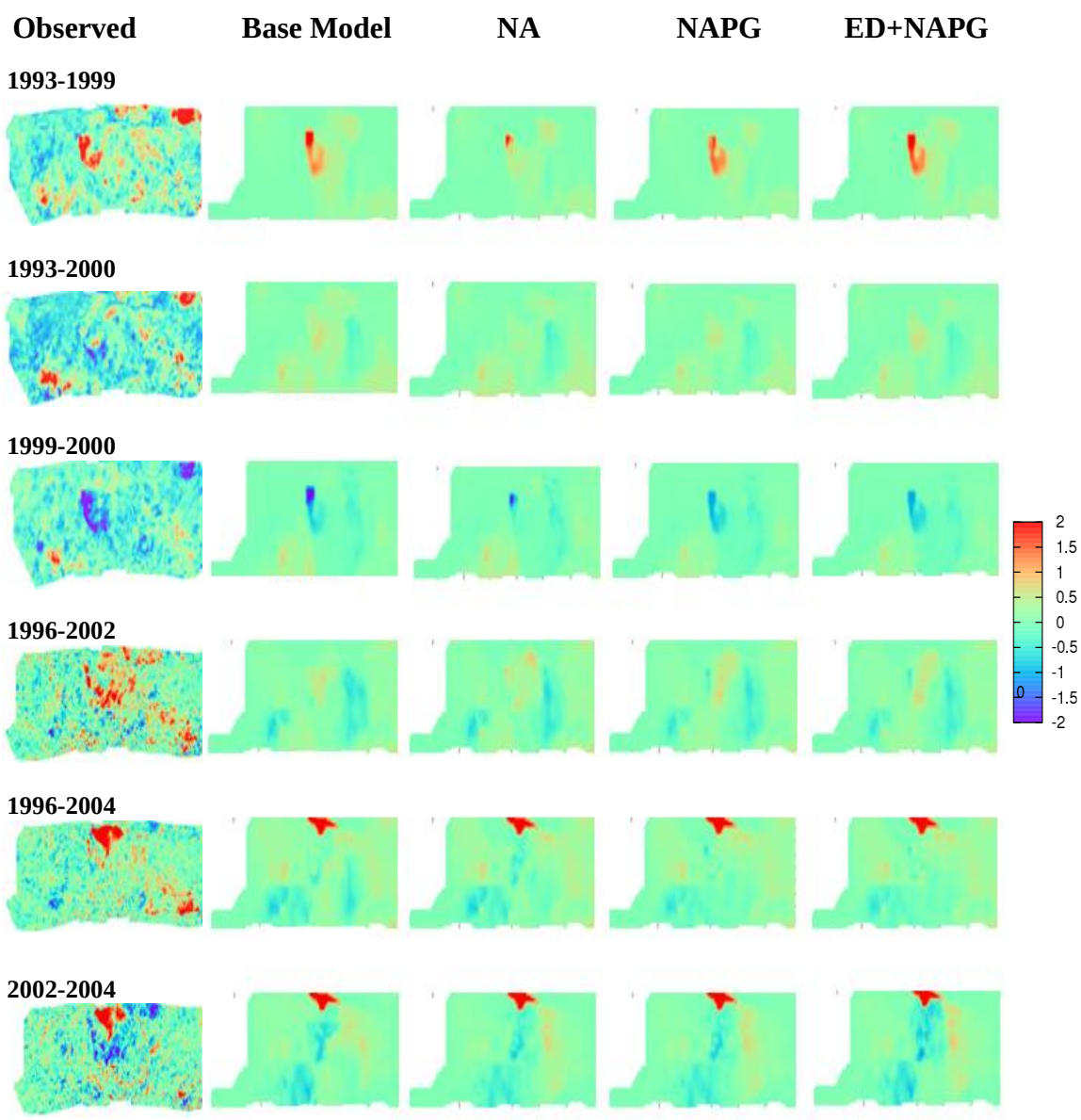

Figure 6.18: Normalized 4D seismic attribute maps as difference in pseudo acoustic impedances for six time increments for the best models compared to the observed and base case. The 4D signatures are normalised by subtracting the mean (μ) of the pre-production maps in 1993 and 1996 and dividing by its standard deviation (σ), and differences are presented in this scale.

6.5 Summary

The main part of this chapter described an application of experimental design to applied to the Schiehallion field. We have presented a method to maximize the information, that can be obtained from a specified number of simulation runs. Response surface and experimental designs are the key concepts. In previous work, we found that one of the main disadvantages of full NA and full NAPG run is that they require a high number of initial models to fill the parameter space. This issue becomes critical when we have a high dimensional problem with more than ten dimensions because of the requirement to use a large number of initial models to start NA or NAPG, which is extremely costly. Proxy models serve as a good tool for analysing the misfit function to determine whether or not such a large number of models is necessary. In this research, we find that Experimental Design can help to not only derive the proxy model but if it is suitable, we can use the initial set of models to start the NAPG process. For a 10D case, the number of initial models was reduced by 85% using CCF, which leads to reduced CPU time. ED can then add to the improved convergence from using proxy model derived gradients.

CHAPTER 7
Stopping Criteria

Overview

Four important issues are to be considered in the (automated) history matching loop: parameterisation, definition of the objective function, choice of optimisation algorithm, and stopping criteria. A stopping criterion is used to define when the history matching process can be terminated. The objective of stopping criteria is to ensure that the proper parameter combinations are found given the data available. In this chapter, the stopping criteria will be studied and we will present different approaches of stopping criteria to terminate the execution of history matching loop.

7.1 Convergence and Termination Criteria

Alvarenga and Mateus, (2004) stated "*an optimization algorithm has converged if it cannot reach new solution candidates anymore or if it keeps on producing solution candidates from a "small" subset of the problem space*". The HM process should not be terminated too early since the quality of the solution may not yet be satisfactory. As mentioned in Chapter 2, the main drawback for the stochastic methods in practice is the high computational cost arising from their slow convergence rate due to their exploratory nature. Also, they may fail to detect promising search directions especially in the final stage of the search where in a real-world problem, the solution is generally not known. Therefore, the question is "*when is it possible to stop the optimization algorithm*?" Since the objective of the algorithm is to minimize the objective function by preferentially sampling the parameter space, the stopping criteria should be directly related to how precise the optimum point is located.

In general, a solution of the inverse problem should not be accepted as an estimate unless it produces a match of the observed data. To discard solutions where the experimental data are not reconciled, convergence and termination criteria should be considered to avoid extended estimations, which are time consuming. For instance, Figure 7.1 illustrates a characteristic plot for the Neighbourhood Algorithms that we

used in this research as an example of outcome of the inversion, showing rapid progress at the beginning and flattening out at the end where the misfit values cannot be get below the noise (and model accuracy) floor. We may stop the iterative process when the models are no longer improving and the misfit is flattening out. It can be seen from the plot that there are many locations within the flat region (from models 4000 to 8000) where we may stop the iterative process to save CPU time. Alternatively we could restart the process by selecting new misfit weights, choose a new search domain or set a new parameterization to find alternative solutions. The general main aim is that the parameters space should be sampled sufficiently to ensure the proper model is found. Otherwise, under-sampling of the parameter space combined with the non-uniqueness of the inverse problem may result in just some local minima being found.

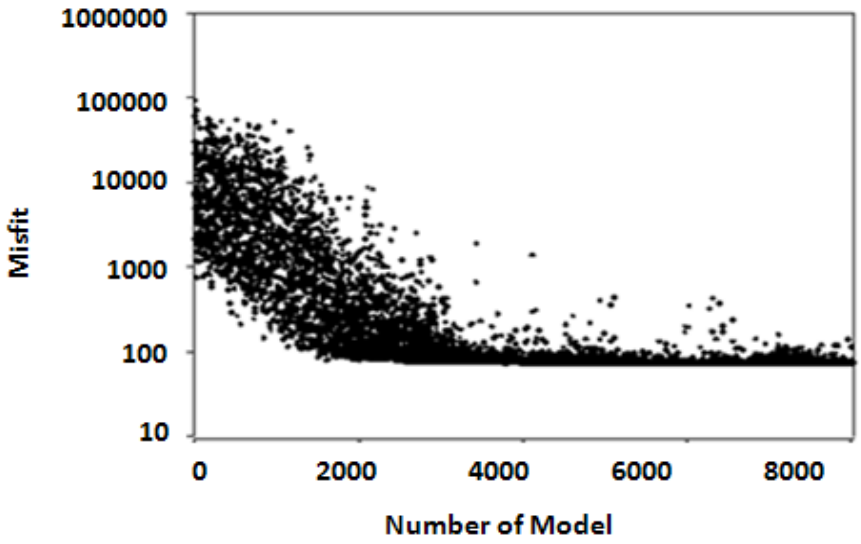

Figure 7.1: Example of convergence behaviour of NA showing flattening out at the end, which means that the algorithm may be stopped at any time potentially (Stephen *et al.*, 2004).

7.2 Stopping Criteria

The definition of an appropriate stopping criterion is complex and problem specific. Strictly speaking, selection of stopping criteria is difficult because determining an acceptable difference in misfits between iterations is complicated. If this criterion is set too relaxed, the model might not be optimally history matched. The selection of a suitable stopping criterion is related to the amount, quality, and type of constraining data available, and type of optimiser used. It is important that the parameter space is properly sampled and the number of iterations is not too limited to capture the solution.

For these reasons, defining suitable criteria to stop the iterative process of SHM is not a straightforward task and it is still a challenge and requires more research. In this study, we suggest different classes of stopping criteria that they might work before reaching the maximum number of iterations to save CPU time.

7.2.1 Stop Criterion 1: Maximum number of Simulations

This is a straightforward criterion where the algorithm stops when the number of iterations exceeds some maximum. However, the main drawback for such a deterministic stopping criteria is that it gives little control on whether the data are over or under-fitted. It is mainly used because a large number of forward model evaluations may represent a waste of computer resources, which may be better used sampling in other regions of the parameter space.

7.2.2 Stop Criterion 2: Misfit to Noise Misfit ratio Criteria

In the Schiehallion field, Stephen *et al.* (2006) found that observed seismic data contained uncorrelated Gaussian noise with standard deviation σ and this is used in the misfit as a weighting term. In Chapter 5, we concluded that for the same case, a misfit of the noise is equivalent to the number of measurements (see Section 5.3.1) which can be subtracted from the total misfit to obtain a misfit as if there was no noise present.

$$J_{noise} \approx N + \frac{\sum \varepsilon_m^2}{\sigma^2} \qquad 7.1$$

The idea is to use the ratio between misfit and misfit of the noise $\left(\frac{J}{J_{noise}}\right)$ as a stopping criterion. We first check if the misfit value has dropped below some threshold, below which we would consider that we are over-fitting to the noise, i.e.

$$(J/J_{noise}) < (1+\delta) \qquad 7.2$$

where $\boldsymbol{J}$ is the misfit and $\boldsymbol{\delta}$ is some small number much less than unity and indicates that we do not wish $\boldsymbol{J_{noise}}$ exactly.

To apply this criterion in stochastic methods, the misfit is estimated as an average per iteration or lowest value of a number of generations. If it falls below a given threshold δ for a number of generations, the optimization run is terminated. In this approach, we may assume errors are Gaussian and uncorrelated and we ignore the error model. On

the other hand, the error model may be important and should be calibrated and included in the misfit (e.g. Stephen, 2007) if necessary. Also in the context of the correlated errors, the noise misfit should be estimated. If the noise contribution to the misfit is not estimated accurately, this criterion cannot be reached easily indicating a poor solution.

7.2.3 Stop Criterion 3: Misfit Convergence Ratio

The change in the objective function can also be used to define a stopping criterion. Hence, the algorithm runs until the average change in value of the objective function in iterations (for stochastic methods is a several misfits per iteration) is less than some defined tolerance. In other words, the iterative process can be set to stop when the objective function (OF) stops changing, i.e.

$$\frac{|\bar{O}(m^l) - \bar{O}(m^{l+1})|}{|\bar{O}(m^{l+1})|} < \in_{o,} \tag{7.3}$$

Where $\bar{O}(m^l)$ is the average objective function of model l and $\in_o$ is the tolerance value. To apply this criterion on stochastic methods, the improvement of the best objective function value or average per iteration is monitored. If it falls below a given threshold m for a number of generations, the optimization run is terminated.

7.2.4 Stop Criterion 4: Parameter convergence ratio

The iterative process may be stopped when the model parameters stop changing, i.e.

$$\max_{1 \le i \le N_d} \left(\frac{\left| m_i^{l+1} - m_i^l \right|}{\left| m_i^{l+1} \right|} \right) \le \in_m \tag{7.4}$$

Where m_i is the value of model parameter i where $i = 1$, N_d and l is the model number index, and N_d is the number of model unknown parameters. The typical tolerance values ϵ_m is 10^{-3} (Oliver and *et al*., 2008). To apply this criterion on stochastic methods, the improvement of the best model parameter convergence value or average per iteration is monitored. If it falls below a given threshold m for a number of generations g, the optimization run is terminated.

7.3 Proposed Stopping Criteria Routine

In the previous section, we suggested different approaches to define the appropriate point to stop the iterative process of SHM. Figure 7.2 shows a workflow for general stopping criteria that we may follow at the end of calculating the misfits for each iteration. First, we check for the maximum number of simulations (it_{max}). If we exceed the maximum number ($it > it_{max}$), then stop the loop.

Otherwise, we ask "*have we reached a solution?*" Therefore, we check if the misfit value has dropped below some threshold which would identify that we are over-fitting to the noise, i.e. ($\boldsymbol{J<J_{noise}\ (1+\delta)}$ (where $\boldsymbol{J}$ is the average misfits per iteration and $\boldsymbol{\delta}$ is some small number much less than unity and indicates that we do not wish to match $\boldsymbol{J_{noise}}$ exactly) as explained for Equation 7.2.

In that case, we check that we have used some minimum number of iterations (it_{min}) before stopping the loop. This is an extra term that basically says we will search with a minimum spendable CPU/license budget but not exceed the maximum. We might have found a good solution at this point but still want to search for alternatives. Therefore, if the number of iterations is greater than it_{min} then we stop. Otherwise, we may check if there could be alternative solutions for the problem by restarting with either:

1. new misfit weights for various data types (e.g. observed seismic or production data) thus varying the importance of the data or
2. a new search domain to search the current parameter space away from where we got stuck or
3. new parameterization.

If we have not reached the solution then we ask "*are we still improving the solution*". "improving" here means that the misfit is declining sufficiently over the iterations. It is measured using the "misfit convergence ratio" and the equivalent for parameters (see Equation 7.3 and Equation 7.4 respectively). If the misfit convergence ratio is less than the specified relative error (ϵ_o) OR the parameter convergence ratio is less than the specified relative error (ϵ_m) then we have stopped improving the solution. Since we have not got a solution that we are happy with yet, we should check if there could be alternative solutions for the problem (points 1-3 above). However, if we are continuing to improve the misfit, we continue the loop with another iteration.

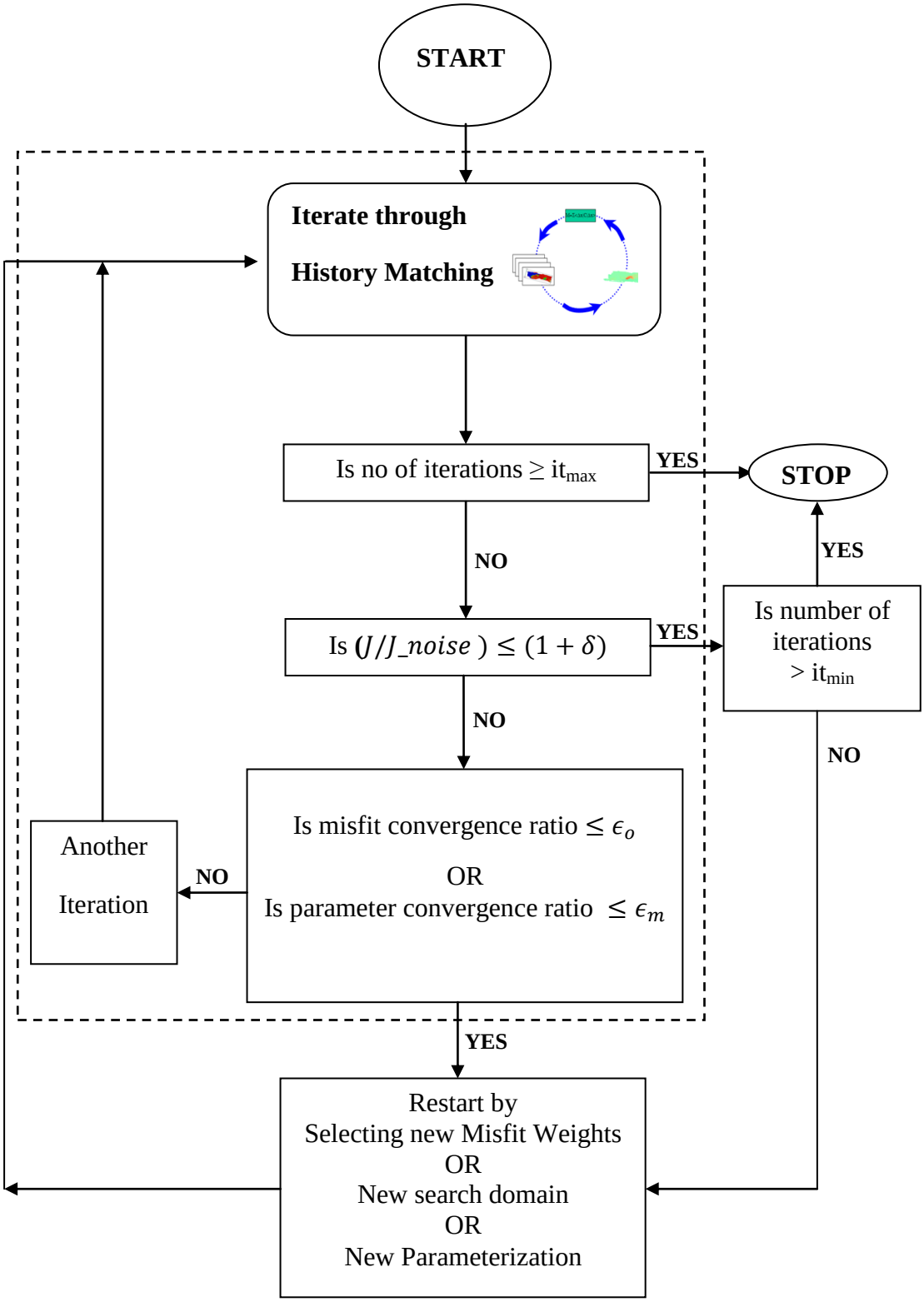

Figure 7.2: SHM loop workflow using different stopping criteria. The dashed box is the automated part of SHM.

7.4 Using the proxy model of the misfit as a stopping criterion

The aim of the work presented in this section is to improve identification of convergence of during history matching using the proxy model and to use the proxy model convergence as a stopping criterion. The plan would be to update the proxy as we sample towards convergence. At each iteration of the history-matching loop, we calculate the proxy using the best N models where N is the optimum number of models that are required to build the proxy model. Adding newer better models from each iteration to update the proxy will lead to a converged and stabilized proxy. Once the proxy has stabilized, no more models are needed and, more importantly, we can stop the iterations of the history-matching loop. There are two steps to achieve this approach. First, what is N likely to be? Second, at what parameter range does the proxy become accurate?

The first step is to estimate the optimum number of models needed (N) to build the proxy model of the misfit. For a 10D case as an example (for details see Chapter 6, Section 6.3), we used 149 models to train the proxy model using Experimental Design (ED). We also now consider proxies derived using an additional 300, 500 or 1024 models obtained from quasi-random sampling of the same region of parameter space in separate scenarios. We tested the convergence of the proxy model coefficients as we add more models and we found that the models defined as a minimum for ED was not enough to complete the necessary convergence of the coefficients as shown in Figure 7.3 and Figure 7.4 for linear and quadratic terms. The convergence of the interaction terms of the proxy model as we add more models is seen in Figure 7.5. In this case, we required an extra 300 models to get convergence of the linear, quadratic and interaction terms coefficients of the proxy model. We observe that ED derived coefficients are quite different but ED+300 are similar to ED+500 and ED+1024. Thus, in this case N is approximately 449 models to build the proxy model of the misfit.

The second step after defining the required models to build the proxy model is to determine the range of parameters where the proxy is accurate. In Chapter 5, we found that a derived proxy model of the misfit was ultimately inaccurate at the minimum and failed to find the solution of a synthetic case from the Schiehallion field where we knew the answer. In other words, it did not recover the original solution, as the parameters were not converging to the known solution and were not stabilized. The whole point is

that as we reduce the search window the misfit should resemble a quadratic equation more and more and the fit of the proxy improves until it cannot improve anymore. This is a simple 2nd order Taylor's expansion with high order terms negligible. Therefore, we consider a reduced sample range to determine how the proxy changes as we approach the proxy zone of validity where we can use the proxy instead of using full numerical simulation. We now want to identify how the coefficients of the proxy converge as the search window is reduced. We chose different parameters ranges, including the original range from Section 6.3 and then reduced by a factor of, 1/3, 1/9, 1/27 of and 1/81. Table 5.2 shows the original parameters range of barrier transmissibility multipliers on a log scale. Because of the normalization process used during the regression analysis where we applied a linear scaling, we needed to denormoralize the coefficients to check if the proxy coefficients converge as we narrow the parameters range.

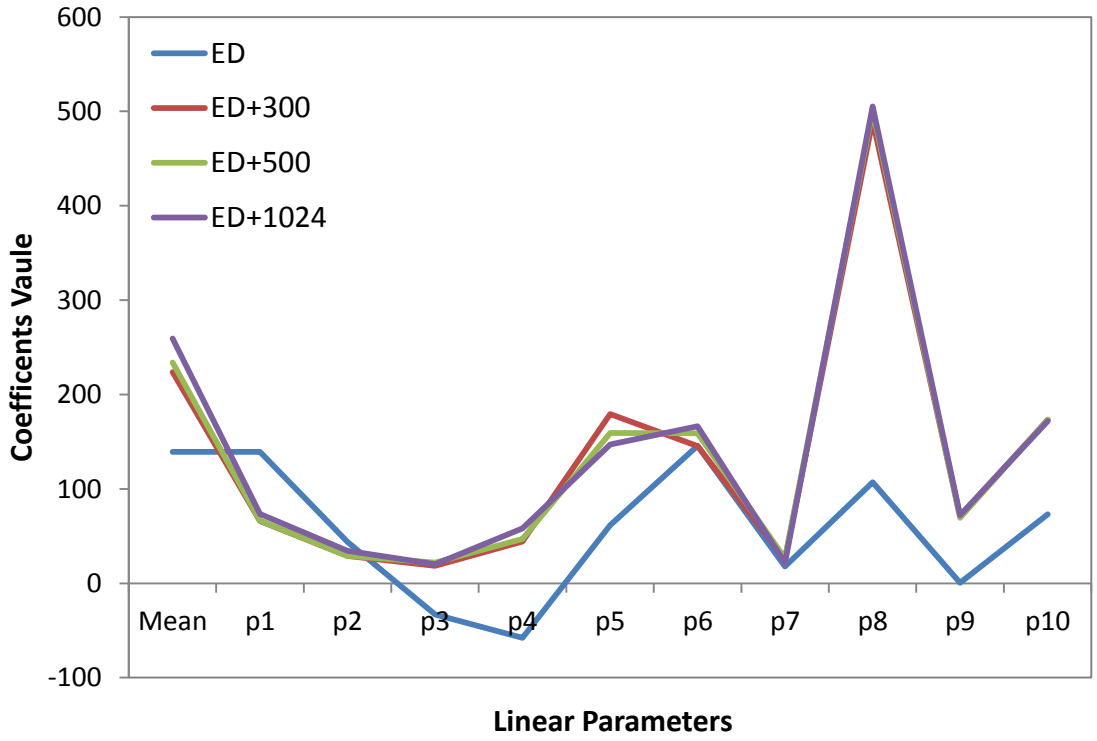

Figure 7.3: Linear terms of the proxy model showing convergence as we added models to the main ED proxy model.

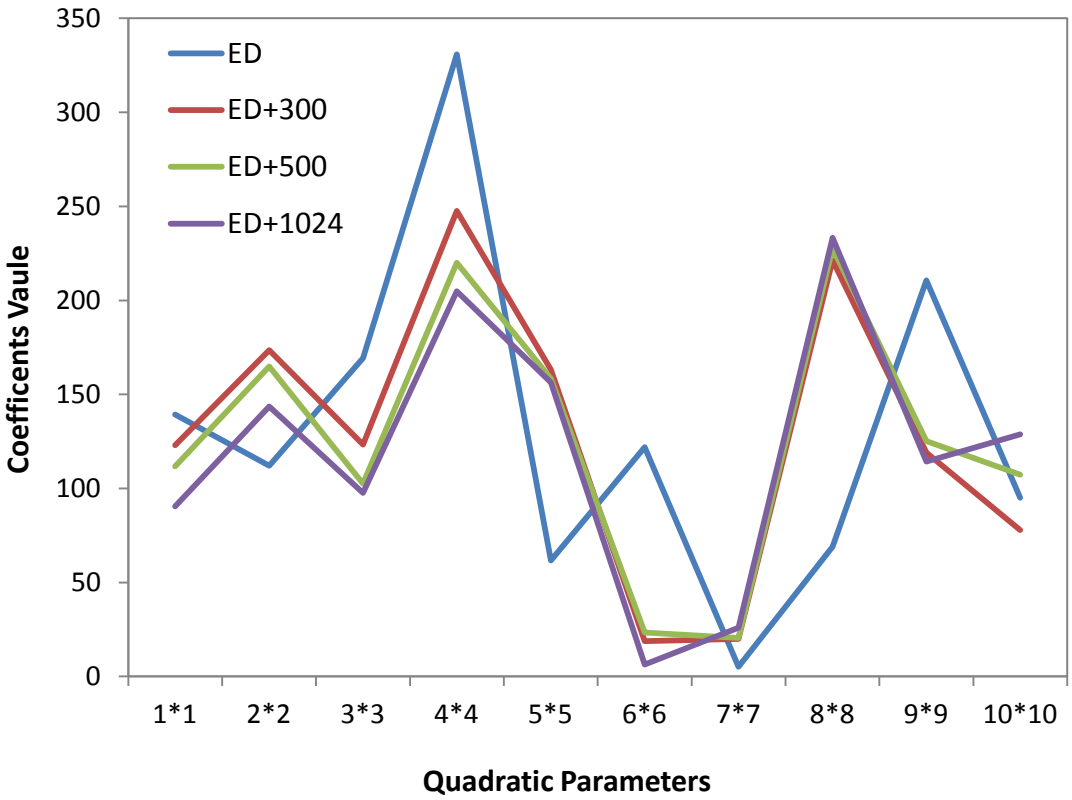

Figure 7.4: Quadratic terms of the proxy model showing convergence as we added models to the main ED proxy model.

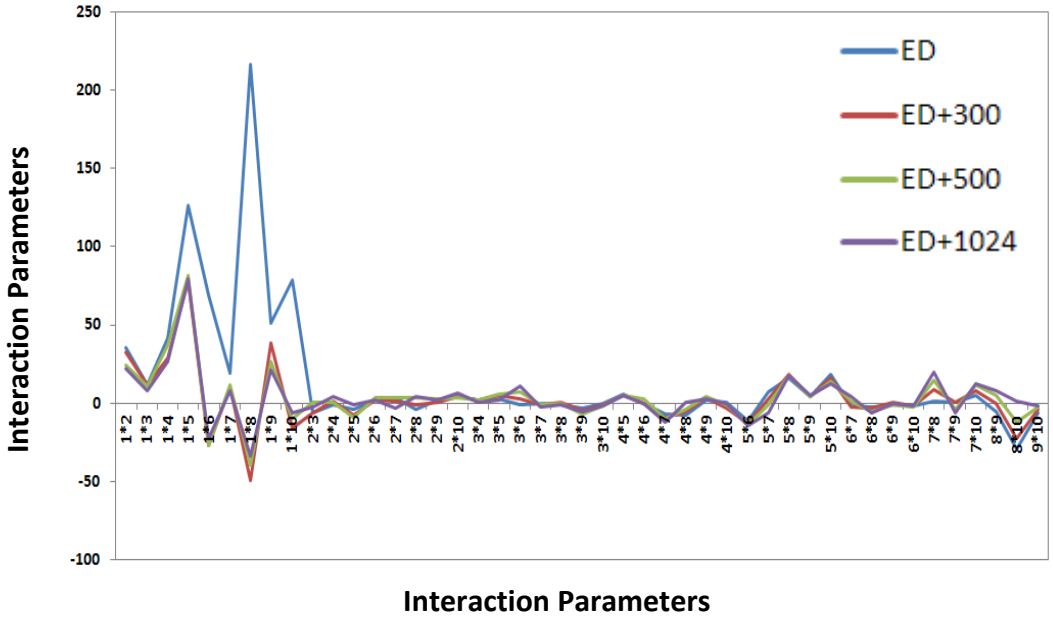

Figure 7.5: Interaction terms of the proxy model showing convergence as we added models to the main ED proxy model.

7.4.1 Coefficient Denormalization

As we change the size of the window, we normalize the parameters. Thus to retrieve the coefficients on their original scale, we need to correct them for the normalization by denormalization. The mathematical derivation of denormalization of the coefficients is presented in this section. We define the proxy model as 2nd order polynomial as:

$$f(\underline{x}) = a + \sum_{i=1}^{N} b_i x_i + \sum_{i=1}^{N} c_i x_i^2 + \sum_{i=1}^{N-1} \sum_{j=i+1}^{N} d_{ij} x_i x_j \tag{7.5}$$

However, when we calculate the coefficients, x_i is a normalized parameter so it lies between -1 and 1 always. So the real parameter is X such that

$$x_i = \frac{X_i - \mu_i}{\sigma_i},$$

$$\mu_i = (x_{max} + x_{min})/2$$

$$\sigma_i = (x_{max} - x_{min})/2 \tag{7.6}$$

Therefore, we need the equation to be written as

$$f(\underline{X}) = A + \sum_{i=1}^{N} B_i X_i + \sum_{i=1}^{N} C_i X_i^2 + \sum_{i=1}^{N-1} \sum_{j=i+1}^{N} D_{ij} X_i X_j \tag{7.7}$$

and then derive its coefficients in terms of those obtained for Equation 7.5. We can write Equation 7.5 in matrix format:

$$f(\underline{x}) = a + \underline{b}.\underline{x} + \underline{x}.\underline{\underline{c}}\,\underline{x} \tag{7.8}$$

The matrix $\underline{\underline{c}}$ is diagonally symmetric, $c_{ii}=c_i$ from Equation 7.5 and $c_{ij}=d_{ij}$.

$$\begin{bmatrix} c_{11} & d_{12} & d_{13} & . & . \\ . & c_{22} & . & . & . \\ . & . & c_{33} & . & . \\ . & . & . & c_{44} & . \\ . & . & . & . & . \end{bmatrix}$$

The conversion is then:

$$f(\underline{X}) = a + \underline{\beta}.(\underline{X} - \underline{\mu}) + (\underline{X} - \underline{\mu}).\underline{\underline{\gamma}}(\underline{X} - \underline{\mu}) \tag{7.9}$$

Where $\beta_i=b_i/\sigma_i$ and $\gamma_{ij}=c_{ij}/(\sigma_i\sigma_j)$.

This gives:

$$f(\underline{X}) = a + \underline{\beta}.(\underline{X} - \underline{\mu}) + \underline{X}.\underline{\underline{\gamma}}\underline{X} - \underline{\mu}.\underline{\underline{\gamma}}\underline{X} - \underline{X}.\underline{\underline{\gamma}}\underline{\mu} + \underline{\mu}.\underline{\underline{\gamma}}\,\underline{\mu} \tag{7.10}$$

Note that because matrix multiplication is not commutative, $\underline{\mu}.\underline{\underline{\gamma}}\underline{X} \neq \underline{X}.\underline{\underline{\gamma}}\underline{\mu}$ however,

$\underline{\underline{\gamma}}^T\underline{\mu}.\underline{X} = \underline{\mu}.\underline{\underline{\gamma}}\underline{X}$ and $\underline{X}.\underline{\underline{\gamma}}\underline{\mu} = \underline{\underline{\gamma}}\underline{\mu}.\underline{X}$ Rearranging gives:

$$f(\underline{X}) = a - \underline{\beta}.\underline{\mu} + \underline{\mu}.\underline{\underline{\gamma}}\,\underline{\mu} + \left(\underline{\beta} - \left(\underline{\underline{\gamma}}^T + \underline{\underline{\gamma}}\right)\underline{\mu}\right).\underline{X} + \underline{X}.\,\underline{\underline{\gamma}}\underline{X} \tag{7.11}$$

Note that $\underline{\underline{\gamma}}^T + \underline{\underline{\gamma}}$ is symmetric.

Thus, this is just

$$f(\underline{X}) = A + \underline{B}.\underline{X} + \underline{X}.\underline{\underline{\gamma}}\underline{X} \tag{7.12}$$

And we relate this to Equation 7.7:

$$A \equiv a - \underline{\beta}.\underline{\mu} + \underline{\mu}.\underline{\underline{\gamma}}\,\underline{\mu}$$

So

$$A \equiv a + \sum_{i=1}^{N} b_i\mu_i/\sigma_i + \sum_{i=1}^{N} c_i\mu_i^2/\sigma_i^2 + \sum_{i=1}^{N-1}\sum_{j=i+1}^{N} d_{ij}\mu_i\mu_j/\sigma_i\sigma_j$$

$\underline{B} \equiv (\underline{\beta} - \left(\underline{\underline{\gamma}}^T + \underline{\underline{\gamma}}\right).\underline{\mu}).\underline{X}$ and

$$B_i = \frac{b_i}{\sigma_i} - 2\frac{c_i\mu_i}{\sigma_i^2} - \sum_{\substack{j=1 \\ j\neq i}}^{N} \frac{d_{ij}\mu_j}{\sigma_i\sigma_j}$$

$C_i = c_i/(\sigma_i^2)$

$D_{ij} = d_{ij}/(\sigma_i\sigma_j)$ (7.9)

We showed the numerical derivation of denormalization of the coefficients for the 10D case of Schiehallion (Section 6.3), which has 66 coefficients. The results of denormalization are shown in Figure 7.6 and Figure 7.7. It can be seen from those plots that as we reduced the parameters range, linear terms of the regression equation would converge to zero as in this case $x^{min} = 0$. In addition, quadratic and interaction terms show convergence where the synthetic misfit is zero when all parameters are the true values assuming no noise added to truth case.

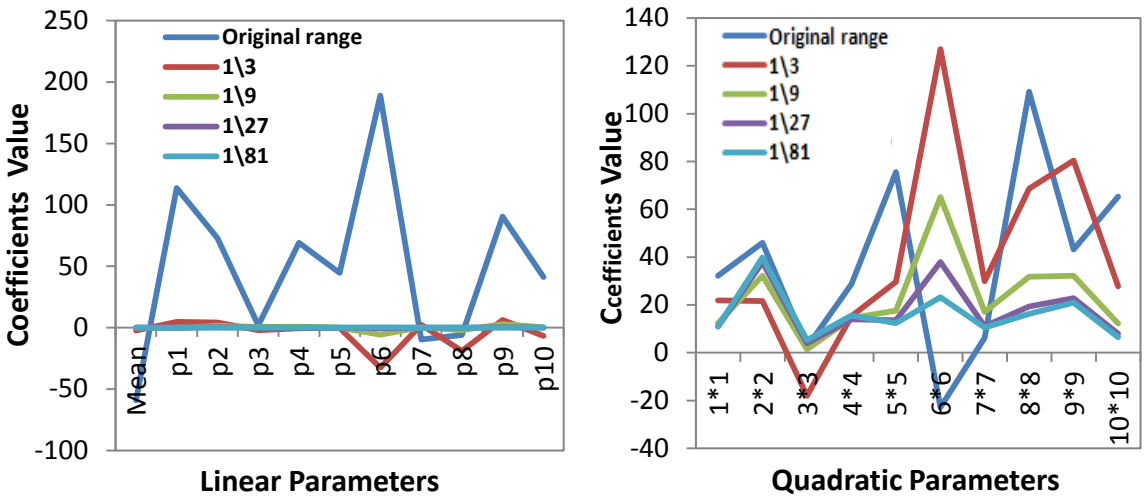

Figure 7.6: Convergence of the denormalized coefficients of the regression equation for **(a)** linear terms and **(b)** quadratic terms. We narrow the parameter range down to 1/81 of the original parameters range.

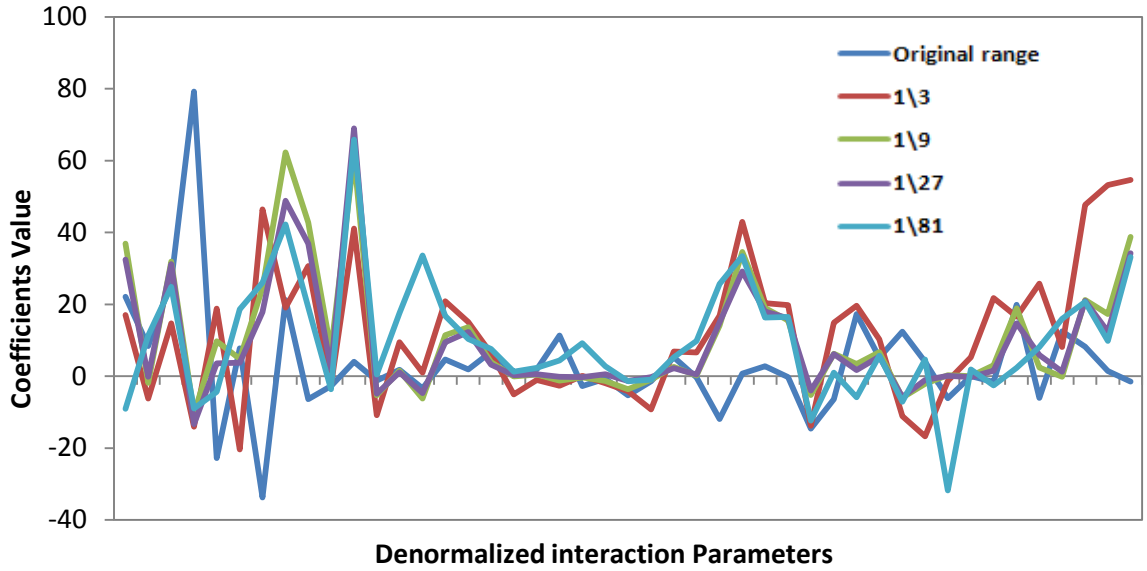

Figure 7.7: Denormalized interaction terms showing convergence of the regression equation.

7.4.2 NAB Analysis

In addition to above criterion of convergence, it is possible to demonstrate the convergence of the proxy coefficients as we reduce the parameter range using 1D marginal of the posterior probability distribution. In this analysis, we use the same Schiehallion case (see Chapter 5, Section 5.3) but here we are sampling the proxy using NA to generate the ensemble that is submitted to NAB routine in order to quantifying parameter uncertainty. (For NAB details, see Appendix B). Figure 7.8 shows the PPDs

for ten parameters and we found that as we sampled closer to the solution the curves would steadily converge. It is obvious from the PPD plots of ten parameters that the proxy model of the misfit is working at a narrow parameters range.

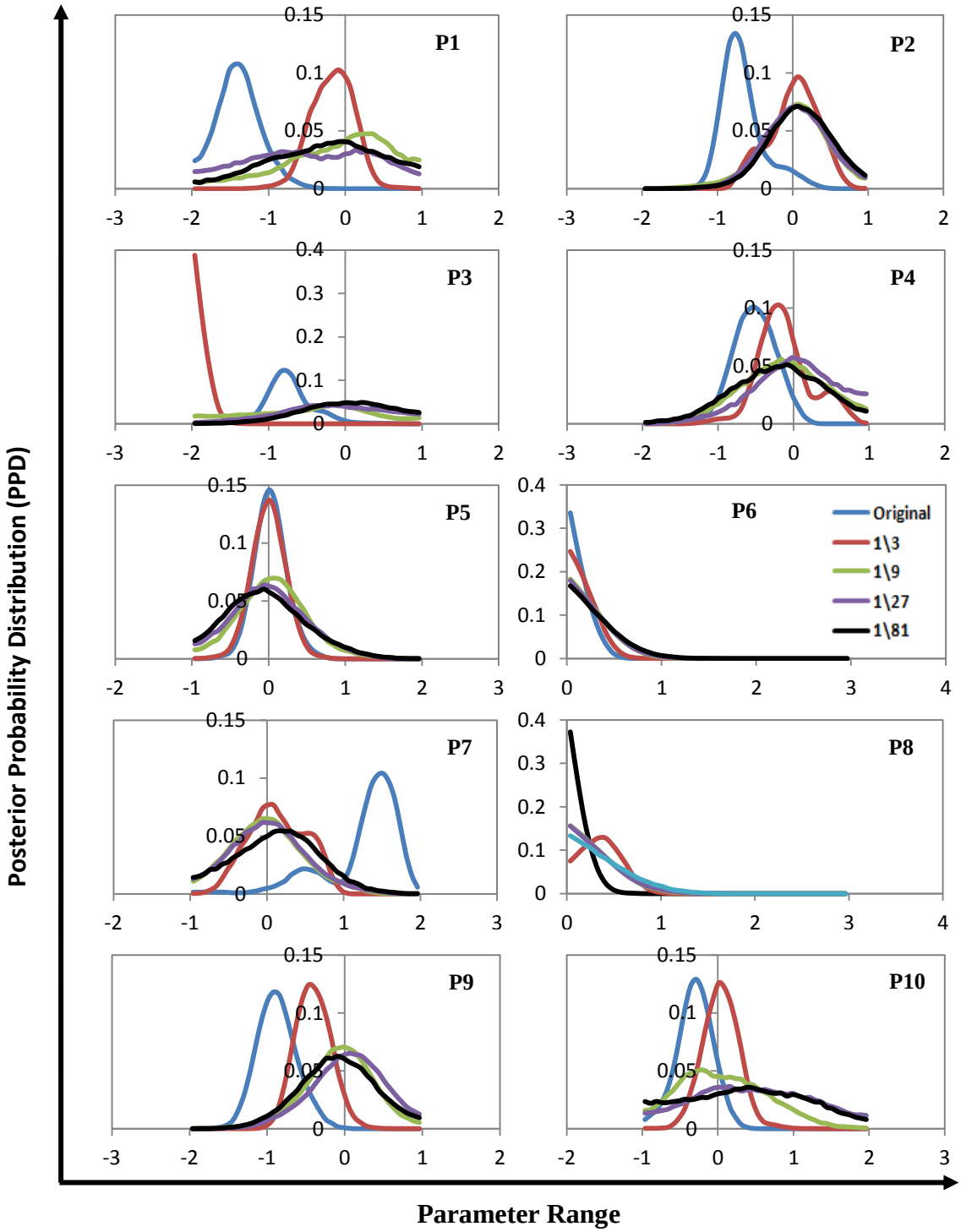

Figure 7.8: NAB outputs as we sample over the original range of parameters. They show convergence as we narrow search range. The symbol "Original" indicates the original parameters range.

7.4.3 Workflow of Stopping Criterion using proxy model

In this section, we present the workflow of the stopping criterion using the proxy model to detect convergence. We know that the derived proxy coefficients converge and the proxy zone of validity exists at certain parameter range. Initially, the proxy model of the misfit at each iteration is calculated using the best N models where N is the optimum number of models that are required to build the proxy model, as illustrated in Section 7.4. There is a range of theta (θ) over which the Taylor expansion of $M(\underline{\theta})$ is accurate We call this the range of validity. In that range, the proxy will be fairly accurate and stabilized otherwise the proxy will be changing. Figure 7.9 shows the general workflow of using proxy convergence as a stopping criterion. The procedure can be summarized in the following steps:

1. Start with N small (e.g. 149 as specified for ED) and get the proxy model of the misfit. In this example, 149 will not be enough as shown, particularly after the ED runs once we have refined the search.
2. Increase N and get the proxy. If N is too small, the proxy will change until there are sufficient models. If it does not stabilize at all, then we are not close to convergence and so another iteration of HM is performed.
3. If we find that as N increases, the proxy stabilizes. We have found the right number AND we are probably "in the proxy zone of validity".
4. Stop

The main challenge of this approach is how we identify a threshold *m* (model number) to detect the boundary of the proxy zone of validity where the proxy model of the misfit is accurate and then we can use proxy coefficients converge as stopping criterion. In practice, this would require the estimation of proxies every few iterations as we have explained.

In summary, all approaches that we have studied in this work need further investigation and are beyond the scope of this thesis.

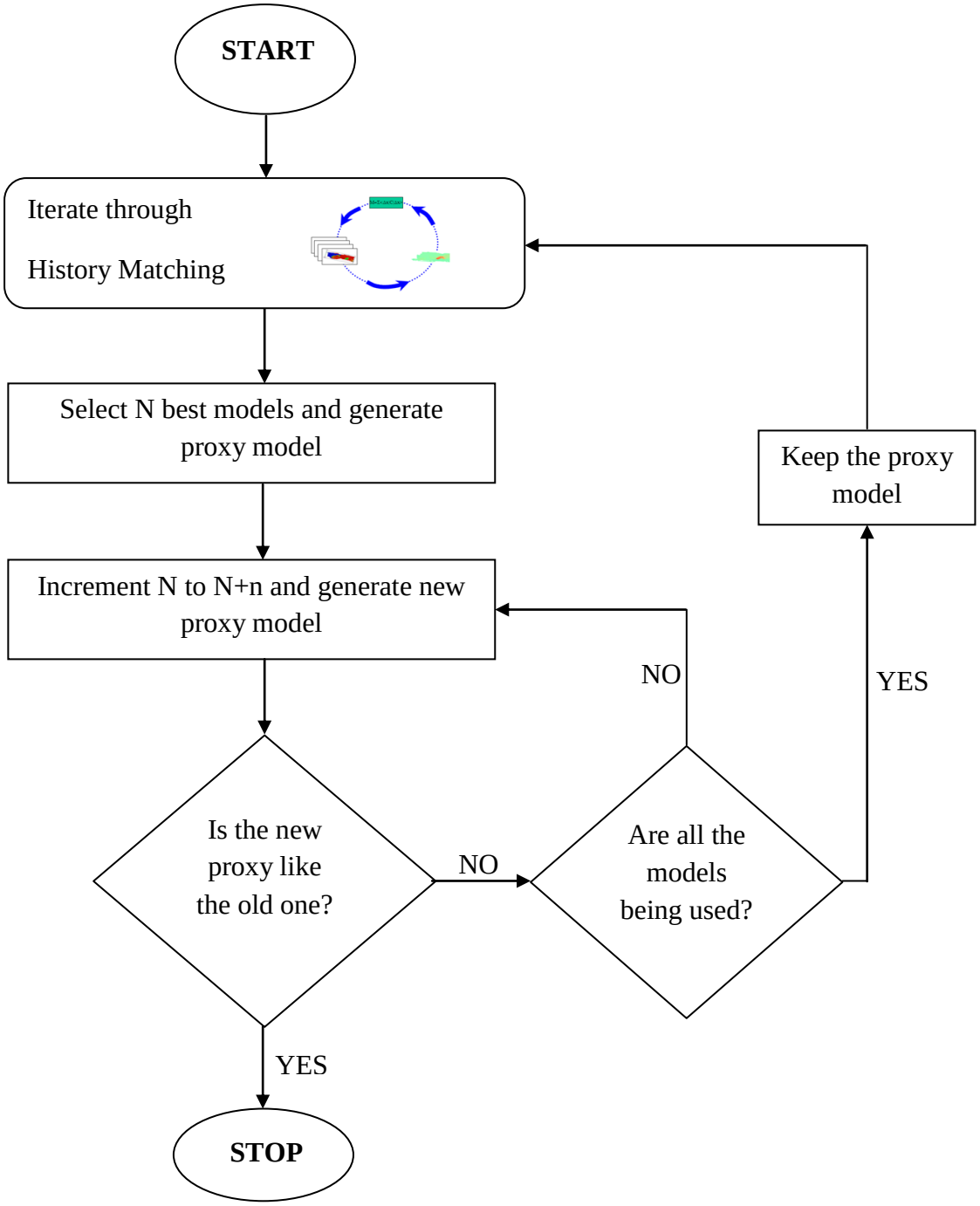

Figure 7.9: Workflow of stopping the criterion using proxy-modelling.

7.4.4 Illustration of the Analysis using a long SHM Run

The aim of this test is to determine whether or not the proxy model coefficients diverge as we add the best models of a long SHM run to update the proxy model. This is equivalent to the inner loop of Figure 7.9. We found that convergence of the coefficients exists as we narrow the parameters range, after that the question is how to identify a threshold *m* where we can use the proxy coefficients convergence as a stopping criterion. We carried out a very long full NA on the 10D case from Schiehallion field to guarantee convergence of history matching as shown in Figure 7.10. We could determine from that run the point at which the analysis of proxies might suggest a stopping point.

The regression analysis (SVD) to generate a proxy was applied to the output of this long SHM run by first taking the best 150 models. Afterwards, we added an additional set of the next best models to the previous ensemble and each time we derived the proxy coefficients to see how they vary**.** In this way, the models that we add to the previous ensemble have higher and higher misfits. Figures 7.11-13 show that as we add more new models to the previous ensemble, the influence of the regions that do not lie on the misfit increases. Also, it can be seen from those plots that the proxy diverges when more than 2000 of the best models were analysed. The best 2000 models, in this case, all have a misfit below 5.8, as indicated by red dashed line in Figure 7.10. This suggests the earliest possibility for detecting convergence. This coincides with the 2000^{th} model in the ensemble. Probably an additional 500 or so models are needed, all with M<5.8, before we would expect any convergence to be detectable. The long run itself is most likely converged according to this approach.

The trend of proxy coefficients can be seen if we normalize them against the coefficients of the first 150 model case. There is a sudden change in the proxy once we use more than the best 2000 models where the proxy breaks down as shown in Figure 7.14 and Figure 7.15. By coincidence this is the misfit of roughly the 2000^{th} model in the series as well as the fact that it is the threshold upon which any chance of detecting convergence has gone with the best 2000 models as illustrated in Figure 7.10.

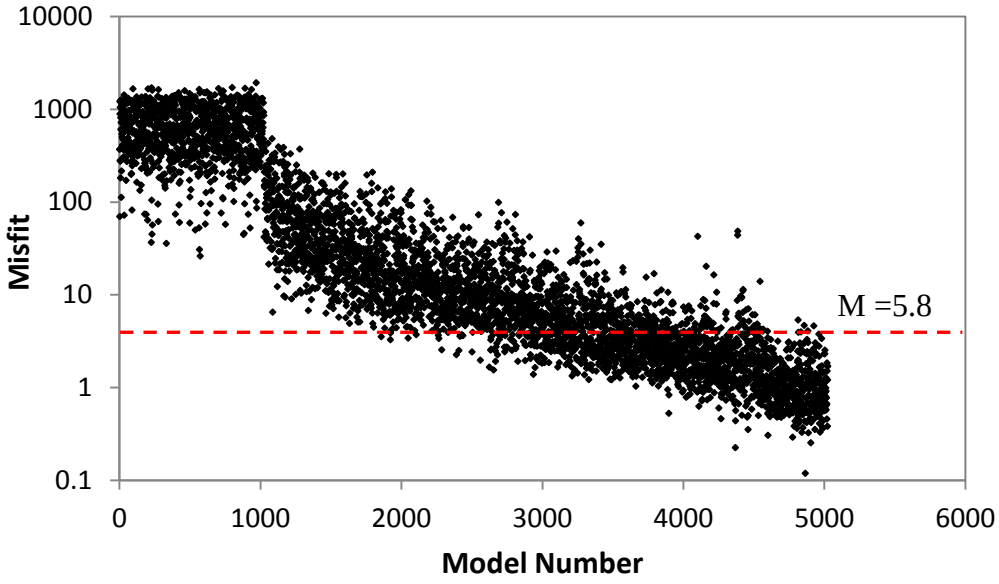

Figure 7.10: Misfit evolution of a long NA run on a synthetic case from the Schiehallion field. The 2000 best models line below the dashed line where M=5.8.

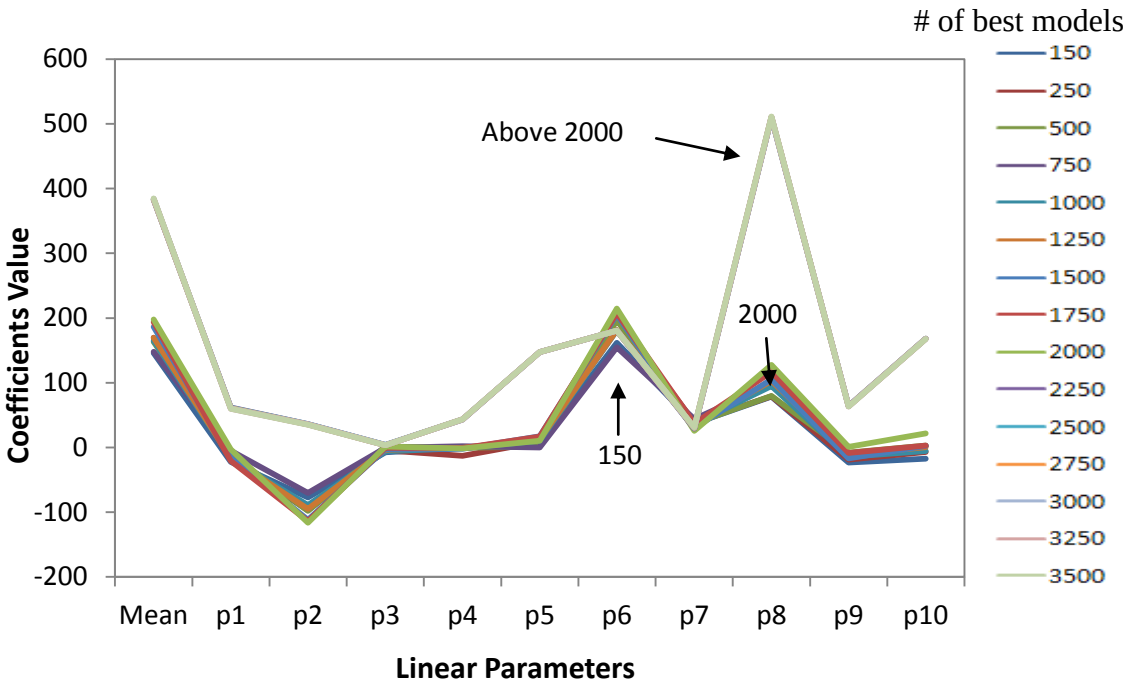

Figure 7.11: Normalised linear coefficients in the proxy as we updated the proxy by adding next best models to the ensemble.

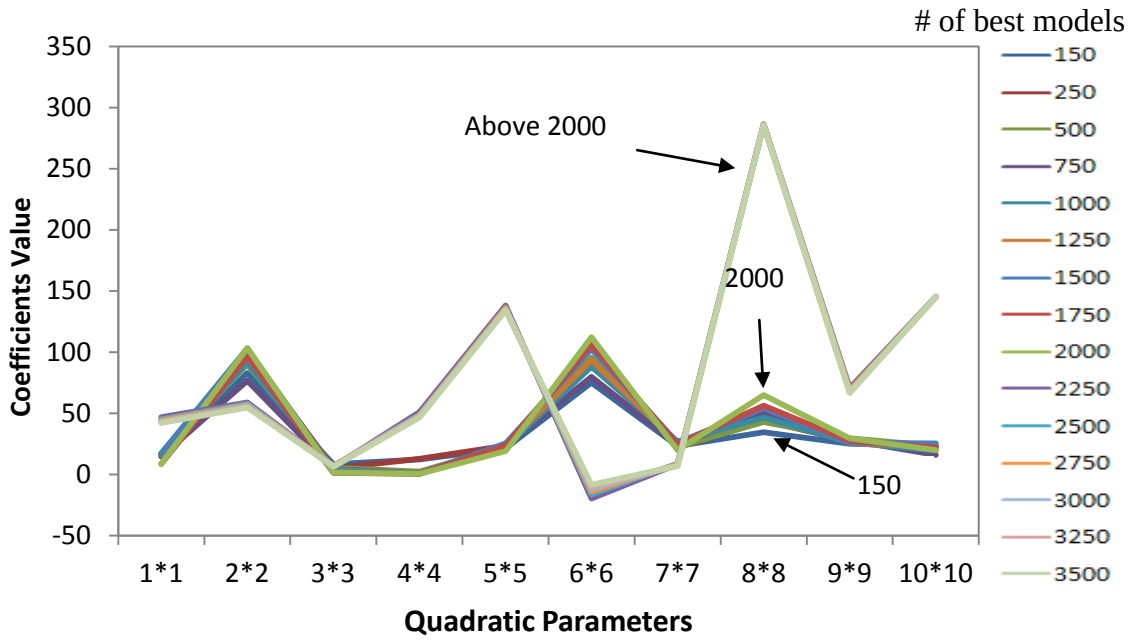

Figure 7.12: Normalised quadratic coefficients the proxy as we updated the proxy by adding next best models to the ensemble.

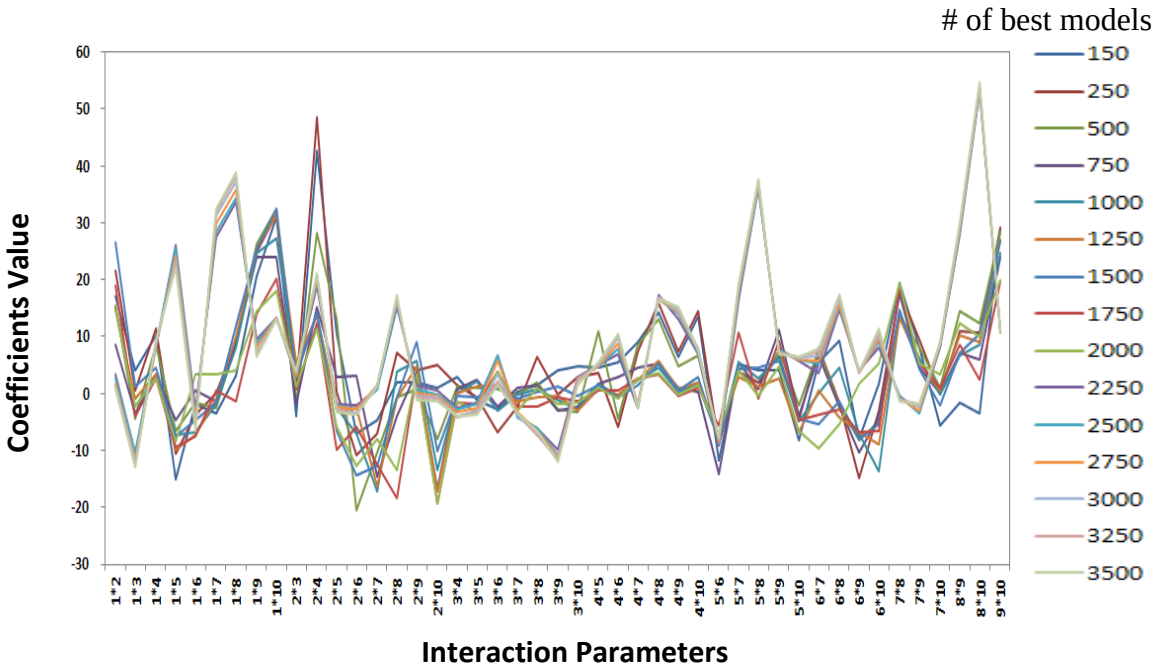

Figure 7.13: Interaction coefficients the proxy as we updated the proxy by adding next best models to the ensemble.

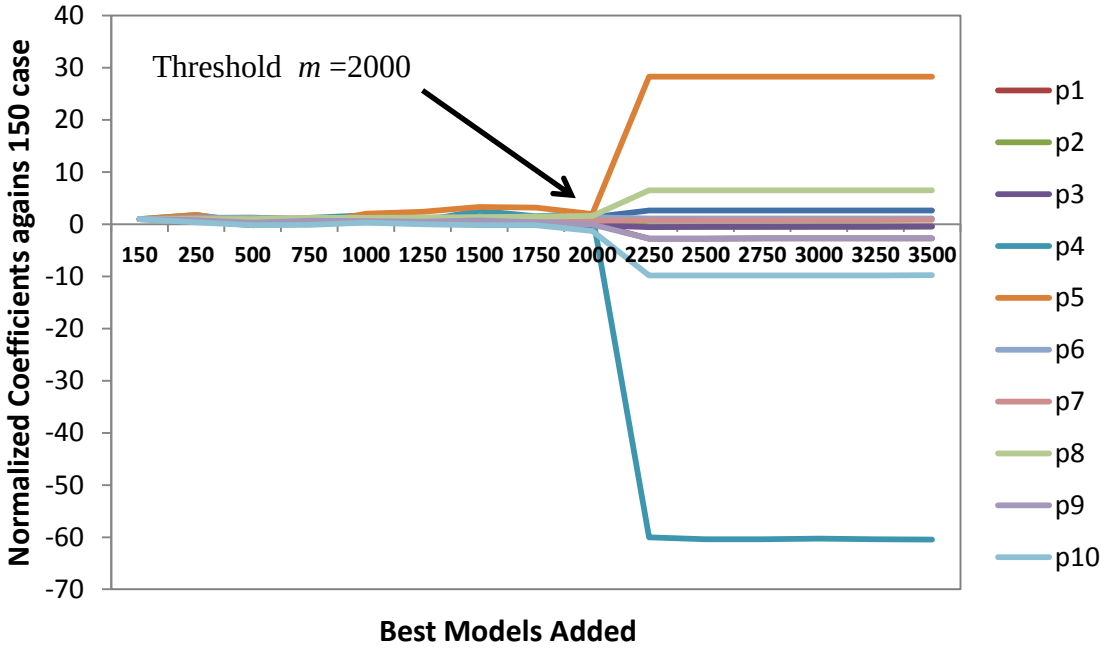

Figure 7.14: Linear coefficients trend after normalizing them against the coefficients of the first 150 models case.

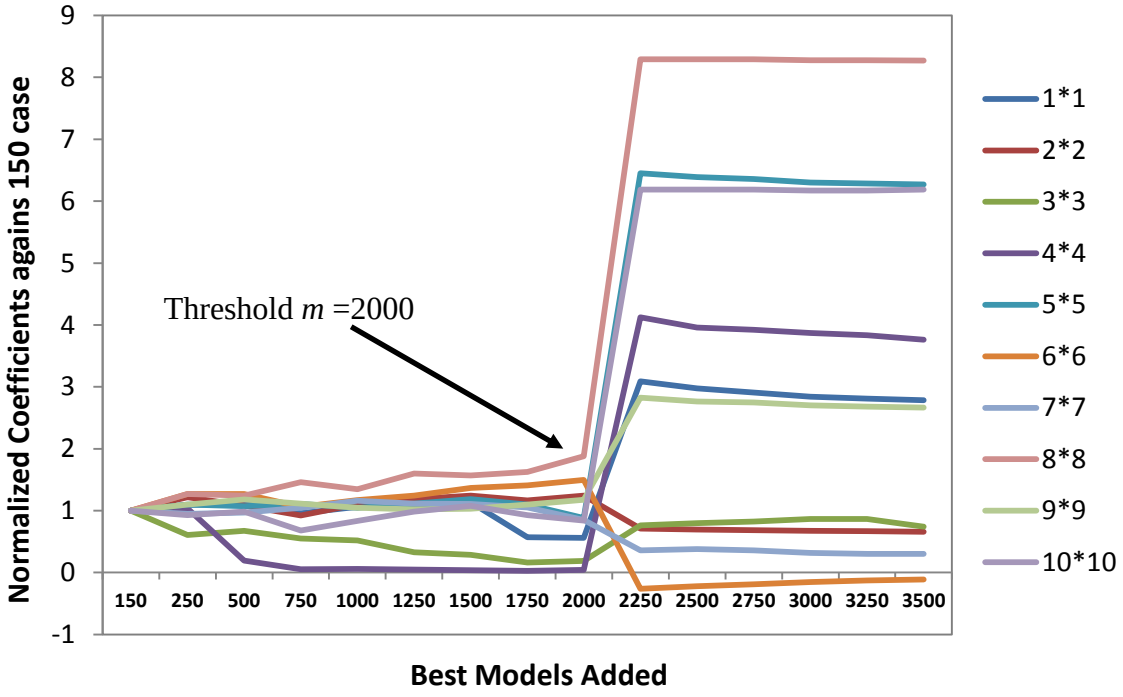

Figure 7.15: Quadratic coefficients trend after normalizing them against the coefficients of the first 150 models case.

7.5 Summary

When using optimization algorithms, the goal is usually clear that the global optimum should be found. Nevertheless, it is not obvious when this goal is achieved, particularly if real-world problems are optimized for which no knowledge about the global optimum is available. Consequently, it is not straightforward to decide when the execution of an optimization algorithm should be terminated. In this chapter, we have investigated some stopping criteria as it is one important factor that affects the convergence rate of the seismic history matching and may save some CPU time. The question was "*when is it possible to stop the assisted history matching process*?" To answer this question, we have suggested different approaches of stopping criteria and we found that the definition of an appropriate stopping criterion is complex and problem specific. We presented a flow chart to apply those criteria based on logical order. In case of none of those criteria work or the solution is not accepted, we may check if perhaps there may be alternative solutions for the problem in the parameter space by restarting the SHM loop using new parameterization or different production and seismic weights or different parameters range.

In addition to the above, we have also studied a few criteria that will be used to improve identification of convergence using the proxy model and to use the proxy coefficients convergence as a stopping criterion. In this section, we aim to find out if we extend the use of proxy models where new models update the proxy model until we saturate the sampling. Therefore, as we add models we update the set of models used to get the proxy, throwing away high misfit models and accepting new better fitting models. Thus, the proxy fit ultimately improves also. Although this approach seems to be very fast and attractive, it is still difficult to define a threshold to switch from full misfit to proxy model calculation and needs further investigation.

To sum up, the challenges of creating proxy-models of a high quality are related to the quality of the input dataset. They are easy to implement and do not require a lot of CPU time. In reservoir simulation, we are dealing with highly non-linear output. The quality of a proxy-model strongly depends on the underlying algorithm and dataset used to create the model. Finally, any decision based on proxy-models requires a thorough understanding of their limitations, and an adequate quality assurance process to quantify proxy-modelling errors is recommended.

CHAPTER 8

Quantifying Parameter Uncertainty using NA and NAPG

Overview

In this chapter, the main objective is to quantify the parameter uncertainty that remains as a result of using the NA and NAPG methods during SHM. Various sampling algorithms are able to find different models of similar history match quality. These are located in different regions of the parameter space. The NA-Bays (NAB) method (Sambridge, 1999b) may be used to approximate the posterior probability, which can then be used to estimate parameter uncertainty. By using Bayes' theorem, the misfits can be used to calculate the conditional likelihood of each model for the given data, and these are used to update prior model probabilities. The updated probabilities may be resampled using Markov chain Monte Carlo (MCMC) methods as part of the uncertainty analysis of the unknown parameters, giving a set of probability distributions. We will apply NAB to synthetic cases and to the Schiehallion field.

8.1 Sources of Reservoir Uncertainty

Finding and developing oil and gas assets has always been a risky business. The industry is surrounded by uncertainties, especially when trying to forecast production. Traditionally, reservoir management is based on the production forecast from a single history matched reservoir model. Risk is assessed by analysing the sensitivity of the forecast from some extra simulation runs. In this manner, not all aspects are taken into account due to the non-uniqueness of the inversion, more than one realization fits the observed data. Each realisation of the reservoir model yields a different production forecast and some realisations are more probable than others. The different realisations and their probability have to be taken into account if the uncertainty is to be quantified. In theory, the entire parameter space needs to be sampled to properly quantify the uncertainty. However, this is not feasible due to the cost associated with the required number of simulations.

Most reservoir data are determined accurately at the reservoir well locations. These well locations account for less that 1% of the reservoir volume even for completely developed and matured fields (Ralf Schulze *et al.*, 2007). Combining this with the fact that most reservoirs are heterogeneous creates the reservoir data highly uncertain, particularly at reservoir locations between wells. The level of uncertainty may be different from one variable to another. The uncertainty of a variable may result from difficulty in directly and accurately measuring the quantity. This is mostly true of the physical reservoir parameters that, at best, can only be sampled at different locations, and are subject to errors caused by the existence of the borehole and borehole fluid or by changes that occur during the transfer of rock and its fluids to laboratory temperature and pressure conditions (Walstrom, 1967; Olea, 1991).

Prediction of reservoir performance is associated with uncertainties arising from the lack of accurate and reliable knowledge about the reservoir rock and fluid properties (Gavalas *et al.*, 1976). Large financial investments required for field development plans have made it necessary to make decisions based on accurate quantification of these uncertainties. Uncertainty influences the decisions about the infill drilling, water flooding scenarios, enhanced oil recovery plans and consequently the design of well surface injection or production facilities (Birchenko *et al.*, 2008).

A large number of uncertainties can be identified in the integrated reservoir modelling process. Therefore, the uncertainty in reservoir models exists everywhere, such as in (1) raw data measurements, (2) data processing and interpretation, (3) structural modelling, (4) facies modelling, (5) petrophysical modelling, (6) transmissibility calculation, and (7) flow simulation, which affects the ability to understand the reservoir behaviour, making reliable production forecasts and risk-free decisions. The spatial and temporal distributions of reservoir properties are important measures of the prediction uncertainty caused by incomplete knowledge of the reservoir heterogeneity. With less uncertainty, there is less risk in many reservoir development and production decisions, which could result in accepting rather than rejecting an economically viable project (Kelkar, 2002).

8.2. Uncertainty quantification

The aim of history matching is to construct a reservoir model to allow forecasting of the production behaviour of the reservoir. Therefore, one of the main challenges within reservoir management is to quantify the production forecast uncertainty. The uncertainty is related to several factors: amount and quality of conditioning data, fluid flow simulation algorithm, upscaling, the parameterisation, mismatch function, etc.

Barker *et al.* (2001) and Floris *et al.* (2001) give an overview of the different approaches to quantify uncertainty. The Markov-Chain Monte-Carlo technique (Hegstad and Omre, 1997) allows a statistically correct sampling. The method requires a large number of samples, even though many adaptations are made to reduce this number. The Bayesian technique has also been widely used to assess uncertainty in reservoir parameter (Stephen *et al* 2004b; Christie *et al* 2006; Barker *et al* 2001; Gao and Reynolds 2005; Nicotra *et al* 2005; Wills *et al* 2004). Bayesian method provides a link between a prior distribution function and posterior probability distribution function through a likelihood function assuming a continuous probability distribution.

8.3 Bayes' Theorem

Bayes theorem regulates the way two events rely on each other providing a means for relating the degree to which an observation confirms the states of nature (Bayes, 1763). The reason why Bayes' theorem is a useful tool is that it relates the posterior probability to the likelihood function, which can be calculated, (Sivia, 1996). The law has been broadly used in many and very different fields, from medicine, disease incidence and propagation, to computer system, for neural network and speech recognition. The oil industry has also found application of Bayes theorem for a number of applications like calculating value of information to help make better decisions, upgrading prospects, and uncertainty analysis. The theorem presumes that any analysis should have available a probability distribution for the alternatives, which express all preceding knowledge to that point. This knowledge is called *prior* distribution, the one that comes before the observation or experiment. Then, another observation is made intending to inform us something about the relative merits of the alternatives. Based on this information we modify the *prior* probability distribution and get a new one, the *posterior* distribution, which is the one that comes after the observation. The theorem may be paraphrased as:

$$Posterior = \frac{likelihood\ x\ prior}{normalizing\ value} \tag{8.1}$$

Here the *likelihood* is defined as the hypothetical probability that an event, which has already occurred, would yield a specific outcome. If another experiment is made then the previous *posterior* distribution becomes *prior* distribution for the next analysis (Papoulis, 1991; Sambridge, 1999b). Bayesian inference is based on *Bayes' theorem*, which is a simple application of the definition of condition probability. So Bayesian *inference* provides a way of evaluating the posterior probability *p(m|d)* of multiple models generated using stochastic optimization such as Neighbourhood Algorithm, Ensemble Kalman Filter or evolutionary algorithms. For the quantities of interest in the inverse problems, this theorem has the form given by equation

$$P(m|d) = \frac{P(d|m)P(m)}{\int_M P(d|m)P(m)dm} \tag{8.2}$$

Here, $P(m|d)$ is called the *posterior probability*, and $P(m)$ and $P(d|m)$ are referred to as the *prior probability* and the *likelihood function*, respectively. The denominator in 8.2 is an integral over the *n*-dimensional model space *M* and acts as a normalizing constant. For many inverse problems, the evaluation of such integrals is intractable. One therefore often uses the alternative formulation of Bayes' theorem given in Equation 8.2, which simply states that $P(m|d)$ is proportional to the product of the likelihood function $P(d|m)$ and the prior probability $P(m)$.

$$P(m|d) \propto P(d|m)\ P(m) \tag{8.3}$$

All the information about the models in the parameter space that is known to the scientist before the measurements are performed is summarized in the prior probability $P(m)$. If no such a priori information is given, $P(m)$ can simply be defined to be the uniform distribution. The likelihood function $P(d|m)$ quantifies how well a model explains the observed data *d*, as a function of the difference between the observed data *d* and the data, $g(m)$, predicted by the model. By using this likelihood function, one does not require the models to reproduce the measured data exactly, but allows for a certain discrepancy between actual and predicated data (Papoulis, 1991; Sambridge, 1999b).

8.4 Markov Chain Monte Carlo (MCMC)

MCMC methods have become standard tools in Bayesian inference and other areas in statistics. MCMC methods are a group of algorithms for sampling from probability distributions based on building a Markov chain that has the desired distribution as its equilibrium distribution (Denison and *et al*., 2002). All the results of Bayesian inference introduced above assume that one is able to evaluate integrals of the form

$$\mathrm{I} = \int_M g(m)P(m|d)dm \tag{8.4}$$

where the function $g(m)$ describes some quantity of interest. However, in many problems involving complex posterior probabilities and high-dimensional parameter spaces, these integrations cannot be performed analytically and direct numerical integration becomes computationally infeasible. A remedy is provided by Markov Chain Monte Carlo (MCMC) methods, which tackle the integration problem by sampling a large set of models, $m^{(1)}, m^{(2)}, \ldots, m^{(N)} \in M$, from the posterior probability density function (PPD) or $P(m|d)$ to estimate the integral I as a simple average over the sample

$$I = \frac{1}{N}\sum_{t=1}^{N} g(m^{(t)}) \tag{8.5}$$

where N is the number of discrete samples in the MC integration. MCMC algorithms belong to the class of Monte Carlo methods since the samples from the specified probability distribution are drawn randomly. For this purpose, Markov chains are constructed whose equilibrium distribution is the very distribution one wishes to approximate (Johannes and Polson, 2007; Oliver and *et al*., 2005)

Definition (Markov chain) *A Markov chain is a sequence of random variables* $X^{(0)}$, $X^{(1)}$, $X^{(2)}$, *. . . in which the distribution of* $X^{(n+1)}$ *only depends on the past through the value of* $X^{(n)}$. *That is,* $P(X^{(n+1)})$.

From the inverse problem point of view, it can be said that MCMC is a purely probabilistic workflow for solving inverse problems where it consist of two parts, the sampling method and the optimization method. The sampling scheme of MC is based on generating a population of reservoir models with reasonable statistical characteristics of a random variable. The random models will be generated from a specific probability distribution. Thousands of possible outcomes of models will be generated then. The

optimization routine of MCMC is based on random walks. This means that the algorithm will move around a marker in multi-dimensional space in order to find the lower misfit (Mosegaard and Sambridge, 2002). There are different random walk MCMC methods (Smith and Roberts 1993) such as:

Gibbs sampling: This method is very broadly applicable to a broad class of Bayesian problems since it does not need any 'tuning'.

Slice sampling: this method employs the idea of sampling from a distribution by sampling uniformly from the region under the plot of its density function.

Metropolis–Hastings algorithm: a random walk can be generated using a proposal density and a method for rejecting proposed moves.

MC methods are simple to apply and analyze, however, they can require a long time to explore all of the space (for a more detailed description, see Neal, 1993). The MCMC-algorithm has been applied to many history-matching applications (Subbey and *et al.*, 2003; Stephen *et al.*, 2005; Wadsley 2005; Ma *et al.*, 2006; Ma *et al.*, 2009; Emerick and Reynolds, 2010). However, the computer expenses to obtain an uncertainty assessment by the MCMC-algorithm are very large, and many papers use approximate sampling algorithms, which include an optimization step, in order to reduce the computational cost.

8.5 Posterior Probability Distribution PPD

The problem of quantifying the uncertainty is the problem of evaluating the posterior probability density function $p(m|d)$, which is, in practice, computationally very expensive. From the Bayesian point of view, the solution to the inverse problem is the posterior probability density function (PPD) as depicted in Figure 8.1. The posterior probability $p(m|d)$ is calculated numerically by Markov Chain Monte Carlo (MCMC) integration and then resampled as part of the uncertainty analysis of modified parameters. The key idea is to replace the real PPD with this approximate PPD, and then the Bayesian integral through MC integration is evaluated. This quantity is used to represent all information available on the model. Its calculation relies on the data, any prior information, and the statistics of all noise present, which must be assumed known (Sambridge, 1999b). Although the PPD is a multidimensional function, it is usually characterized in terms of its properties in model space. The model, which maximizes

the PPD, is one property of interest, and in the lack of prior information would match to the best data fit model. In addition to this, they are most useful if the PPD has a single dominant peak, and become less useful if multiple 'significant' maxima are present (Sambridge, 1999b). When for example, this probability distribution only reveals one single peak in a certain region of the model space, this region can be pointed out as containing the best-fitting models. Then, the width of the peak reveals with how much accuracy the true model can be determined.

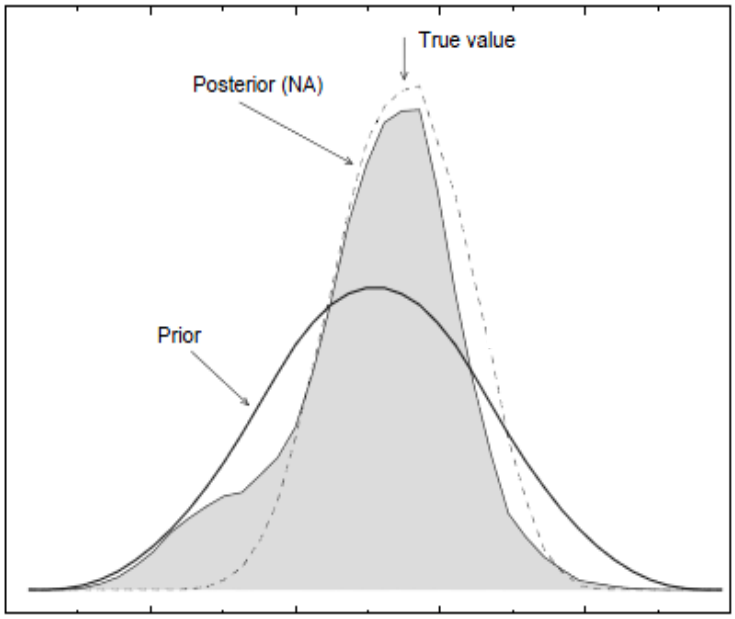

Figure 8.1: The prior and posterior marginal showing that PPD is the solution to the inverse problem (Sambridge, 1999b).

8.6 One-dimensional marginal distributions (1D-marginal)

A marginal PPD is another kind of PPD property that may be useful, even when multiple maxima are present. The one-dimensional marginal distribution of one individual model parameter m_i can be extracted from the PPD by holding the value of this parameter fixed while 'integrating over' the other parameters:

$$P(m_i|d) = \int p(m|d) \prod_{\substack{j=1,n \\ j \neq i}}^{n} dm_j \tag{8.5}$$

Analogously, marginal distributions for several model parameters can be calculated by integrating over all possible values of the remaining parameters. The 1-D marginals

indicate how well the data constrain the individual model parameters. That is, they reflect how much uncertainty is inherent in the parameter estimates that are made based on the prior knowledge and the observed measurements. The area under a distinct peak of such a curve represents the probability that the true parameter value belongs to this range of values. Furthermore, the existence of several separated peaks that are similarly high indicates that models from different parts of the model space cannot be distinguished on the basis of the available information.

Sambridge, 1999b applied the Neighbourhood Approximation to the sampling from the posterior probability distribution (PPD) in Bayesian framework, (NA-Bayes Algorithm). Presume that we have obtained the information on the PPD through the history matching with NA or NAPG. After that, we make use of MCMC to evaluate the posterior expectation without conducting any extra flow simulations. By simply setting the known PPD of each model to be constant inside its Voronoi cell, we can build an approximate PPD from a fixed ensemble. This approximation allows us to avoid computing the real PPD of the new proposed models at each step of MCMC (Okano *et al*., 2005). Further details of the NA-Bayes Algorithm are described in Appendix B.

8.7 Bayesian credible intervals

In Bayesian statistics, the Bayesian confidence interval is an interval in the domain of a posterior probability distribution used for interval estimation (Edwards *et al.*, 1963). Results from the Posterior Probability Distribution PPDs often are expressed as the Bayesian credible intervals (Erbas, 2007). Such intervals predict that the true values of the parameters (true model) have a particular probability of lying in the credible interval given the data actually obtained. Therefore, a narrower credible interval is equivalent to the more confidence in history matched reservoir model and less uncertainty is associated with them. To determine these intervals, the Cumulative Posterior Distribution (CDF) is needed from the posterior, which can be calculated by summation of PPDs arranged in an ascending order (Christie *et al.*, 2005). In this thesis, the Bayesian credible interval is reported as the interval of parameters corresponding to 10% to 90% CDF values [p90- p10] as shown in Figure 8.2.

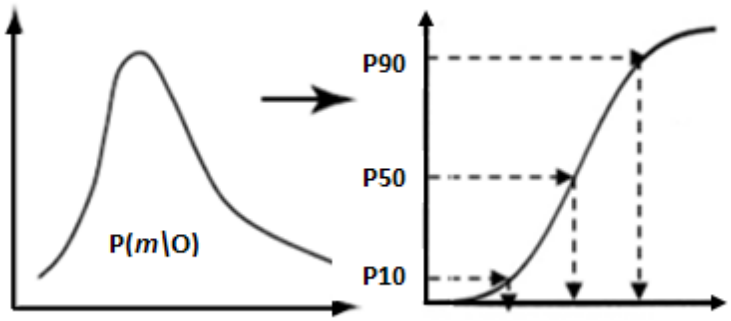

Figure 8.2: PPD's to CDF's to estimate Bayesian credible interval (P90-P10).

8.8 Applications

We applied uncertainty analysis using NAB to three scenarios as different algorithms may find different models of similar history match quality located in different regions of the parameter space. The first scenario is a 6D fourth order polynomial function with two global minima with different sampling densities (see Equation 5.1). The second scenario is the 6D synthetic case from the Schiehallion field (see Chapter 5, Section 5.2). The third scenario is the 10D real Schiehallion Field case (as seen in Chapter 6, Section 6.3). The effect of using NA and NAPG algorithms on uncertainty analysis was analysed in this work.

8.8.1 Case Study 1: 6D - Fourth Order Polynomial Function

The details of this function can be found in Chapter 5, Section 5.1.1. We found that the convergence rate is much improved with the new approach (NAPG) compared to the original NA. We used three different scenarios: under-sampled, well-sampled and over-sampled cases as shown in Section 5.1, Chapter 5. This function has two minima which are in 6D: (+1,0,0,0,0,0) and (-1,0,0,0,0,0). Therefore, the exact solution of this function is known and the PPD should converge to showing those minima as peaks. The ensemble of three cases generated by NA and NAPG were submitted to the NAB routine in order to quantifying parameter uncertainty. We found in Chapter 5, Section 5.1.1 that NAPG converged faster than NA and the parameter space should be saturated well to detect two minima. As part of solving the inverse problem, we found the approximate PPDs and then converted to 1D marginals. For the under-sampled case, it can be seen from Figure 8.3 that the solution is not exactly the same. Therefore, NA and NAPG missed one minimum of the function (sub-optimal solution) and found

different solution because of insufficient sampling. In reality, we have to avoid such scenario to get models that are more accurate for forecasting. Figure 8.4 shows that we get better results when we saturated the parameter space. Here we easily detect double minima and there was a little difference in parameter uncertainty. In the over sampled scenario, both methods got the same answer and two minima were detected because the misfit is so small and therefore the differences are small between the "models" as shown in Figure 8.5. Therefore, for both well-sampled and over-sampled scenarios, NA and NAPG have the same solution but over-sampled scenario should be avoided in real cases due to CPU time.

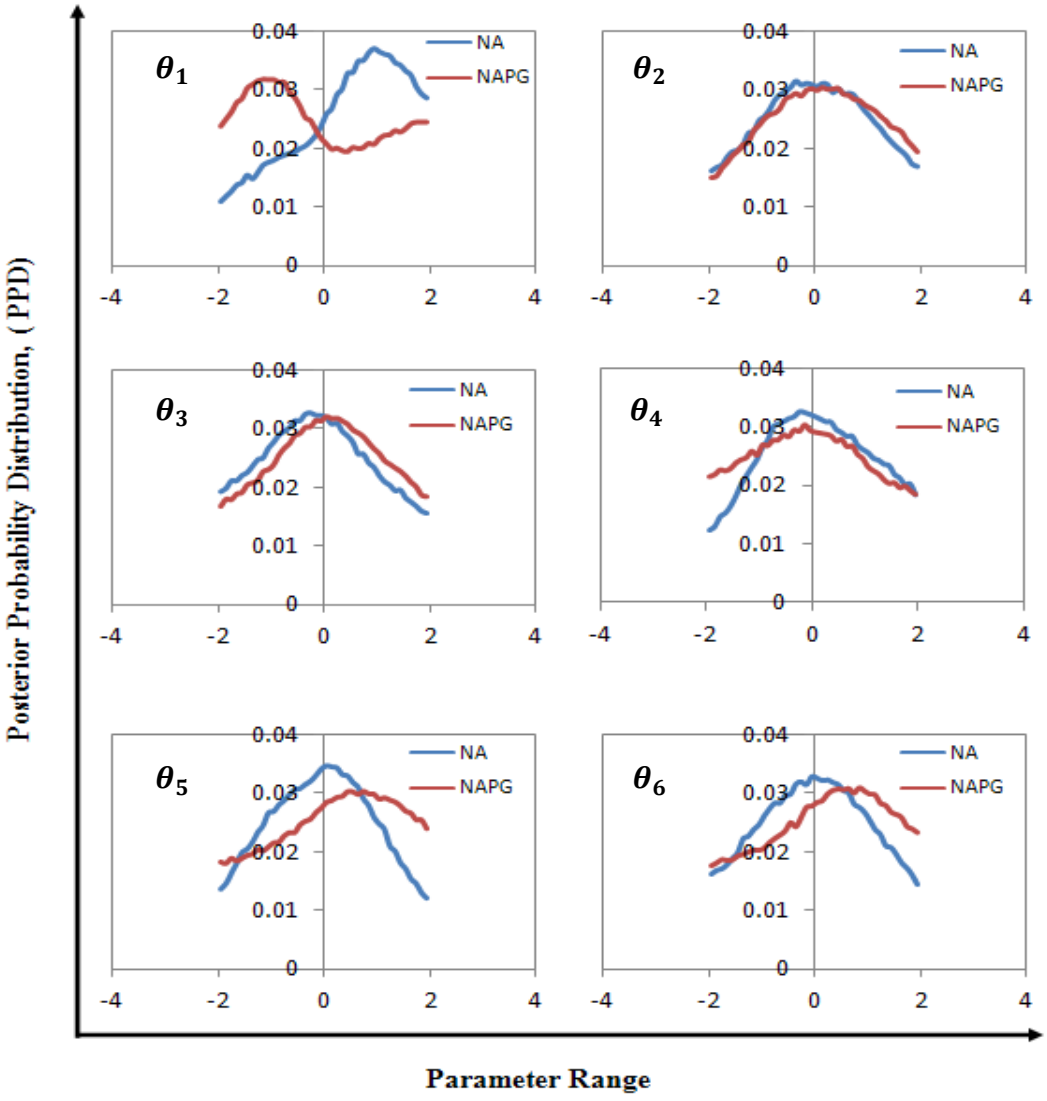

Figure 8.3: 1D marginal plots for the fourth order polynomial function with two global minima (Equation 6.1) when we have under sampled the parameter space.

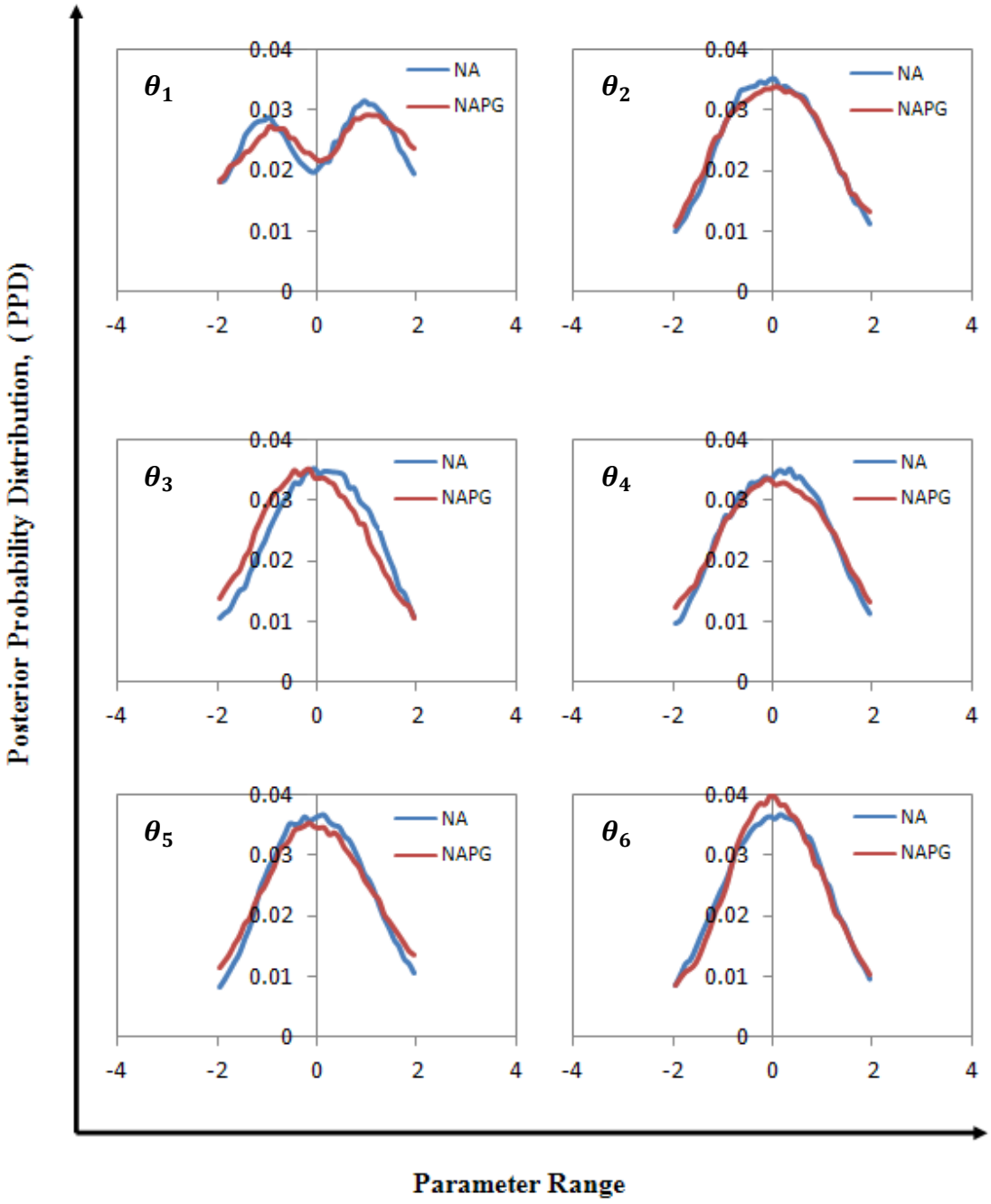

Figure 8.4: 1D marginal plots for the fourth order polynomial function with two global minima (Equation 6.1) when we have well-sampled the parameter space.

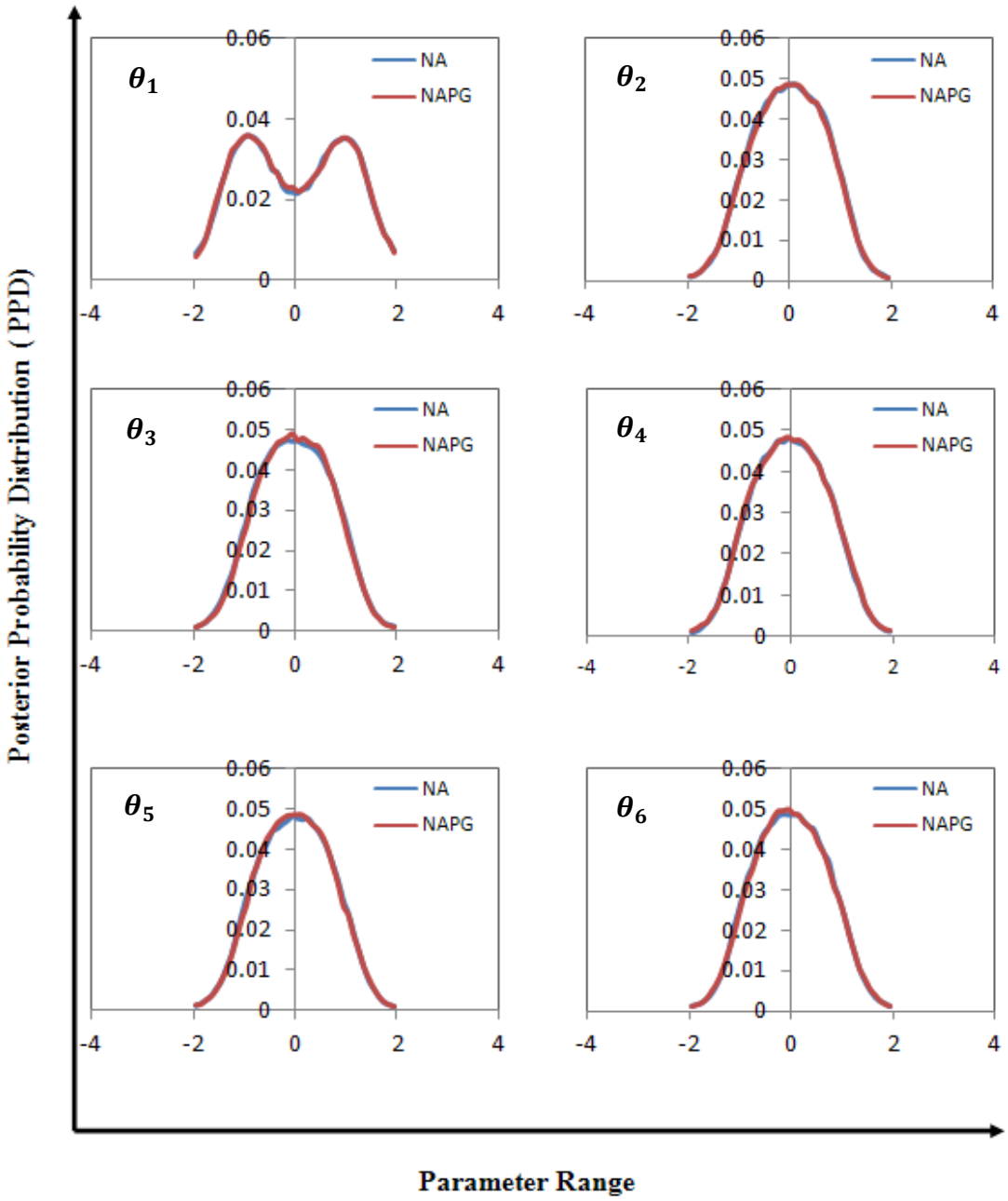

Figure 8.5: 1D marginal plots for the fourth order polynomial function with two global minima (Equation 6.1) when we have over sampled the parameter space.

There is another way of viewing the uncertainty by calculating Bayesian Credible interval (**P90-P10**) where no inference can be made just based on PPD unless determining the model with highest PPD as the most probable model. This can be done by converting these posterior probability densities to cumulative probabilities (CDF's) which provide the potential for updating reservoir model based on observations as shown in Figure 8.2. The case with narrower credible interval (P90-P10) is the case with less uncertainty. Narrowest credible interval is the one in which the difference

between the bounds of this interval is the lowest one. Therefore, it can be seen from the histogram chart as shown in Figure 8.6 that both NA and NAPG have the same Bayesian Credible interval (P90-P10) which means equal parameter uncertainty.

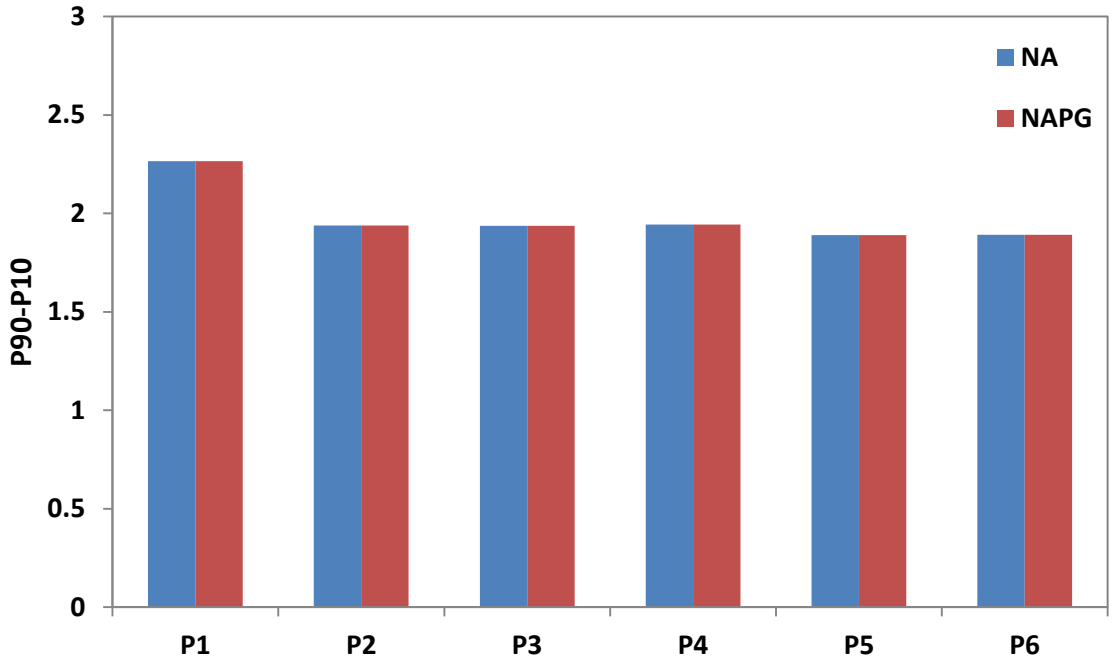

Figure 8.6: Bayesian Credible interval (P90-P10) of the well-sampled 6D quadratic equation.

8.8.2 Case Study 2: 6D Synthetic Case

This synthetic case consists of a model analogous to the Schiehallion field. The details of this model were given in Chapter 5, Section 5.2. The aim of this synthetic case is to examine the convergence of two approaches using posterior probability distributions PPD where we know the answer. We found that the misfit evolution and the six parameters converged more quickly to zero with the new approach (NAPG) compared to NA. Here we assessed the posterior probabilities to determine whether or not both algorithms found the exact solution. According to the output of NAB, PPD's of all six parameters are the same for NA and NAPG as shown in Figure 8.7. This means the CDF's are also the same and then they will have the same degree of parameter uncertainty.

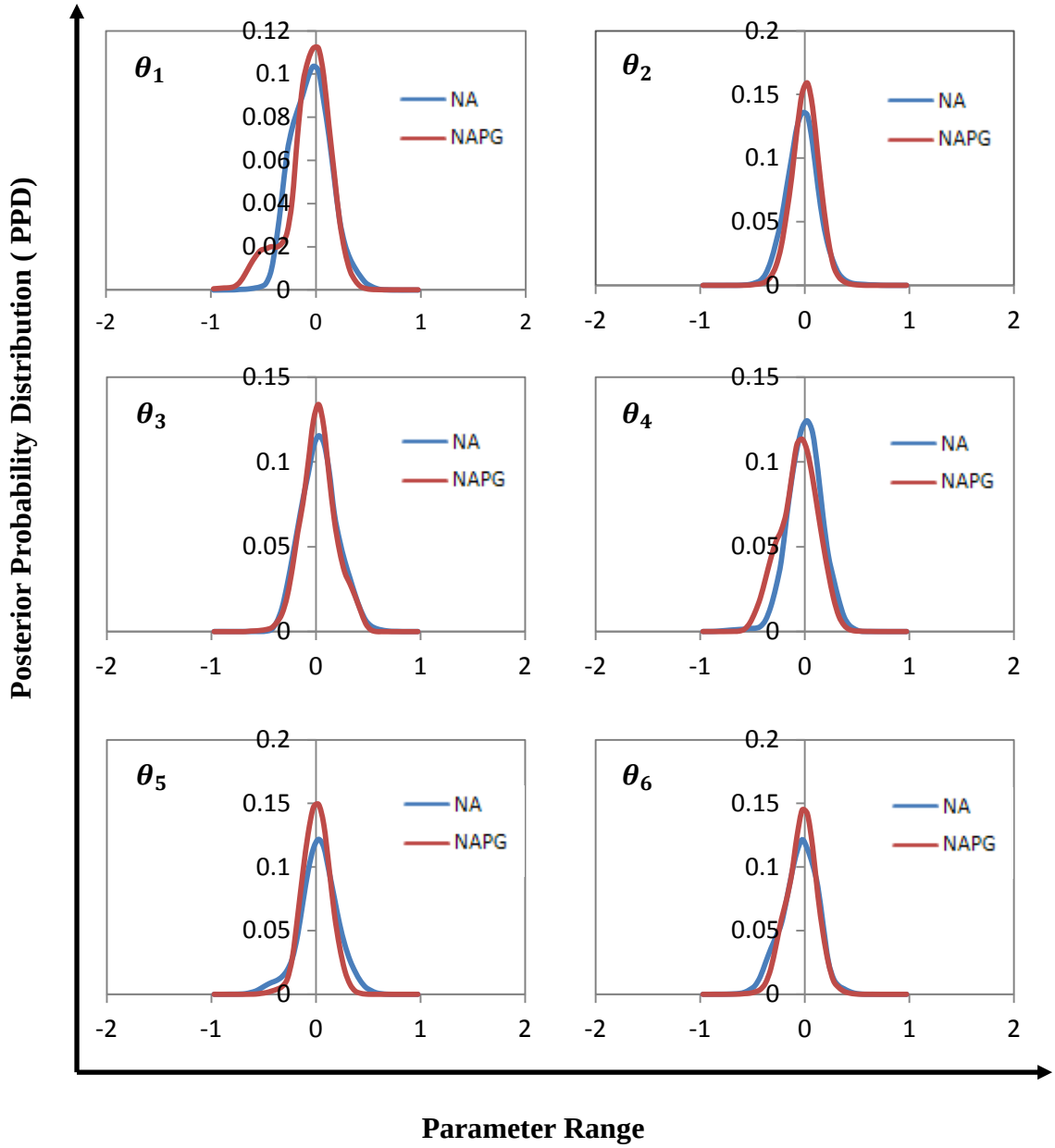

Figure 8.7: 1D marginal plots for 6D problem Synthetic model from the Schiehallion field.

8.8.3 Case Study 3: Schiehallion Field

In this application, the same Schiehallion model that was described in Chapter 6, Section 6.3 were used to quantify parameter uncertainty when using NA, NAPG and ED+NAPG methods. The misfit evolutions of the three approaches are shown in Figure 6.10 in Chapter 6. The NAB routine is applied (for details see Appendix B) to the whole ensemble of models generated by NA, NAPG and ED+NAPG in order to assess the parameter uncertainty. Figure 8.8 shows 1D-marginal plots and we observe that the three methods produce different PPDs outputs, which means they have different solutions. We found in Chapter 6, Section 6.4 that the NAPG converged more quickly than the original NA but some parameters such as a, e, g, i and K_h1 may need longer run with NA to converge (see Figure 6.10 and Figure 6.12). These results may signify the non-uniqueness of this history matching problem and the existence of the multiple solutions that have been obtained using different search methods.

Moreover, NAB depends on the size of voronoi cells of the best models and those models are closer together. The voronoi cells are smaller with NAPG due to improved convergence. Also, the size of the misfit is large and the voronoi cells of the best models are very small in the case of NAPG. For this reason, we derive different approximation of PPD. i.e. approximate PPD is a function of the misfit size. In other words, if the misfit variation is too strong, we will depend on the sampling method and then NA will give a different result from NAPG. In addition, it can be seen from Figure 8.9 that there are slight variations in the Bayesian Credible interval where the narrowest credible interval is the one with less uncertainty. Therefore, from this chart, NAPG and ED+NAPG appear to have less parameter uncertainty than NA.

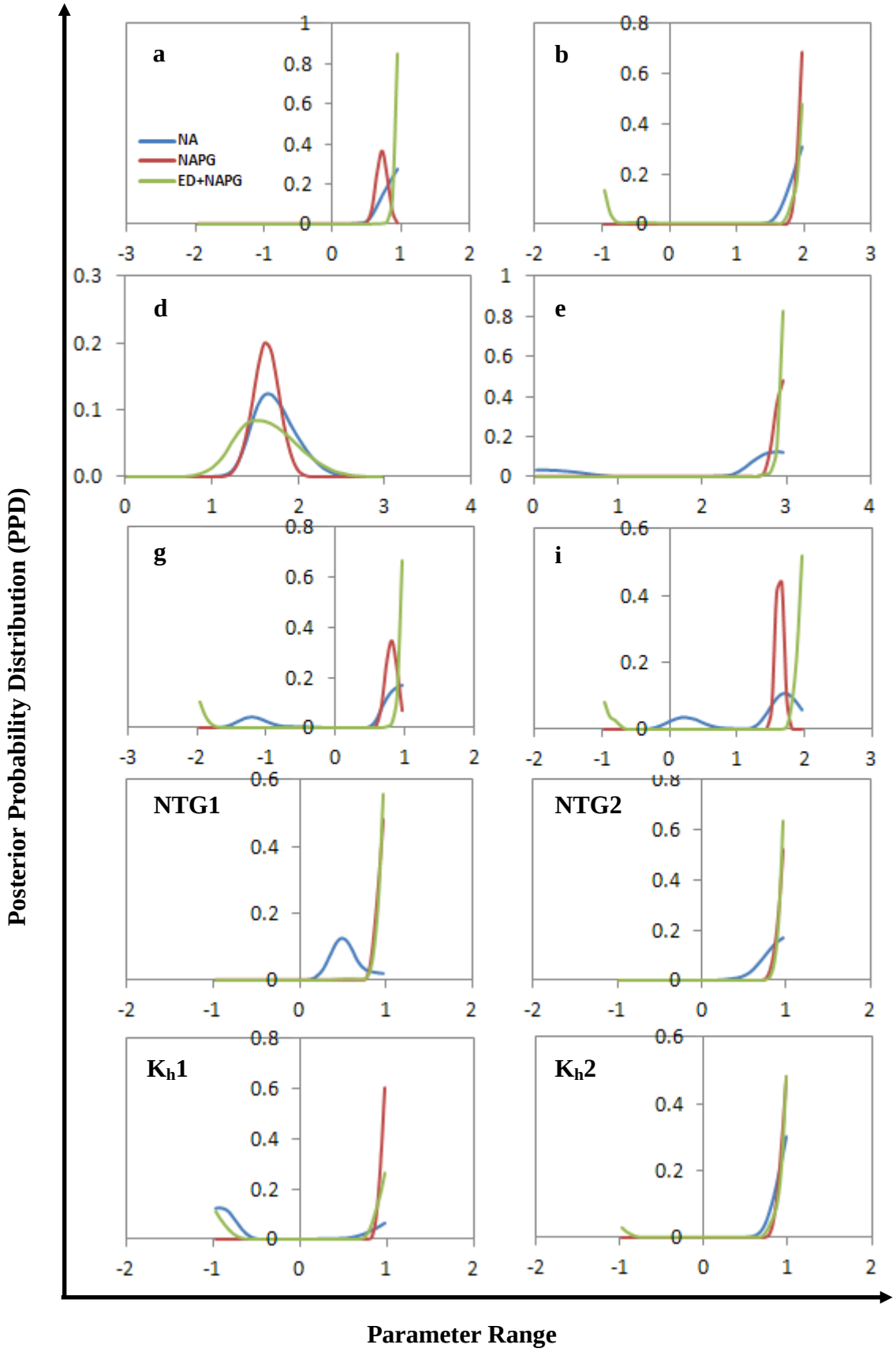

Figure 8.8: 1D marginal plots for 10D problem of Schiehallion field where blue indicates NA and red for NAPG and green is for ED+NAPG.

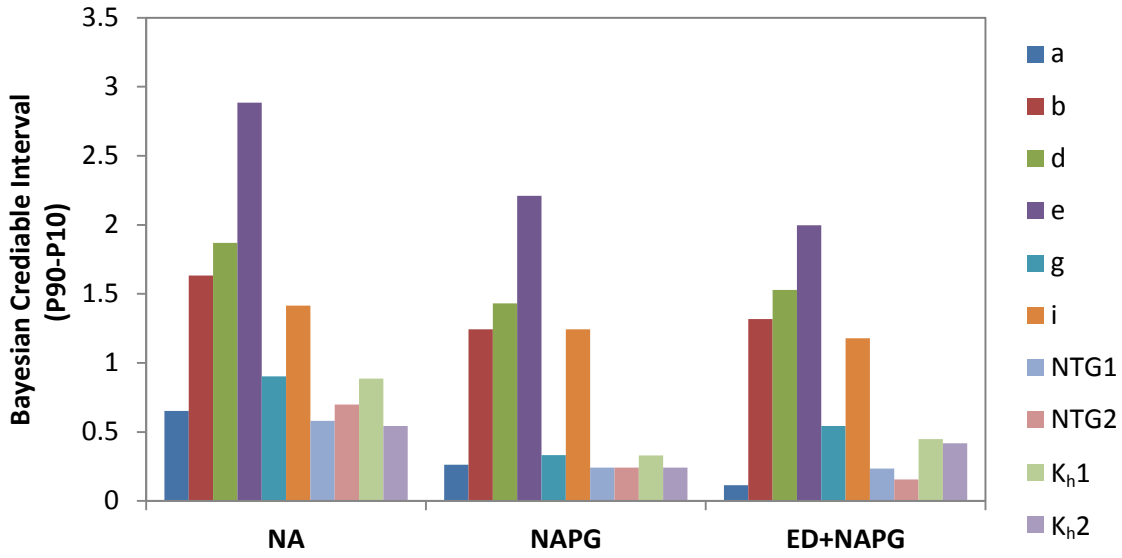

Figure 8.9: Bayesian Credible interval (P90-P10) of Schiehallion field.

In summary, when analysing the Schiehallion field case, we found that the misfits were quite large and so the approximate nature of NA-Bayes was then affected by the sampling method. According to these results in this particular case, NAB probably is not that useful as a tool due to the difference between misfit values within each method. In addition, the results may be adversely affected by not having sampled enough in the good data fitting regions of parameter space. Because NAB is sampling the voronoi cell of the best models, the NA should have the same level of convergence as NAPG to make the comparison.

In addition, we needed to estimate the production and seismic weighting terms in the single objective function, as part of the problem is that the seismic misfit is too big. This arises because we downscale the prediction to the seismic grid and then take differences where the prediction can never match the detail of the seismic. The question that arises here is "*what if we increase degree of data or model error?*" The effect of using data with greater measurement error will be considered here by reducing the size of the misfit. We decrease the misfit magnitude to make the data error bigger by a factor of 10 and $\sqrt{10^3}$. This means that the total misfits reduce by a factor of 100 and 1000 respectively. Figure 8.10 and Figure 8.11 illustrated the answer to the above question by varying the data error (σ_D). Changing the data error does not affect the misfit rank and the solutions are the same. However, the probabilities of sampling models outside the best model go up with increasing the data error, which leads to

increase parameters uncertainty. It can be seen from those plots that as we increase the data error, the parameter uncertainties of NA and NAPG converge. The data error that was estimated for the seismic and/or production data will increase the uncertainty and to a point where both methods get the same solution. However, the differences for NA and NAPG at lower data error estimates are due to the approximate nature of the PPD estimation.

8.9 Summary

The effect of using NAPG on uncertainty analysis was analysed and the NA-Bayes approach was used which approximates the posterior probability and uses it to estimate parameter uncertainty. This approach randomly samples the parameter space using the ensemble of models derived via history matching.

For synthetic cases where we know the answer, NA and NAPG produce the similar posterior probabilities (PPD) because the misfits are quite similar but NAPG converged faster than NA as shown Chapter 5. We found that for synthetic cases there was little difference in parameter uncertainty. However, when analysing the Schiehallion field case, we found that the misfits were quite large and so the approximate nature of NA-Bayes was then affected by the sampling method. The process was dependent on the size of the voronoi cell in parameter space associated with the best models of NA and NAPG. Because NAPG obtained better convergence rate this was smaller. To get a similar answer, we should take NA to the same level of convergence as NAPG.

In addition, we showed that data error plays an important factor affects the PPDs output of NAB. Therefore, as we increase the data error, the parameter uncertainties of NA and NAPG converge similarly.

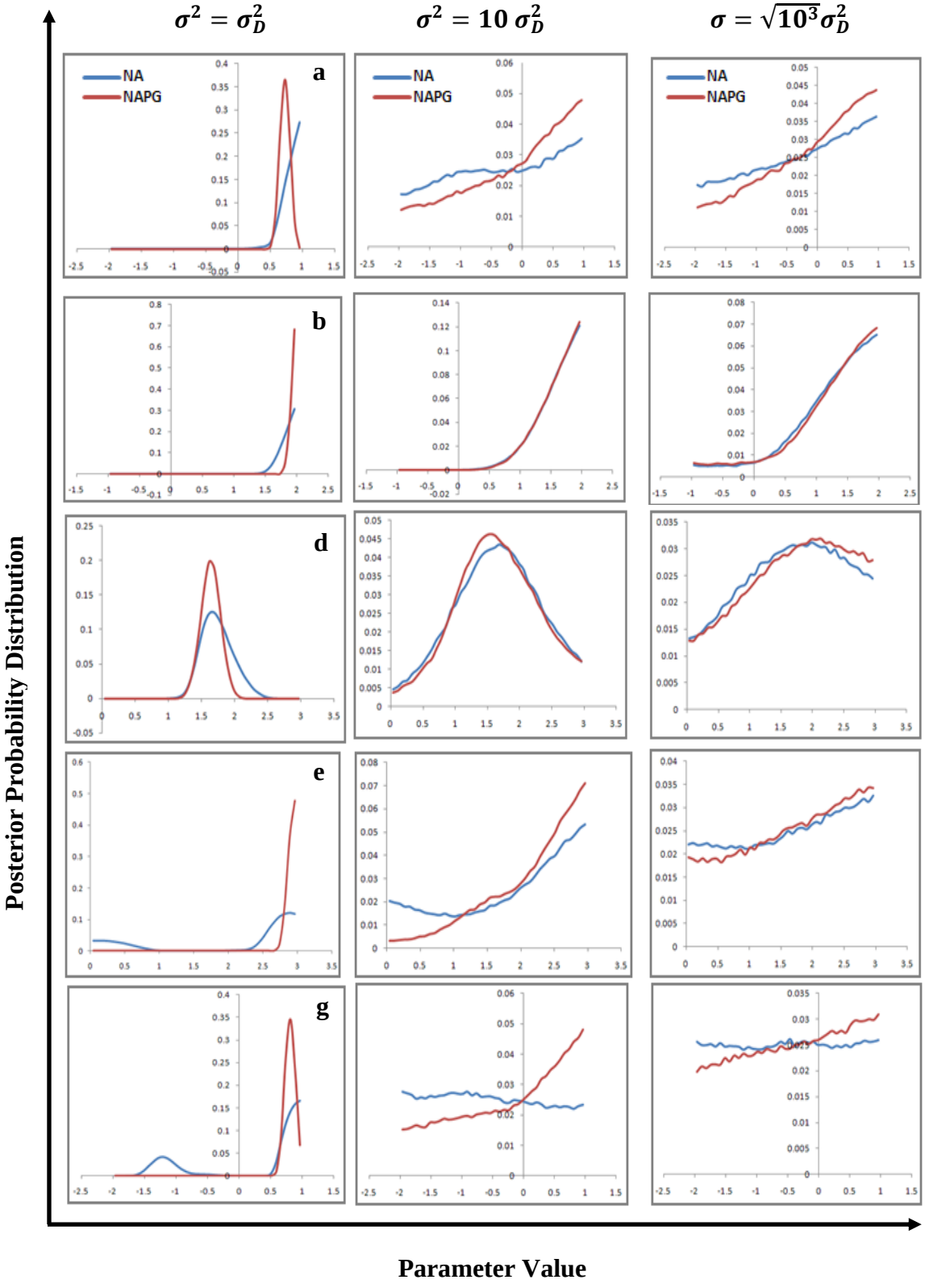

Figure 8.10: 1D marginal plots of Schiehallion field for barriers a to g when we have different degree of data error ($\boldsymbol{\sigma_D}$). As we increase the data error, NAB gives similar results for both NA and NAPG.

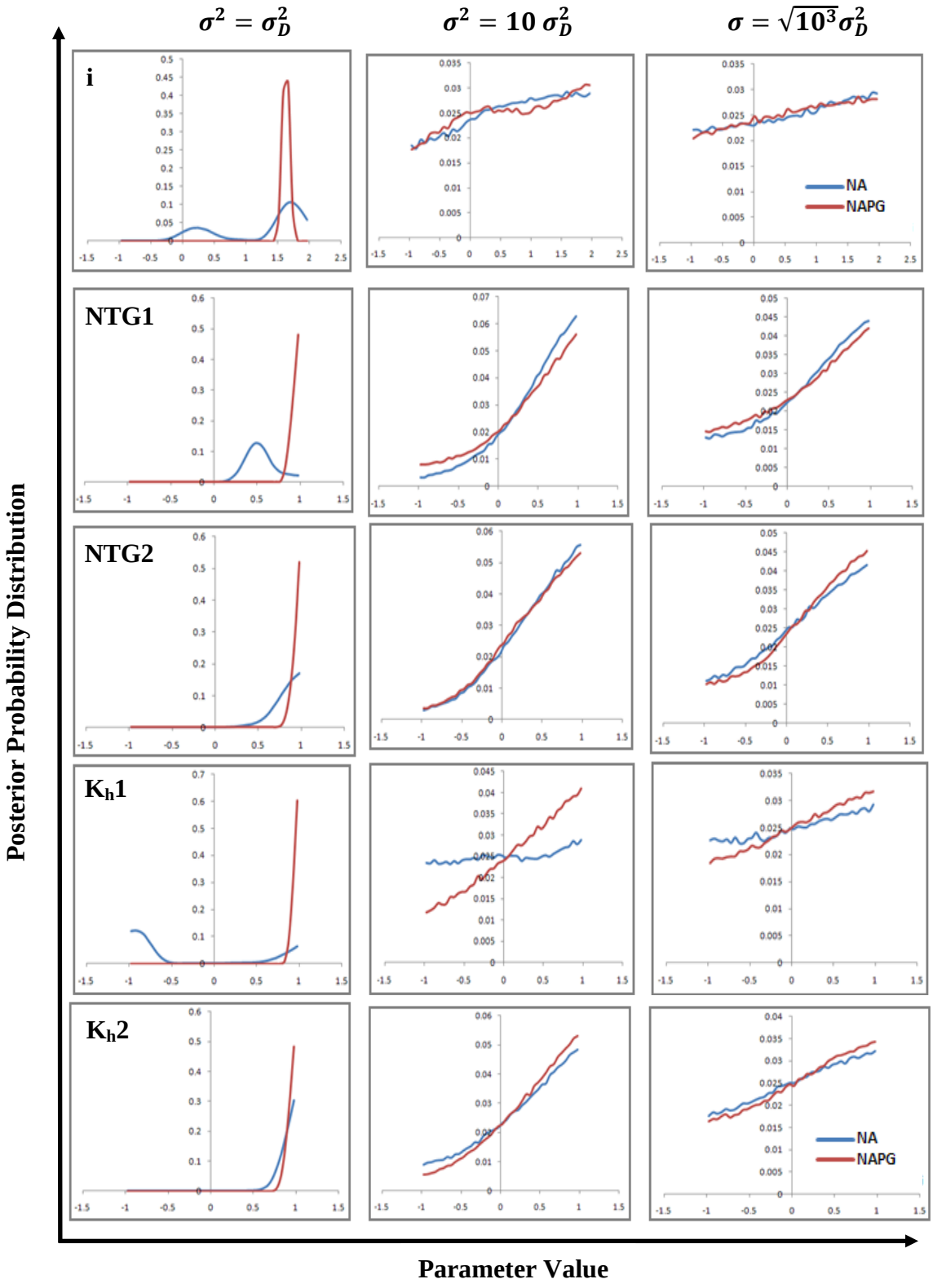

Figure 8.11: 1D marginal plots of Schiehallion field for barrier i and NTG & permeabilities when we have different degree of data error ($\boldsymbol{\sigma_D}$). As we increase the data error, NAB gives similar results for both NA and NAPG.

CHAPTER 9

Summary, Conclusions and Future Work

9.1 Summary

In this thesis, the cycle of integration of time-lapse seismic data with production data is described using an appropriate assisted history matching workflow in order to properly update the simulation model. The general aim of this thesis was to investigate different approaches to improve the convergence rate of assisted seismic history matching. An assisted history matching method had been developed where predictions are quantitatively compared to observed seismic and production data and then the model is updated in an objective manner. The automated procedure allows engineers to work more efficiently with larger reservoir models and extensive dynamic conditioning data sets. The main aim of the research is to improve convergence of the assisted history matching. We developed a new method named NAPG (NA with Proxy derived Gradients) to improve the convergence rate of SHM and also this approach can be applied to other stochastic methods such as Genetic Algorithm (GA).

The neighbourhood algorithm (NA) is able to identify global minima and those that are local. One of our key focuses in the sampling method of the Neighbourhood Algorithm is the reduction of the convergence rate towards the solution. We found that the original NA can be improved if we can estimate the probabilities to distribute the new models instead of using a uniform probability. Therefore, if we can approximate the probability of the models within the Voronoi cell as being a linear function of the parameter values, we can use this to steer the search towards better models.

Verification of the proposed method is done using analytical tests (e.g. fourth order polynomial function with two global minima and the Branin function), a synthetic field model and both synthetic and real cases from the Schiehallion field. We have studied this field previously and use it as a laboratory to apply our new technique where the field has two pre-production and several monitor surveys. With improved convergence, we have the ability to run fewer models or search the parameter space more widely.

This leads to an improved set of final reservoir models, which in turn can be used more effectively in reservoir management decisions.

9.2 Conclusions

The NA with Proxy derived Gradients method has been shown to be successful in speeding up the convergence rate of seismic history matching. However, like other algorithms it has advantages and disadvantages. The following conclusions are drawn from applying NA and NAPG on analytical functions, synthetic models and Schiehallion field.

Verification of NAPG

By applying various synthetic cases where we know the solution of these synthetic problems, we found the following:

- The combination of global optimization and gradient-like one is an attractive approach. Its use of can reduce the computational effort which increases exponentially with the dimension of the problem and it is a difficult task to sample and search in high-dimensional spaces.
- Proxy derived sensitivities are used to steer sampling in Voronoi cells and leads to improved the exploitation phase in the NA.
- Proxy models of the misfit based on regression equations misfits fail to capture the magnitude of the misfit near minima so they cannot be used in place of the full misfit calculation. Therefore, the regression equation itself is of limited use to replace predictions close to the minima but it provides excellent sensitivity information. In NAPG, inaccuracy of the proxy model near minima can encourage the parameter search in the wrong direction.
- Measurement and model error should be calibrated before history matching. We should calibrate the noise and model error to reduce its effect on history matching. In the Schiehallion field, we found that the effect of Gaussian noise can be removed from the misfit if the data error is estimated accurately.

Updating Regression Misfit Sensitivities

The efficiency of using regression misfit sensitivities can be improved near minima if we update the regression equation coefficients. For updating the regression equation coefficients, we considered three ways "Full ensemble", "Best so far" and "Latest models" approaches. These reflect the accuracy that we are likely to obtain in representing the misfit surface close to the minimum. We found that:

- By using the "Latest Models" to estimate the proxy, we got the best results compared to other approaches. Therefore, NAPG works better with updating the regression equation sensitivities instead of using single regression equation sensitivities.

- Updating the regression equation as we progress improves convergence further as the minimum is approached. By continuing updating of the proxy, the convergence rate is three times faster obtained but also better models can be found.

Combining Experimental Designs with NAPG

One of the main disadvantages of NA and NAPG is the large number of initial models needed to the fill parameter space in a high dimensional problem. Therefore, instead of the random selection to fill the parameter space, we used Experimental design (ED) to train the proxy model. We found that:

- Experimental design reduces the number of models to initialise the stochastic approach. For a 10D case, the number of initial models was reduced by 85% using Central Composite Faced Designs (CCF), which leads to reduced CPU time. Such an approach is then especially attractive of higher dimensional cases where thousands of initial models are required to saturate the space.

- ED method helps to explore the parameter space in a more efficient way by providing maximum information from the least number of simulation runs.

Stopping Criteria

Stopping criteria is one significant factor that affects the convergence rate of the assisted seismic history matching. The question was "*when is it possible to stop the assisted history matching process?*" and "*when should we restart the SHM process to search elsewhere to find alternative solutions for the problem*?". To answer this question, we suggested different approaches to define a suitable point to stop SHM loop. According to this study, we found that:

- The definition of the stopping criteria is related to the amount, quality, and type of constraining data available, and type of optimiser used. Therefore, it is complex and problem specific and needs further investigation.
- Improved identification of convergence using the proxy model coefficients can be used as a stopping criterion. Thus, if the proxy model stops changing during iterations, this is an indication of when to stop. We found that the proxy model of the misfit works within a specific window of the parameter range instead of the full misfit calculation and its coefficients can be used to define a stopping criterion within a specific parameters range.
- Although, this approach seems very attractive and fast, it is still requires more research especially the boundary of "proxy zone of validity" where the proxy model is quite accurate and when to look elsewhere to find another solutions.

Uncertainty Analysis of NA and NAPG

In this thesis, the NA-Bayesian (NAB) algorithm is used as a tool to capture parameter uncertainty and calculates an approximation of the posterior probability distribution (PPD) via a Gibbs sampler. Bayes theory provides the ultimate means of quantifying uncertainty in reservoir model performance. We used NA and NAPG algorithms to generate an ensemble of history match models. Once we created sufficient models, the misfits were used to update model probabilities from the prior, $p(m)$. We found that:

- The NAB algorithm is able to extract the information given by the generated model ensemble provided.
- For purely synthetic cases, NAB works well where the misfits are quite similar. NAB produces the similar posterior probabilities (PPD) for both NA and NAPG.

- For the Schiehallion field real case, we found very large misfits (increased by the volume of 4D data) which translated to very large probability ratios. Therefore, if the misfit variation is too big, the sampling method is important and then NA will give a different result from NAPG. This is because of the strength of the misfit and the fact that the voronoi cells are smaller with NAPG due to improved convergence.
- To get a similar answer in the Schiehallion field real case, we should take NA to the same level of convergence as NAPG.
- Data error plays an important factor that affects the PPDs of the NAB. However, with reduced accuracy of measured or modelled data, misfits are more similar and NAB gives the same results. Therefore, we would get better NAB results if we estimate data error in seismic and production data correctly.

9.3 Limitation of the NA with Proxy derived Gradients

NAPG like other algorithms it is not without limitations. According to our application, we have noticed the following limitations:

- If the misfit surface is very asymmetrical and complicated, the proxy equation will not be well represented by the symmetrical 2^{nd} order quadratic polynomial especially for a wider parameter range. In this case, it is therefore possible that we lose the benefit of the proxy model sensitivities and they could even work against us by directing the search in the wrong direction. On the other hand, we can eliminate this problem by updating the regression equation sensitivities as we progress towards the minima.

- In high dimensional problems, a large number of initial models are required to fill the parameter space as the original NA, which is extremely costly. We found that some filtering is needed to focus on important parameters such as experimental design could solve this problem. Alternatively, in order to sample the parameter space efficiently to find all minima, parameter space should be separated into several sub-volumes so that they can then be sampled separately but simultaneously using the NA or NAPG (e.g. Sedighi and Stephen, 2010).

9.4 Suggested Future work

The broadness of the subject and the fact that time-lapse seismic technology is rapidly advancing means that this thesis can neither be complete, nor that problems and solutions can be covered in all details. It is limited to some of the main problems. Below, a list of recommendations for future work.

- Since these results have been obtained on a single field dataset, further studies on more complex fields will be needed to establish definitive guidelines.
- When comparing predicted and observed seismic data, it is often quite difficult to determine the data error. We have found that noise is uncorrelated with the signal and that it can be determined by spectral analysis. Correlated noise may introduce biasing and it is recommended to develop schemes that properly account for this in the misfit evaluation. Examining the type of noise that the seismic contains will improve the misfit evaluation and enhance forecasting.
- It is recommended to investigate the exploration phase of NAPG. The computational effort will be more effectively directed to exploration by deriving measures of model diversity to prevent over sampling of the parameter space in volumes, where negligible new information is obtained. Such measures linked to misfits but also other variables such as saturations, pressures, permeabilities etc.
- It is recommended to apply the proxy derived gradient (PG) approach on other stochastic algorithms to speed up the convergence rate.
- Another proxy models method should be considered such as Multivariate kriging model (KG), Thin-plate splines model (TSP) and Artificial neural network (ANN) and design a criteria to verify the proxy model and assess the proxy-model prediction accuracy to choose the best proxy model method.
- More investigations are needed to define a suitable stopping criterion to stop the iterative process of SHM or when we should restart the process for searching elsewhere to find another solution. A lot of CPU time can be saved and a broad selection of models will therefore be found more efficiently.

Appendix A

The Batzle and Wang empirical correlations

Batzle and Wang (1992) combined thermodynamic relationships and empirical trends from published data in order to predict the effects of pressure, temperature and composition on the seismic properties of fluids. They examined the properties of gases, oils and brines: the three primary types of pore fluid present in most reservoirs. The fluid properties predicted include density and bulk modulus as functions of fluid temperature and pressure, when the pore-fluid composition is known or estimated.

1. Brine density

Brine density is a function of temperature (T in °C), pressure (P in MPa) and salinity (S in ppm). The density of pure water is first obtained:

$$\rho_w = 1 + 1\,\text{x}10^{-6}\begin{pmatrix} -80T - 3.3T^2 + 0.00175T^3 + 489P - 2TP \\ +0.016T^2P - 1.3\,\text{x}\,10^{-5}T^3P - 0.333P^2 - 0.002TP^2 \end{pmatrix} \quad (\text{A. 1})$$

Brine density is then deduced from pure water density:

$$\begin{aligned} \rho_B = \rho_w + S\big[&0.668 + 0.44S \\ &+ 1\,\text{x}\,10^{-6}\big(300P - 2400PS \\ &+ T(80 + 3T - 3300S - 13P + 47PS)\big)\big] \end{aligned} \quad (\text{A. 2})$$

Where $\rho_w$and $\rho_B$are the densities of water and brine in g/cm^3, and S is the weight fraction (ppm/1000000) of sodium chloride.

Brine velocity

Similarly to density, brine velocity is function of *T*, *P* and *S*, and is deduced from the velocity of pure water W_w, which is a polynomial function of temperature and pressure. The included constant w_{ij} coefficients are listed in Table A.1:

$$W_w = \sum_{i=0}^{4}\sum_{j=0}^{3} w_{ij} T^i P^j \qquad (A.3)$$

$$V_B = V_W + S(1170 - 9.6T + 0.055T^2 - 8.5 \text{ x } 10^{-5}T^3 + 2.6P - 0.0029TP - 0.0476P^2) + S^{1.5}(780 - 10P + 0.16P^2) - 820S^2 \qquad (A.4)$$

Table A.1: The bulk modulus of oil as a function of temperature, pressure, and composition (Batzle and Wang, 1992)**.**

w_{00}=1402.85	w_{02}=3.437x10^{-3}
w_{10}=4.871	w_{12}=1.739x10^{-4}
w_{20}=-0.04783	w_{22}=-2.135x10^{-6}
w_{30}=1.487x10^{-4}	w_{32}=-1.455x10^{-8}
w_{40}=-2.197x10^{-7}	w_{42}=5.230x10^{-11}
w_{01}=1.524	w_{03}=-1.197x10^{-5}
w_{11}=-0.0111	w_{13}=-1.628x10^{-6}
w_{21}=2.747x10^{-4}	w_{23}=1.237x10^{-8}
w_{31}=-6.503x10^{-7}	w_{33}=1.327x10^{-10}
w_{41}=7.987x10^{-10}	w_{34}=-4.614x10^{-13}

2. Oil density

Batzle and Wang (1992) make the distinction between live and dead oil. In our experiment, dead oil was chosen in order to simplify the understanding of the production. The density of oil at 15.6 °C under atmospheric pressure is given by:

$$\rho_o = \frac{141.5}{API + 131.5} \qquad (A.5)$$

where API is the oil gravity number. Under different temperature and pressure condition (respectively *T* and *P*), the oil density is calculated by:

$$\rho_{\text{oil}} = \frac{\rho_o + (0.00277P - 1.71 \text{ x } 10^{-7}P^3)(\rho_o - 1.15)^2 + 3.49 \text{ x } 10^{-4}P}{(0.972 + 3.81 \text{ x } 10^{-4}(T + 17.78)^{1.175})} \quad (A.6)$$

3. Oil velocity

The oil velocity under the same conditions is given by the following empirical equation:

$$V_{oil} = 2096\sqrt{\frac{\rho_{\text{oil}}}{2.6 - \rho_{\text{oil}}}} - 3.7T + 4.64P + 0.0115\left(4.12\sqrt{\frac{1.08}{\rho_{\text{oil}}} - 1} - 1\right)TP \quad (A.7)$$

The oil and brine bulk moduli can be now obtained, using:

$$K = V^2\rho \quad (A.8)$$

4. Gas density

$$\rho_{\text{g}} = \frac{28.8gP}{ZRT_a} \quad (A.9)$$

where g is the gas-specific gravity, P is pressure, R is the gas constant, Z is the gas compressibility factor and T_a = Absolute temperature. The Z and T_{a} are calculated using:

$$Z = 0.03 + 0.00527\left(3.5 - T_{\text{pr}}\right)^3 P_{\text{pr}} + \left(0.642T_{\text{pr}} - 0.007{T_{\text{pr}}}^4 - 0.52 + E\right) \quad (A.10)$$

$$T_{\text{a}} = T(°\text{C}) + 273.15 \quad (A.11)$$

and T_{pr}, P_{pr} and E are given by:

$$T_{\text{pr}} = \frac{T_{\text{a}}}{94.72 + 170.75\text{g}}, P_{\text{pr}} = \frac{P}{4.892 - 0.404\text{g}} \quad (A.12)$$

Where T_{pr} is the pseudo-reduced temperature, T_a is the absolute temperature and P_{pr} is the pseudo-reduced pressure.

$$E = 0.109(3.85 - T_{\text{pr}})^2 \exp\left[\frac{-\left(0.45 + 8\left(0.56 - \frac{1}{T_{\text{pr}}}\right)^2 {P_{\text{pr}}}^{1.2}\right)}{T_{\text{pr}}}\right] \quad (A.13)$$

5. Gas bulk modulus

$$K_g = \frac{P}{\left(1 - \frac{P_{\mathrm{pr}}}{Z} - \frac{\partial Z}{\partial P_{\mathrm{pr}}}\right)_T} \gamma_o \qquad (\mathrm{A.14})$$

$$\gamma_o = 0.85 + \frac{5.6}{\left(P_{\mathrm{pr}} + 2\right)} + \frac{27.1}{\left(P_{\mathrm{pr}} + 3.5\right)^2} - 8.7\exp\left(-0.65\left(P_{\mathrm{pr}} + 1\right)\right)$$

Where values of $\frac{\partial Z}{\partial P_{\mathrm{pr}}}$ ae easily obtained from Equations A.10 and A.13. More details can be found in Batzle and Wang (1992)

Appendix B
Neighbourhood Bayes Algorithm (NAB)

B.1 Neighbourhood Bayes Algorithm (NAB)

This section describes a way to extract robust information from the model ensemble generated during the search stage of an inverse problem. This appraisal step is performed in a Bayesian framework using the NA-Bayes (NAB) algorithm (Sambridge, 1999b), which can be seen as a complement to the NA algorithm in that it makes use of the same geometrical concept of representing the model space as a Voronoi diagram. In this approach, the solution of the inverse problem will be carried out in two steps:

- Approximation stage: generation of approximate likelihood function and,
- MCMC stage: evolution of MCMC solution of the problem using generated approximation.

This approach named Neighbourhood Bayes Algorithm (NAB). The whole ensemble of previously generated models is re-sampled and analysed in a Bayesian framework in order to evaluate the posterior density functions of the uncertain parameters (Rotondi *et al.*, 2006). The ensemble generated can be quantitatively inferred in a Bayesian framework by means of NA-Bayes (NAB). Two advantages of using NAB for the uncertainty quantification problem are:

1. It refers the information from the complete ensemble, not only a subset of it, and
2. It does not require running reservoir simulation of each model "resampled". NAB sampling is referred to as "resampling" in this thesis, as it samples from an ensemble already generated by sampling the parameter space using a search algorithm (e.g. NA or NAPG).

NAB constructs an approximation of the posterior probability (PPD) by a Gibbs sampler (Geman & Geman 1984; Smith & Roberts 1993). In other words, after

producing an ensemble of irregularly distributed models at the search stage, a second 'resampled' ensemble is created that represents the gathered information in a consistent, probabilistic way. However, using this resampled ensemble $m_{NA}^{(1)}, m_{NA}^{(2)}, m_{NA}^{(3)}, \dots, m_{NA}^{(N)}$ in the MC estimation (to estimate the integral I_{NA} as a simple average over the sample as depicted in Equation B.1) clearly cannot retrieve information that was missed during the search process performed before.

$$I_{NA} = \frac{1}{N}\sum_{t=1}^{N} g\left(m_{NA}^{(t)}\right) \tag{B.1}$$

Where N is the ensemble size and $g(m_{NA})$ is the function that describes some quantity of interest.

The resampled ensemble is generated using a Gibbs sampler where Voronoi cells are used to represent the model space and to interpolate the PPD of unknown points in the high-dimensional parameter space. The Voronoi interpolation is done simply by setting the known PPD of each model to be constant inside its cell. Figure B.1 illustrates a two-dimensional example where a random walk collects four successive models (for parameter x and y). Starting from some point (x_0, y_0) in cell E which we write as m_E (This can be a model from the input ensemble.), a new value for parameter x is proposed, this time randomly chosen between the lower and upper bounds of the parameter range, l_x and u_x. This value x_1 is accepted if a second random deviate r from the interval (0, 1) satisfies

$$r \leq \frac{P_{NA}(x_1|y_0)}{P_{NA}(x^{max}|y_0)} \tag{B.2}$$

where $P_{NA}(x_1|y_0)$ is the probability density for parameter x conditioned on the fixed value of y and $P_{NA}(x^{max}|y_0)$ is the maximal value of this conditional (in this case the value in cell D as indicated Figure B.1). It is clear that the conditional $P_{NA}(x_1|y_0)$ is just the function $P_{NA}(m)$ sampled along the i^{th} axis, which passes through m_E. As these conditionals only appear in a quotient, they can simply be taken as the values of the joint probability $P_{NA}(m)$, because the normalizing factor (here, $P_{NA}(y_0)$) cancels out. If the proposal point is rejected, the procedure is repeated until one value is accepted. In the next

step, a new value for parameter y is produced resulting in the model (x_1, y_1). This mechanism can directly be transferred to higher-dimensional spaces, and it yields a random walk that asymptotically converges to the equilibrium $P_{NA}(m)$ (see Sambridge, 1999b). Again, all information that is needed are the intercepts of the axis of the current parameter with the boundaries of the Voronoi cells, and these are obtained by the formula given in Sambridge, 1999a. Note that the values of $P_{NA}(m)$ are constant within the cells. Therefore, in the whole process, the probability of entering a cell is determined by the value $P_{NA}(m^{(i)})$ of its generator point and the size of the cell. The most important feature of this algorithm is that it does not require any further evaluations of the objective function (solving of the forward problem), which leads to low computational costs. To sum up, after many independent walks starting from different locations, the constructed conditional PDF is believed to be a good approximation to the true posterior distribution. More details of NAB mechanism can be found in Sambridge, 1999b.

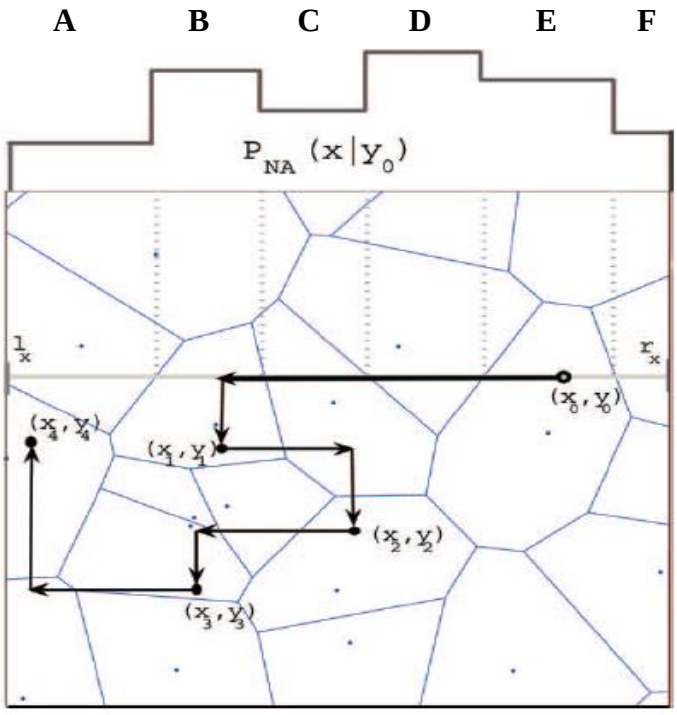

Figure B.1: A Gibbs sampler generating four new points in the search space (Sambridge, 1999b).

The accuracy of NAB depends on the complexity of the misfit space, Voronoi cell size and the size of samples to represent this space. The shape and size (volume) of Voronoi cells are determined by distribution of the models using the optimization (sampling) algorithm. If there is a complex misfit surface (large change of misfit value within short distance) or limited number of samples (large Voronoi cells), then the NAB approach should be used carefully (Hajizadeh *et al.*, 2009, 2010).

References

Aanonsen, S. I., Aavatsmark, I., Barkve, T., Cominelli, A., Gonard, R., Gosselin, O., Kolasinski, M., Reme, H.: "Effect of scale dependent data correlation in an integrated history matching loop combining production data and 4D seismic data," paper SPE 79665, presented at SPE reservoir simulation symposium, Houston, Texas, U.S.A., 3-5 February 2003.

Aanonsen, S.I., Nævda, G., Oliver, D.S., Reynolds, A.C.; and Vallès, B.: "The Ensemble Kalman Filter in Reservoir Engineering-a Review," SPE Journal, Vol. 14, No. 3, pp. 393-412, 2009.

Abacioglu, Y., Oliver, D.S., and Reynolds, A.C.: "Efficient Reservoir History Matching Using Subspace Vectors," Computational Geosciences, Vol. 5, No. 2, pp.151-172, 2001.

Alan S. E., William J. M.: "History Matching Finite Difference Models With 3D Streamlines," paper SPE 49000, presented at the SPE Annual Technical Conference and Exhibition, New Orleans, Louisiana, 27-30 September 1998.

Alvarenga, G. B. and Mateus, G. R.: "Hierarchical tournament selection genetic algorithm for the vehicle routing problem with time windows," In 4th International Conference on Hybrid Intelligent Systems, pp. 410-415, 2004.

Anderson, J. L.: "An ensemble adjustment Kalman filter for data assimilation," Monthly Weather Review, Vol. 129, No. 12, pp. 2884–2903, 2001.

Anderson, M.J., Whitcomb, P.J.: "RSM simplified: optimizing processes using response surface methods for design of experiments," Productivity Press, New York, 2005.

Anterione, F., Eymard, R. V., and Karcher, B.: "Use of Parameter Gradients for Reservoir History Matching," paper SPE 18433, presented at SPE Symposium on Reservoir Simulation, Houston, TX, 6-8 February 1989.

Andersen T., Zachariassen E., Otterlei C., Hatland K., and Liestol F..: "Method for conditioning the reservoir model on 3D and 4D elastic inversion data applied to a fluvial reservoir in the North sea," paper 100190, presented the SPE Europec/EAGE Annual Conference & Exhibition, Vienna, Austria, 2006.

April, J., Glover, F., Kelly, J., Laguna, M., Erdogen, M., Mudford, B., and Stegemeier, D.: "Advanced Optimization Methodology in the Oil and Gas Industry: The Theory of Scatter Search Techniques with Simple Examples," paper SPE 82009, presented at the SPE Hydrocarbon Economics and Evaluation Symposium, Dallas, TX, 5-8 April, 2003.

References

April, J., Glover, F., Kelly, J., Laguna, M..: "A New Optimization Methodology for Portfolio Management," paper SPE 84332, presented at the SPE Annual Technical Conference and Exhibition in Denver, CO, 5-8 October, 2003.

Arenas, E., Kruijsdijk, C. V. and Oldenziel, T.: "Semi-automatic history matching using the pilot point method including time-lapse seismic data," paper SPE 71634, presented at the 2001 SPE Annual Technical Conference and Exhibition held in New Orleans, Louisiana, USA, 30 September - 3 October, 2001.

Arenas, E. M., Oldenzeil, T. and Van Kruijsdijk, C. P. J. W.: "History matching reservoir model to Time-Lapse seismic using pilot point method," EAGE 63rd Conference and Technical Exhibition, Amsterdam, The Netherlands, 11 - 15 June, 2001.

Arwini, S. and Stephen, K.D.: "A New Method to Improve Convergence Rates with Seismic History Matching," paper SPE 131545, presented at the 72nd EUROPEC/EAGE Conference & Exhibition, Barcelona, Spain, 14-17 June, 2010.

Arwini, S., and Stephen, K.D.: "Combining experimental design with proxy derived sensitivities to improve convergence rates in Seismic History Matching," paper SPE 143528, presented at the 73rd EUROPEC/EAGE Annual Conference and Exhibition Vienna, Austria, 23-26 May, 2011.

Asadollahi, M. and Nævdal, G.: "Waterflooding Optimization Using Gradient Based Methods," paper SPE 125331, presented at SPE/EAGE Reservoir Characterization and Simulation Conference, Abu Dhabi, 19-21 October, 2009.

Backus, G. E.: "Long-wave Elascit Anisotropy Produced by Horizontal Layering," J. Geophysical Research, Vol. 67, No. 11, pp.4427- 4440, 1962.

Badru, O., and Kabir, C. S.: "Well Placement Optimization in Field Development.," paper SPE 84191, presented at the Annual Technical Conference and Exhibition, Denver, Colorado, 5-8 October 2003.

Baker, R. O.: "Streamline Technology: "Reservoir History Matching and Forecasting = Its Success, Limitations, and Future," Journal of Canadian Petroleum Technology, April 2001, Vol. 40, No. 4, pp. 23-27, 2001.

Barker, J.W. Cuypers, M. and Holden, L.: "Quantifying Uncertainty in Production Forecasts: Another Look at the PUNQ-S3 Problem," Journal of Petroleum Technology, pp. 433-441, December 2001.

Ballin, P.R., Aziz, K., Journel, A.G.: "Quantifying the Impact of Geological Uncertainty on Reservoir Performing Forecasts," paper SPE 25238, presented at the 12th SPE Symposium on Reservoir Simulation, New Orleans, USA, 28 February – 3 March, 1993.

Barton, R. R., Meckesheimer, M.: "Metamodel-based simulation optimization," Henderson SG, Nelson BL, eds. Handbooks in Operations Research and Management Science, Vol. 13, pp. 535-574, Elsevier, Amsterdam, 2006.

Batzle, M. and Wang, Z.: "Seismic properties of pore fluids," Geophysics, Vol. 57, No. 11, pp. 1396–1408, 1992.

Bayes, T.: "An essay towards solving a problem in the doctrine of chances,'' Philosophical Transactions of the Royal Society, Vol. 53, pp.370-418, 1763.

Benabentos, M., Mallick, S., Sigismondi, M., and Soldo, J.: "An Overview of Exploration Geophysics-Recent Breakthroughs in Geophysics and Recognition of Challenging new Problems," CSEG Journal, Vol. 11, No. 1, pp. 7–15, 1975.

Benabentos, M., Mallick, S., Sigismondi, M., and Soldo, J.: "Seismic Rreservoir Description Using Hybrid Seismic Inversion," The Leading Edge, Vol. 21, No. 10, pp.1002–1008, 2002.

Bernardo, J. and Smith, A. F.: "Bayesian theory," John Wiley & Sons, New York, 1994.

Bi, Z.: "Conditioning 3D Stochastic Channels to Well-Test Pressure Data," PhD dissertation, U. of Tulsa, Tulsa, Oklahoma, 1999.

Bi, Z., Oliver, D.S. and Reynolds, A.C.: "Conditioning 3D Stochastic Channels to Pressure Data," Soc. Petrol. Eng. J., Vol. 5, No. 4, pp. 474-484, 2000.

Bi, Z., Oliver D.S., and Reynolds, A.C.: "Conditioning 3D Stochastic Channels to Pressure Data," paper SPE 67954, presented at the SPE Annual Technical Conference and Exhibition held in Houston, 3–6 October 1999.

Birchenko, V.M., Demyanov, V.V., Konopczynski, M.R., and Davies, D.R.: "Impact pf Reservoir Uncertainty on Selection of Advanced Completion Type," paper SPE 115744 presented at the SPE Annual Technical Conference and Exhibition, Denver, 21-24 September 2008.

Bissell, R.: "Calculating Optimal Parameters For History-Matching," paper presented at the European Conference on the Mathematics of Oil Recovery, Røros, Norway, 7-10 June 1994.

Bissell, R.C., Dubrule, O., Lamy, P., Swaby, P., and Lepine, O.: "Combing Geostatistical Modelling with Gradient Information for History Matching: The Pilot Point Method," paper SPE 38730, presented at the SPE Annual Technical Conference and Exhibition, San Antonio, TX, 5-8 October 1989.

References

Bissell, R. C., Dubrule, O., Lamy, P., Lepine, O.: "Combining geostatistical modelling with gradient information for history matching: the pilot point method," paper SPE 38730, presented at the SPE Annual Technical Conference, San Antonio, Texas, 5-8 October, 1997.

Bissell, R.C., Sharma, Y., and Killough, J.E.: "History Matching Using the Method of Gradients: Two Case Studies," paper SPE 28590 presented at the SPE Annual Technical Conference and Exhibition, New Orleans, LA, 25-28 September, 1994.

Bittencourt, A. C., and Horne, R. N., "Reservoir Development and Design Optimization", paper SPE 38895, presented at the SPE Annual Technical Conference and Exhibition, San Antonio, Texas, 5-8 October 1997.

Bonet-Cunha, L., Oliver, D.S., Redner, R.A. and Reynolds, A.C.: "A Hybrid Markov Chain Monte Carlo Method for Generating Permeability Fields Conditioned to Multiwell Pressure Data and Prior Information," paper SPE 36566, presented the SPE Annual Technical Conference and Exhibition, Denver, Colorado, 6-9 October 1996.

Box, G. E. P. and Draper, N.R.: "Empirical model-building and response surfaces," New York: John Wiley & Sons, 1987.

Box, G. E. P., Hunter,W.G., Hunter, J.S. and Hunter,W.G.: "Statistics for Experimenters: Design, Innovation, and Discovery," 2nd Edition, Wiley, 2005.

Box, G. E. P. and Wilson, K.B.: "On the Experimental Attainment of Optimum Conditions," Journal of the Royal Statistical Society, Series B, Vol. 13, No. 1, pp 1–45, 1951.

Brand, C.W., Heinemann, Z.E., Aziz, K., "The grid orientation effect in reservoir simulation," paper SPE 21228, presented at the 11th SPE Symposium on Reservoir Simulation held in Anaheim, California, 17-20 February 1991.

Brook, R., Landrum, R., and Sallas, J.: "Report to the SEG Technical Standards Committee Regarding Polarity Convention for Vibratory Source/Recording System," In SEG Report, Tulsa, Oklahoma, Society of Exploration Geophysicists, 1993.

Brouwer, D.R., Jansen, J.D., van der Starre, S., Van Kruijsdijk, C.P.J.W., and Berentsen, C.W.J.: "Recovery Increase through Water Flooding with Smart Well Technology," paper SPE 68979, presented at the SPE European Formation Damage Conference, The Hague, The Netherlands, 21-22 May, 2001.

Brouwer, D.R., Naevdal, G., Jansen, J.D., Vefring, E.H., and Van Kruijsdijk, C.P.J.W.: "Improved Reservoir Management through Optimal Control and Continuous Model Updating," paper SPE 90149, presented at the SPE Annul Technical Conference and Exhibition, Houston, TX, 26-29 September 2004.

References

Brown, A.: "Interpretation of Three-Dimensional Seismic Data," The American Association of Petroleum Geologists, Vol. 9, pp. 233-281. Society of Exploration Geophysics, Tulsa, Oklahoma, 1999.

Burke, E. K., Gustafson, S. M. and Graham Kendall, G.: "Diversity in genetic programming: An analysis of measures and correlation with fitness," IEEE Transactions on Evolutionary Computation, Vol. 8, No. 1, pp. 47-62, 2004.

Caers, J.: "Efficient Gradual Deformation Using a Streamline-Based Proxy Method," Journal of Petroleum Science and Engineering, Vol. 39, pp. 57-83, 2003.

Caers, J: "Markov chain theory for spatial stochastic simulation," Stanford for Reservoir Forecasting, Stanford University, Report No. 12, Vol. 1, May 13-14, 1999.

Cancelliere, M., Verga, F., and D. Viberti, D.: "Benefits and Limitations of Assisted History Matching," paper SPE 146278, presented at the SPE Offshore Europe Oil and Gas Conference and Exhibition held in Aberdeen, UK, 6–8 September 2011.

Carter, R.D., Kemp, L.F., Pierce, A.C., and Williams, D.L.: "Performance Matching with Constraints," Soc. Petrol. Eng. J., Vol. 14, No. 4, pp. 187-196, 1974.

Carter, J.N., and Ballester, P.: "A real parameter genetic algorithm for cluster identification in history matching," In: The Proceedings of the 9th European Conference on the Mathematics of Oil Recovery, Cannes, France, 30 August–02 September 2004.

Castellini, A., Landa, J.L., and Kikani, J.: "Practical Methods for Uncertainty Assessment of Flow Predictions for Reservoirs with Significant History- A Field Case Study," 9th European Conference on the Mathematics of Oil Recovery, Cannes, France, 2004.

Chapin, M., Terwogt, D., and Ketting, J.: "From Seismic to Simulation Using New Voxel Body and Geologic Modeling Techniques," Schiehallion Field, West of Shetlands. The Leading Edge, Vol. 19, No. 4, pp. 408–412, 2000.

Chavent, G.M., Dupuy, M., and Lemonnier, P.: "History Matching by Use of Optimal Control Theory," Soc. Petrol. Eng. J., Vol. 15, No. 1, pp. 74-86, 1975.

Chen, W.H., Gavalas, G.R., Seinfeld, J.H., and Wasserman, M.L.: "A New Algorithm for Automatic History Matching," Soc. Petrol. Eng. J., Vol. 14, No. 12, pp. 593-608, 1974.

Cheng, H., Kharghoria, A., He, Z., and Datta-Gupta, A.: "Fast History Matching of Finite-Difference Models Using Streamline-Derived Sensitivities," SPE Res Eval & Eng , Vol. 8, No. 5, pp. 426-436, 2005.

Cheng, K., Wei, Y. N., Wu, W. and Holditch, S. A.: "A Novel Optimization Model for Analyzing Production Data," paper 132545, presented at the SPE Western Regional Meeting held in Anaheim, California, USA, 27 –29 May 2010.

References

Christie, M. A.: "Upscaling for Reservoir Simulation," SPE Distinguished Author Series, Journal of Petroleum Technology, Vol. 48, No. 11, pp. 1004–1010, 1996.

Christie, M., Demyanov, V., and Erbas D.: "Uncertainty Quantification for Porous Media Flows," Journal of Computational Physics, Vol. 217, pp. 143–158, 2006.

Christie, M., MacBeth, C., and Subbey S.: "Multiple History-Matched Models for Teal South," The Leading Edge, Vol. 21, No. 3, pp. 286-289, March 2002.

Christie, M., Glimm, J., Grove, J.W., Higdon, D.M., Sharp, D.H, Wood-Schultz, M.M "Error Analysis and Simulations of Complex Phenomena," Los Alamos Science, Vol. 29, 2005

Christopher O. A., Randle J., Fitzmorris R.: "Quantifying Uncertainties in a New Field Development: A Swamp Field Case," paper SPE 88888, presented at the 28th Annual SPE International Technical Conference and Exhibition, Abuja, Nigeria, 2 – 4 August 2004.

Chu, L., Reynolds, A.C., Oliver, D.S.: "Computation of sensitivity coefficients for conditioning the permeability field to well-test data," In Situ, Vol. 19, No. 2, pp. 179–223, 1995.

Chung, C.B. and Costas, K.: "Incorporation of A Priori Information in Reservoir History Matching by Regularization," paper SPE 21615, SPE Journal, 1990.

Coats, K. H., Dempsey, J. R., and Henderson, J. H.: "A New Technique for Determining Reservoir Description From Field Performance Data," SOC. Pet. Eng. J. pp. 66-74, March 1970.

Cooper, M., Thorogood, E., O'Donovan, A., Kristiansen, P. and Christie. P.: "Foinaven active reservoir management: The time-lapse signal," SEG, Expanded Abstracts, 1999.

Cooper, M., Thorogood, E., O'Donovan, A., Kristiansen, P., and Christie, P.: "Foinaven Active Reservoir Management: The Time-Lapse Signal," In SEG International Exposition and Annual Meeting, Houston, Texas, 1999a.

Cooper, M.,Westwater, P., Thorogood, E., Kristiansen, P., and Christie, P.: "Foinaven Active Reservoir Management :Towed Streamer and Buried Sea-Bed Detectors in Deep Wter for 4D Seismic," In SEG International Exposition and Annual Meeting, Houston, Texas, 1999b.

Cooper, M.,Westwater, P., Thorogood, E., Kristiansen, P., Christie, P., and Probert, T.: "Foinaven Active Reservoir Management : The Benefits from the Baseline Surveys," In SEG International Exposition and Annual Meeting, Houston, Texas, 1999c.

Corrigan, A.F.: "Estimation of recoverable reserves: the geologists job," In J. R. Parker. Petroleum Geology of Northwest Europe: Proceedings of the 4th Conference, pp. 1473-1482. The Geological Society, London, 1993.

Craig, P.S., Goldstein, M., Seheult, A.H. and Smith, J.A.: "Pressure matching for hydrocarbon reservoirs: a case study in the use of Bayes linear strategies for large computer experiments (with discussion)," in Gatsonis et al. (eds), Case Studies in Bayesian Statistics, Vol. III, Springer, pp 37–93, 1997.

Cullick, A.S., Johnson, D., and Shi, G.: "Improved and More Rapid History Matching with a Nonlinear Proxy and Global Optimization," paper SPE 101933, presented at the SPE Annual Technical Conference and Exhibition, San Antonio, TX, 24-27 September 2006.

Cullick, A.S., Heath, D., Narayanan, K., April, J., and Kelly, J.: "Optimizing Multiple-Field Scheduling and Production Strategy with Reduced Risk," paper SPE 84239, presented at the SPE Annual Technical Conference and Exhibition, Denver, CO, 5-8 October 2003.

Cuong, T. Q, Ngoc, T. B., Wisup, B. and Taemoon, C.: "Global and Local History Matching Optimization. The Successful Key of Reservoir Simulation: High Heterogeneous Field CaseStudy," paper 2009-021 accepted for the Proceedings of the Canadian International Petroleum Conference (CIPC) 2009, Calgary, Alberta, Canada, 16-18 June 2009.

Dadashpour, M., Kleppe, J., and Landro, M.: "Porosity and permeability estimation by gradient-based history matching using time-lapse seismic data," paper SPE 104519, presented the 15th SPE Middle East Oil & Gas Show and Conference held in Bahrain International Exhibition Centre, Kingdom of Bahrain, 11–14 March 2007.

Dadashpour, M., Martin Landrø, M., Kleppe, J.: "Nonlinear inversion for estimating reservoir parameters from time-lapse seismic data," J. Geophys. Eng. Vol. 5, pp. 54-66, 2008.

de Marsily, G., Lavedan, G., Boucher, M., and Fasanino, G.: "Interpretation of Interference Tests in a Well Field Using Geostatistical Techniques to Fit the Permeability Distribution in a Reservoir Model," In Geostatistics for Natural Resources Characterization, Part 2, pp. 831–849, Kluwer Academic Publishers, 1984.

Debye, P.: "Näherungsformeln für die Zylinderfunktionen für große Werte des Arguments und unbeschränkt veränderliche Werte des Index," Mathematische Annalen, Vol. 67, No. 4, pp. 535–558, English translation in Debye, Peter J. W. (1954), The collected papers of Peter J. W. Debye, Interscience Publishers, Inc., New York, 1909.

Denison, D.G., Holmes, C.C., Mallick B.K. and Smith A.F.: "Bayesian Method for Nonlinear Classification and Regression," Wiley series in probability and statistics, 2002.

Dey, T.: "Handbook of Discrete and Computational Geometry," CRC.Press, Boca Raton, U.S.A, 1998.

Ditzhuijzen, R. V., Oldenziel, T. and Kruijsdijk, V.: " Geological parameterization of a reservoir model for history matching incorporating time-lapse seismic based on a case study of the statfjord field," paper SPE 71318, presented at the SPE Annual Technical Conference and Exhibition held in New Orleans, Louisiana, USA, 2001.

Dobbyn, A. and Marsh M.: "Material Balance: A Powerful Tool for Understanding The Early Performance of The Schiehallion Field," paper SPE 71819, presented at the Offshore Europe Conference, Aberdeen, Scotland, 4-7 September, 2001.

Dong, Y., Gu, Y. and Oliver, D. S.: "Sequential Assimilation of 4D Seismic Data for Reservoir Description Using the Ensemble Kalman Filter," Journal of Petroleum Science and Engineering, Vol. 53, No. (1-2), pp. 83–99, 2006.

Dong Y and Oliver D.: "Quantitative use of 4D seismic data for reservoir description," SPE Journal, SPE 84571, 2005.

Dong and D. Oliver.: "Reservoir simulation model updates via automatic history matching with integration of seismic impedance change and production data," In Proceedings of the International Petroleum Technology Conference, Kuala Lumpur, Malaysia, 2008.

Dougherty, E. L. and Khairkhah, K.: "History matching of Gas Simulation Models Using Optimal Control Theory," paper SPE 5371, presented at the 45th SPE Annual California Regional Meeting, Ventura, CA, April 2-4, 1975.

Dorigo, M.: "Learning and Natural Algorithms," PhD thesis, Politecnico di Milano, 1992.

Dorigo, M., and T. Stutzle.: " Ant Colony Optimization," MIT Press, Cambridge, Mass, 2004.

Doyen, P.: "Seismic reservoir characterization: An earth modeling perspective," EAGE Publications, The Netherlands, 2007.

Eastwood, J., Johnston, D., Huang, X., Craft, K. and Workman, R.: "Processing for robust time-lapse seismic analysis: Gulf of Mexico example," Lena Field, SEG Expanded Abstracts, 1998.

Edriz, N., Stephen, K. D., Shams, A., and MacBeth, C.: " Updating Barrier Transmissibilies in Simulations by Successively Adding Data to an Automated Seismic History Matching Processes: A Case study," paper SPE113557, presented at the SPE Europec/EAGE Annual Conference and Exhibition, Rome, Italy, 9–12 June, 2008.

Edwards, W., Lindman, H., Savage, L.J.: "Bayesian statistical inference in statistical research," Psychological Review, Vol. 70, pp. 193-242, 1963

Eisenmann, P., Gounot, M. T., Juchereau, B. and Whittaker, S. J.: "Improved Rxo measurements through semi-active focusing," paper SPE-28437, presented at the SPE 69th Annual Technical Conference and Exhibition, New Orleans, LA, USA, 25-26 September 1994.

Elabed, S.: "Analysis of the Neighbourhood Algorithm Applied to History Matching Under Uncertainty," Technical report, Heriot-Watt University, Institute of Petroleum Engineering, 2003.

Emerick, A.A., Moraes, R.J and Rodrigues, J.R.P.: "History Matching 4D Seismic Data with Efficient Gradient Based Methods," paper SPE 107179, presented at the SPE EUROPEC/EAGE Annual Conference and Exhibition, London, United Kingdom, 11-14 June, 2007.

Emerick, A., Reynolds, A.C.: "EnKF-MCMC," paper SPE 131375, presented at the EUROPEC/EAGE Annual Conference and Exhibition, Barcelona, Spain, 14-17 June 2010.

Erbas, D. and Christie, M.A.: "Effect of Sampling Strategies on Prediction Uncertainty Estimation," paper SPE 106229 presented at the SPE Reservoir Simulation Symposium, Houston, TX, 26-28 February, 2007.

Eriksson, K., Estep, D., Hansbo, P. and Johnson, C.: "Computational Differential Equations," Cambridge University Press, Sweden, 1996.

Evensen, G.: "Sequential data assimilation with a nonlinear quasi-geostrophic model using Monte Carlo methods to forecast error statistics," Journal of Geophysical Research, Vol. 99, No. C5, pp. 143-162, 1994.

Evensen, G.: "The ensemble Kalman filter: Theoretical formulation and practical implementation," Ocean Dynamics, 2003.

Evensen, G., Hove, J., Meisingset, H. C., Reiso, E., Seim, K. S. and Espelid, Ø.: "Using the EnKF for Assisted History Matching of a North Sea Reservoir Model," paper SPE 106184, presented at the SPE Reservoir Simulation Symposium, Houston, TX, 26–28 February, 2007.

Fasanino G, Molinard J E, de Marsily G and Pelcé V.: "Inverse Modeling in Gas Reservoirs," SPE 15592, 61st SPE Annual Technical Conference and Exhibition, New Orleans, Texas, October 5-8, 1986.

Fishman, G.S.: "Monte Carlo: Concepts, Algorithms and Applications," New York, Springer-Verlag, 1996.

Fletcher, R.: "Practical Methods of Optimization," 2nd Edition, John Wiley & Sons, New York, 1987.

Fletcher, J., Seymour, G., Flynn, T., and Burchell, M.: "Formation pressure testing while drilling for deepwater field development," paper SPE 96321, presented at the SPE Offshore Europe Conference, Aberdeen, UK, 2005.

Floris, F., Bush, M., Cuypers, M., Roggero, F., and Syversveen, A. R.: "Methods for quantifying the uncertainty of production forecasts: a comparative study," Petroleum Geoscience , Vol. 7(SUPP), pp. 87–96, 2001.

Floricich, M., Soldo, J., and MacBeth, C.: "An Engineering Approach for Pressure and Saturation Estimation from Time-Lapse Seismic Data," In XII Congreso Venezolano de Geofisica, Caracas, Venezuela, 2004.

Floricich, M.: "An engineering-consistent approach for pressure and saturation estimation from time-lapse seismic data," PhD thesis, Heriot-Watt University, 2006.

Floricich, M., A. Evans, D. McCormick, G. Jenkins, and Stammeijer, J.: "Adding the temporal coherence dimension to 4D seismic data-assessing connectivity in the Schiehallion field," 70th Annual Conference and Exhibition, EAGE, Extended Abstracts, E017, Rome, Italy, 9–12 June, 2008.

Fox, M.J., Chedburn, A.C.S., and Stewart, G.: "Simple Characterization of Communication Between Reservoir Regions," paper SPE 18360, presented at the SPE European Petroleum Conference, London, 16–19 October, 1998.

Friedmann, F., Chawathe, A. and Larue, D.K.: "Assessing Uncertainty in Channelized Reservoirs Using Experimental Designs," paper SPE 71622, presented at the Annual Technical Conference and Exhibition, New Orleans, 30 September - 3 October, 2001.

Fujita, K., and Kounoe, Y.: "High-Order Polynomial Response Surface with Optimal Selection of Interaction Terms," Department of Mechanical Engineering, Osaka University, Suita, Osaka 565-0871, Japan, 2005.

Gainski, M., Macgregor, A. G., Freeman, P. J. and Nieuwland, H. F.: "Turbidite reservoir compartmentalization and well targeting with 4D seismic and production data: Schiehallion Field, UK," Geological Society, London, Vol. 347, pp. 89-102, 2010.

Gao, G. and Reynolds, A.C.: "An Improved Implementation of the LBFGS Algorithm for Automatic History Matching," Soc. Petrol. Eng. J., Vol. 11, No. 1, pp. 5-17, 2006.

Gao, G., Zafari, M. and Reynolds, A.C.: "Quantifying Uncertainty for the PUNQ-S3 Problem in a Bayesian Setting with RML EnKF," paper SPE 93324, presented at the SPE Reservoir Simulation and Symposium, 2005.

Gassmann, F.: "Elastic waves through a packing of spheres, Geophysics," Vol. 16, No. 4, pp. 673–685, 1951.

Gauss C. F.: "Theoria Motus Corporum Coelestium," 1809.

Gavalas, G. R., Shah, P. C., and Seinfeld, J. H.:"Reservoir History Matching by Bayesian Estimation,'' SPE Journal, Vol. 16, No. 6, pp. 337-350, 1976.

Ghosh, S. and Rao, C. R.: "Design and Analysis of Experiments," Handbook of Statistics. Vol. 13, Amsterdam: North-Holland, 1996.

Gilks, W.R., Richardson, S. and Spiegelhalter, D.J.: "Markov Chain Monte Carlo in Practice," Chapman & Hall, London, 1996.

Glover, F.: "Heuristics for Integer Programming Using Surrogate Constraints," Decision Sciences, Vol. 8, pp. 156-166, 1977.

Glover, F.: "Genetic Algorithms and Scatter Search: Unsuspected Potentials," Statistics and Computing, Vol. 4, pp. 131-140, 1994.

Glover, F. and Laguna, M.: "Tabu Search, Kluwer Academic Publishers," Boston, 1997.

Goldberg, David E.: "Genetic Algorithms in Search, Optimization & Machine Learning," Addison-Wesley, Reading, Massachusetts, pp. 1-5, 1989.

Gómez-Hernánez, J.J., Sahuquillo, A., and Capilla J.E.: "Stochastic Simulation of Transmissivity Fields Conditional to Both Transmissivity and Piezometric Data I Theory," Journal of Hydrology, Vol. 203, pp. 162-174, 1997.

Gosselin, O., den Berg, V. and Chowdhury, S. D.: "A gradient-based approach for history-matching of both production and 4D seismic data," Tech. rep., preprint, 2001.

Gosselin, O., van den Berg, S., and Cominelli, A.: "Integrated History-Matching of Production and 4D Seismic Data," paper SPE 71599, presented at the SPE Annual Technical Conference and Exhibition, New Orleans, Louisiana, U.S.A, 30 September-3 October, 2001.

Gosselin, O., Aanonsen, S.I, Aavatsmark, I., Cominelli, A., Gonard, R., Kolasinski, M., Ferdinandi, F., Kocvacic, L. and Neylon, K.: "History Matching Using Time-Lapse Seismic (HUTS)", paper SPE 84464, presented at 2003 SPE Annual Conference and Exhibition, Denver, USA, 5-8 October, 2003.

Govan, A., Primmer, T., Douglas, C., Moodie, N., Davies, M., and Nieuwland, F.: "Reservoir management in a deepwater subsea field - The Schiehallion Experience," paper SPE 96610, presented at the SPE Offshore Europe Conference, Aberdeen, UK, 2005.

Govan, A., Primmer, T., Douglas, C., Moodie, N., Davies, M., and Nieuwland, F.: "Reservoir management in a deepwater subsea field - The Schiehallion Experience," SPE 96610-PA. SPE Journal, Vol. 8, No. 5, pp. 382-390, 2006.

Gray, D., Goodway, B., Chen, T.: "Bridging the gap: Using AVO to detect changes in fundamental elatsic constants," EAGE conference, Annual Technical Conference, Helsinki, 1999.

Guohua G, Gaoming L and Reynolds A. C.: "A stochastic optimization algorithm for automatic history matching," paper SPE 90065, presented at SPE Annual Technical Conference and Exhibition, Houston, Texas, September 26-29, 2004.

Guyaguler, B., Horne, R. N., Rogers, L., and Rosenzweig, J. J.: "Optimization of Well Placement in a Gulf of Mexico Water flooding Project," paper SPE 63221, presented at the Annual Technical Conference and Exhibition, Dallas, Texas, 1-4 October 2000.

Hadamard, J.: "Sur les problemes aux derivees partielles et leur signification physique," Bull. Univ. Princeton, Vol. 13, pp. 49-52, 1902.

Hajizadeh, Y., Christie, M., and Demyanov, V.: "Ant colony optimisation for history matching," paper SPE 121193, presented at the Proceedings of EUROPEC/EAGE Conference and Exhibition, 8–11 June, Amsterdam, The Netherlands, 2009.

Hajizadeh, Y., Christie, M., and Demyanov, V.: "Ants Can Do History Matching," paper SPE 141137, presented at the SPE International Student Paper Contest at the SPE Annual Technical Conference and Exhibition held in Florence, Italy, 19–22 September 2010.

Hajizadeh, Y.: "Population-Based Algorithms for Improved History Matching and Uncertainty Quantification of Petroleum Reservoirs", PhD thesis, Heriot Watt University, Edinburgh, UK, 2011.

Han, D., Nur, A. and Morgan, D.: "Effects of porosity and clay content on wave velocities in sandstones," Geophysics, Vol. 51, No. 11, pp. 2093-2107, 1896.

Handels, M., Zandvliet, M.J, Brouwer, D.R., and Jansen, J.D.: "Adgoint-Based Well-Placement Optimization Under Production Constraints," paper SPE 105797, presented at the SPE Reservoir Simulation Symposium, Houston, USA, 26-28 February, 2007.

Hanea, R.G., Przybysz-Jarnut, J.K. Krymskaya, M.V., Heemink, A.W. and Jansen, J.D.: "The Choice of a 'Best' Assisted History Matching Algorithm," paper SPE 131088, presented at the SPE EUROPEC/EAGE Annual Conference and Exhibition held in Barcelona, Spain, 14–17 June 2010.

Harris, P.E., Henry, B.: "Time-lapse processing: A North Sea case study," SEG Annual Technical Conference, New Orleans, 1998.

Huang X, Meister L and Workman R.: "Reservoir characterization by integration of time-lapse seismic and production data," paper SPE 38695, presented at SPE Annual Technical Conference, San Antonio, Texas, 1997.

Haugen, V., Natvik, L.-J., Evensen, G., Berg, A., Flornes, K., and Nævdal, G.: "History Matching Using the Ensemble Kalman Filter on a North Sea Field Case," paper SPE 102430, presented at the SPE Annual Technical Conference and Exhibition, San Antonio, TX, 24–27 September 2006.

He, N., Reynolds, A.C., and Oliver, D.S.: "Three-Dimensional Reservoir Description from Multiwell Pressure Data and Prior Information," Soc. Petrol. Eng. J., Vol. 2, No. 3, pp. 312-327, September 1997.

He, N., Oliver, D.S., and Reynolds, A.C.: "Conditioning Stochastic Reservoir Models to Well-Test Data," paper SPE 38655, presented at SPE Annual Technical Conference and Exhibition, San Antonio, TX, October 5 – 8, 1997.

Hestenes, M. R. and Eduard S.: "Methods of Conjugate Gradients for Solving Linear Systems," Journal of Research of the National Bureau of Standards, Vol. 49, No. 6, 1952.

Hirasaki, G. J.: "Sensitivity Coefficients for History Matching Oil Displacement Processes," SOC. Pet. Eng. J. pp. 39-49, 1975.

Holland, J.H.: "Adaptation in Natural and Artificial Systems," University of Michigan Press, Ann Arbor, 1975.

Holland, C. W. and Cravens, D. W.: "Fractional factorial experimental designs in marketing research," Journal of Marketing Research, Vol. 10, pp. 270-276, 1973.

Houtekamer, P. L. and Mitchell, H. L.: "Data assimilation using an ensemble Kalman filter technique," Monthly Weather Review, Vol. 126, No. 3, pp. 796–811, 1998.

Houtekamer, P. L. and Mitchell, H. L.: "A sequential ensemble Kalman filter for atmospheric data assimilation," Monthly Weather Review, Vol. 129, No. 1, pp. 123–137, 2001.

Hu, L.: "Gradual Deformation and Iterative Calibration of Gaussian-Related Stochastic Models," Mathematical Geology, Vol. 32, No. 1, pp. 87-108, 2000.

Hu, L. and Jenni, S.: "History Matching of Object-Based Stochastic Reservoir Models," Soc. Petrol. Eng. J., Vol. 10, No. 3, pp. 312-323, September 2005.

Huang, X., Bentley, L.R. and Laflamme, C.: "Integration of Production History and Time-Lapse Seismic Data Guided by Seismic Attribute Zonation," paper SPE 68819, presented at SPE Western Regional Meeting, Bakersfield, USA, 26-30 March, 2001.

Huang, X., Will R., Khan, M. and Stanley L.: "Reservoir characterization by integration of time-lapse seismic and production data," paper SPE 38695, presented at SPE Annual Technical Conference and Exhibition held in San Antonio, Texas, USA, 1997.

Huang, X., Meister, L., and Workman, R.: "Improvement and Sensitivity of Reservoir Characterization Derived From Time-Lapse Seismic Data," paper SPE 49146, presented at the at the SPE Annual Technical Conference and Exhibition, New Orleans, 27–30 September, 1998.

Huston, D. and Backus, M.: "Offset-Dependent Mis-Tie Analysis at Seismic Line Intersections," Geophysics, Vol. 54, No. 8, pp. 962–972, 1998.

Iwegbue, M., Appah, D., Ogwo, E.A.: "Crude Oil Metering Experience in the Niger-Delta," paper SPE 111906, presented at the Nigeria Annual International Conference and Exhibition, Abuja, Nigeria, 6-8 August, 2007.

Jackson, D.D.: "The Use of a Priori Data to Resolve Non-Uniqueness in Linear Inversion," Geophys. J. R. Astr. Soc., Vol. 57, pp. 137-157, 1979.

Jacquard, P., and Jain, C.: "Permeability Distribution from Field Pressure Data," Soc. Petrol. Eng. J., Vol. 5, No. 4, pp. 281-294, 1965.

Jahns, H.O.: "A Rapid Method for Obtaining a Two-Dimensional Reservoir Description from Well Pressure Response Data," Soc. Petrol. Eng. J., Vol. 6, No. 12, pp. 315-327, 1966.

Jansky, J., Zahradnik, J., Novotny, O., Plicka, V., Stavrakakis, G.: "Waveform inversion of M4 events in the Gulf of Corinth Poster presentation at the First European Conference on Earthquake Engineering and Seismology, 3-8 September 2006, Geneva, Switzerland.

Jaynes, E. T. and Brethorst, G. L.: "Probability Theory: The Logic of Science. Cambridge," MA: Cambridge University Press, 2003.

Johannes, M. and Polson, N.: "MCMC methods for continuous-time financial econometrics," in Handbook of Financial Econometrics, Y. Ait-Sahalia and L. P. Hansen, eds., Amsterdam: North-Holland, 2003.

John K. Hughes.: "Examination of seismic repeatability as a key element of time-lapse seismic monitoring," paper SPE 50627, presented at the SPE European Petroleum Conference held in The Hague, The Nethedands, 1998.

Jorge L. L. and Roland N. H.: "A procedure to integrate well test data, reservoir performance history and 4-D seismic information into a reservoir description," paper SPE 38653, presented at SPE Annual Technical Conference and Exhibition held in San Antonio, Texas, 1997.

Junkin, J.E., Sippel, M.A., and Lord, M.E.: "Well Performance Evidence for Compartmented Geometry of Oil and Gas Reservoirs," paper SPE 24356, presented at the SPE Rocky Mountain Regional Meeting, Casper, Wyoming, 18–21 May, 1992.

Jutila, H.A. and Goodwin, N.H.: "Schedule Optimization to Complement Assisted History Matching and Prediction under Uncertainty," paper SPE 100253, presented at the SPE Europec/EAGE Annual Conference and Exhibition, Vienna, Austria, 12-15 June, 2006.

Kabir, C. S., Young, N. J.: "Handling Production-Data Uncertainty in History Matching: The Meren Reservoir Case Study," paper SPE 87823-PA, presented at the SPE Reservoir Evaluation & Engineering, Vol. 7, No. 2, pp 123-131, 2004

Kelkar, M, Godofredo, P.: "Applied Geostatistics for Reservoir Characterization," published by SPE, 2002.

Kalman, R. A.: "New Approach to Linear Filtering and Prediction Problems," Trans. ASME, J. Basic Eng., Vol. 82(D), pp. 35–45, 1960.

Kazemi, A., Stephen, K. D. and Shams, A.: "Seismic History Matching of Nelson Using Time-Lapse Seismic Data: An Investigation of 4D Signature Normalization," SPE Reservoir Evaluation & Engineering, Vol. 14, No. 5, pp. 621-633, 2011.

Kennedy, J., and Eberhart, R.: "Particle swarm optimization," In Proceedings of the IEEE International Conference on Neural Networks, Vol. 4, pp. 1942–1948, Piscataway, New Jersey, 1995.

Kirsch, A.: "An Introduction to the Mathematical Theory of Inverse Problems," Vol. 120, Applied Mathematical Sciences, New York: Springer-Verlag, 1996.

Kitanidis, P.K.: "Quasi-Linear Geostatistical Theory for Inversing," Water Resour. Res., Vol. 31, No. 10, pp. 2411-2419, 1995.

Kitandis, P. K.: "The Minimum Structure Solution to the Inverse Problem," Water Res. Research, Vol. 33, pp. 2263-2272, 1997.

Kleijnen, J. P. C.: "Statistical testing of optimality conditions in multi-response simulation-based optimization," Seminar at the Statistics Department of Stanford University, 26 July 2005.

Kleijnen, J.P. C., and Van Groenendaal, W.J. H.: "Two-stage versus sequential sample-size determination in regression analysis of simulation experiments," American Journal of Mathematical and Management Sciences, Vol. 15, pp. 83-115, 1995.

Knai, T. A. and Knipe, R. J.: "The impact of faults on fluid flow in the Heidrun Field," In: Jones, G., Fisher, Q. J. and Knipe, R. J. (editors) Faulting, Fault Sealing and Fluid Flow in Hydrocarbon Reservoirs. Geological Society, London, Special Publication, Vol. 147, pp. 269–282, 1998.

Kretz V, Le Ravalec-DupinMand Roggero F.: "An integrated reservoir characterization study matching production and 4D seismic," paper SPE 77516 presented at the SPE AnnualTechnical Conference and Exhibition, San Antonio, USA, 2002.

Kromah, M.J., Liou, J., and MacDonald, D.G.: "Step Change in Reservoir Simulation Breathes Life into a Mature Oil Field," paper SPE 94940, presented at the SPE Latin American and Caribbean Petroleum Engineering Conference, Rio de Janeiro, Brazil, 20-23 June 2005.

Kruger W. D.: "Determining Areal Permeability Distribution by Calculations," J. Pet. Tech., Vol. 691, 1961.

Kruijsdijk, C.P.J.W. van: "Integrating reservoir engineering into Geosciences," Joule II–Reservoir Engineering Project, JOU2-0182, Delft University of Technology and TNO Institute of Applied Geoscience, 2001.

Kuo R.J.' Hong S.Y. and Huang Y.C., : "Integration of particle swarm optimization-based fuzzy neural network and artificial neural network for supplier selection," Applied Mathematical Modelling Volume 34, Issue 12, Publisher: Elsevier Inc., pp. 3976–3990, December 2010

Lach, J., McMillen, K., Archer, R., Holland, J., DePauw, R., and Ludvigsen, B.E.: "Integration of Geologic and Dynamic Models for History Matching, Medusa Field," paper SPE 95930, presented at the SPE Annual Technical Conference and Exhibition, Dallas, TX, 9-12 October, 2005.

Lake, L.W., and Jenson, J.L.: "A review of heterogeneity measures used in reservoir characterization", SPE Journal, SPE 20156, 1989.

Lamers, E. and Carmichael, S.: "The Palaeocene Deepwater Sandstone Play West of Shetland," Proceedings of 5th Conference Petroleum Geology of Northwest Europe, London, United Kingdom. The Geological Society, 1999.

Lancaster, S. and Whitcombe, D.: "Fast-Track Coloured Inversion," SEG International Exposition and Annual Meeting, Calgary, Canada, 2000.

Landa, J., Kamal, M. and Jenkins, C. D.: "Reservoir Characterization Constrained to Well Test Data: A Field Example," paper SPE 36511, presented at the SPE Annual Technical Conference and Exhibition, Denver, Colorado, 6-9 October, 1996.

Landa, J., Kalia, R.K., Nakano, A., Nomura, K., and Vashishta, P.: "History Match and Associated Forecast Uncertainty Analysis - Practical Approaches Using Cluster Computing," International Petroleum Conference. Doha, Qatar, 21-23 November 2005.

Landa, J. and Horne, R.: "A procedure to integrate well test data, reservoir performance history and 4D seismic information into a reservoir description," paper SPE 38653, presented at the SPE Annual Technical Conference and Exhibition, San Antonio, USA, 1997.

Landro M.: "Discrimination between pressure and fluid saturation changes from time-lapse seismic data," Geophysics, Vol. 66, No. 3, pp. 836-844, 2001.

Le Ravalec-Dupin, M., Hu, L.-Y.: "Combining the Pilot Point and Gradual Deformation Methods for Calibrating Permeability Models to Dynamic Data," Oil & Gas Science and Technology, Vol. 62, No. 2, pp. 169-180, 2007.

Le Ravalec, M., Hu, L. Y., and Noetinger, B.: "Sampling the conditional realization space using the gradual deformation method," Geostatistics 2000 Cape Town, Vol. 1, pp. 176–186, 2000.

Leach, H. M., Herbert, N., Los, A. and Smith, R. L.: "The Schiehallion development," In Fleet, A. J. and Boldy, S. A.R. (eds) Petroleum Geology of Northwest Europe, Proceedings of the 5th Conference, p683-692. The Geological Society, London, UK, 1999.

Leeuwenburgh, O., Brouwer, J., Trani, M.: "Ensemble-based conditioning of reservoir models to seismic data," Computational Geosciences, Vol. 16, pp. 1-20, 16 September, 2010

Li, R., Reynolds, A. C. and Oliver, D. S.: "History matching of three-phase flow production data," SPE Journal, Vol. 8, No. 4, pp. 328–340, 2003.

Li, B. and Friedmann, F.: "Novel multiple resolution design of experiment/response surface methodology for uncertainty analysis of reservoir simulation forecasts," SPE Reservoir Simulation Symposium, Woodlands, Texas, U.S.A., 31 Jan. -2 Feb. 2005.

Li, R., Reynolds, A.C., and Oliver, D.S.: "History Matching of Three-Phase Flow Production Data," paper SPE 66351, presented at the SPE Reservoir Simulation Symposium, Houston, TX, 11-14 February, 2001.

Li, R., Reynolds, A.C., and Oliver, D.S.: "Sensitivity Coefficients for Three-Phase Flow History Matching," Journal of Canadian Petroleum Technology, Vol. 42, No. 4, pp. 70-77, 2003.

Liang, B.: "An Ensemble kalman filter model for automatic history matching," PhD thesis, University of Texas, 2007.

Liang, B., Alpak, F.O., Sepehrnoori, K., and Delshad, M.: "A Singular Evolutive Interpolated Kalman Filter for Rapid Uncertainty Quantification," paper SPE 106170, presented at the SPE Reservoir Simulation Symposium, Houston, 26–28 February 2007.

Liang, B., Sepehrnoori, K., and Delshad, M.: "An Automatic History Matching Module with Distributed and Parallel Computing," Petroleum Science and Technology, Vol. 27, No. 10, pp. 1092-1108, 2009.

Lindley D.V.: "Theory and Practice of Bayesian Statistics," Cambridge University Press, 1983.

Litvak, M., Christie, M., Johnson, D., Colbert, J., and Sambridge, M.: "Uncertainty Estimation in Prediction Predictions Constrained by Production History and Time-Lapse Seismic in a GOM Oil Field," paper SPE 93146, presented at the SPE Reservoir Simulation Symposium, Houston, TX, 31 January-2 February, 2005.

Liu, N., Betancourt, S., and Oliver, D.S.: "Assessment of Uncertainty Assessment Methods," paper SPE 71624, presented at the 2001 SPE Annual Technical Conference and Exhibition, New Orleans, LA, 30 September-3 October, 2001.

Liu, N. and Oliver, D.S.: "Evaluation of Monte Carlo Methods for Assessing Uncertainty," SPEJ, Vol. 8, No. 2, pp. 188-195, 2003

Liu, N. and Oliver, D.S.: "Experimental Assessment of Gradual Deformation Method, "Mathematical Geology, Vol. 36, No. 1, pp. 65-77, 2004.

Lord, M.E. and Collins, R.E.: "Detecting Compartmented Gas Reservoir Through Production Performance," paper SPE 22941, presented at the SPE Annual Technical Conference and Exhibition, Dallas, 6–9 October, 1991.

Lumley, D.E. Nunns, A.G. Delorme, G.and Bee. M.F.: “Meren field, Nigeria: A 4d seismic case study,” SEG 1999 Expanded Abstracts, 1999.

Ma, X., Al-Harbi, M., Datta-Gupta, Akhil and Efendiev, Y.: “A Multistage Sampling Method for Rapid Zuantification of Uncertainty in History Matching Geological Models,” paper SPE 102476, presented at the SPE Annual Technical Conference and Exhibition, San Antonio, Texas, 24-27 September, 2006.

Ma, X., Datta-Gupta, A., Efendiev, Y.: “A Multistage MCMC Method with Nonparametric Error Model for Efficient Uncertainty Quantification in History Matching,” paper SPE 115911, presented at the Annual Technical Conference and Exhibition, Denver, Colorado, USA, 21-24 September 2008.

MacBeth, C.: "How can anisotropy be used for reservoir characterisiation?," First Break, Vol. 13, No. 1, pp.31-37, 1995.

MacBeth, C.: “An introduction to quantitave 4D seismic interpretation for dynamic reservoir description,” EAGE education day, 2007.

MacBeth, C., Stephen, K. D. and McInally, A.: "The 4D Seismic Signature of oil-water Contact Movement Due to Natural Production in a Stacked Turbidite Reservoir," Geophysical Prospecting, Vol. 53, No. 1, pp. 183-203, 2005.

MacBeth, C., and Stephen, K.: “Seismic scale saturation relations in turbiditer reservoirs undergoing waterflood,” European Association of Geoscientists & Engineers, Geophysical Prospecting, Vol. 56, pp.693–714, 2008.

MacBeth, C., Soldo, J., and Floricich, M.: “Going Quantitative with 4D Seismic Analysis,” In SEG International Exposition and Annual Meeting, Denver, Colorado, 2004.

Macdonald, C. J., Tosdevin, M., and Tothill, M. D.: “Report on the Schiehallion Full Field VIP Model,” FFM2003, 2004.

MacMillan, D. J., Pletcher, J. L., and Bourgeois, S. A.: “Practical Tools To Assist History Matching”, Paper SPE 51888, presented at the SPE Reservoir Simulation Symposium, Houston, Texas, February 14-17, 1999.

Makhlouf, E.M., Chen, W.H, Wasserman, M.L., and Seinfeld, J.H.: “A General History Matching Algorithm for Three-Phase, Three-Dimensional Petroleum Reservoirs,” SPE Advanced Technology Series, Vol. 1, No. 2, pp. 83-92, 1993.

Mandel, J.: “Use of the singular value decomposition in regression analysis,” Amer. Statistician, Vol. 36, pp. 15–24, 1982.

Manceau, E., Mezghani, M. Zabalza-Mezghani, I. and Roggero, F.: "Combination of experimental design and joint modeling methods for quantifying the risk associated with deterministic and stochastic uncertainties - an integrated test study," paper SPE paper 71620, presented at the SPE Annual Technical Conference and Exhibition held in New Orleans, Louisiana, 30 September - 3 October 2001.

Manzocchi, T., Walsh, J. J., Nell, P., and Yielding, G.: "Fault transmissibility multipliers for flow simulation models," Petroleum Geoscience, Vol. 5, pp. 53–63, 1999.

Marco D. and Thomas S.:" Ant Colony Optimization," Bradford Book, 2004.

Marsh, J.M., Whitcombe, D.N., Raikes, S.A., Parr, R.S. and Nash, T.: "BP's Increasing Systematic Use Of Time-Lapse Seismic Technology," Petroleum Geoscience, Vol 9, pp. 7-13, 2003.

Marsh, M.: "4D in reservoir management - Successes and Challenges," IOR Views e-Newsletter, No. 8, 2004.

Marsily, G., Lavedan, G., Boucher, M., Fasanino, G.: "Interpretation of Interference Tests in a Well Field Using Geostatstical Techniques to Fit the Permeability Distribution in a Reservoir Model," in the edited book Geostatistics for Natural Resources Characterization, Part 2, pp. 831-849, Kluwer Academic Publishers, 1984.

Matheron, G.: "The theory of regionalized variable and its applications," Les Cahiers du Centre de Morphologie Mathematique de Fontainebleau, Technical Report 5, published by the Ecole Nationale Superieure de Mines du Paris, 1971.

McCulloch, R, Rossi, P. and Singpurwalla, N.D.: "Case Studies in Bayesian Statistics," Vol. III of Lecture Notes in Statistics, No. 121, pp. 37–93, Springer-Verlag, New York, USA, 1997.

Meadows, M.A.: "Enhancements to landro's method for separating time-lapse pressure and saturation changes," San Antonio, Expanded Abstracts, 2001.

Metropolis, N., Rosenbluth, A.W., Rosenbluth, M.N., Teller, A.H., Teller, E.: "Equation of State Calculation by Fast Computing Machines," J. of Chem. Phys., Vol. 21, pp. 1087-1091, 1953.

Mezghani, M., Fornel, A., Langlais, V., and Lucet, N.: "History matching and quantitative use of 4D seismic data for an improved reservoir characterization," paper SPE 90420, presented at the SPE Annual Technical Conference and Exhibition, Houston, USA, 2004.

Migon, H. S. and Gamerman, D.: "Statistical Inference: an Integrated Approach," New York: Arnold, 1999.

Mohamed, L. Christie, M., Demyanov, V., Robert, E. and Kachuma, D.: "Application of Particle Swarms for History Matching in the Brugge Reservoir," paper SPE 135264, presented at the SPE Annual Technical Conference and Exhibition, Florence, Italy, 19-22 September 2010.

Monico, C.: "Mathematic comparisons of different history match runs," 6th European Conference on the Mathematics of Oil Recovery, Peebles, Scotland, Paper B-25, 1998.

Montgomery, D.C.: "Design and analysis of experiments," New York, John Wiley & Sons, 1997.

Montgomery, D. C.: "Design and Analysis of Experiments," 5th Edition, John and Wiley Sons, Inc., New York, 2000.

Murphy, W., Reischer, A., and Hsu, K.: "Modulus Decomposition of Compressional and Shear Velocities in Sand Bodie," Geophysics, Vol. 58, pp. 227-239, 1993.

Myers, R.H. and Montgomery, D.C.: "Response surface methodology: process and product optimization using design of experiments," John Wiley & Sons, New York, 1995.

Myers, R.H. and Montgomery, D.C.: "Response Surface Methodology: Process and Product Optimization Using Designed Experiments," 2nd edition, John Wiley & Sons, Inc, 2002.

Neal, R.M.: "Probabilistic Inference Using Markov Chain Monte Carlo Methods," tech. report, Department of Computer Science, University of Toronto, Toronto, Canada,, 1993.

Nelder, J.A.: "An alternative interpretation of the singular-value decomposition in regression," Amer. Statistician, Vol. 39, pp. 63–64, 1985.

Nicotra, G., Godi, A., Cominelli, A., Christie, M.: "Production Data and Uncertainty Quantification: A Real Case Study," paper SPE 93280, presented at the SPE Reservoir Simulation Symposium, Houston, TX, 31 January-2 February, 2005.

NIST/SEMATECH: "e-Handbook of Statistical Methods," http://www.itl.nist.gov/div898/handbook/, 2012.

O'Sullivan, A., Christie, M.: "Simulation Error Models for Improved Reservoir Prediction. Reliability Engineering and System Safety," Vol. 91, Issues 10-11, pp. 1382-1389, 2006.

Okabe, A., Boots, B., Sugihara, K.: "Spatial Tessellations: Concept and applications of Voronoi diagrams," John Wiley& Sons, Chichester, 1992.

Okano, H., Pickup, G.E., Christie, M.A., Subbey, S., Sambridge, M. and Monfared, H.: "Quantification of Uncertainty in Relative Permeability for Coarse-Scale Reservoir Simulation," paper SPE 94140, presented at the SPE Europec / EAGE Annual Conference, Madrid, 13-16 June 2005.

Oldenziel T.: " Geologic parameterization of reservoir model enhances history-match procedure," The Leading Edge), Vol. 21, No. 6, pp.544, 2002.

Oldenziel T.: "Time-lapse seismic within reservoir engineering," PhD Thesis, Delft University of Technology, The Netherlands, 2003.

Olea, R.A.: "Geostatistical Glossary and Multilingual Dictionary," Oxford University Press, 1991.

Oliver, D. S.: "Incorporation of transient pressure data into reservoir characterization," In Situ, Vol. 18, No. 3, pp. 243–275, 1994.

Oliver, D.S.: "Multiple Realizations of the Permeability Field from Well-Test Data," Soc. Petrol. Eng. J., Vol. 1, No. 2, pp.145-154, 1996.

Oliver, D., Reynolds, A., Liu, N.: "Inverse Theory for Petroleum Reservoir Characterization and History Matching," 1st Edition, Cambridge University Press, New York, 2008.

Oliver D. S., Cunha L. B., and Reynolds A. C., "Markov chain Monte Carlo methods for conditioning a permeability field to pressure data," Mathematical Geology, vol. 29, number 1, pp. 61–91, 1997.

Omre, H., Hegstad, B.K., Tjelmeland, H.: "Alternative history matching approaches," Tech. rep., Department of Mathematical Sciences, Norwegian University of Science and Technology, Trondheim, Norway, 1996.

Omre; H. and Tjelmeland; H.: "Petroleum Geostatistics; in Baafi and Schofield (Ed.)," Geostatistics Wollongong 1996, Vol. I, Kluwer Academic Publishers, pp. 41-52, 1997.

Onwunalu J.E. and Durlofsky L.J.: "Application of a particle swarm optimization algorithm for determining optimum well location and type," Computational Geosciences 14: pp. 183–198, 2010.

Onwunalu J.E. and Durlofsky L.J.: "A new well pattern optimization procedure for large-scale field development," SPE Journal (in press), 2011.

Osterloh, W. T.: "Use of Multiple-Response Optimization to Assist Reservoir Simulation Probabilistic Forecasting and History Matching," paper SPE 116196, presented at the Annual Technical Conference and Exhibition, Denver, Colorado, 21-24 September 2008.

OUENES, A., BREFORT, B., MEUNIER, G. and DUPERE, S.: "A New Algorithm for Automatic History Matching: Application of Simulated Annealing Method (SAM) to Reservoir Inverse Modeling," paper SPE 26297, unsolicited unpublished manuscript, 1993.

Otake, M.: "Hierarchical Geostatistical Modeling and History Matching Strategies in a Volcanic Formation," paper SPE 115931, presented at the SPE Asia Pacific Oil and Gas Conference and Exhibition, Perth, Australia, 20-22 October, 2008,

Panda, M.N. and Lake, L.W.: "Parallel Simulated Annealing for Stochastic Reservoir Modeling," paper SPE 26418, presented at the SPE Annual Technical Conference and Exhibition, Houston, TX, 3-6 October, 1993.

Paffenholz J., Monk, D. and Fryar, D.: "Random and Systematic Navigation Errors: How Do They Affect Seismic Data Quality?" paper 1993-0527, presented at SEG Conference Paper, Huston, USA, 1993.

Papoulis, A.: "Probability, random variables, and stochastic processes," McGraw-Hill, Inc, 1991.

Parr, R., Cowper, D., and Michener, B.: "The Search for Mountains of Oil: Exploration Activity in the Atlantic Margin, West of Shetland," paper SPE56897, presented at the SPE Offshore Europe Conference, Aberdeen, Scotland, 1999.

Parr R.S., Marsh M. and Griffin T.: "Interpretation and integration of 4-D results into reservoir management, Schiehallion Field, UKCS," 70th SEG meeting, Calgary, Canada, Expanded Abstracts, pp. 1464-1467, 2000.

PBQuad204Project, "Environmental Statement," BP Exploration Operating Company Ltd, November 2010.

Peaceman, D.W.: "Fundamentals of Numerical Reservoir Simulation," Elsevier Scientific Publishing Company, Amsterdam, 1977.

Peaceman, D.W.: "Effective Transmissibilities of a Gridblock by Upscaling - Comparison of a Direct Methods with Renormalization, paper SPE 36722, SPE Journal, 1997.

Peake, W. T., Abadah, M., Skander, L.: "Title Uncertainty Assessment using Experimental Design: Minagish Oolite Reservoir," paper SPE 91820-MS, presented at the Reservoir Simulation Symposium, The Woodlands, Texas, USA, 31 January-2 February 2005.

Pearson, K.: "On Lines and Planes of Closest Fit to Systems of Points in Space," Philosophical Magazine, Vol. 2, No. 6, pp. 559-572, 1901.

Peng, C.Y., and Gupta, R.: "Experimental Design and Analysis Methods in Multiple Deterministic Modelling for Quantifying Hydrocarbon In-Place Probability Distribution Curve," paper SPE 87002, presented at the Asia Pacific Conference on Integrated Modelling and for Asset Management, Kuala Lumpur, Malaysia, 29-30 March 2004.

Plackett, R.L. and Burman, J.P.: "The Design of Optimum Multifactorial Experiments," Biometrika, Vol. 33, No. 4, pp. 305-325, 1946.

Portella, R.C.M and Emerick, A.A.: "Use of Quantitative 4D-Seismic Data in Automatic History Match," paper SPE 94650, presented at the SPE Latin American and Caribbean Petroleum Engineering Conference held in Rio de Janeiro, Brazil, 20 – 23 June, 2005.

Portellaand, R.C.M. and Prais, F.: "Use of Automatic History Matching and Geostatistical Simulation to Improve Production Forecast," paper SPE 53976, presented at the Latin American and Caribbean Petroleum Engineering Conference, Caracas, Venezuela, 21-23 April, 1999.

Porter-Hirsche, J. and Hirsche, K.: "Repeatability study of land data acquisition and processing for time lapse seismic," 1998 SEG Expanded Abstracts, 1998.

Press, W. H., Teukolsky, S. A., Vetterling, W. T., and Flannery, B. P.: "Numerical recipes in FORTRAN: the art of scientific computing," Cambridge University Press, New York, 1998.

Ramammorthy, R., Murphy, W.F., and Coll. C.: "Total porosity estimation in shaly sands from shear modulus," SPWLA 36th Annual Logging Symposium Transactions, 1995.

RamaRao, B.G., LaVenue, A.M., Marsily, G., Marietta, M.G.: "Pilot Point Methodology for Automated Calibration of an Ensemble of Conditionally Simulated Transmissivity Fields, 1, Theory and Computational Experiments," Water Resour. Res., Vol. 31, No. 3, pp.475-494, 1995.

Rechenberg, I.: " Cybernetic Solution Path of an Experimental Problem, Royal Aircraft Establishment," Library Translation Number 1122, Farnborough, UK, 1965.

Reynolds A. C., He N., Chu L., Oliver D. S.: "Reparameterization techniques for generating reservoir descriptions conditioned to variograms and well-test pressure data," Soc. Petrol. Eng. J., Vol. 1, No. 4, pp. 413-426, 1996.

Richardson, S., Herbert, N., and Leach, H.: "How Well Connected is the Schiehallion Reservoir? Paper SPE38560, presented at the SPE Offshore Europe Conference, Aberdeen, Scotland, 1997.

Ripley, B.D.: "Spatial Statistics," Wiley, pp. 252, 1981

Rodrigues, J.R.P.: “Calculating Derivatives for History Matching in Reservoir Simulators,” paper SPE 93445, presented at the SPE Reservoir Simulation Symposium, Houston, TX, 31 January-2 February 2005.

Roggero, F.: "Direct Selection of Stochastic Model Realizations Constrained to Historical Data," paper SPE38731, presented at the SPE ATCE, San Antonio, Texas, 5-8 October 1997.

Roggero, F., Ding, D. Y., Berthet, P., Lerat, O., Cap, J. and Schreiber, P.E.: “Matching of Production History and 4D Seismic Data-Application to the Girassol Field, Offshore Angola,” paper SPE 109929, presented at the Annual Technical Conference and Exhibition held in Anaheim, California, U.S.A., 11-14 November, 2007.

Roggero, F. and Guerillot, D.: “Gradient Method and Bayesian Formalism Application to Petrophysical Parameter Characterization,” paper presented at the 5th European Conference on the Mathematics of Oil Recovery, Leoben, Austria, 3-6 September, 1996.

Roggero, F. and Hu, L.Y.: “Gradual Deformation of Continuous Geostatistical Models for History Matching,” paper SPE 49004, presented at the SPE Annual Technical Conference and Exhibition, New Orleans, LA, 27-30, September 1998.

Romero C E, Carter J N, Zimmerman R W, and Gringarten A C.: “Improved reservoir characterization through evolutionary computation,” paper SPE 62942, presented at the SPE Annual Technical Conference and Exhibition , Dallas, Texas, October 1–4 2000.

Romero, C.E., Carter, J.N., Gringarten, A.C., and Zimmerman, R.W.: “A Modified Genetic Algorithm for Reservoir Characterisation,” paper SPE 64765, presented at the SPE International Oil and Gas Conference and Exhibition in China, Beijing, China, 7-10 November 2000.

Rotondi, M., Nicotra, G., Godi, A., Contento F.M., Blunt M.J., and Christie, M.A.: “Hydrocarbon Production Forecast and Uncertainty Quantification: A Field Application,” paper SPE 102135, presented at the SPE Annual Technical Conference and Exhibition, San Antonio, TX, 24-27 September, 2006.

Rwechungura, R., Dadashpour, M., Kleppe, J.: “Application of Particle Swarm Optimization for Parameter Estimation Integrating Production and Time Lapse Seismic Data,” paper SPE 146199, presented at the SPE Offshore Europe Oil and Gas Conference and Exhibition held in Aberdeen, UK, 6–8 September 2011.

Rwechungura, R., Dadashpour, M., Kleppe, J.: “Advanced History Matching Techniques Reviewed,” paper SPE 142497, presented at the SPE Middle East Oil and Gas Show and Conference, Manama, Bahrain, 25-28 September 2011.

Sacks, J., Welch, W. J., Mitchell, T. J., and Wynn H. P.: "Design and analysis of computer experiments," Statistical Science, Vol. 4, No. 4, pp. 409-435, 1989.

Sambridge M.: "Finding Acceptable Models in Nonlinear Inverse Problems Using a Neighbourhood Algorithm," Inverse Problems, Vol. 17, pp. 387-403, 2001.

Sambridge, M.: "Geophysical Inversion with a Neighbourhood Algorithm-I. Searching a Parameter Space," Geophys. J. Int., Vol. 138, p. 479-494, 1999a.

Sambridge, M.: "Geophysical Inversion with a Neighbourhood Algorithm-II. Appraising the Ensemble," Geophys. J. Int., Vol. 138, p. 727-746, 1999b.

Sambridge, M. and Kennett, B.: "Seismic Event Location: Nonlinear Inversion Using a Neighbourhood Algorithm," Pure and Applied Geophysics, Vol. 158, No. (1-2), pp.427-440, 2001.

Sarma, P., Durlofsky, L.J., and Aziz, K.: "Efficient Closed-Loop Production Optimization under Uncertainty," paper SPE 94241, presented at the SPE/EAGE Annual Conference, Madrid, Spain, 13-16 June 2005.

Sarma, P., Aziz, K., and Durlofsky, L.J.: "Implementation od Adjoint Solution for Optimal Control of Smart Wells," paper SPE 92864, presented at the SPE Reservoir Simulation Symposium, The Woodlands, Texas, USA, 31 January-2 February 2005.

Sarma, P., Chen, W.H., Durlofsky, L.J., and Aziz, K.: "Production Optimization with Adjoint Models under Nonlinear Control-State Path Inequality Constraints," paper SPE 99959, presented at the Intelligent Energy Conference and Exhibition, Amsterdam, The Netherlands, 11-13 April 2006.

Saxby, I.: "Impact of 4-D seismic reservoir monitoring in Schiehallion Field, UKCS," AAPG Annual Meeting, Denver, Colorado, 2001.

Scheidt, C., and Caers., J.: "Representing spatial uncertainty using distances and kernels," Mathematical Geosciences, Vol. 41, pp. 397-419, 2009.

Schulze-Riegert, R., Axmann J K, Haase O, Rian D T, and You Y L.: "Evolutionary algorithms applied to history matching of complex reservoirs," SPE Reservoir Evaluation & Engineering, Vol. 52, 2002.

Schulze-Riegert, R., Haase O and Nekrassov A.: "Combined global and local optimization techniques applied to history matching," paper SPE 79668, presented at the SPE Reservoir Simulation Symposium, Houston, Texas, 3-5 February 2003.

Schulze-Riegert R., Shawket G.: "Modern Techniques for History Matching," 9th International Forum on Reservoir Simulation, Abu Dhabi, United Arab Emirates, 9-13 December 2007.

Sedighi, F. and Stephen K.: "Faster Convergence in Seismic History Matching by Dividing and Conquering the Unknowns," SPE 121210-PA. SPE Journal, Vol.12, No. 4, pp. 1077-1088, 2010.

Sedighi, F.: "Faster Convergence in Seismic History Matching by Dividing and Conquering the Unknowns," PhD thesis, Heriot-Watt University, Edinburgh, UK, 2011.

Seiler, A., Evensen, G.,. Skjervheim, J., Hove, J. and Vabø, J.G.: "Advanced Reservoir Management Workflow Using an EnKF Based Assisted History Matching Method," Paper SPE 118906, presented at the SPE Reservoir Simulation Symposium held in the Woodlands, Texas, USA, 2-4 February 2009.

Selvi V. And Umarani R.: "Comparative Analysis of Ant Colony and Particle Swarm Optimization Techniques," International Journal of Computer Applications (0975 – 8887), Vol. 5, No.4, 2010.

Sen, M. K. and Stoffa, P. L.: "Global optimization methods in geophysical inversion Advances in Exploration Geophysics," Vol. 4, Elsevier, Amsterdam, 1995.

Sheriff, R. E.: "Basic petrophysics and geophysics, in Reservoir Geophysics," In Sheriff, R., editor, Investigations in Geophysics No. 7, Society of Exploration Geophysicists, Tulsa, Oklahoma, pp. 37-49, 1992.

Sivia, D.S.: "Data Analysis – A Bayesian Tutorial. Claredon Press, Oxford, 1996.

Skjervheim, J.-A., Evensen, G., Aanonsen, S. I., Ruud, B. O., and Johansen, T. A.: " Incorporating 4D seismic data in reservoir simulation models using ensemble Kalman filter," paper SPE 95789, presented at the SPE Annual Technical Conference and Exhibition held in Dallas, Texas, U.S.A., 9-12 October, 2005.

Skjervheim, J.-A., Evensen, G., Aanonsen, S. I., Ruud, B. O., and Johansen, T. A.: " Incorporating 4D seismic data in reservoir simulation models using ensemble Kalman filter," SPE J., Vol. (12), No. 3, pp. 282-292, SPE 95789, 2007.

Smith, A. F. M., and Roberts, G. O.: "Bayesian computation via the Gibbs sampler and related Markov chain Monte-Carlo methods (with discussion)," J. Roy. Stat. Soc. Series B 55: pp. 3-23, 1993.

Smith, C., Tracy, G, Farrar, R.: "Applied Reservoir Engineering", Vol. 2, Oil & Gas Consultants International, Tulsa, 1992.

Socha, K., Dorigo, M.: "Ant Colony Optimization for Continuous Domains, European Journal of Operational Research," Vol. 185, No.3, pp. 1155-1173, 2008.

Soldo, J.: "Quantitative Integration of Time-Lapse Seismic Data," PhD Thesis, Heriot-Watt University, Edinburgh, Scotland, 2005.

Sotirios Vardakos, S., Gutierrez, M., Caichu, X.: "Back-Analysis of Tunnel Response Using Simulated Annealing," ISRM paper published by International Society for Rock Mechanics and the University of Hong Kong, SINOROCK, Hong Kong, China, 2009.

Sousa, S.H.G., Maschio, C., and Schiozer D.J.: "Scatter Search Metaheuristic Applied to the History-Matching Problem," paper SPE 102975, presented at the SPE Annual Technical Conference and Exhibition, San Antonio, TX, 24-27 September, 2006.

Staples, R., Lamens, Y., and Smith, B.: "Monitoring injection in the Northern North Sea," SPE/EAGE joint workshop, Copenhagen, Denmark, 2004.

Stephen, K.D.: "Scale and process dependent model errors in seismic history matching," Oil & Gas Science and Technology-Revue de l' IFP, Vol. 62, No. 2, pp. 123-136, 2007.

Stephen, K.D. and Arwini, S.: "Improving Stochastic Inversion Methods in History Matching using Proxy Models", ECMOR XII, 12th European Conference on the Mathematics of Oil Recovery, Oxford, UK, 6-9 September 2010.

Stephen, K., Soldo, J., Macbeth, C. and Christie, C.: "Multiple-model seismic and production history matching: A case study," SPE 94173, SPE Journal, Vol. 11, No. 4, pp. 418-430, 2006.

Stephen, K. D., and MacBeth, C.: "Reducing Reservoir Prediction Uncertainty Using Seismic History Matching," paper SPE 100295, presented at the SPE Europec/EAGE Annual Conference and Exhibition held in Vienna, Austria, 12–15 June, 2006a.

Stephen, K. D., and MacBeth, C.: "Inverting For the Petro-elastic Model Via Seismic History Matching," Society of Exploration Geophysicists International Expansion and 76th Annual Meeting, New Orleans, Louisiana, 1-6 October 2006b.

Stephen K.D. & Edriz N.: "Assessing the Value of Time-lapse Seismic in History Matching and Forecasts of the Schiehallion," SPE Europec/EAGE Annual Conference and Exhibition, Amsterdam, 7–14 June 2009.

Stephen, K. D., Soldo, J., MacBeth, C. and Christie M.: "A multiple model approach to history matching and uncertainty analysis using time-lapse seismic," Proceedings of the 9th European Conference on the Mathematics of Oil Recovery, Cannes, France, 20 Aug.-2nd Sept, 2004.

Stephen, K. D., Soldo, J., MacBeth, C., and Christie, M.: "Multiple Model Seismic and Production History Matching: A Case Study," paper SPE94173, presented at the 14th Europec Biennial Conference held in Madrid, Spain, 13–16 June, 2005.

Stephen, K., Soldo, J., Macbeth, C. and Christie, C.: "Multiple-model seismic and production history matching: A case study," SPE 94173-PA, SPE Journal, Vol. 11, No. 4, pp. 418-430, 2006.

Stephen, K.D., Soldo, J., MacBeth, C., and Christie, M.: "Multiple-Model Seismic and Production History Matching: A Case Study," SPE J., Vol. 11, No. 4, pp. 418-430, SPE-94173-PA, 2006.

Subbey, S., Christie, M., and Sambridge, M.: "A Strategy for Rapid Quantification of Uncertainty in Reservoir Performance Prediction," paper SPE 79678, presented at the SPE Reservoir Simulation Symposium, Houston, TX, 3-5 February, 2003.

Subbey, S., Christie, M., and Sambridge, M.: "Prediction under Uncertainty in Reservoir Modeling," Journal of Petroleum Science and Engineering, Vol. 44, pp. 143-153, 2004.

Subbey, S., Christie, M., and Sambridge, M.: "Uncertainty Reduction in Reservoir Modeling," In Chen, Z. and Ewing, R. (editors), Fluid Flow and Transport in Porous Media: Mathematical and Numerical Treatment, Vol. 295 of Contemporary Mathematics, pp. 1-10. American Mathematical Society, Providence, Rhode Island, 2002.

Suzuki, S. and Caers, J.: " History Matching with an Uncertain Geological Scenario," paper SPE 102154, presented at the SPE Annual Technical Conference and Exhibition, San Antonio, TX, 24-27 September, 2006.

Szklarz, S. P., Hanea, R.G. and Peters, E.: "A Case study of the History Matching Of A Sector Of The Norne Field Using the Ensemble Kalman Filter," paper SPE 143004, presented at the SPE EUROPEC/EAGE Annual Conference and Exhibition, Vienna, Austria, 23-26 May 2011.

Trani, M., Arts, R., Leeuwenburgh, O., and Brouwer, J.:" Estimation of changes in saturation and pressure from 4D seismic AVO and time-shift analysis," Geophysics, Vol. 76, No. 2, pp. C1-C17, March-April 2011.

Tarantola, A., and Valette, B.: "Inverse Problems Quest for Information," Journal of Geophysics, Vol. 50. No. 2, pp.159-170, 1982.

Tarantola, A.: "Inverse Problem Theory: Methods for Data Fitting and Model Parameter Estimation," Elsevier, Amsterdam, The Netherlands, 1987.

Tokuda, N., Takahashi, S. and Watanabe, M.: "Application of Genetic Algorithm to history matching for core flooding," paper SPE 88621, presented at the SPE Asia Pacific Oil and Gas Conference and Exhibition, Perth, Australia, October 18-20, 2004.

Traine A., Donatella A., and Marcelo, B.: "Seismic applications throughout the life of the reservoir," Oilfield review 2002, pp. 40-65, 2002.

Trefethen, L. N. and Bau, D.: "Numerical linear algebra," Philadelphia: SIAM, 1997.

Tura, A. and Lumley, D.: "Estimating pressure and saturation changes from time-lapse AVO data," Extended Abstracts, SEG Annual Meeting, 1999.

Van Ditzhuijzen, R., Oldenziel, T., Groot Bril, de and van Kruijsdijk, C.P.J.W.: "Geological Parameterization of a Reservoir Model for History Matching Incorporating Time-Lapse Seismic Based on a Case Study of the Statfjord Field, " paper SPE 71318, presented at the SPE Annual Technical Conference and Exhibition, New Orleans, Louisiana, 30 September-3 October 2001.

Van Leeuwen, P. J.: "Comment on "Data assimilation using an ensemble Kalman filter technique," Monthly Weather Review, Vol. 127, No. 6, pp. 1374-1377, 1999.

Valjak, M.: "History Matching and Forecasting with Uncertainty, Challenges and Proposed Solutions for Real Field Application," PhD Thesis, Institute of Petroleum Engineering, Heriot Watt University, 2008.

Vasco, D.W., Yoon, S., and Datta-Gupta, A.: "Integrating Dynamic Data Into High-Resolution Reservoir Models Using Streamline-Based Analytic Sensitivity Coefficients," SPE Journal, Vol. 4, No. 4, pp. 389-399, 1999.

Vauthrin, R., Brid, B., Will, B., Eastwood, J., Johnston, D.: "Improvements in 4D legacy data quality and repeatability through reprocessing," Lena Field, SEG 1999 Annual Technical Conference, Houston, 1999.

Vega, S., and Berteussen, K.: "Uncertainty Signal Analysis for a 4D-Seismic in a Middle East Carbonate," paper SPE 118153, presented at the Abu Dhabi International Petroleum Exhibition and Conference held in Abu Dhabi, UAE, 3-6 November, 2008.

Venkataraman, R.: "Application of the Method of Experimental Design to Quantify Uncertainty in Production Profiles," paper SPE 59422, presented at the SPE Asia Pacific Conference on Integrated Modeling for Asset Management, Yokohama, Japan, 25 - 26 April 2000.

Voronoi, M.G.: "Nouvelles applications des parame`tres continus a` la the´orie des formes quadratiques," J. reine Angew Math, Vol. 134, pp. 198-287, 1908.

Wadsley, A.W.: "Markov Chain Monte Carlo Methos for Reserves Estimation," paper SPE 10065, presented at the International Petroleum Technology Conference. Doha, Qatar, 21-23 November 2005.

Waggoner, J.R.: "Lessons learned from 4D projects," SPE Res. Eval. & Eng., Vol. 3, pp. 310-318, 2000.

Waggoner, J., Cominelli, A., and Seymour, R.: "Improved reservoir modeling with time-lapse seismic in a Gulf of Mexico gas condensate reservoir," paper SPE 77514, presented at the SPE Annual Technical Conference and Exhibition, San Antonio, USA, 2002.

Walder, D. R., Howes, D. R., Mountford, C. F., and Parr, R. S.: "Development Drilling Innovations for the Foinaven and Schiehallion fields, in the UK Atlantic Margin," OTC 10990, Houston, 1999.

Walstrom, J.E., Mueller, T.D., McFarlane, R.C.: "Evaluating Uncertainty in Engineering Calculations," Journal of Petroleum Technology, pp. 1595, 1976.

Wang, Z.: "The Gassmann equation revisited: comparing laboratory data with Gassmann's predictions," SEG, Vol. 3, No. 19, pp. 8-23, 2000.

Wang, Z., Nur, A.: "Effect of temperature on wave velocities in sands and sandstones with heavy hydrocarbons," SPE Reservoir Eng., Vol.3, No.1, pp. 158-164, 1988.

Wasserman, M. L., Emanuel, A. S. and Seinfeld, J. H.: "Practical Applications of Optimal Control Theory to History Matching Multiphase Simulator Models," SPE 5020, SPE-AIME 49th Annual Fall Meeting, Houston, Texas, October 6-9, 1974.

Watts, G., Jizba, D., Gawith, D., and Gutteridge, P.: "Reservoir Monitoring of the Magnus Field through 4D Time-Lapse Seismic Analysis," Petroleum Geoscience, Vol. 2, No. 4, pp. 361-372, 1996.

Watson, A.T., Seinfeld, J.H., Gavalas, G.R., Woo, P.T.: "History Matching in Two-Phase Petroleum Reservoirs," paper SPE 8250, presented at the SPE Annual Technical Conference and Exhibition, Las Vegas, NV, 1979.

Wen, X., Deutsch, C.V., Cullick, A.S.: "High Resolution Reservoir Models Integrating Multiple-Well Production Data," paper SPE 38728, presented at the SPE Annual Technical Conference and Exhibition, San Antonio, TX, 5-8 October, 1997.

Wences, P. G., Cullick, A.S., Deutsch, C. V.: "An optimization framework for reservoir characterization," SEG 1998 Annual Technical Conference, New Orleans, RC 1.2, 1998

White, C.D. and Roy, S.A.: "Experimental Design as a Framework for Reservoir Studies," paper SPE 79676, presented at the 2003 SPE Reservoir Simulation Symposium, Houston, 3 - 5 February, 2003.

Wills, H.A., Graves, R.M. and Miskimins, J.: "Don't Be Fooled by Bayes," paper SPE 90717, presented at Annual Technical Conference and Exhibition, Houston, TX, 26-29 September 2004.

Wolff, M.: "Probabilistic Subsurface Forecasting - What Do We Really Know?," paper SPE 118550, Journal of Petroleum Technology, Vol. 62, No. 5, pp. 86-92, 2005.

Wolf, M.: "Probabilistic Subsurface Forecasting," SPE 132957, unsolicited unpublished manuscript, 2010.

Wu, Z., Reynolds, A.C., and Oliver, D.S.: "Conditioning Geostatistical Models to Two-Phase Production Data," Soc. Petrol. Eng. J., Vol. 3, No. 2, pp. 142-155, 1999.

Xue, G. and Datta-Gupta: "Structure Preserving Inversion: An Efficient Approach to Conditioning Stochastic Reservoir Models to Dynamic Data," paper SPE 38727, presented at the SPE Annual Technical Conference and Exhibition, San Antonio, TX, 5-8 October, 1997.

Yadav, S.: "History Matching Using Face-Recognition Technique Based on Principal Component Analysis," paper SPE 102148, presented at the SPE Annual Technical Conference and Exhibition held in San Antonio, Texas, U.S.A., 24–27 September 2006.

Yao, H., C. Beghein, and Van der Hilst, R.D.: "Surface wave array tomography in SE Tibet from ambient seismic noise and two-station analysis: II. Crustal and upper-mantle structure," Geophys. J. Int., Vol. 173, No. 1, pp. 205-219, 2008.

Yeten, B.: "Optimization of Field Development," Proceedings of 9th International Forum on Reservoir Simulation, Abu Dhabi, UAE, 9-13 December, 2007.

Yeten, B., Castellini, A., Guyaguler, B., and Chen,. W.H.: "A Comparison Study on Experimental Design and Response Surface Methodologies," paper SPE 93347, presented at the SPE Reservoir Simulation Symposium, Houston, Texas, USA, 31 January - 2 February 2005.

Yeten, B., Durlofsky, L., and Aziz, K.: "Optimization of Well Type, Location and Trajectory," paper SPE 77565, presented at the SPE Annual Technical conference and Exhibition, San Antonio, TX, September 29-October 2, 2002.

Yeten, B., Durlofsky, L.J., and Aziz, K.: "Optimization of Smart Well Control," paper SPE 79031, presented at the SPE International Thermal Operation and Heavy Oil Symposium and International Horizontal Well Technology Conference, Calgary, Alberta, Canada, 4-7 November 2002.

Yielding, G., Overland, J. A., and Byberg, G.: "Characterisation of fault zones in the Gullfaks field for reservoir modeling," In: Petroleum Geology of Northwest Europe: Proceedings of the 5th Conference, Geological Society, London, Vol. 5, pp. 1177-1185, 1999a.

Yielding, G., Overland, J. A., and Byberg, G.: "Characterisation of fault zones for reservoir modelling: An example from the Gullfaks Field, Northern North Sea," American Association of Petroleum Geologists Bulletin, Vol. 83, No. 6, pp. 925–951, 1999b.

Yu, T., Wilkinson, D., and Castellini, A.: "Constructing Reservoir Flow Simulator Proxies Using Genetic Programming for History Matching and Production Forecast Uncertainty Analysis," Journal of Artificial Evolution and Applications Volume 2008.

Zhang, F., Reynolds, A.C.: "Optimization Algorithms for Automatic History Matching of Production Data," paper presented at the 8th European Conference on the Mathematics of Oil Recovery, Freiberg, Germany, 3-6 September, 2002.

Zhang, F., Skiervheim, J.A., Reynolds, A.C., and Oliver, D.S.: "Automatic History Matching in a Bayesian Framework, Example Applications," paper SPE 84461, presented at the SPE Annual Technical Conference and Exhibition, Denver, CO, 5-8 October, 2003.

Zubarev, D.I.: "Pros and Cons of Applying Proxy-Models as a Substitute for Full Reservoir Simulations," paper 124815, presented at the SPE Annual Technical Conference and Exhibition held in New Orleans, Louisiana, USA, 4-7 October 2009.